CHEMICAL CHARACTERISATION OF THE UROPYGIAL SECRETION OF *RHINOPOMASTUS CYANOMELAS*

by

NEGASSI GHEBREALFA KAHSAI

Thesis presented in fulfilment of the

requirements for the degree of

Master of Science

in

Chemistry

at the

University of Stellenbosch

Promoter: Dr M. le Roux

Co-promoter: Prof B.V. Burger

Stellenbosch

April 2004

DECLARATION

I the undersigned hereby declare that the work contained in this thesis is my own original work and has not previously in its entirety or in part been submitted at any other university for a degree.

N.G. Kahsai

SUMMARY

The uropygial gland of most birds produces a variety of hydrocarbons, lipids, waxes, fatty acids, alcohols and other organic compounds. These compounds have two widely recognized functions, *viz.* they are considered essential for the maintenance of a good plumage condition, and may be used for fungicidal, bactericidal or other hygienic purposes.

Scimitar-billed woodhoopoes, *Rhinopomastus cyanomelas,* are group-territorial birds that live in groups comprising between two and twelve individuals. Individuals enter the roost cavities shortly after sunset and exit the following morning soon after sunrise. During the period that the birds are inside the roost, they are vulnerable to a range of vertebrate predators, including snakes, genets and rats. When disturbed while roosting, woodhoopoes immediately face away from the threat hence presenting their uropygial glands in the direction of the threat. Typically, a drop of brown, highly pungent secretion is then formed at the tip of the papilla to the uropygial gland, and kept in place by a few tuft-like feathers. This response pattern has led some observers to believe that the secretion serves an anti-predatory role. It has been found that the synthetic volatile constituents of the uropygial secretion of the green woodhoopoe, *P. purpureus*, individually or as a mixture, have potent defensive properties against feline and reptilian predators. In addition, the compounds also showed activity against a range of bacteria.

The aim of the present study was to determine the chemical composition of the uropygial secretion of the scimitar-billed woodhoopoe, *Rhinopomastus cyanomelas*, as a first step towards the evaluation of, *inter alia*, the semiochemical function of the secretion. Using gas chromatography-mass spectrometry, 179 constituents of the uropygial secretion of the scimitar-billed woodhoopoe have been identified. The majority of the constituents of the secretion are branched and unbranched aldehydes (aliphatic and aromatic), acids (aliphatic and aromatic), sulfides and ketones. This group of volatile compounds is responsible for the obnoxious odour of the secretion and

possibly also for its defensive action against predators. The secretion also contains a large number of branched and unbranched alkanes and wax esters.

The chemical composition of the secretion was compared with the secretion of *P. purpureus* as well as with that of the hoopoe, *Upupa africana*. The uropygial gland secretion of the scimitar-billed woodhoopoe is quite similar to that of the green woodhoopoe, although it is much more complex than that of the green woodhoopoe. In contrast to the uropygial secretions of the green and the scimitar-billed woodhoopoes, the secretion of *Upupa africana* does not have a strongly obnoxious odour and it also does not contain large quantities of alkanes and wax esters.

OPSOMMING

Die uropigiale klier van die meeste voëls produseer 'n verskeidenheid van koolwaterstowwe, lipiede, was-esters, vetsure, alkohole en ander organiese verbindings. Hierdie verbindings het twee algemeen erkende funksies, naamlik die instandhouding van die goeie kondisie van die vere, en 'n swam- en kiemdodende werking.

Swartbekkakelaars (Engels: scimitar-billed woodhoopoes), *Rhinopomastus cyanomelas,* is groep-territoriale voëls wat in groepe van tussen twee en twaalf saam woon. Individue gaan hul neste net na sononder binne en verlaat dit weer die volgende oggend net na sonsopkoms. Terwyl die voëls binne die neste is, is hulle kwesbaar ten opsigte van aanval deur verskeie gewerwelde roofdiere, insluitende slange, muskeljaatkatte en rotte. Wanneer hulle in hul neste gesteur word, sal kakelaars onmiddellik wegdraai van die bedreiging sodat die uropigiale klier in die rigting van die bedreiging gekeer is. 'n Druppel bruin, uiters onwelriekende afskeiding vorm dan by die punt van die papil na die uropigiale klier, en word in posisie gehou deur 'n verekwassie. Hierdie gedragspatroon het aanleiding gegee tot die gedagte by sommige waarnemers dat die afskeiding as afweerstof teen roofdiere dien. Daar is gevind dat die sintetiese vlugtige komponente van die uropigiale afskeiding van die groenkakelaar, *P. purpureus*, individueel of as 'n mengsel, sterk afweer-eienskappe teen katte en reptiele toon. Daarbenewens het die verbindings ook aktiwiteit getoon teen 'n reeks van bakterieë.

Die doel van die huidige studie was om die chemiese samestelling van die uropigiale afskeiding van die swartbekkakelaar, *Rhinopomastus cyanomelas*, te bepaal as 'n eerste stap met die oog op die evaluering van, onder andere, die semiochemiese funksie van die afskeiding. Deur van gaschromatografie-massaspektrometrie gebruik te maak, is 179 komponente van die uropigiale afskeiding van die swartbekkakelaar geïdentifiseer. Die meeste van die komponente is vertakte en onvertakte aldehiede (alifaties en aromaties), sure (alifaties en aromaties), sulfiede en ketone. Hierdie groep vlugtige verbindings is verantwoordelik vir die afstootlike reuk van die

afskeiding en waarskynlik ook vir sy afweer-aksie teen roofdiere. Die afskeiding bevat ook 'n groot aantal vertakte en onvertakte alkane en was-esters.

Die chemiese samestelling van die afskeiding is vergelyk met die van *P. purpureus* sowel as dié van die hoepoe, *Upupa africana*. Die uropigiale klierafskeiding van die swartbekkakelaar stem tot 'n groot mate ooreen met dié van die groenkakelaar, alhoewel dit veel meer kompleks is as dié van die groenkakelaar. In teenstelling met die uropigiale afskeidings van die groen- en die swartbekkakelaars, het die afskeiding van *Upupa africana* nie 'n afstootlike reuk nie en bevat dit ook nie groot hoeveelhede alkane en was-esters nie.

ACKNOWLEDGEMENTS

My thanks and gratitude extend to the following

- To my advisor Dr. M.le Roux and co-advisor Prof. B.V. Burger for their close follow-up and guidance throughout my study.
- To Mr. Gary Scott for his unreserved support and cooperation.
- To members of LECUS, especially Mrs. W.J.G. Burger for creating a pleasant atmosphere.
- To Mr Aron Hailemichael for providing relevant documents, and Mr. Amanuel Ghebresadik and Mr. Jomal Adem for their kind support.
- To my family.

To my family for their

material and moral support

CONTENTS

CHAPTER 1

INTRODUCTION AND OBJECTIVES

1.1 Introduction

In this chapter a short summary is given of the different modes of communication that exist between animals of the same species or of different species. The interaction between animals and their environment is, however, not dealt with. An attempt is made to briefly discuss the main types of communication in both higher and lower animals with emphasis being given to vertebrates. Since the research discussed in this thesis deals with a secretion that is possibly used by a bird to communicate chemical information, a comparative approach, between birds and other animals, is used in the discussion. In addition, considerable attention is given to odour-producing organs and anatomical descriptions of those body parts that participate in the process of chemical communication. At the end of this chapter brief mention is made of the composition and functional role of the uropygial gland and the identity of the bird that was studied.

Bearing in mind that the main objective of the research focused on the chemical characterisation of the secretion from the uropygial gland, an exhaustive discussion of the chemical nature of secretion is given in the second chapter. The discussion of biological aspects, which is the focus of this chapter, is intended as an introduction to this research in the whole.

1.2 Behaviour

Behaviour, in short, is the response of a living organism to some form of stimulus, although the response can be affected by many variables. The simplest type of behaviour consists of automatic or reflex maintenance activities, so-called because their function is to maintain the animal in a suitable environment[1].

No animal lives independently. Every individual comes into contact with

other animals at some stage during its lifetime. While in contact, each animal species shows characteristic ways of performing certain functions and rarely departs from them. These characteristic ways, sometimes called behavioural patterns, are organized segments of behaviour having special functions. Although the nature of these behavioural patterns is determined chiefly by heredity, it is also greatly modified by learning and training.

The primary function of behaviour is to enable an animal to adjust itself to certain changes in its environment; whether living or inanimate. Most animals have a variety of behavioural patterns that can be tried out in a given situation, and in this way they learn to apply that one which produces the best adjustment. These changes in the behaviour to external stimuli are not passive; they are active, reversible and directed actions, that is, actions promoting survival of the animal.

However, before an animal can assimilate the results of its behaviour there must first be a situation which calls forth a response. Each behavioural pattern has some sort of primary stimulus which elicits behaviour in the absence of any previous experience. In other words there must be some form of communication between the animal and its environment[2,3].

1.3 Communication

There is considerable disagreement on the precise definition of the term communication. The widely used and accepted definition with regard to animals is the following, as formulated by Wilson: Communication occurs when the action of, or cue given by, one organism is perceived by and alters the probability pattern of behaviour in another organism in a fashion adaptive to either one or both of the participants[4].

Animals communicate for a variety of fundamental reasons associated with their need for food, reproduction, territorial marking, alarm and social regulation and recognition. The necessity for interspecific communication is obvious for animals, such as honey-bees, rabbits, and man that live in complex societies. At the other end of the scale of complexity, the need for

communication is less obvious but nevertheless essential for animals that appear to live alone. For example, prior to mating in bisexual species, communication must be used to bring the two sexes - or at least their gametes - together[5].

The degree to which animals use communication systems in their daily lives is directly related to the level of development of their sensory-nervous systems. Animals such as jelly fish, that have a simple nervous system, have few channels for communication, and hence communicate little in general. On the other hand, animals such as insects and vertebrates that have well-developed senses and highly developed nervous systems, use a multitude of signals for a wide variety of purposes[6].

In the course of communication a variety of stimulus modalities and associated sense organs may be used by the communicating animals, the major ones being chemical, visual and acoustic. Many animals use more than one sensory channel, and some of the higher animals can use all the channels in the course of their communication[7].

1.3.1 Visual communication

The signals for visual communication are used in varying degrees by most vertebrates. In some fish, lizards, many birds, and the primates, vision is probably the most important sensory modality for communication[8]. One interesting difference between most vertebrate eyes and the bird eye is that the vertebrate lens filters out wavelengths of light below 400 nm which renders ultraviolet radiation invisible. However, the bird lens is optically clear and appears to transmit wavelengths of light down to about 350 nm, which makes near ultraviolet radiation visible to the bird, filtering out only those ultraviolet wavelengths that are dangerous to the bird. It is suspected that birds may secrete a substance from the uropygial (preen) gland that is spread on the feathers and that is visible in the ultraviolet range. It is thought that this may be one way in which a bird may visually discern the sex of other birds, namely through the differences in the ultraviolet colour of the feathers[9,10].

Birds are highly visual and have evolved a vast diversity of patterns of coloured feathers and body appendages that can be incorporated into complex displays used in communication, e.g. male peacocks have evolved brilliant tail plumage, which they display to the females during courtship. These elaborate tail feathers are folded away when the bird is not displaying[11].

Among invertebrates only certain arthropods use visual communication to an equivalent degree. The most specialised form of optical signals in insects is the flashes produced by luminous organisms such as fire-flies. These signals are produced by special photophoric organs, which utilize complex chemical reactions to produce almost cold light as a means of communication[12,13].

1.3.2 Acoustic communication

Many animal sounds, apart from being used as alert signals, are subject to cyclic variation with different phases of the breeding cycle and are intimately associated with the complex nature of reproductive activities. Within this complexity several different functions may be served. Male crickets, for example, have been known to produce different sounds for establishing initial contact and courtship with the female, courtship interruption and the repelling of males[14].

The vocal repertoire of birds is as rich and varied as any to be found in the animal kingdom. These signals are often most structured, discrete and continuous. The song of birds, usually though not always the prerogative of males, tends to be associated with territorial defence, establishment and maintenance of pair bonds, control of reproductive cycle of male and female, or combinations of these[15]. In certain birds it is of prime importance, as demonstrated by Schleidt[16]: The female was surgically deafened, laid and sat on her eggs normally, but after the young hatched, she did not seem to be able to distinguish them from predators and killed them as she would predators that approached the nest.

1.3.3 Chemical (olfactory or gustatory) communication

The most widely used channels for communication in the animal kingdom are the chemical senses. In man, two chemical senses are used, namely smell and taste. In many other animals, however, it is difficult to separate these two accurately. Generally the sense of smell, or the "distance chemical sense", is most important in communication[17].

The one great advantage of chemical signals is their capacity, exploited for social integration especially by terrestrial mammals, to serve as vehicles for future communication. Unlike acoustic and many visual stimuli, chemical stimuli persist after emission for varying lengths of time, and their potential durability makes possible their transmission over great distances. They can be left behind as a continuous signal after the animal has departed and serve as a source of continuous communication into the future. Chemical secretions are commonly used as territorial and trail markers as well as for marking individual nests[18,19].

Until recently birds were considered to have a poorly developed sense of smell. It was found that ducks whose uropygial glands had been surgically excised were badly treated by their congeners[20]. This result, together with the observation of the ability of young goslings to react to a heated metal block impregnated with the uropygial secretion of their mother[21], leads to the conclusion that the uropygial gland plays a role in olfactory communication. In opposition to the previous notion that birds have a poorly developed sense of smell, it is now well-established that many avian species have a very well-developed sense of smell[22].

1.4 Semiochemicals

Semiochemicals are volatile chemical substances that bring about behavioural changes when perceived by living organisms. These odourants must posses certain molecular properties in order to provide sensory stimulation. An odourant must have some water solubility, sufficiently high vapour pressure, high lipophilicity and surface activity. Most odourants possess

molecular weights between 80 and 300 amu[23].

Unlike visual or acoustic signals which travel very fast from the point of origin to the receiver, odourants (chemical signals) travel relatively slowly in still air according to Graham's law of diffusion:

$$U(r,t) = \frac{Q}{2D\pi r} f\left[\frac{r}{\sqrt{4Dt}}\right]$$

where $U(r,t)$ is the concentration of odourant in molecules/cm^3 air, r is the distance (cm) from the source of the odour to the receiver, t is the time (sec) from the start of emission, Q is the rate of emission of the odourant (molecules/sec), D is the coefficient of diffusion of the odourant molecules in air (cm^3/sec) and f is a complex correction function for error. This law is important since it enables the estimation of K, the threshold concentration, which is the value of $U(r,t)$ at which behavioural or physiological response in the animals can be detected and recorded. Below this value a sensation or stimulus can not be evoked[24,25].

The minimum stimulus required to evoke a sensation varies with type of odourant and animal species. Some substances, like mercaptans, can be detected by mammals in the air at a very high dilution as can be seen from Table 1.1.

The term *semiochemical*, which is derived from the Greek word "semeion" meaning a signal or sign, refers to all chemicals that mediate, through taste and smell, the interactions between organisms[26].

On the basis of their functional role, semiochemicals can act between individuals of the same species (intraspecific) or between individuals of different species (interspecific) for which the terms *pheromones* and *allelochemicals* are used respectively[27].

Table 1.1: Threshold concentrations (molecules/cm^3 air) of various odourants for canines and humans[28].

Odourants	Dog	Man
acetic acid	5×10^5	5×10^{13}
propanoic acid	2.5×10^5	4.2×10^{11}
butanoic acid	9.0×10^3	7.0×10^9
valeric acid	3.5×10^4	6.0×10^{10}
caproic acid	4.0×10^4	2.0×10^{11}
capryloic acid	4.5×10^4	2.0×10^{11}
ethyl mercaptan	2.0×10^5	4.0×10^8
α-ionone	1.0×10^5	3.0×10^8

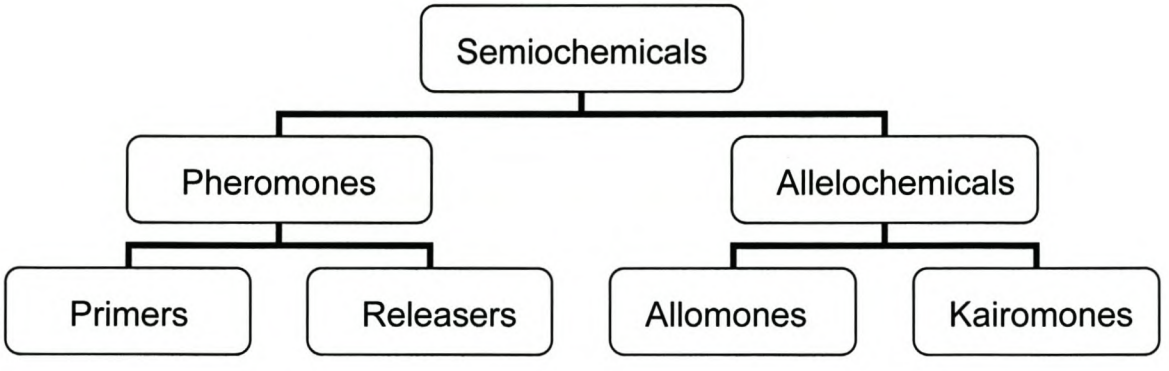

Fig. 1.1: Classification of types of chemical signals

1.4.1 Pheromones

Pheromones are one channel for biological communication. The term pheromone, first proposed and defined by Karlson and Lischer in 1959, refers to a group of biologically active substances resembling hormones in some respects, yet which can not be included among them as they evidently do not come from endocrine glands[29]. The presently widely accepted definition of pheromones is "substances which are secreted to the outside by an individual and received by a second individual of the same species in which they release a specific reaction, for example a definite behavioural or developmental change". The word pheromone is derived from the Greek word "pherein", meaning to carry or transfer and "horman" to excite or stimulate. Pheromones are active substances which invoke behavioural response as a single compound or as a mixture of compounds, often in extremely low concentrations.

Each pheromone is used in a particular context, for example, to indicate or influence reproductive states, to proclaim social status, to mark territory, and to label self and kin[30]. Based on the type of behavioural changes they induce, Wilson in 1963 classified pheromones as *releasers* and *primers*[31]. Those pheromones which act directly on the central nervous system to evoke an immediate and reversible change of behaviour in the receiver are termed as releasers; for example female sex pheromones attracting male insects or alarm messages in fish. Primers on the other hand trigger permanent physiological changes in the receiver. There may be no immediate change in behaviour, but the organism develops new response potentials which can be evoked by new stimuli, such as stimulation of sexual maturation in insects and mammals or controlling caste differentiation in insects.

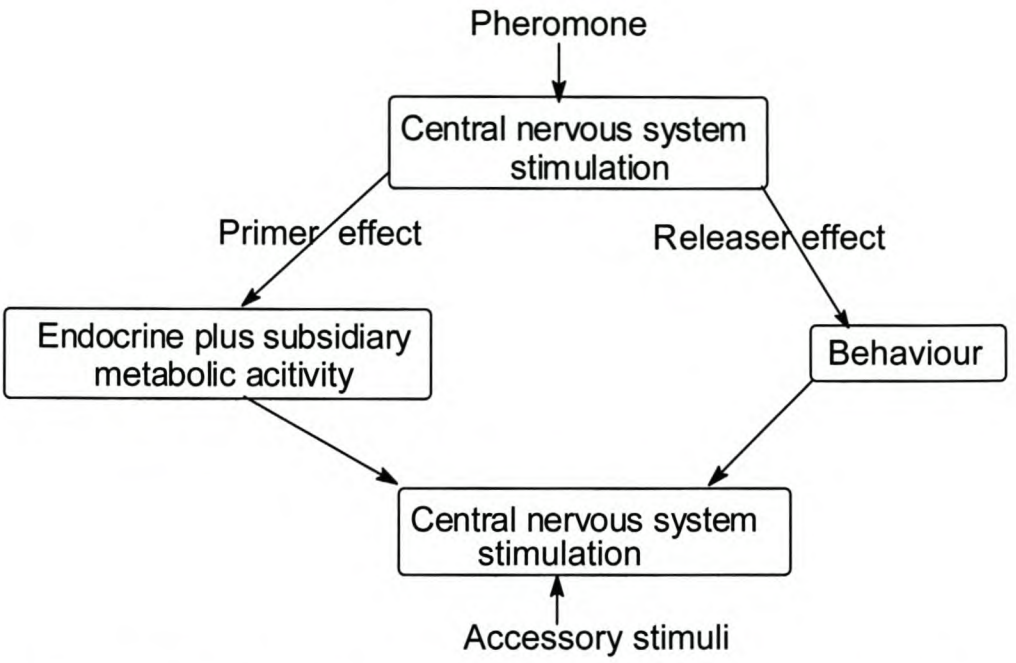

Fig 1.2: Effect of releaser and primer pheromones on behaviour

Sometimes a single substance can have both releaser and primer effects. For example, 9-keto-2-decenoic acid which is produced by the honey-bee queen is used both as a releaser and primer pheromone for such purposes as attracting a retinue of workers around her, attracting drones on mating flights, preventing workers from reproducing at the individual (worker egg-laying) and colony (swarming) level, and regulating several other aspects of colony functions[32,33].

1.4.2 Allelochemicals

Those chemical interactions which affect the growth, health, and behaviour or population biology of individuals of other species have been termed allelochemicals. Allelochemicals are further subdivided into several groups depending on whether the response is to the advantage of receiver, the sender or of mutual benefit[34].

Allomones are allelochemicals that confer adaptive advantages to the producer (sender), such as repellent secretions or venoms which protect a predator from its prey. *Kairomones* give the adaptive advantage to the receiving organism and include food attraction stimuli or secretion from a prey species

that attracts a predator.

Within species allelochemical interactions can be autotoxins, auto-inhibitors or pheromones. Autotoxins are repellents or wastes that are toxic or inhibitory to individuals of the releasing population with or without selective advantage through detriment to some other species. Adaptive auto-inhibitors on the other hand limit the population to numbers that do not destroy the host or produce excessive crowding, e.g. staling substance in algae.

1.5 Olfactory system in Vertebrates

Mammals: The olfactory system in mammals is organized a bit differently than most other vertebrate sensory systems. Unlike the optical and acoustic receptors that are surrounded by a complex system in the reception and interpretation processes, olfactory receptor cilia lie bare in a small patch of mucus secreting membranes (the olfactory membranes) in the upper part of the nasal cavity. These receptors extend their axons into the olfactory bulb, a projection of the brain that in most primates lies over the nasal cavity and in other vertebrate lies posterior to the nose, in the anterior region of the brain. Axons from the olfactory bulb enter the brain *via* the olfactory tract (cranial nerve I) and project to the primary olfactory cortex, also called pyriform cortex (Fig 1.3).

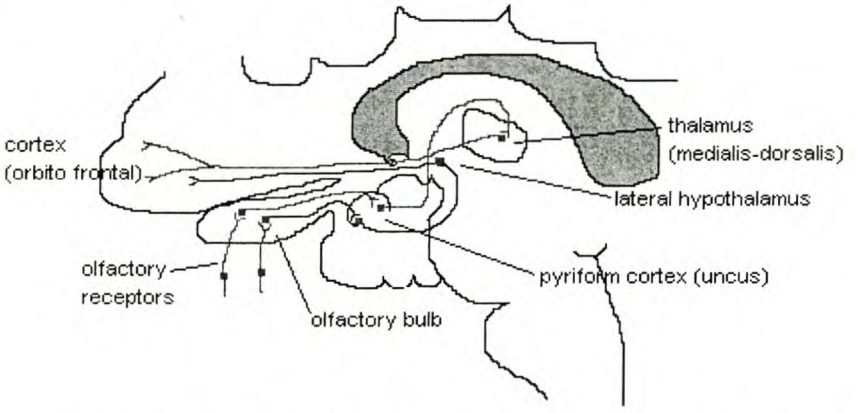

Fig 1.3: Anatomy of the sense organ (sense of smell) of mammals[35].

Together with the axons from the olfactory tract that bypass the pyriform cortex, axons from the pyriform cortex project to the entarhimal cortex. Both

pyriform and entarhimal axons are projected to the limbic system, the part of the brain most intimately associated with neuroendocrine regulation and emotion, food gathering, and sexual behaviour. Other axons extend to the orbitofrontal cortex where primary discrimination of odours (and in primates, conscious recognition) takes place[36].

Birds: The avian olfactory system differs slightly from that of mammals. In birds two typical nasal ducts, separated by a thin bony partition, originate at the external nostrils, run across the palate of upper beak and end as two large openings (choanae) which connect the tubes with the mouth cavity. Each of these tubes swells, in anteroposterior sequence, into three chambers. In each of these chambers the walls form either a fold or a spiral scroll (cochae) which increases the surface over which inhaled air must pass. Out of these three chambers only the one, called the turbinates of the olfactory chamber (posteriosuperior chamber) has olfactory receptors in its lining epithelium which are slender, columnar, each with one or more olfactory hairs extending to the surface of the nasal epithelium. Impulses from these cells are carried to the brain by the olfactory cranial nerve I. The vomeronasal (Jacobsen's) organ is absent in birds which led to the misconception that birds have a poorly developed sense of smell[37,38].

The anatomy of the olfactory bulb in vertebrates suggests that interactions among higher-order neurons are as important for stimulus characterization as are neural influences from the periphery. For an odourant to be detected, molecules of the substance must diffuse to the region of the olfactory mucosa layer. This layer which is produced by Bowman's glands of the olfactory epithelium, is a lipid-rich secretion that coats the surface of the receptors at the epithelium surface[39]. Once there, the odourant molecules first dissolve in the layer and then bind to receptor sites. Odourant-binding proteins in the mucus covering the receptors interact with the odourant molecules, transport them to the receptors, and facilitate the binding of odourants to specific receptors on the olfactory neurons for final interpretation[40, 41].

1.6 Odour producing organs in vertebrates

The odours used by animals to demarcate their own space or to communicate with other animals may come from different sources such as urine, faeces, saliva and most importantly, from special odour producing skin glands, the secretions from which may increase the communication power of faeces and saliva[42,43].

1.6.1 The integument

The skin of mammals contains a striking variety of external appendages and numerous different glands. The familiar odour-producing glands found in vertebrates are the sebaceous and the sweat glands.

1.6.1.1 Sebaceous glands secrete fats and oily substances which have an odorant property that keeps the skin supple. Most of these glands swell into the hair canals and are so intimately associated with hair follicles that they are part of the pilocebaceous units[44].

1.6.1.2 Sweat glands are numerous in the skin of vertebrates, but in no other animals are they as numerous as in the primates and particularly in man. Two types of sweat glands exist: the large, apocrine glands, which secrete a milky fluid, and smaller eccrine glands, which secrete watery sweat. The sweat glands in most vertebrates are apocrine, whereas those in man are eccrine glands which are restricted to the axillae, the outer ear canal, the nipple of breasts, the external genitalia, and around the orifice of the anus. The friction areas in the body of mammals are, in general, very rich fields of eccrine glands[45,46].

1.6.2 Urine

The pheromonal function of urine has been described for many species. Such urinary odours mainly originate from accessory sexual organs such as the preputial glands which are small paired glands lined between the pubic skin and the body wall. These introduce their secretions into the urine *via* a duct that opens near the urethra orifice. Urinary odours may also arise by mixing urine

with secretions from the accessory sexual organs such as coagulating glands. They may also be present in bladder urine[47,48].

1.6.3 Vaginal secretions

Secretions from the vaginal layers are notable for their pheromonal properties in many species. The production of these secretions seems to depend upon the bacteria of the vagina, and the ovarian hormones which exert their influence on odour production in the animal by determining the availability of nutrients for the bacteria[49].

1.6.4 Accessory glands of the eye

The Harderian gland is a tubulo-alveolar gland, with alveoli composed of cells which contain lipid droplets[50]. There are two types of alveolar cells, Type I and Type II: both are columnar but Type I is smaller with few lipid droplets while Type II cells contain many lipid droplets. The lumen of these alveoli may contain porphyrins[51].

It has been shown that the Harderian gland in the gerbil produces a pheromone[52]. In the rat androsta-4,16-dien-3-one, the precursor of androstenol and anderestenone produced by the boar submandibular gland, accumulates in both Harderian and extraorbital luctrial glands and it has been suggested that these glands may therefore be pheromone producing organs[53].

1.6.5 Salivary glands

These glands develop from the ectoderm of the oral mucosa. They have a complex branching duct system which terminates in secretory cells called secretory acini[54]. Pigs and primates are notable for the production of odoriferous secretion by the salivary glands. In boars it has been shown that androstenol (3α-hydroxy-5α-androst-16-ene) and androstenone (5α-androst-16-ene-3-one), which elicit the immobilization response in oestrous gilts, are produced by the submandibular salivary glands[55].

Some animals are known to develop other odour secreting glands during

the breeding season. One of the typical examples of this phenomenon is found in the *salaria pavo*. During the breeding season, *Salaria pavo* males develop an androgen-dependent anal gland (AG) from the first two rays of the anal fin, which has been hypothesised to be a source of substances that attract sexually active females to nesting sites. The results of an investigation of the secretion of this gland suggest that a putative pheromone from the AG promotes female attraction and influences female mate choice, thereby affecting male reproductive success[56].

1.6.6 The uropygial gland

This gland is found only in birds. Although most birds have this gland, the odorous nature of this gland is restricted to a few species. The uropygial gland (also known as the oil gland or preen gland) is a bilobed sebaceous gland found in birds and lies between the dorsal skin and the muscles at the base of the tail. Each lobe of the gland is composed of numerous acinar tubules arranged radially around a central cavity, which collects the secretion from the tubules. Ducts convey the secretion caudally to the surface where they open, in some birds at the tip of a papilla. The total number of orifices varies among birds from one in the Hoopoe (*upupa epops*) to eighteen in a pelican (*pelecanus sp.*). The skin over the gland may be bare or feathered, but the papilla is usually bare except at the tip, where there is commonly a tuft of down feathers, the uropygial wick. In all cases, the location of the gland is concealed by the body feathers except when a bird exposes it in preening. The gland is enclosed in a capsule of connective tissue and is sometimes embedded in fat. It receives its blood supply from branches of the caudal artery, and is drained by branches to the caudal vein. The gland is innervated by the first pair of caudo-spinal nerves and by sympathetic fibres. Stimulation of the sympathetic fibres is thought to cause dilation of the sphincter muscles around the external openings of the ducts.

The secretory alveoli are supplied with oil formed from modified epidermal cells that do not become keratinised. Each epidermal cell has a

prominent golgi apparatus (generally associated with the lopogenesis) and as it matures the cells become filled with droplets. Finally the lipids coalesce to form a globule and cytolysis causes the cell to dissolve completely and release its product to the duct. The act of preening causes a nervous reflex which stimulates the secretion to flow onto a nipple of feathers. When massaged, a small amount of greasy secretion exudes from the tip of the gland. It is held on the tip of the gland by the tuft of feathers. The bird wipes its beak on the papilla and spreads the resulting secretion over its body.

The uropygial gland is present in most avian species, and is relatively large in some aquatic species. The shape of this gland varies between species and families of birds and has been used as a taxonomic marker. The gland is absent in certain species, including the ostrich, emu, cassowary, many pigeons, bustard, frogmouth, many woodpeckers and certain species of psittacines (hyacinth macaw, *Anodorhynchus hacinthinus*, Lear's macaw, *Anodorhynchus leavi*). The gland is however present in other psittacine species and in canaries and most finches. None of the parrots of the genus *Amazona* possess an uropygial gland[57].

1.7 Composition of the uropygial gland secretion

1.7.1 Wax esters

Sebaceous-gland lipids generally have unusual compositions and differ in structure from all other body lipids (e.g. depot fat) in most animals. This is particularly true for birds, and thus the uropygial gland is a unique source of unusual lipids, especially monoester waxes. Moreover, the qualitative composition of lipids varies at the ordinal and in some cases at the familial level[58]. The chemical composition of preen gland waxes is very complex and varies significantly between taxa. Preen gland secretions consist predominantly of wax esters, which are composed of fatty acids esterified to an alcohol moiety. Usually a mixture of fatty acids and alcohols or diols with varying chain lengths and degree and location of branching is involved, resulting in a complex mixture

composed of hundreds of individual wax esters[59].

What is most intriguing about the waxes from the uropygial gland is their seasonal variation. It was found that adult female mallards secrete three different types of compositions, presumably representing three physiological states[60]. Most of the year the secretion contained wax esters containing short chain acids. During the breeding season these monoester waxes were replaced by diesters of 3-hydroxy fatty acids. After the breeding season, the females went into eclipse similar to that found in males generating monoesters of long chain fatty acids[61]. When eclipse was over, the shorter chain esters returned as the major products.

A similar shift in preen wax composition from the lower molecular weight monoesters to higher molecular weight diesters was also observed in individuals of the Sand Piper species which were about to leave for tundra breeding[62]. The timing of the shift indicated that diester waxes serve as a quality signal during mating choice. Both sexes produced the diester waxes during the incubation period until hatching, in addition to the short period of courtship, indicating that functions of the diesters extend beyond that of a sexually related make-up. The lowest likelihood of secreting diesters in non-incubating birds indicated a functional role for diester preen waxes during incubation. This finding led to the conclusion that diester preen waxes enhance olfactory crypticism at the nest.

1.7.1.1 Monoester waxes: Esters of aliphatic alcohols and fatty acids are the predominant type of lipid occurring in the uropygial gland secretions. Both the acids and the alcohols can be even- or odd-numbered, normal or branched. Though methyl-substituted acids predominate, other alkyl-substituted acids (e.g., ethyl-, propyl- or butyl-) have been identified in birds. Moreover, the degree of substitution (mono-, di-, tri...,) and the position of the substitution (C2, C3, C4…,) may vary. It must, however be mentioned that all acids and alcohols hitherto investigated are saturated, except in Apterygiformes. Unsaturated lipids tend to be oxidized by atmospheric oxygen, and this would lead to resination during impregnation of plumage. Hence unsaturated constituents would be

disadvantageous for the bird, which perhaps explains their absence in uropygial gland secretions. The structural variability of these constituents, which can be combined randomly, leads to a multiplied variability of the waxes[63].

1.7.1.2 Diester waxes: Although restricted to a few orders, a number of diester waxes have been reported to exist in the uropygial gland: Diester waxes containing 2-hydroxy acids esterified with *n*-alkanols and unbranched fatty acids[64]; diester waxes containing 3-hydroxy acids esterified with *n*-alkanols and unbranched fatty acids[65]; diester waxes containing alkane-1,2-diols that are esterified with unbranched fatty acids[66]; diester waxes containing *erythro*-alkane-2,3-diols that are esterified with unbranched fatty acids[67] and the same diesters but with *threo*-alkane-2,3-diols[68].

1.7.1.3 Triester waxes: Triester waxes composed of alkyl hydroxymalonic acids, *n*-alkanols, and unbranched fatty acids are common in uropygial gland secretions and distributed in various orders[69].

1.7.2 Glycerides

Triglycerides have been detected in almost all uropygial secretions, but in most cases they must be considered as regular products of cell decomposition and not as true secretion constituents. Only some ciconiiform species produce triglycerides as a main constituent of the secretion of the uropygial gland (e.g. *Ardea cinerea*). Mono- and diglycerides have not been found to occur in preen secretions, but together with free fatty acids that have been detected in the plumage lipids from *Leptoptilos crumeniferus*. These have been suggested to originate from triglycerides by microbial liposysis[70].

1.7.3 Sterols

Cholesterol seems to occur in minor amounts in the preen gland of some birds. Sterols have, however, been found to be major constituents of the secretion, e.g. cholestannol in *Anas platyrhynchos*[71].

1.7.4 Hydrocarbons

Squalene has been shown to occur as a major constituent in the preen secretions of some birds[72]. In some species, unbranched, monomethyl- and dimethyl-substituted saturated alkanes, as well as unsubstituted alkenes and alkadienes, have been observed.

1.7.5 Other compound types

Beside waxes, the uropygial gland of birds is also known to contain non-lipid compounds. Several proteins, inorganic substances containing K, Na, Ca, Mg, and Cl, polysaccharides, ascorbic acid, alkaline phosphatase and acid phosphatase have been detected in the secretion. Iron is also found in the secretion of some birds. Apart from the seasonal variation, the composition of the uropygial gland is also found to depend on the type of diet. In geese and ducks a variation in the composition of the secretion, specially in the number of branched and straight chain acids, was observed when the birds were fed a diet containing corn oil or a fat-free diet[73].

1.8 Functions of the uropygial gland

Chemicals produced by the uropygial gland of birds have been the subject of intensive investigations. It is generally accepted that the preen wax, mainly composed of monoesters of fatty acids and alcohols, protects the plumage against wet. However, some additional functions can be assumed from the very complex structure of the lipids, which are known to be highly species-dependent. The uniqueness of this waxy material manifests itself in the number and kind of carbon skeletal types, in the wide range of chain lengths, and in the unusual patterns of substitution. Although much has still to be explained, from these variations a new taxonomy of birds has evolved. By studying the structure of relevant components, one may gain clues to the understanding of the functions of these externally secreted lipids[74].

The following are some of the functions of the uropygial gland.

1.8.1. As water-proofing agent

The secretion of the uropygial gland is well known for its role as a protection against moisture. It keeps feathers, the rhamphotheca, and the podetheca from drying, thereby helping to keep them supple and in good condition. The lipids in the secretion are hydrophobic and are a necessary supplement to the meshwork of the barbs in making feathers water repellent. This is achieved by making the feather keratin flexible. Removal of the gland in some birds showed a significant degradation of plumage[75,76].

1.8.2. As a supplement of vitamin D

The secretion from the uropygial gland contains the precursor for vitamin D (ergosterol) that is spread over the feathers during preening. With exposure to sunlight during preening these precursor secretions are converted to an active form of vitamin D by UV radiation which is then ingested while the bird preens itself. This vitamin is known to protect the bird against rickets. Removal of this gland caused young domestic chicks and ducks to show symptoms of rickets in spite of normal diet and exposure to sunlight[77]. This gland was also known to have an effect on the rate of growth of birds. This effect on the rate of growth differs amoung bird species. In some ducks a decrease in the rate of growth was observed, in other birds (e.g. fowl) removal of the gland enhanced the growth rate[78].

1.8.3. As antibacterial and antifungal agents

The preen secretion covers a broad spectrum of plumage hygiene. It has been shown that fatty acids and feather waxes can be inhibitory to dermatophyte, saprophytic keratinophilic, as well as non-keratinophilic fungi[79]. On the other hand, feather lipids may stimulate certain fungi[80], for example *Arthroderma currey,* and thus serve as a suitable diet for non-pathogenic dermatophytes, which could possibly avoid an overcrowding by pathogenic ones. In this manner the secretion from the uropygial gland may be considered to regulate the microflora of the plumage.

Besides the effect of chemical hygiene, the preen waxes possess advantages as cleaning material for lipoidal residues in the plumage.

1.8.4. As a means of defence and individual recognition

The secretion of the uropygial gland is odourous in some birds like Musk ducks and the Hoopoes. In Hoopoe it is used as a defence when the bird is threatened by predators. When in danger the bird rubs its uropygial gland to exude its secretion which deters predators from attacking[81]. Recent research shows that the bird's eye is sensitive to light in the ultraviolet range. The secretion from the uropygial gland may also play a role in the identification of the sex of a bird, and may be involved with individual identification of birds as well[82]. Although a detailed study is needed, there is reason to assume that the secretion from the uropygial gland plays a role as protection from UV light and as a pheromone.

1.9 The Scimitar-billed woodhoopoe

The Scimitar-billed woodhoopoe, *Rhinopomastus cyanomelas*, is one of the eight existing woodhoopoe (Phoeniculinae) families. These woodhoopoes are found only in forested Africa south of the Sahara and are confined specifically to southern Africa and east Africa. In South Africa they are absent from the extreme south and most of the Highveld. The Scimitar-billed woodhoopoe prefers open acacia to dense forest, and their distribution reflects this predilection. They frequent open and cultivated lands with some trees. The male bird has black plumage with a metallic blue sheen and tinged violet on the back, while being green on the underparts. Although of similar general appearance, the female is slightly smaller and duller in colour than the male. Her face and underparts are dark brown, without metallic sheen and her bill is more slender. Woodhoopoes have long, sharp clawed toes, ideally suited to climbing trees where, they pick insects from the bark, often in an upside position.

These birds are usually solitary or in pairs, but are sometimes seen in

small family groups.

Fig. 1.4: The Scimitar-billed woodhoopoe (*Rhinopomastus cyanomelas*)

Woodhoopoes forage mainly in outer branches of trees and less often also on the bark of trunks (like Red-billed woodhoopoes). Occasionally they hawk insects on the ground. Scimitar-billed woodhoopoes are agile and restless and often hang upside down while probing with their bills. They probe with the lower jaw only and with the bill open. Their favourite foods include insects, specially larvae, spiders, cockroaches, etc., and also seeds, buds and nectar. While feeding they are silent. They seem to have little need of water, for apparently they never drink. After feeding in tree tops they glide to lower parts of the next tree. Their flight is graceful and buoyant. At night Scimitar-bills roost on the bark of tree trunks, or in groups of up to four birds in a hole in a tree trunk.

The breeding season for Scimitar-billed woodhoopoes extends from August to December with a marked peak in September to October. Like Hoopoes, woodhoopoes nest in holes and have little use for nest lining. Some hoopoes line the hole with bits of straw or feathers, but usually they use no nesting material. A favourite nesting site is a tree cavity, but crevices in walls and building also serve as nests. The same nest site may be used in successive years.

The female merely makes a slight hollow for the eggs, which are greenish blue with fine white pores and when freshly laid have a translucent appearance. However, within a few days, the eggs become nest-stained with brownish marks and by the end of the incubation period the original colour fades considerably. A clutch size on average is between two and four. A striking feature of these birds is the consistency of the egg size within clutches, especially in width. This contrasts markedly with the Red-billed hoopoes where egg size within a clutch may vary considerably.

Once incubation begins the female rarely leaves the nest. The female bird, known to be a particularly tenacious sitter, incubates the eggs alone for 15-17 days during which time the male feeds her assiduously. When the eggs hatch the shells are not removed and eventually disintegrate in the nest. Initially the female and chicks are fed by the male and she rarely leaves the nest. Only

after the fourth day does she emerge to assist the male with feeding the chicks, although she still continues to brood them on a regular basis. The male doesn't feed the nestlings directly and never enters inside the nest. He simply passes the food to the mother at the entrance for relaying to the chicks.

The nestling period ranges on average from 21-24 days after which the male calls repeatedly to the last remaining nestling and will not feed it until it leaves the nest. This behaviour suggests that the male is deliberately enticing it to fly. Once the young leave the vicinity of the nest soon after fledging they do not return to roost in it. The nestlings usually remain with their parents for a few weeks. However, family groups have been reported to remain together for up to six months.

Scimitar-billed woodhoopoes are notorious for their foul, smelly nests, from which they never remove droppings or food debris. In addition, the female has a strongly repulsive musty smell that emanates from her preen gland, and is believed to have a protective function like attar of the skunk[83-86].

Hoopoes are pictured on the walls of ancient tombs and temples in Egypt and Crete. Medieval writers mention them in connection with magic and the supernatural. Soothsayers recommended using various Hoopoe organs in concoctions to stimulate vision or aid the memory. The species appears in the Old Testament list of foods proscribed by the sanitary law, incorrectly translated from the Hebrew in the Authorised Version as "lapwing." Their filthy nesting habits were doubtless responsible for their place on the ancient Hebrews' proscribed list, yet other peoples eat them readily, and some even consider them a delicacy[87].

Table.1.2: The calls of Scimitar-billed woodhoopoes' and their context

Call	Context
1. Plaintive, ventriloquial *wheep-wheep-wheep*	May be given by the male only; when used in flight 3-4 m above tree-tops this call serves the purpose of territorial advertisement
2. Rapidly repeated *kwi-kwi-kwi*	Appears to maintain contact between the pair when separated in wood land; used by male to alert female on approaching the nest with food; may sometimes be interspersed with call (3) in situations of excitement
3. Harsh chattering *ker-ker-ker…*	Used at high intensity in a situation of excitement or alarm; e.g. by male to attract the female to the nest or when species such as barbets attempt to inspect an occupied nest
4. Soft, squeaky high-pitched *sweee-sweee-sweee*	Used mainly as a begging call by the female in the nest, but also by small chicks in the nest and also after leaving the nest

1.10 Objective of this Study

When disturbed while roosting, woodhoopoes immediately face away from the threat hence presenting their uropygial glands in the direction of the threat. Typically, a drop of brown, highly pungent secretion is then formed at the tip of the papilla to the uropygial gland, and kept in place by a few tuft-like feathers. This response pattern has led some observers to believe that the secretion serves an anti-predatory role. Previous studies on the uropygial secretion of the Green woodhoopoe, *P. purpureus*, showed that the secretion contains very volatile, low molecular weight compounds with obnoxious odour. It has been found that these synthetic volatile constituents, individually or as a mixture, have potent defensive properties against feline and reptilian predators. In addition, the compounds also showed activity against a range of bacteria.

The aim of the present study was the chemical characterisation of the uropygial secretion of the Scimitar-billed woodhoopoe, *Rhinopomastus cyanomelas*, as a first step towards the evaluation of, *inter alia*, the semiochemical function of the secretion, by determining whether in fact compounds with similar repellant and antibiotic activity existed in the secretion.

The chemical composition of the scretion was compared with the secretion of *P. purpureus* as well as with that of the African hoopoe, *Upupa africana,* which, in contrast to the uropygial secretions of the Green and the Scimitar-billed woodhoopoes, does not have a strongly obnoxious odour and also does not contain large quantities of alkanes and wax esters.

References: Chapter 1

1. J.L. Cloudsley-Thompson, "Animal Behaviour", Oliver and Boyd, Edinburgh, (1960), p. 5
2. E.S.E. Hafez, "The Behaviour of Domestic Animals", Bailliere, Tindall and Cassell, London, (1969), pp. 3-4
3. V.G. Dethier and E. Stellar, "Animal Behavior: Its Evolutionary and Neurological Basis", Prentice-Hall, Englewood Cliffs, (1961), pp. 1-2
4. E.O. Wilson, "Sociobiology: The New Synthesis", The Belknap Press of Harvard University Press, Cambridge, (1975), p. 176
5. H.H. Shorey, "Animal Communication by Pheromones", Academic Press, New York, (1976), p. 1
6. Hubert and M. Frings, "Animal Communication", Blaisdell, Waltham, (1964), p. 5
7. T.A. Sebeok, Science, **147**, 1006 (1965)
8. P. Marler and W.J. Hamilton III, "Mechanisms of Animal Behavior", John Wiley, New York, (1966), pp. 322-23
9. A.S. King and J. McLelland, "Birds, Their Structure and Function", Bailliere Tindall, London, (1984) pp. 28, 29 (as sited in *http://www.exoticpetvet.net/avian/uropygial.html*, 14 Nov 2003)
10. J.E. Cooper, G.J. Harrison. Dermatology. In: B.W. Ritchie, G.J. Harrison, L.R Harrison (eds) "Avian Medicine: principles and application", Lake Worth, F.L. Wingers, (1994), pp. 613-61 (as sited in *http://www.exoticpetvet.net/avian/uropygial.html*, 14 Nov 2003)
11. W.K. Purves, G.H. Orians, and H.C. Heller, "Life: The Science of Biology", Sinaver, Massachusetts, (1995), pp. 1040-1041

12. J.E. Lloyd, Ann. Rev. Entomol., **16**, 97 (1971)

13. Reference 6, p. 15

14. R.D. Alexander, Evolution, **16**, 443 (1962)

15. Reference 8, pp. 442-443

16. M. Schleidt and M. Magg, Behaviour, **16**, 254 (1960) (as cited in T.A. Sebeok "Animal Communication: Techniques of Study and Results of Research", Indiana University Press, Bloomington, (1968), p. 128

17. Reference 6, p. 12

18. T.A. Sebeok, "Perspectives in Zoosemiotics", Mouton, The Hague, (1972), p. 90

19. K. Ralls, Science, **171**, 443, (1971)

20. P. Paris, Arch. Zool. Exp. Gen. **53**, 139 (1913) (cited in Reference 58, p. 307)

21 I. Wurdinger, Proc. Cong. Int. Ornithol.,17th, (1978), 1415 (as cited in Reference 58, p. 307)

22. B. Wenzel, "Handbook of Sensory Physiology, Vol. 4", Springer-Verlag, Berlin, (1971), p. 432 (as cited in Reference 59, p. 307)

23. J.H. Law and F.E. Regnier, Ann. Rev. Biochem., **40**, 533 (1971)

24. A.J. Macleod, "Chemistry of Odours", Symp. Zool. Soc. Lond., **45**, 16 (1980)

25. W.H. Bossert and E.O. Willson, J. Theoret. Biol., **5**, 443 (1963)

26. B.A. Sommerville and D.M. Broom, Appl. Anim. Behavior Science, **57**, 269 (1998)

27. F.E. Regnier, Biol. Reprod., **4**, 309 (1971)

28. D.M. Stoddart, "Mammalian Odours and Pheromones", Edward Arnold,

London, (1976), p. 9

29. M.C. Birch, "Pheromones", North-Holland, Amsterdam (1974), p. 1
30. P. Karlson and A. Butenandt, Ann. Rev. Entomol., **4**, 39 (1959)
31. E.O. Wilson, Sci. Amer., **208**, 100 (1963)
32. C.G. Butler, Symp. Roy, Entomol. Soc. London, **2**, 66 (1964) (as cited in Reference 18)
33. C.I. Keeling, K.N. Slessor, H.A. Higo and M.L. Winston, Proc. of the National Academy of Sciences of the United States of America, **100**, 4486 (2003)
34. R.H. Whittaker and P.P. Feeny, Science, **171**, 757 (1971)
35. *http://www.cf.ac.uk/biosi/staff/jacob/teaching/sensory/olfact1.html*
36. F. Delcomyn, "Foundations of Neurobiology", W.H. Freeman, New York, (1998), pp. 311-312
37. P.D. Sturkie, "Avian Physiology", Springer-Verlag, New York, (1976), p. 43
38. A.J. Marshal, "Biology and Comparative Physiology of Birds (II)", Academic Press, New York, (1961), pp. 42-45
39. Ya.A. Vinnikov, "Sensory Reception: Cytology, Molecular Mechanisms and Evolution", Chapman and Hall, London, (1974), pp. 181-193
40. A.J. Vander, J.H. Sherman, and D.S. Luciano, "Human Physiology: The Mechanisms of Body Function", McGraw-Hill, New York, (1994), p. 267
41. G. Ohloff and A.F. Thomas, "Gustation and Olfaction", Academic Press, London, (1971), pp. 239-240
42. Reference 27
43. D.M. Stoddart, Nature, **246**, 501 (1973)

44. Reference 26, p. 12

45. D.M. Stoddart, "Olfaction in Mammals", Academic Press, London, (1980), pp. 60-61

46. A. Comfort, Nature, **230**, 432 (1971)

47. F.H. Bronson and W.K. Whitten, J. Reprod. Fert., **15**, 131 (1968)

48. R.L. Brahmachary, Endeavour, **10**, 65 (1986)

49. B. Keverne, New Scientist, **63**, 22 (1974)

50. J.R.M. Innes and M.F. Stanton, Am. J. Path, **38**, 455 (1961)

51. H.B. Muller, Z. Zellforsch. Mikrosk. Anat., **100**, 42 (1969)

52. D. Thiessen and M. Rice, Psychol. Bull., **83**, 505 (1976)

53. F.J. Ebling, E. Ebling, V. Randall and J. Skinner, J. Endocr., **66**, 401 (1975)

54. M.R. Kare and J.G. Brand, "Interaction of Chemical Senses with Nutrition", Academic Press, Orland, (1986), p. 4

55. R.L.S. Patterson, J. Sci. Fdn. Agric., **19**, 434, (1968)

56. E.N. Barata, R. Serrano, L.Gomes and A.V.M. Canario, Comparative Biochemistry and Physiology-Part A Molecular and Interaction Physiology, **12**, 63 (2002)

57. D.F. Farner, J.R. King, and K.C. Parkes, "Avian Biology, Vol.II", Academic Press, New York, (1972), pp.50-51

58. D.S. Farner, J.R. King, and K.C. Parkes, "Avian biology, Vol VI", Academic Press, New York, (1982), p. 255

59. *http://www.nioz.nl/en/deps/mbt/projects/gland_waxes.html*

60. P.E. Kolattukudy, S. Bohnet and L. Rogers, J. Lipid Research, **28**, 582 (1987)

61. P.E. Kolattukudy, S. Bohnet. and L. Rogers J. Lipid Research, **26,** 989 (1985)

62. J. Reneerkens, T. Piersma and J.S.S. Damste, Proceedings of the Royal Society of London Series: Biological Sciences, **269**, 2135 (2002)

63. Reference 58, pp. 255-262

64. J. Jacob, Lipids, **11**, 816 (1976)

65. J. Jacob and A. Zeman, Z. Physiol. Chem., **353**, 492 (1972) (as sited in Reference 58)

66. K. Saito and M. Gamo, Comp. Biochem. Physiol., **458**, 603 (1973)

67. B.Y. Tang and I.A. Hansen, Comp. Biochem. Physiol., **54B,** 483 (1976)

68. E. Edkins and I.A. Hansen, Comp. Biochem. Physiol., **398**, 1 (1971)

69. J. Jacob and J. Poltz, Biochem. Syst. Ecol., **3**, 263 (1975)

70. J. Jacob, Biochem. Syst. Ecol., **6**, 347 (1978)

71. J. Jacob and D.E. Pomeroy, Comp. Biochem. Physiol., **64B**, 301 (1979)

72. J. Jacob, Comp. Biochem. Physiol., **72B**, 161 (1982.)

73. M. Apandi and H.M. Edwards, Poultry Sci., **43**, 1445 (1964)

74. Q.T. Yu, B.N. Liu, J.Y. Zhang, and Z.H. Huang, Lipids, **30**, 804 (1988)

75. B.R. Moyer, A.N. Rock and D.H. Clayton, AUK, **120**, 490 (2003)

76. Reference 10, pp. 1099-1100

77. H.C. Hou, Chin. J. Physiol., **5**, 11, (1931) (as cited in Reference 57)

78. Reference 57 p. 53

79. J.F. Pugh and M.D. Evans, Trans. Br. Mycol. Soc, **54**, 241 (1970) (as cited in Reference 57, p. 306)

80. J.F. Pugh, Ibid, 114, **172**, (1972) (as cited in Reference 58, p. 306)

81. J.D. Ligon and S.H. Ligon, Living Bird, **16**, 159 (1978)

82. Reference 10

83. G.L. MacLean, "Roberts' Birds of Southern Africa", CTP Book Printers, Cape, S.A., (1993), p. 391

84. I. Sinclair, P. Hockey, and W. Tarboton, "Birds of Southern Africa", Struik, Cape Town, (2002), p. 268

85. P. Steyn, Ostrich, **70**, 173 (1999)

86. J. Gooders, "Birds: An Illustrated Survey of the Bird Families of the World", The Hamlyn, London, (1975), p. 217

87. L. Oliver and J.R. Austin, "Birds of the World", Golden Pleasure Books, Florida, (1961), p. 182

CHAPTER 2

CHEMICAL CHARACTERIZATION OF THE UROPYGIAL GLAND SECRETION OF THE SCIMITAR-BILLED HOOPOE, *RHINOPOMASTUS CYANOMELAS*.

2.1 Introduction

The total ion chromatogram (TIC) obtained from the uropygial gland secretion of *Rhinopomastus cyanomelas* (Fig. 2.1) will be used as a reference in the discussion of the different components found in the secretion. Each component will be referred to by its number in the gas chromatogram. The compounds identified in the secretion are listed in Tables 2.1 (p. 97) and 2.2 (p. 99).

Individual components were identified by interpreting their low-resolution electron impact (EI) mass spectra, taking into account the relative gas chromatographic retention times of members of homologous series of compounds and of similar compound types (e.g. branched and unbranched aldehydes, etc). The interpretation was further aided by comparison of the respective mass spectra with those in the available NBS and Wiley mass spectra libraries, containing *ca*. 200,000 spectra in total. Only chemical structures based on correlations of more than 80% in almost all cases between unknown mass spectra and library data were considered as viable and served as evidence in the identification of the constituents of the secretion.

It must be mentioned that in some cases, the *m/z* values reported in the text for certain ions are not visible in the corresponding spectra. They are visible only after the spectra have been magnified. In the case of some components, especially those having aromatic structures, whose molecular ions are expected to be visible, the molecular ions are in fact also absent from the spectra due to the low total ion current value

Although a field trip to Kimberley and surrounding area was undertaken, no uropygial secretion could be collected for gas chromatographic retention

time comparison purposes, because of the scarcity of the particular bird. It was not possible to schedule another field trip within the time limits of this particular study, but it is planned to take place during the next breeding season as part of the ongoing research on the semiochemical secretions of avian species.

2.2 Structural determination of the components of the uropygial gland secretion of *Rhinopomastus cyanomelas.*

2.2.1 Hydrocarbons (Aliphatic)

2.2.1.1 Alkanes

The molecular ion in aliphatic saturated hydrocarbons may be described as a non-localized type[1]. This class of compounds appears to break down mainly by an initial non-selective cleavage of C-C bonds, followed by further step-wise decomposition of the primary products, with intervening energy–releasing rearrangements to give a characteristic product distribution:

$$R{-}CH_2{-}CH_2{-}CH_2{-}\overline{R_1}\,|^{+\bullet} \longrightarrow R{-}CH_2{-}\overset{+}{C}H_2 + R_1{-}\dot{C}H_2$$

Simple sigma fission is the primary fragmentation mode which leads to even electron (EE^+) fragment ions[2], which in turn can undergo further cleavage with expulsion of unsaturated species. The mass spectra of unbranched saturated hydrocarbons typically exhibit clusters of ions, spaced 14 amu apart. The largest peak in each cluster represents a $(C_nH_{2n+1})^+$ ion, accompanied by $(C_nH_{2n-1})^+$ and $(C_nH_{2n})^+$ ions. Abundance maxima occur at C3 and C4 and fragment abundances decrease up to the $(M - C_2H_5)^+$ ion[3]. The prevalence of these ions could be explained in terms of further decomposition of the higher species by ejection of olefin neutral molecules, as evidenced by observation of corresponding meta-stable peaks. Because of the instability of the CH_3 radical, loss of CH_3 from a parent ion is not a likely process.

Molecular ions are usually present, even in long-chain aliphatic

hydrocarbons, although with low intensity. The presence of branching in aliphatic hydrocarbons decreases the intensity of parent ions or causes them to be virtually absent in highly branched alkanes. The presence of branching causes preferential cleavage at the site of branching and a break in the normal gradual decline in the abundance of fragments exhibited by straight-chain hydrocarbons owing to the higher stability of secondary and tertiary carbonium ions over primary ions, which are the result of simple sigma fission. Cleavage with charge retention usually occurs at the branched carbon with preferential discharge of large alkyl groups as neutral radicals[4]. An exception is found in the fragmentation of isoalkanes which show dominant loss of the isopropyl radical while the charge remains on the primary ion[5].

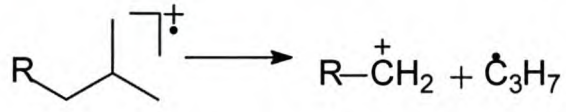

The fragment resulting from cleavage at a branch tends to lose a hydrogen atom leading to a prominent $(C_nH_{2n})^+$ ion which is sometimes more intense than the corresponding $(C_nH_{2n+1})^+$ ion.

The EI mass spectrum of component 2264 (Fig. 2.2) in the total ion chromatogram (TIC) of the uropygial secretion of *Rhinopomastus cyanomelas* (Fig. 2.1) shows typical clusters of $(C_nH_{2n+1})^+$ ions separated by 14 amu. The mass spectrum possesses a molecular ion peak at *m/z* 184 which is in agreement with the general formula for alkanes, namely C_nH_{2n+2}. Hence component 2264 was identified as tridecane and this was confirmed by the results of a computerised mass spectral library search.

Similar mass spectra, typical of unbranched hydrocarbons, were also observed for components 2682, 3080, 3460, 3827, 4169, 4525, 4819, 5178, 5458, 5749, 6014, 6268, and 6479 (Fig. 2.3 - 2.15). These components form a homologous series of straight-chain saturated alkanes, 14 mass units apart, ranging from C_{14} to C_{26}.

The effect of branching can be seen in the mass spectrum of component 3692 (Fig. 2.18). The absence of M^+ at *m/z* 240 and presence of a distinct ion

at *m/z* 225 indicates branching. A prominent ion at *m/z* 197 in the high mass region indicates methyl branching is indeed in the iso-position and in agreement with this conclusion, a computerised library search also proposed 2-methylhexadecane as the most likely structure.

Careful investigation of the relevant mass spectra (Fig. 2.16, 2.17, 2.19 - 2.24) led to the identification of components 579, 1151, 3981, 4070, 4667, 5258, 5854, and 6413 as branched alkanes in which the branching is found in different positions, as indicated in Table 2.1.

2.2.1.2 Alkenes

In alkenes hydrogen rearrangements in the molecular ion are prevalent, resulting in the migration of the radical sites along the chain[6]. As a result, the mass spectra of mono-unsaturated alkenes with the double bond in different positions are normally quite similar, except in cases where the double bond is highly substituted[7]. The usual fragmentation pattern for alkenes is rupture of the allylic bond (beta to the unsaturation) giving rise to a resonance-stabilized allylic cation. Since the allylic radical is also stabilized, the fragmentation may give rise to ions corresponding to charge retention by either of the fragments[8].

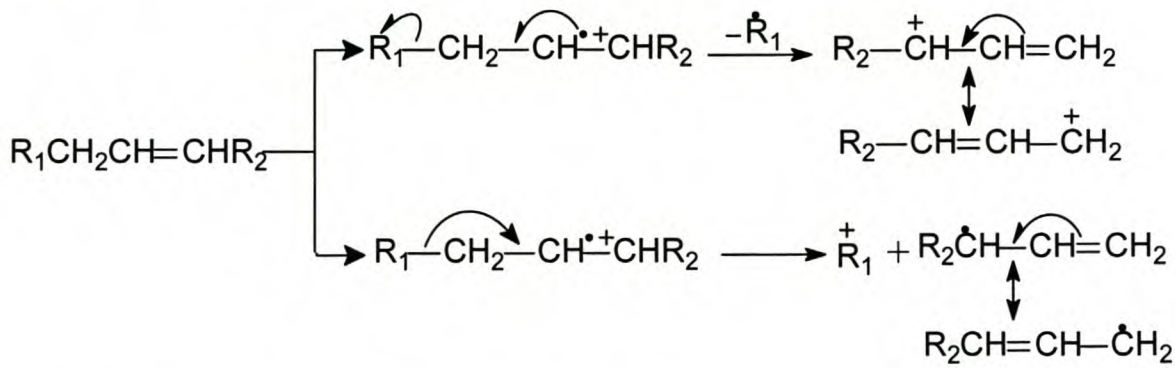

Cleavage of a bond beta to the double bond accompanied by the intramolecular rearrangement of a hydrogen atom is also prominent, giving rise to $(C_nH_{2n})^+$ ions. The simplest alkene which could undergo such a reaction is 1-pentene because it has the minimum required chain length for such a rearrangement. Studies on alkyl substituted 1-pentenes showed that such a fragmentation is facilitated by substitution in the 2-position, but is lowered by substituents in other positions[9]. Although substitution in the 1-position has the

same electron donating effect as that of the 2-position, steric hindrance restricts migration of the incoming hydrogen atom.

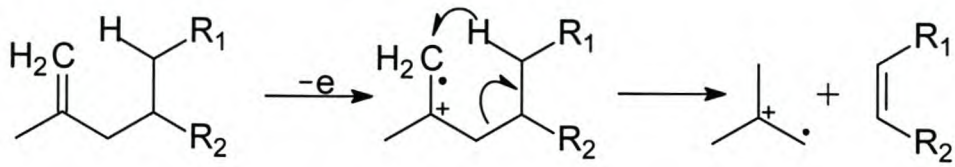

Similarity between mass spectra of *cis*- and *trans*- isomers of a given alkene is attributed to isomerization in the molecular ion or in the transition state prior to fragmentation.

Unlike alkanes, the mass spectra of olefins are dominated by $(C_nH_{2n-1})^+$ ions accompanied by $(C_nH_{2n})^+$ and $(C_nH_{2n+1})^+$ ions which gradually decrease in intensity as the *m/z* value increases. Ions at *m/z* 69, 83, 97,..., which are 2 amu lower than the corresponding ions in the spectra of alkanes, correspond to the retention of charge on the unsaturated fragment after C-C bond rupture[10].

Because of better stabilization of the positive charge formed from the π-bond, molecular ions of alkenes are much more intense than those of alkanes.

All the features mentioned above can be seen in the mass spectrum of component 3733 (Fig. 2.25). The distinctive ion at *m/z* 238 was found to be the molecular ion and the mass spectrum exhibits clusters of $(C_nH_{2n-1})^+$, $(C_nH_{2n})^+$ and $(C_nH_{2n+1})^+$ ions which are characteristic for alkenes. According to a computerized library search a heptadecene was a possible structure but the position of the double bond could not be determined with certainty.

The mass spectra of seventeen further components (Fig. 2.26 - 2.42) were found to be similar to that of component 3733 and similar reasoning showed that components 3755, 4409, 4427, 4455, 4477, 4743, 5039, 5075, 5090, 5346, 5367, 5929, 5945, 5970, 6152, 6174, and 6193 are also straight-chain alkenes as shown in Table 2.1.

The mass spectrum of component 5862 (Fig. 2.43), with *m/z* 336 as the molecular ion, is similar to that of component 5929 (Fig. 2.37) except that it has an ion at *m/z* 321. The presence of this ion indicates the presence of methyl branching. Since the position of the double bond is not known it is difficult to

locate the position of the branching. Hence component 5862 is identified as a methyl branched tetracosene. This conclusion is also supported by this component having a shorter retention time than component 5929 which was identified as unbranched tetracosene.

2.2.1.3 Alkynes

The mass spectra of alkynes are similar to those of alkenes. Due to stabilization of the charge they have more prominent molecular ions than the alkanes and their fragmentation patterns usually correspond to that of the alkenes. Prominent ions in the spectra of acetylenes occur at *m/z* values 67, 81, 95,..., that is 2 amu less than the corresponding ions in the spectra of alkenes and 4 amu less than those of alkanes[11].

Interpretation of their mass spectra (Fig. 2.44 - 2.48) and computer library data showed that components 5010, 5279, 5560, 5874, and 6099 are C_{21}-C_{25} alkynes. The position of the triple bond in these components is uncertain.

2.2.2 Alcohols

2.2.2.1 Aliphatic alcohols (saturated)

Alcohols upon EI ionization lose one of the non-bonded electrons of the oxygen atom to give an odd electron (OE^+) molecular ion in which the charge is retained by the oxygen atom[12]. Since (EE^+) are more stable than OE^+ ions, the ion thus formed from the alcohol undergoes further fragmentation. The most favoured fragmentation in primary alcohols occurs through α-cleavage to give a stable oxonium ion at *m/z* 31. If no α-carbon is present, as in methanol where R = H, α-fission occurs through expulsion of a hydrogen atom bonded to the C-atom.

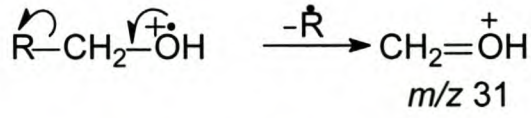

Alcohols, apart from the loss of a hydrogen atom from the α-carbon, show $(M - 2)^+$ and $(M - 3)^+$ ions because of the consecutive loss of the hydroxyl hydrogen and an additional hydrogen from the carbinol carbon[13]. The $(M - 2)^+$

ions are sometimes prominent in the spectra of long-chain alcohols and are useful in locating the molecular ion peak.

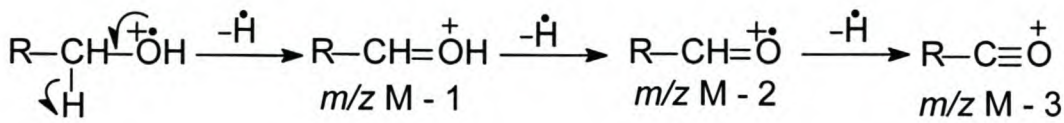

The mass spectra of primary alcohols (especially long-chain) consist of two types of ions. One type arises from primary fragmentation to produce weak alcohol type $C_nH_{2n+1}O^+$ ions (*m/z* 31, 45, 59…) and alkane type $(C_nH_{2n+1})^+$ ions (*m/z* 29, 43, 57…). The second type of ions consists of ions typical of olefins i.e. $(C_nH_{2n})^+$ and $(C_nH_{2n-1})^+$ (*m/z* 41, 42, 55, 56,…)[14].

When an alternative exists as in secondary and tertiary alcohols, the larger substituent is always expelled more readily since the electron in the neutral radical can be stabilized more easily in larger fragments, either by rearrangement or further fragmentation.

Another type of fragmentation that occurs in alcohols is elimination of water to give *m/z* $(M - 18)^+$ ions. This elimination, unlike thermal elimination, which is 1,2-elimination, was found to occur predominantly through 1,4-elimination (≈ 90%) with small contributions from 1,3- and 1,5-elimination[15].

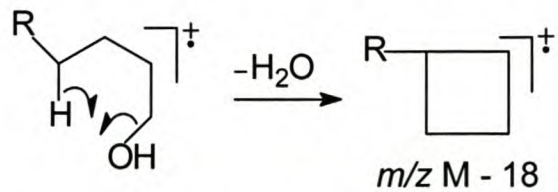

Labelling experiments showed that elimination of water can also occur from fragment ions containing a hydroxyl group. But in this case abstraction of a hydrogen atom is less specific (≈ 30% each for 1,3- and 1,4-elimination)[16]. Elimination of water, either from the molecular ion or fragment ions, is usually accompanied by expulsion of C_2H_4. Depending on the chain-length of the alcohol, this expulsion of C_2H_4 can be repeated in succession[17].

The mass spectrum of component 4304 (Fig. 2.49) is dominated by

$C_nH_{2n+1}O^+$, $(C_nH_{2n+1})^+$, $(C_nH_{2n})^+$, and $(C_nH_{2n-1})^+$ ions which are typical for long-chain alcohols. The ion at *m/z* 224 indicates the loss of water. Intermittent loss of C_2H_4 molecules results in the formation of ions at *m/z* 196, 168, 140, 112, 84, and 56. On account of this mass spectrometric evidence and comparison with spectral library data component 4304 was identified as 1-hexadecanol.

In the mass spectrum of component 5248 (Fig. 2.51) the ion at *m/z* 282 represents the loss of two hydrogen atoms. The presence of an ion at *m/z* 282 together with ions at *m/z* 266 and *m/z* 238 allows location of the molecular ion at *m/z* 284. Therefore component 5248, which has fragmentation patterns similar to those of component 4304, was identified as 1-nonadecanol.

The mass spectrum of component 3963 (Fig. 2.54) is identical to that of component 4304. Its elution prior to component 4304 (1-hexadecanol) indicates it is a branched C_{16} or C_{14} or C_{15} alcohol. On account of *m/z* 182, which is formed by loss of H_2O and C_2H_2, component 3964 was labelled as a C_{15} alcohol. The presence of an abundant *m/z* 154 ion indicates methyl branching at the iso-position. The *m/z* 154 $(M - 74)^+$ ion is formed by expulsion of a carbinol group and a terminal isopropyl group from the ionized molecule. Hence component 3963 was identified as 13-methyl-1-tetradecanol.

The mass spectrum of component 2127 (Fig. 2.55) has a base peak at *m/z* 59, characteristic of secondary alcohols. The subtraction of 30 amu (CH-OH) from *m/z* 59 and *m/z* 115 led to the characterisation of the two alkyl groups on either side of the α-carbon as ethyl and hexyl respectively. Therefore component 2125 was tentatively identified as 3-nonanol.

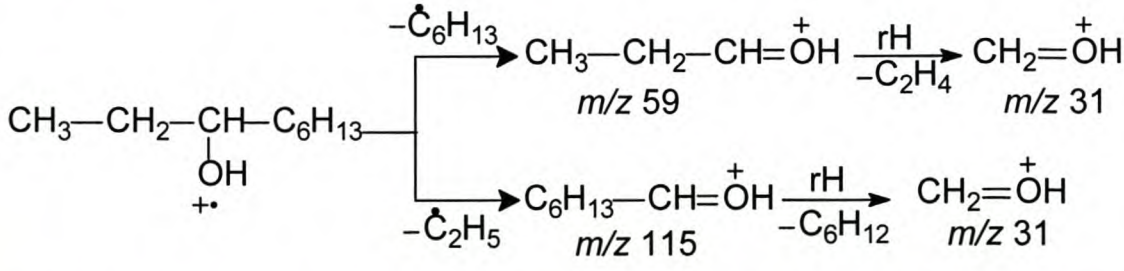

The ion at *m/z* 97 is formed by the expulsion of a water molecule from the *m/z* 115 ion. Successive removal of C_2H_4 molecules from the ion at *m/z* 97

results in the formation of the ions at *m/z* 69 and 41.

Confirmation of the identity of component 2127 as 3-nonanol was obtained by computerised comparison of its mass spectrum with library data.

Interpretation of the relevant mass spectra (Fig. 2.50, 2.52-2.53) led to the identification of components 4959, 5385 and 3769 as 1-octadecanol, 1-docosanol and 12-methyl-1-tridecanol respectively.

2.2.2.2 Aromatic alcohols

The greater stability of the molecular ions of aromatic alcohols, in contrast to aliphatic alcohols with their weak or undetectable molecular ions, is attributed to the resonance stabilization of the unpaired electron on the oxygen atom by the aromatic ring[18]. In aromatic alcohols, with the exception of benzyl alcohols, the ion at *m/z* $(M - 1)^+$ is insignificant

The mass spectrum of component 500 (Fig. 2.56) shows a base peak at *m/z* 98 and prominent ions at *m/z* 39, 42, 53, 69, and 81.The characterisation of this component as 2-furanylmethanol was in agreement with the results of a computer library search. The ion at *m/z* 98 is therefore the molecular ion and *m/z* 97 is the $(M - 1)^+$ ion.

The formation of some of the ions can be rationalized as follows:

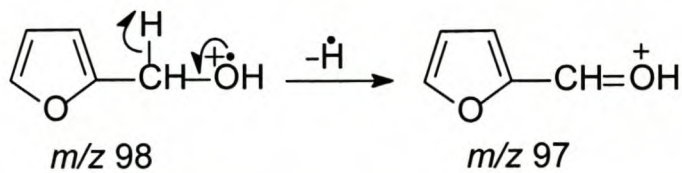

m/z 98 *m/z* 97

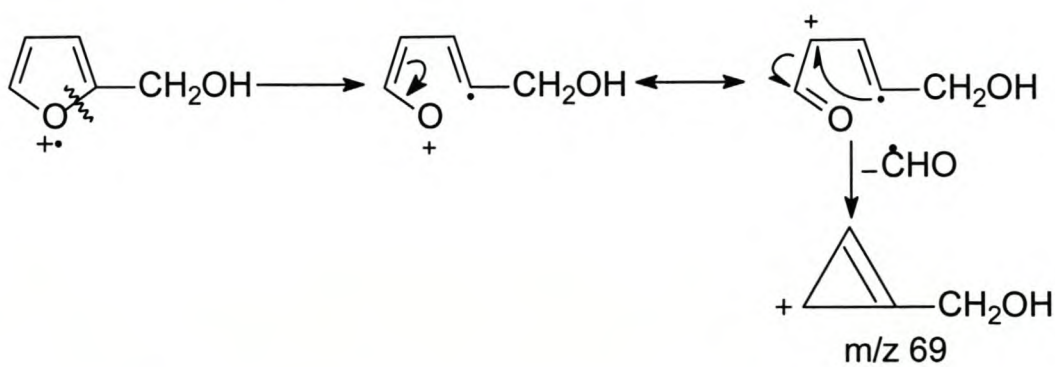

m/z 69

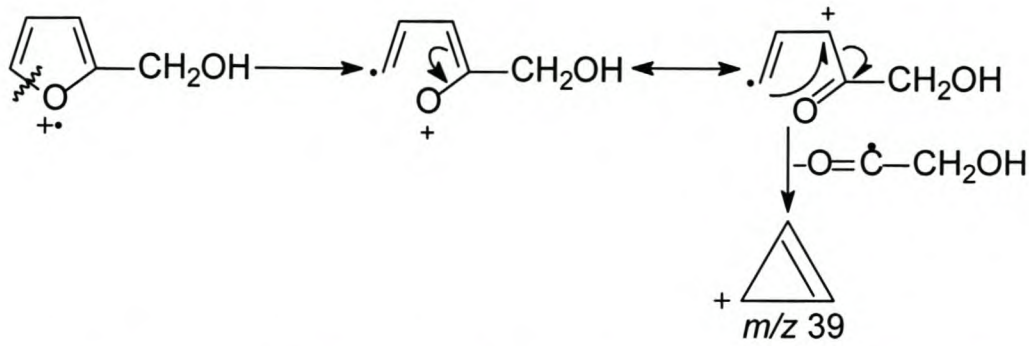

The expulsion of OH through β-fission with respect to the furan ring is generally favoured because the resulting cation can be stabilized by resonance or ring expansion to a fully aromatic pyrylium ion with *m/z* 81[19].

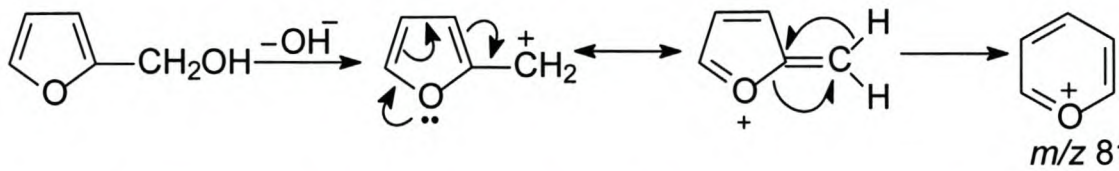

The mass spectrum of component 972 (Fig. 2.57) has a base peak which is also the molecular ion peak at *m/z* 94. The ions at *m/z* 39, 50, 55, 65, and 66 are characteristic for a benzene ring.

The abundant ion at *m/z* 66 is formed due to the loss of a CO molecule. Studies using isotope labelling confirmed that the *m/z* 66 ion is formed through cyclohexadienone as an intermediate[20].

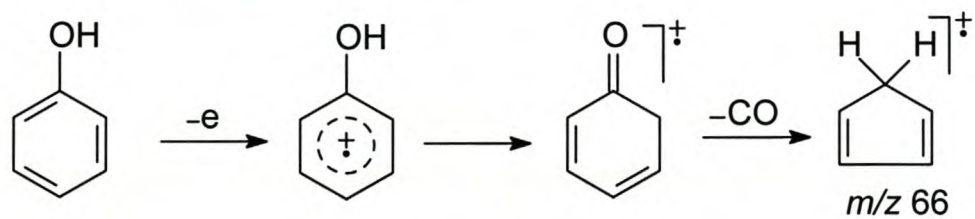

The ion at *m/z* 66 is accompanied by *m/z* 65 of comparable intensity. This ion at *m/z* 65 is formed by expulsion of a formyl radical from the molecular ion in which the hydrogen atom comes from the hydroxyl group to an extent of 33% with the rest from the ring hydrogen atoms.

Interpretation of its mass spectrum and correlation with mass spectral library data led to the conclusion that component 972 is indeed phenol.

2.2.3 Aldehydes

2.2.3.1 Aliphatic aldehydes

Fragmentation in aliphatic aldehydes is dominated by bond cleavage between the carbonyl carbon and α-carbon atom with the positive charge usually remaining on the oxygen-containing fragment. Although not as prominent as this C-C bond cleavage, C-H bond rupture between the carbonyl carbon and aldehydic hydrogen atom results in an $(M - 1)^+$ ion which has important structural diagnostic value[21].

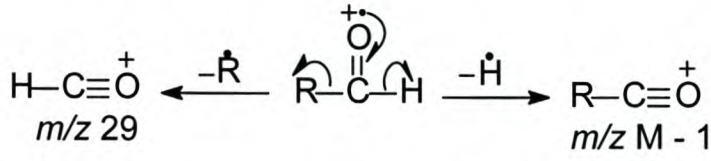

Molecular ions, especially for the lower and unbranched members of this compound group, are relatively prominent.

In the spectra of higher aldehydes ions appear at *m/z* 29, 43, 57..., corresponding to either $(C_nH_{2n+1})^+$ or $(C_nH_{2n+1}CO)^+$ ions. As a result, high-resolution mass spectrometry is needed to differentiate between the compositions of these ions. Studies using ^{18}O-labelled aldehydes showed that the *m/z* 29 ion in the first three members, C_1-C_3, is totally due to the formyl (CHO^+) ion, whereas in aldehydes containing more than four C-atoms it is solely due to $C_2H_5^+$. In butanal, although $C_2H_5^+$ is the prime contributor, there is some contribution (≈ 20%) from CHO^+ as well[22]. This shows a shift in mode of fragmentation in going from C_3 to C_4 and higher aldehydes.

For the first three members from formaldehyde to propanal the base peak appears at *m/z* 29 due to α-cleavage; for C_4-C_7 at *m/z* 44 because of rearrangement and for the higher members at *m/z* 43 or *m/z* 57.

From its simple mass spectrum component 47 (Fig. 2.58) was identified as propanal with its base peak at *m/z* 29 and molecular ion at *m/z* 58. Shift of the base peak to *m/z* 43, the presence of an ion at *m/z* 57 and a molecular ion at *m/z* 72 in the mass spectrum of component 63 (Fig. 2.59) indicates methyl branching. Hence component 63 was identified as 2-methylpropanal. In both

components the base peak is the result of α-cleavage. The identities of components 47 and 63 were confirmed by excellent agreement with computer library data.

Aldehydes with more than three carbon atoms undergo McLafferty rearrangement through a 6-membered ring transition state. This rearrangement is a two-step process in which an α-β cleavage occurs following γ-hydrogen transfer to the ionized carbonyl oxygen. Ions formed from this rearrangement appear at *m/z* 44 or *m/z* 44 + 14n depending on the nature of the substituents on the α-carbon atom.

The mass spectrum of component 77 (Fig. 2.60) is characterised by a base peak at *m/z* 44 and molecular ion at *m/z* 72. This component was identified as *n*-butanal on account of a computer library search.

While the ion at *m/z* 44 is the result of a McLafferty rearrangement, the *m/z* 43 ion with abundance comparable to that of the *m/z* 44 ion, is the result of direct σ-fission.

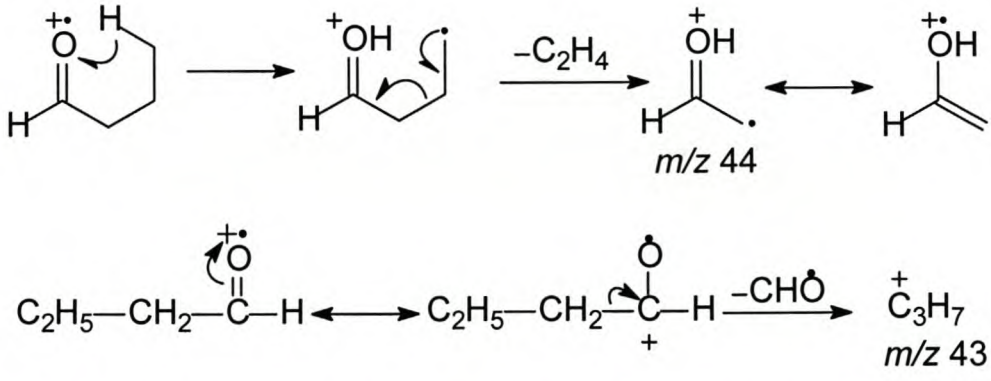

The mass spectrum of component 148 (Fig. 2.63) has a base peak at *m/z* 44, and M^+ and $(M - H)^+$ at *m/z* 86 and *m/z* 85 respectively. From the *m/z* 86 ion it is evident that the component could represent pentanal. The ion at *m/z* 44 indicates the absence of substituents on the α-carbon and is formed because of the formation of a resonance stabilized enol ion radical with concomitant expulsion of propene[23].

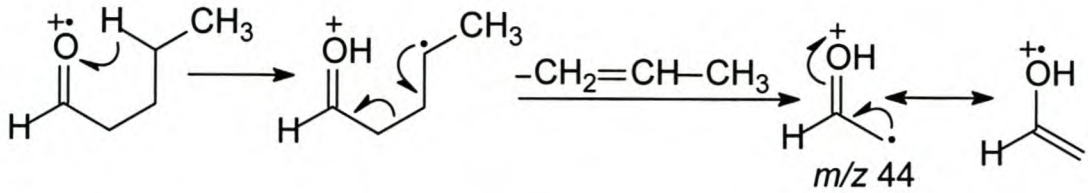

Usually an ion from a McLafferty rearrangement is accompanied by another ion, although of lower intensity, 13 amu higher. This so-called "McLafferty + 13" rearrangement[24] occurs when there is an available hydrogen atom at or beyond the δ-carbon atom. Fragmentation is first initiated by hydrogen transfer from the δ- or higher carbon atom to the ionized oxygen atom followed by reciprocal hydrogen rearrangement from the α-carbon and cleavage of the C-C bond in the β-γ position with respect to the carbonyl group.

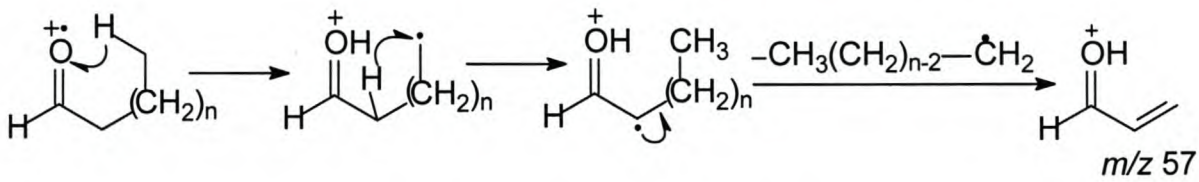

The driving force for the "McLafferty + 13" rearrangement is the high stability afforded by the α-, β-unsaturation of the protonated carbonyl group.

The most prominent rearrangement ion in the mass spectrum of component 120 (Fig. 2.62), which is isomeric with component 148, is found at *m/z* 58. The shift of the base peak from *m/z* 44 to *m/z* 57 and presence of intense ion at *m/z* 58 indicate methyl branching at the α-carbon (R_1 = CH_3, R_2 = H). The presence of methyl branching is further confirmed by a distinctive ion at *m/z* 71 which is the result of $(M - 15)^+$. Hence the component was characterised as 2-methylbutanal.

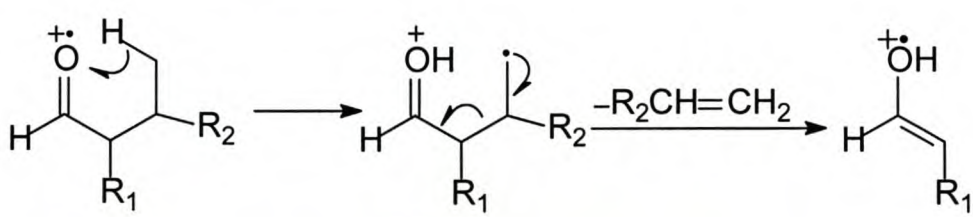

Component 113 which represents the third C_5 aldehyde isomer, is readily distinguishable from components 120 and 148 by distinctive ions at *m/z* 43 and *m/z* 71 (Fig. 2.61). While the ion at *m/z* 71 shows methyl branching, its location

at the α-carbon is excluded because of the presence of a rearrangement ion at *m/z* 44. Therefore the only possible position for branching reconcilable with the mass spectrum is at the β-carbon (R_1 = H, R_2 = CH_3). This is also confirmed by an ion of high intensity at *m/z* 43 which is of low intensity in the mass spectrum of the former two isomers.

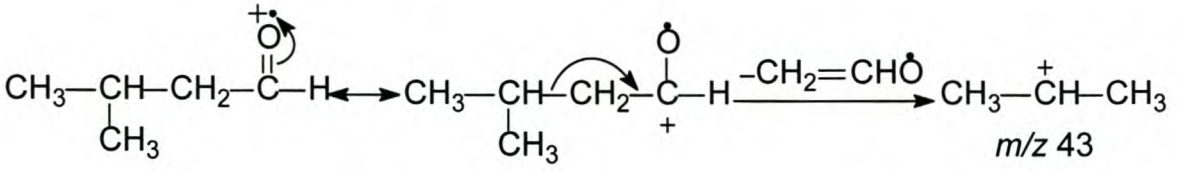

Therefore, components 113, 120, and 148 were identified as 3-methylbutanal, 2-methylbutanal and pentanal respectively.

In the fragmentation of α-unsubstituted aldehydes prominent ions of diagnostic value occur at $(M - 44)^+$, $(M - 43)^+$, $(M - 28)^+$ and $(M - 18)^+$ [25]. The $(M - 44)^+$ ions are produced by hydrogen rearrangement followed by β-fission as in the McLaffery rearrangement, but the charge in this case remains with the olefin part because of the heterolytic bond cleavage.

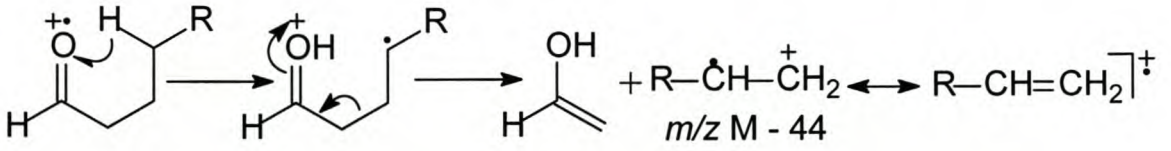

Unlike the McLaffery rearrangement, however, studies with deuterated C_{16}-C_{18} aldehydes showed that the source of hydrogen atom is not restricted to the γ-carbon atom. This rearrangement can also involve β-, γ- and δ-hydrogen atoms.

β-Cleavage without hydrogen rearrangement is also prominent in aldehydes and gives rise to $(M - 43)^+$ ions with general composition C_nH_{2n+1}.

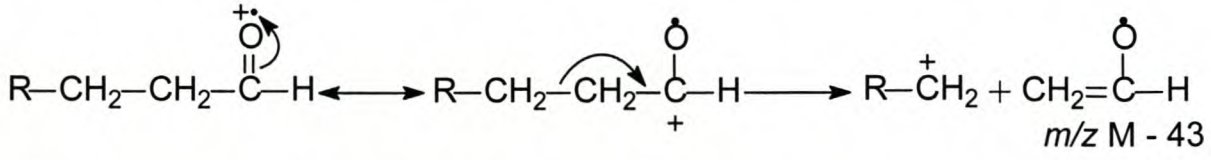

Components 227 (Fig. 2.64) and 292 (Fig. 2.65) are both C_6 aldehydes. Elution of component 227 ahead of 292 indicates branching in the former

component. The shift of the base peak from *m/z* 44 to *m/z* 57 and presence of intense ion at *m/z* 58 indicate the position of branching is at the α-carbon. This is further confirmed by the presence of an intense ion at *m/z* 71 which is the result of the loss of a CHO radical.

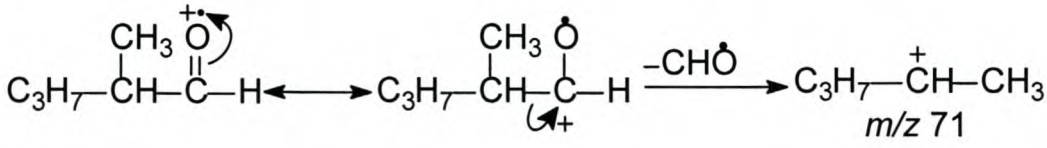

Unlike the mass spectrum of component 227, which lacks ions at *m/z* 72 and *m/z* 82 because of branching, the mass spectrum of component 292 is characterised by abundant ions at *m/z* 44 (base peak), 72, and 82 which indicate the absence of branching. While the ion at *m/z* 44 is because of the rearrangement, the ions at *m/z* 72 and 82 arise from the expulsion of respectively ethylene and water from the molecular ion. Hence components 227 and 292 were identified as 2-methylpentanal and hexanal respectively.

Ions at $(M - 28)^{+}$ [26] and $(M - 18)^{+}$ [27] corresponding to the elimination of C_2H_4 and H_2O respectively, are generally prominent in straight-chain hexanal and higher aldehydes. The formation of these ions is initiated by hydrogen rearrangement followed by expulsion of the neutral species, i.e. ethylene or water.

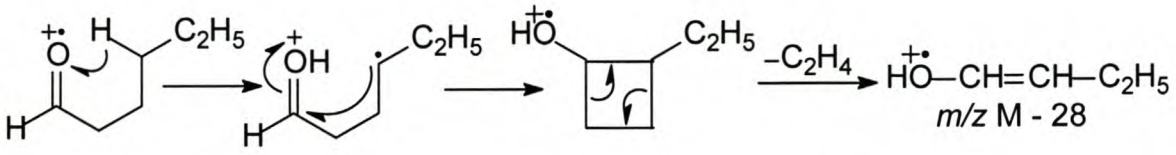

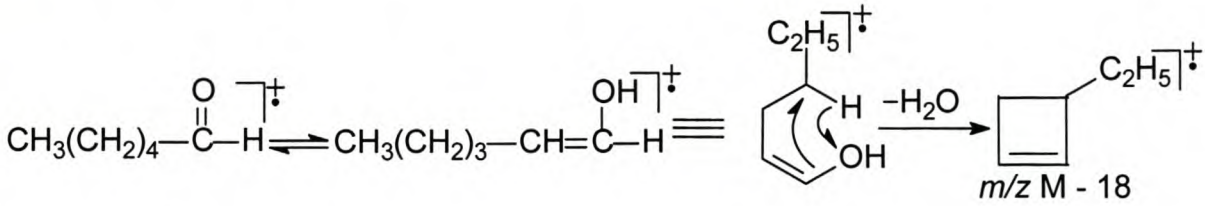

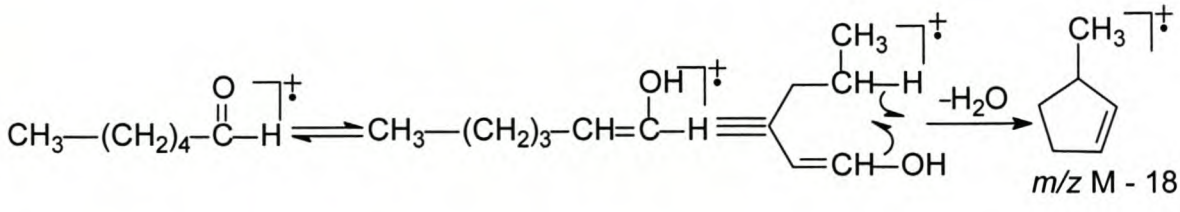

For higher aldehydes, as the number of carbon atoms increases, fragmentation because of the hydrocarbon part dominates that of the aldehyde part. As a consequence, typical hydrocarbon fragmentation with peak maxima at C3 and C4 occurs. Beside these $(C_nH_{2n+1})^+$ ions, a series of even mass ions at *m/z* 68 + 14n (n = 0, 1, 2, 3) appears in the spectra of long-chain aldehydes with *m/z* 82 as the most intense ion. These ions are formed because of the high probability of the formation of 5 to 7-membered rings where the enol formed from the aldehyde expels an alcohol molecule through a cyclic transition state. The mechanism for the formation of these rings is similar to the elimination of water[28].

All the above-mentioned fragmentation processes are observed in the mass spectrum of component 929 (Fig. 2.67). Although the molecular ion is absent, ions separated by 10 amu at *m/z* 110 $(M - H_2O)^+$ and *m/z* 100 $(M - C_2H_4)^+$ indicate the component to be octanal. Ions at *m/z* 68 and *m/z* 82 are because of ring formation with expulsion of an ethanol and propanol molecule respectively.

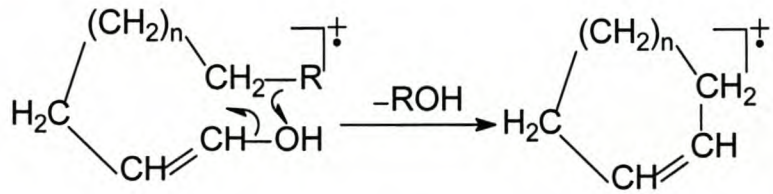

m/z 68, n = 1, R = C_3H_7
m/z 82, n = 2, R = C_2H_5

Based on the interpretation of their respective mass spectra, the comparison of their relative gas chromatographic retention times and confirmation by computerised library searches, components 47, 63, 77, 113, 120, 148, 227, 292, 556, 929, and 1361 were identified as the respective branched and unbranched aldehydes shown in Table 2.1.

Component 3331 which was tentatively identified as nonanal *O*-methyloxime, has prominent ions at *m/z* 41, 73 (base peak), 86, 114, and 156 in its mass spectrum (Fig. 2.69). The fragmentation observed in this component is most likely similar to that of its analogous oximes.

The ion at *m/z* 73 is formed by a McLafferty rearrangement in which the charge is retained by the nitrogen atom[29]. This ion undergoes further

fragmentation to give the ion at *m/z* 41 which has been shown by high-resolution mass spectrometry to have the composition $C_2H_3N^+$.

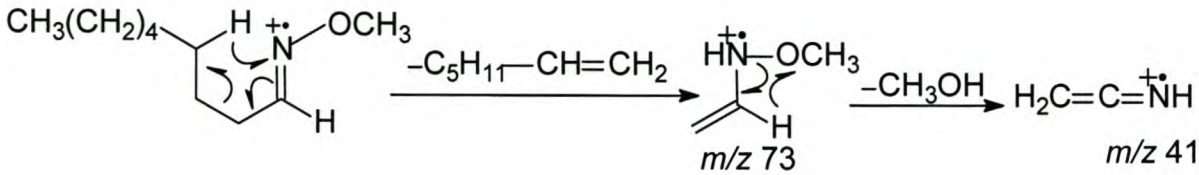

In the case of unbranched oximes γ-fission gives a prominent ion at *m/z* 72. Therefore by analogy γ-fission in *O*-methyloximes is expected to lead to the formation of an ion at *m/z* 86. The high abundance of the *m/z* 86 ion is because of alternative pathways for the formation of more stable cyclic ions in which the charge resides on either the oxygen or nitrogen atom. Of these two alternatives the latter pathway, with the charge at the nitrogen atom, is favoured because it has only a single heteroatom in the ring:

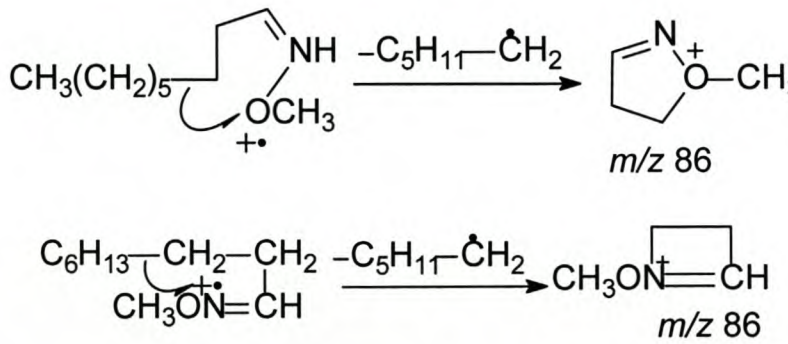

This is in agreement with the characterisation of component 3331 as nonanal *O*-methyloxime.

2.2.3.2 Aromatic aldehydes

Owing to better stabilization of the molecular ion through resonance by the aromatic ring, aromatic aldehydes have prominent molecular ions. Unlike aliphatic aldehydes which show predominantly C-C bond cleavage, bond cleavage between the carbonyl carbon and aldehydic hydrogen also gives prominent $(M - 1)^+$ ions which sometimes appear as the base peak. These $(M - 1)^+$ ions help to distinguish aromatic aldehydes from aromatic hydrocarbons, aromatic esters, or aromatic carboxylic acids[30].

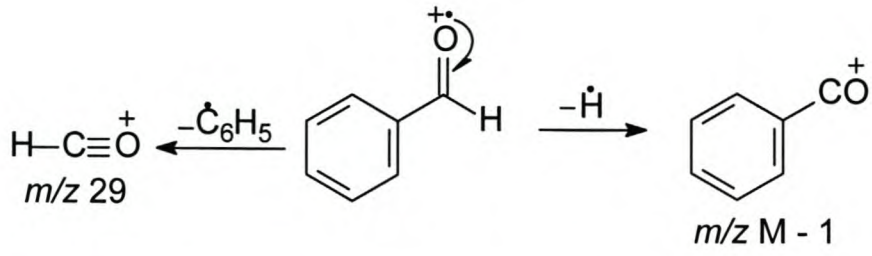

Even though aromatic aldehydes contain a benzene ring, the typical ion at *m/z* 91 is absent. The absence of this ion is used to distinguish aromatic aldehydes (where the acyl part is directly attached to the ring) from their isobaric alkyl benzenes. This indicates that there is no ring expansion in aldehydes as is a common phenomenon in alkyl benzenes to give the tropylium ion $(C_7H_7)^{+}$[31].

Component 743 has prominent ions in its mass spectrum (Fig. 2.70) at *m/z* 105 and *m/z* 106. The presence of ions at *m/z* 39, 50, 51, and 77 reveals the presence of a benzene ring that undergoes ring disintegration. Benzaldehyde was therefore suggested as a likely candidate by a computer library search.

While the ion at *m/z* 106 is the molecular ion, the *m/z* 105 ion is formed due to the loss of a hydrogen radical to give the $(M - 1)^{+}$ ion. Deuterium labelling experiments[32] showed that the $(M – 1)^{+}$ ion originates exclusively from the loss of a hydrogen atom from the α-carbon atom. The high intensity of this peak is because of resonance stabilization from the ring nucleus i.e.

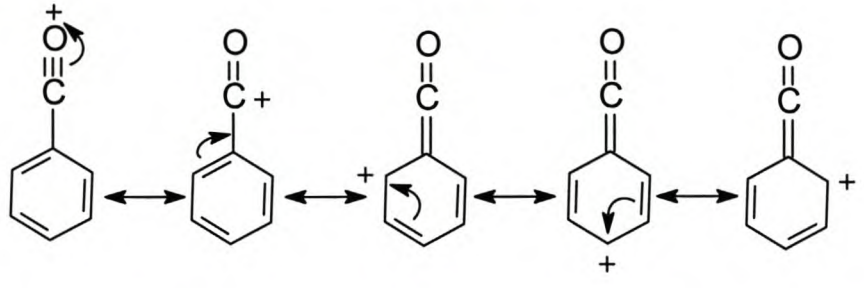

The ion at *m/z* 77 can be formed in either of two ways, either by expulsion of CO followed by a hydrogen radical from the parent ion, or by removal of neutral CO from the $(M – H)^{+}$ ion.

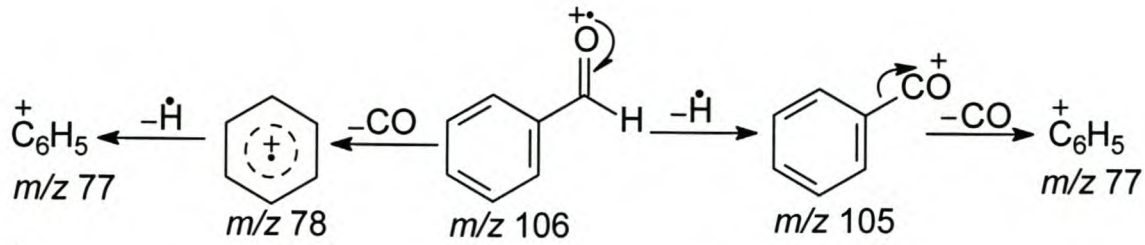

In the lower mass range, the ion at *m/z* 51 is because of expulsion of C_2H_2 from $C_6H_5^+$ and the ion at *m/z* 29 is because of the loss of an aryl radical by direct α-cleavage. Labelling experiments also showed that the hydrogen atom in CHO^+ (*m/z* 29) is the one originally attached to the alpha carbon.

On account of this mass spectral evidence and excellent agreement with mass spectral library data, component 743 was identified as benzaldehyde.

2.2.4 Ketones

2.2.4.1 Aliphatic ketones (saturated)

Fragmentation of ketones, like corresponding aldehydes, can best be interpreted by both α- and β-cleavages. Alpha cleavage adjacent to both sides of the carbonyl group always results in the formation of two acylium ions which are stabilized by mesomerism. The controlling factor for α-cleavage is the relative stability of the expelled alkyl radicals. Hence α-cleavage with the expulsion of the larger alkyl radical from either side of the carbonyl group is usually favoured[33].

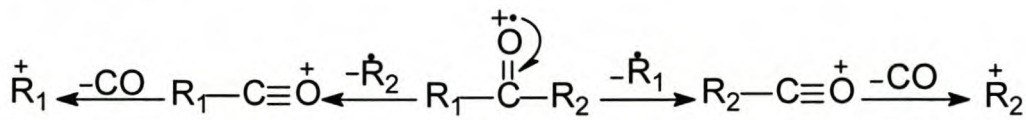

Further expulsion of a molecule of CO from the acylium ions results in the formation of hydrocarbon ions (R_1^+ and R_2^+) from which the structure of the ketone can be deduced by noting the two pairs of ions separated by 28 amu corresponding to R_1^+ and R_1CO^+ and R_2^+ and R_2CO^+ [34].

Important rearrangement ions occur in the mass spectra of ketones through McLafferty rearrangement. This rearrangement occurs if either or both of the groups adjacent to the carbonyl functional group contain a γ-hydrogen

atom. In straight-chain methyl ketones or those which are branched beyond the α-carbon this rearrangement gives an abundant ion, which most of the time is the base peak for the lower ketones, at *m/z* 58 because of the formation of a $C_3H_6O^+$ ion[35].

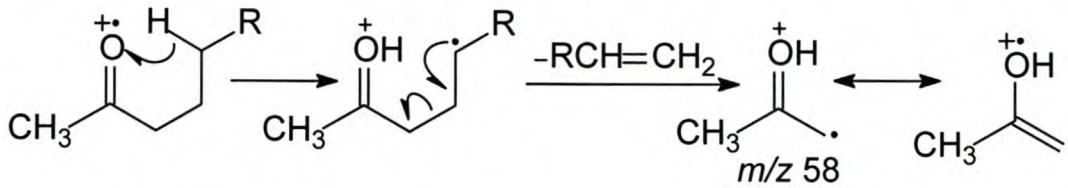

In methyl ketones without a substituent at the α-position, bond rupture between C4 and C5 produces the *m/z* 71 ion. A displacement to *m/z* 72 observed in deuterated 2-octanone has led to the conclusion that reciprocal hydrogen transfer processes must be operative in the formation of this ion[36].

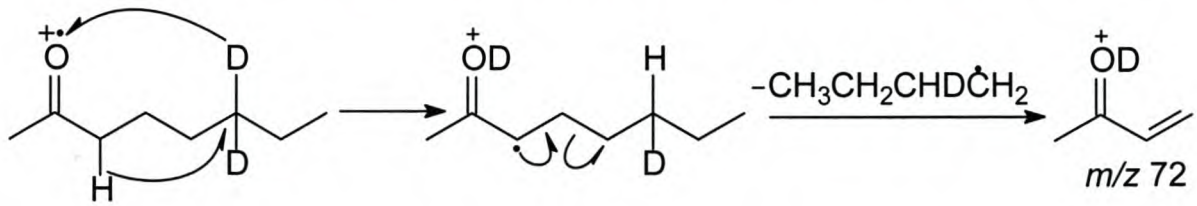

Unlike unbranched aldehydes, which are characterised by *m/z* 44 because of McLafferty rearrangement, β-fission in ketones does not furnish a specific *m/z* value for the following two reasons[37]:

(1) The mass of the rearranged ion can vary with the size of the alkyl group which is not involved in the rearrangement. (2) When there are more than two carbon atoms in each alkyl group, further rearrangement becomes possible since the enol produced from the primary rearrangement can again fragment similarly through a 6-membered transition state.

In the EI mass spectrum of component 276 (Fig. 2.71) the ions at *m/z* 43 and *m/z* 58 indicate the component to be a methyl ketone. Since the ion at *m/z* 100 corresponds to the molecular mass of a C_6 ketone, this component was identified as 2-hexanone. The ions at *m/z* 43 and *m/z* 85 are because of α-cleavage on either side of the carbonyl functional group. The abundant ion at *m/z* 58 indicates there is no branching at the α-carbon.

The mass spectrum of component 1311 (Fig. 2.73) has prominent ions at *m/z* 43, 58, 71, and 113 which are important for structural elucidation. The ions at *m/z* 43 and *m/z* 58 indicate the component to be a methyl ketone without substituents on the α-carbon. Therefore the ion at *m/z* 113 is considered to originate from the expulsion of a methyl radical by α-fission. The absence of the molecular ion is probably because of branching. The presence of ions at *m/z* 71 and 99 and absence of an ion at *m/z* 85 indicate that methyl branching is most probably at C5. Based on the study of its mass spectrum and a computer library search, the component was identified as 5-methylheptan-2-one.

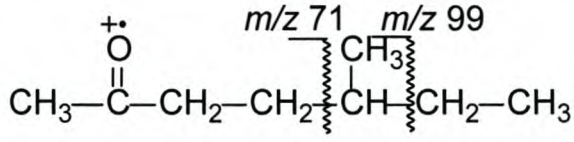

The mass spectrum of component 2602 (Fig. 2.76) has a base peak at *m/z* 72. This rearranged ion at *m/z* 72 can be formed from either an α-methyl substituted methyl ketone or an ethyl ketone. The high abundance of the ions at *m/z* 57 and *m/z* 155 indicate that the component is an ethyl ketone. Therefore the ions at *m/z* 57 and 155 are because of α-cleavage on either side of the carbonyl group. Hence component 2602 was identified as 3-dodecanone.

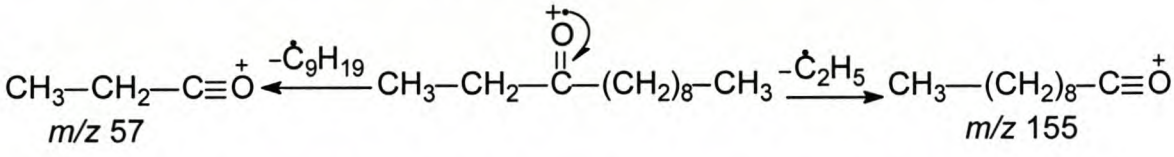

The base peak at *m/z* 72 is because of a McLafferty rearrangement:

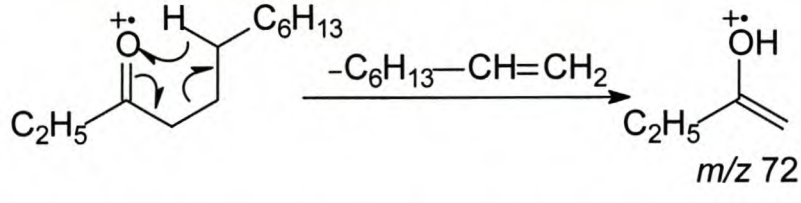

The ion at *m/z* 85 is most probably because of a "McLafferty + 13" fragmentation and *m/z* 122 to simultaneous loss of a CH_3 radical and a H_2O molecule from the ion at *m/z* 155.

Close investigation of their mass spectra (Fig. 2.72, 2.74, 2.75, 2.77-2.81) led to the identification of components 525, 1600, 1759, 2200, 3010,

3030, 3789, and 4357 as indicated in Table 2.1. The allocated structures are in good agreement with structures suggested by computerised library search.

2.2.4.2 Cyclic ketones

The mass spectrum of component 404 (Fig. 2.82) has a base peak at *m/z* 81 and molecular ion at *m/z* 116. From the ratio of the intensities of the M^+ and $(M+2)^+$ ions, which is approximately 3:1, it could be deduced that one chlorine atom is most likely present in the component. This is in agreement with the results of a computer library search which led to the tentative identification of this compound as 4-chloro-2-cyclopentene-1-one.

Apart of the presence of the chlorine atom and the double bond, the fragmentation pattern of component 404 is similar to those of cyclic ketones, especially cyclopentanone[38]. The formation of some of the ions can be rationalised as follows:

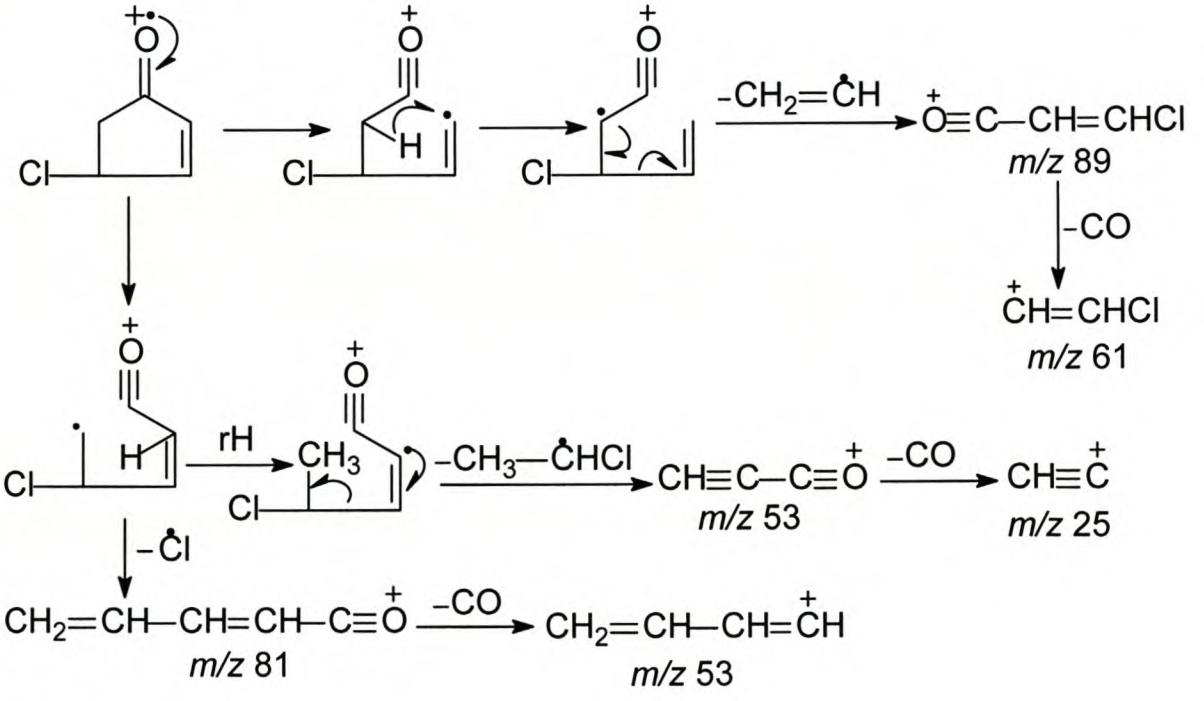

2.2.4.3 Diketones

Studies on alpha diketones showed that fragmentation occurs predominantly between the carbonyl groups to give an acylium ion and a radical[39].

The mass spectrum of component 2664 (Fig. 2.83) is characterised by a

base peak at *m/z* 105. The simplicity of its mass spectrum indicates that component 2664 could be a symmetrical diketone. This component was identified as diphenylethanedione with its typical fragmentation pattern.

The ion at *m/z* 105 is ascribed to C-C fission between the two carbonyl groups to give a benzoyl ion and a benzoyl radical.

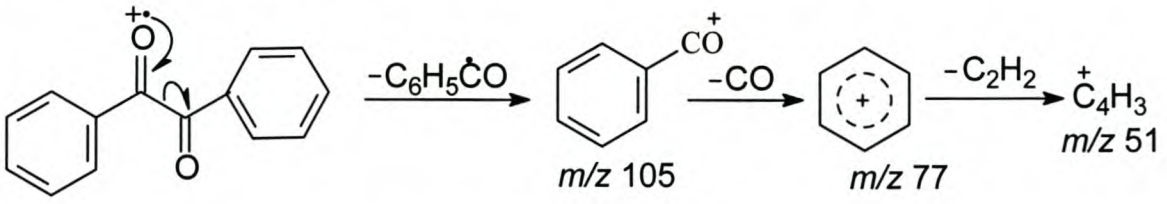

2.2.5 Carboxylic acids

2.2.5.1 Aliphatic carboxylic acids

The molecular ion peak of unbranched short-chain mono-carboxylic acids is readily distinguishable, although weak. The most characteristic ion of structural significance is the ion at *m/z* 60 which is found in those acids having a γ-hydrogen atom. Isotope labelling experiments with ^{13}C showed that the carbon atom of the carboxyl group is always retained in this ion[40]. In the lower members prominent ions with *m/z* $(M - 17)^+$ and *m/z* 45 arise because of α-cleavage on either side of the carbonyl group.

Mass spectra of long-chain carboxylic acids are characterised by two series of ions which correspond to retention of the charge on either fragment, namely on the fragment containing oxygen atoms $(C_nH_{2n-1}O_2)^+$ or on the hydrocarbon fragment $(C_nH_{2n+1})^+$.

Component 239 shows prominent ions at *m/z* 73 and *m/z* 74 in its mass spectrum (Fig. 2.84). While the *m/z* 74 ion is the molecular ion, the former ion is produced by loss of the acidic proton through σ-fission. The ions at *m/z* 57 and 45 are formed by loss of hydroxyl and ethyl radicals respectively through α-fission. The fragmentation pattern observed in this mass spectrum is typical for propanoic acid which is further confirmed by mass spectral library data.

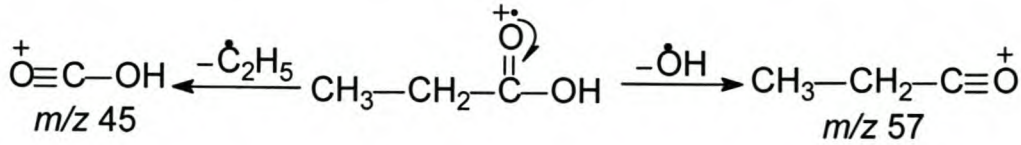

The molecular ion at *m/z* 88 in the mass spectrum of component 340 (Fig. 2.85) shows the component to be a C_4 acid. The absence of an abundant ion at *m/z* 60 indicates the absence of an available γ-hydrogen for the formation of this rearrangement ion. Therefore, it is obvious that the C_4 acid must be a branched one. As the only possible position of branching for a C_4 acid is at the C2 position, component 340 was identified as 2-methylpropanoic acid.

The ion at *m/z* 73 is formed by loss of a methyl radical from the molecular ion:

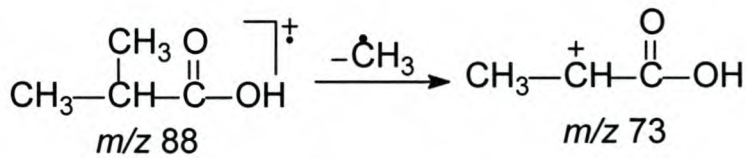

The base peak at *m/z* 43 is formed as a result of an inductive cleavage induced by the radical. Cleavage occurs preferentially at the branched carbon while the charge remains with the hydrocarbon fragment:

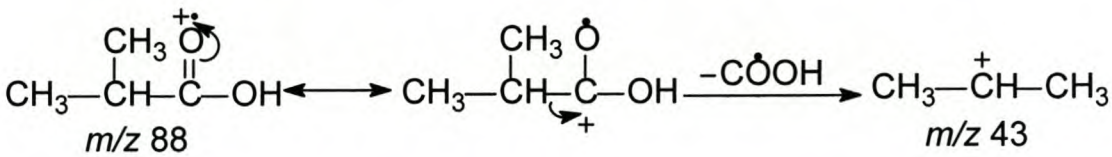

Although molecular ions are absent in the mass spectra of components 487 (Fig. 2.86) and 520 (Fig. 2.87), the molecular masses can be determined. The absence of the molecular ions is an indication of the presence of branching. If branching is assumed to arise only from a mono-methyl type, a prominent *m/z* 87 ion should, therefore, arise from loss of a methyl radical. Hence, as a working hypothesis these components were assumed to be branched C_5 acids. The base peaks at *m/z* 60 and *m/z* 74 in the two components respectively indicate that branching is at C3 in the former (R_1 = H, R_2 = CH_3) and at C2 in the latter (R_1 = CH_3, R_2 = H). The *m/z* 69 ion which is formed as a result of simultaneous expulsion of H_2O and a methyl radical is

found in both the spectra. Therefore, components 487 and 520 were identified as 3-methylbutanoic acid and 2-methylbutanoic acid respectively.

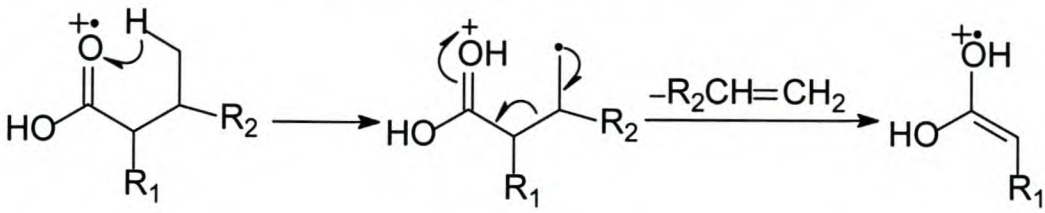

Component 610, the third isomer of the C_5 acids has its base peak at *m/z* 60 and weak molecular ion at *m/z* 102 in its mass spectrum (Fig. 2.88).The absence of branching is confirmed by the low abundance of the *m/z* 87 ion which is prominent in the former two C_5 acids. Another confirmation for the absence of branching is the absence of an *m/z* 69 ion which is the result of simultaneous loss of water and a methyl radical, characteristic of methyl branched acids. Therefore component 610 was identified as the unbranched C_5 acid, pentanoic acid.

From the study of their respective mass spectra, components 894 and 961 were concluded to be C_6 acids. The fact that component 894 elutes earlier than component 961 indicates the presence of branching in component 894.This is further confirmed by the presence of low abundance of the *m/z* 60 ion and of prominent ions at *m/z* 101 $(M - CH_3)^+$ and *m/z* 83 $[M - (CH_3 + H_2O)]^+$ in the mass spectrum of component 894 (Fig. 2.89).

Therefore component 894 was considered to be either 3- or 4-methylpentanoic acid. The high abundance of *m/z* 73 and 74 ions excludes the possibility of branching at C3 because branching at C3 should not give these ions in high abundance. Hence, component 894 was identified as 4-methylpentanoic acid and this was confirmed by comparison with library data. The *m/z* 74 ion is formed by a modified McLafferty rearrangement:

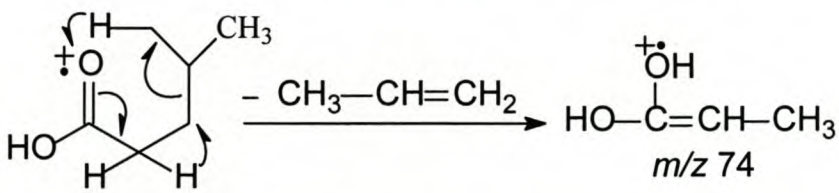

The base peak at *m/z* 57 in the mass spectrum of this component is due to β-fission with the charge remaining on the hydrocarbon fragment. The reason for the higher abundance of this ion is assumed to be the formation of a stable rearranged isobutyl ion:

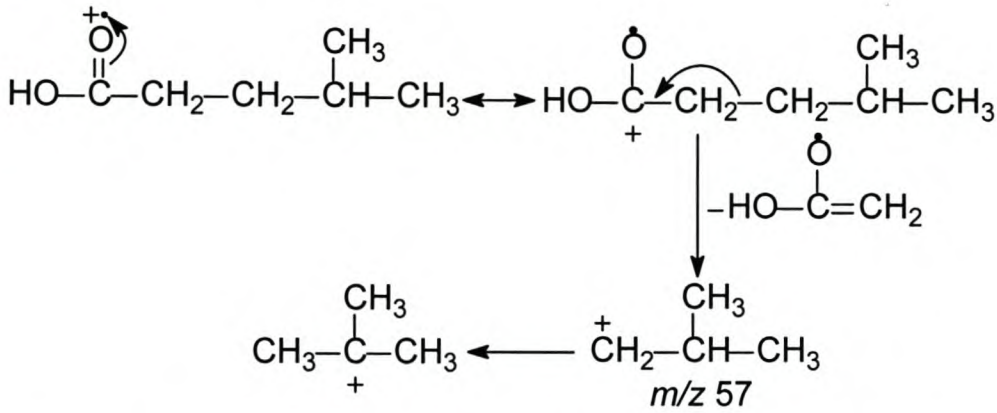

The mass spectrum of component 961 (Fig. 2.90), which was identified as hexanoic acid, shows the normal fragmentation pattern found in straight-chain acids.

Taking into account their relative retention times, components 894 and 961 were identified as 4-methylpentanoic acid and hexanoic acid respectively.

Preliminary structural elucidation of component 1817 was made using the ions at *m/z* 45, 88, 113 and 129 in its mass spectrum (Fig. 2.91). The ions at *m/z* 45 $(COOH)^+$ and 113 $(M - 45)^+$ indicate the component to be a carboxylic acid with a molecular ion at *m/z* 158. The base peak at *m/z* 88, combined with low abundance of the *m/z* 60 ion indicates ethyl branching at the alpha position. The presence of an ethyl chain is further supported by the *m/z* 129 ion $(M - 29)^+$. Therefore component 1817 was identified as 2-ethylheptanoic acid.

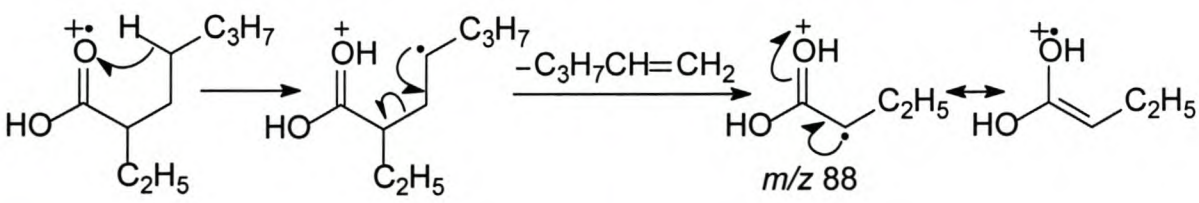

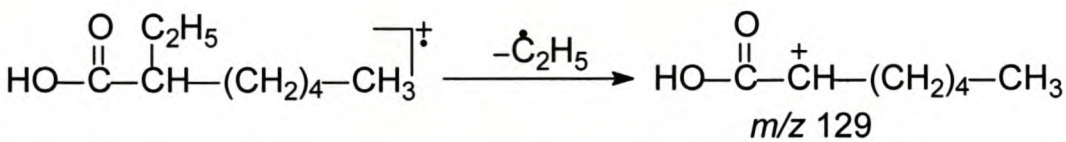

The comparable intensities of the ions at *m/z* 60 and 74 in the mass spectrum of component 1260 (Fig. 2.92) is typical for a carboxylic acid with methyl substitution at the 4-position. These ions are formed by McLafferty and modified McLafferty rearrangements respectively. Further supporting evidence for branching at C4 is obtained by the low abundance of the *m/z* 87 ion in relation to its neighbouring ions (*m/z* 73 and *m/z* 101). Hence, this component was thought to be either 4-methylheptanoic acid or 4-methyloctanoic acid. The *m/z* 101 ion can be formed by loss of an ethyl or propyl radical respectively from the corresponding acids. Since the ions at *m/z* 70 and 84 can, respectively, be the complimentary of these acids, final identification was not possible on account of the mass spectrum only. The elution of 4-methyloctanoic acid at higher retention time (component 2388) helps to identify component 1260 as 4-methylheptanoic acid.

The mass spectrum of component 2582 (Fig. 2.94) has a prominent ion at *m/z* 60 as the base peak and an *m/z* 73 ion as its "McLafferty + 13" rearranged ion. The relatively less abundant molecular ion peak at *m/z* 158 is in agreement with nonanoic acid.

The fact that component 2388 elutes earlier than component 2582 indicates that component 2388 should be a straight-chain acid with less than nine carbon atoms or a branched acid having nine carbon atoms. The ions at *m/z* 143 and *m/z* 125 in the mass spectrum of component 2388 (Fig. 2.93) are in fact evidence that the component is a methyl branched C_9 acid. The ion at *m/z* 125 is because of simultaneous expulsion of H_2O and a methyl radical while the one at *m/z* 143 is because of loss of a methyl radical. Therefore components 2388 and 2582 were identified as 4-methyloctanoic acid and nonanoic acid respectively.

The mass spectra of components 4044 (Fig. 2.95), 4704 (Fig 2.96), and 5887 (Fig 2.97), are characterised by prominent ions at *m/z* 60 and *m/z* 73 indicating they belong to the same aliphatic acid series with different chain lengths. All these acids have prominent molecular ion peaks of which the relative intensity increases with the molecular weight which is characteristic of

acids with more than six carbon atoms. The mass spectrum of component 4704 will be discussed as a representative of this group. In the mass spectrum of component 4704 (Fig. 2.96) the ion at *m/z* 60 is formed because of the obvious McLafferty rearrangement while the molecular ion appears at *m/z* 256.

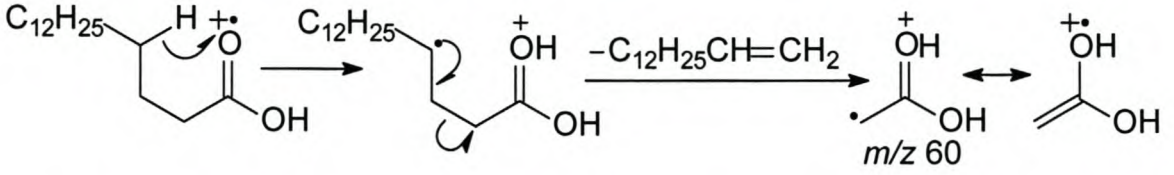

The formation of ions with the general formula $[(CH_2)_nCOOH]^+$, where n = 2, 6, 10, 14,..., at *m/z* values which differ by 56 amu (73, 129, 185,...) is favoured in the long straight-chain aliphatic carboxylic acids. These ions are formed even at low source temperatures and low electron beam energies, indicating that their formation is energetically favoured. The formation of these ions is initiated by prior hydrogen radical migration from C6 to the ionized carbonyl oxygen. Subsequent homolytic bond fission between C7 and C8 leads to the formation of the *m/z* 129 ion.

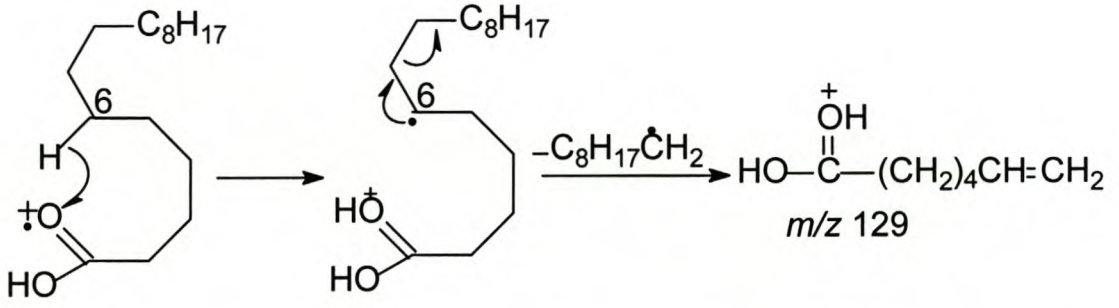

Further rearrangement of a hydrogen radical through a six-membered transition state, i.e., from C2 to C6 followed by homolysis of C3-C4, or from C10 to C6 followed by homolysis of C11- C12, furnishes ions with *m/z* values 73 and 185 respectively.

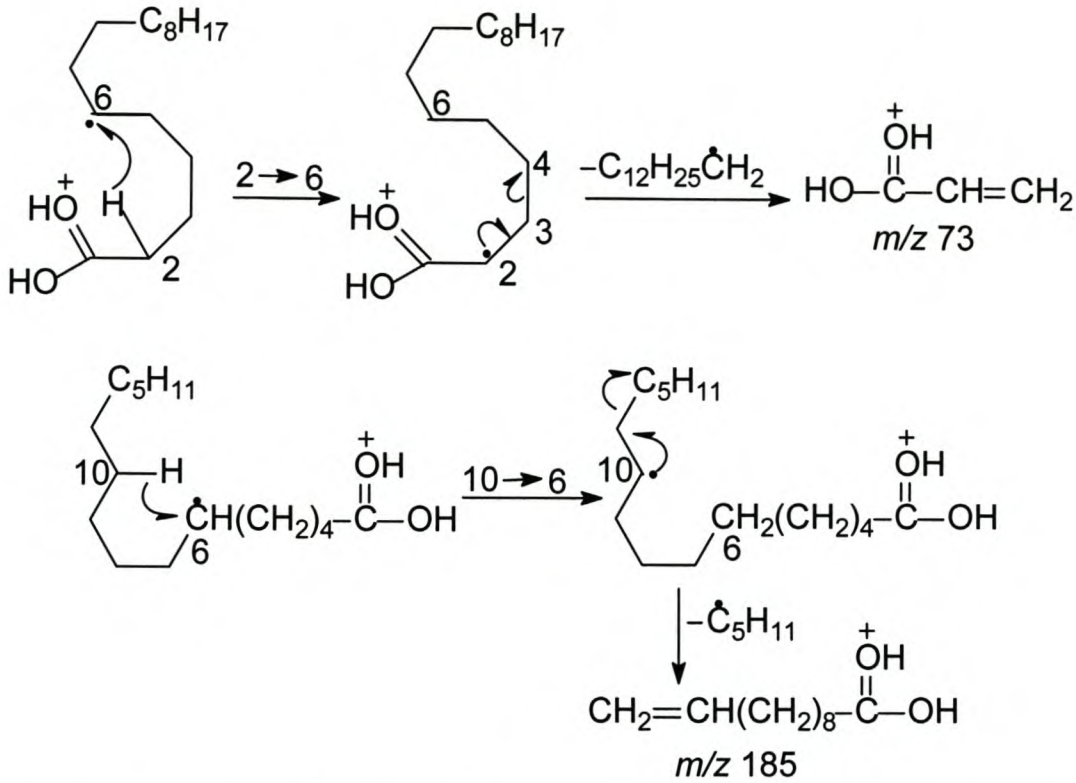

Another moderately abundant ion which belongs to the $[(CH_2)_nCOOH]^+$ series for which n = 12, is the *m/z* 213 ion. This ion is formed by loss of a C_3H_7 radical $(M - 43)^+$. Isotope labelling experiments revealed that the carbon atoms lost in the formation of this ion are C2, C3, and C4 following hydrogen transfer from C6 to C4 and recombination of the two terminal sides[41].

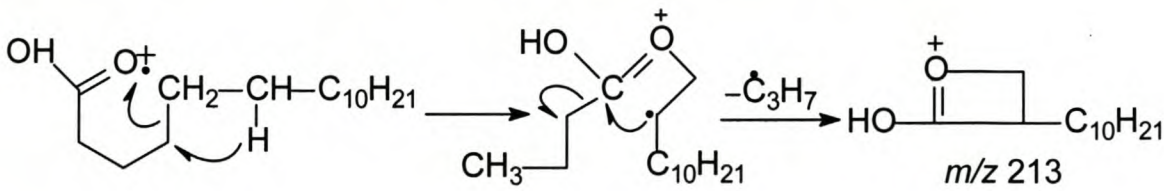

The formation of series of ions at *m/z* 73, 87, 101..., $[(CH_2)_nCOOH)]^+$ where n = 2, 3, 4, could also be accounted for by simple σ-cleavage with the charge residing on the oxygen-containing fragment[42]. Ions formed by σ-cleavage with the charge remaining on the hydrocarbon side are found at *m/z* 29, 43, 57, 71....

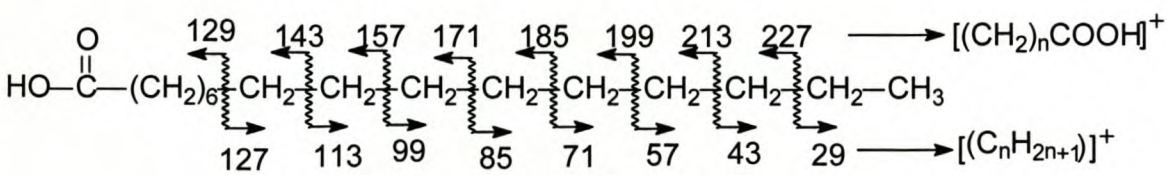

On account of this mass spectral evidence, components 4044, 4704, and 5887 were identified as tetradecanoic, hexadecanoic, and eicosanoic acids respectively.

2.2.5.2 Aromatic carboxylic acids

Aromatic acids can easily be identified from their simple mass spectra. The presence of ions typical for a ring system together with a strong molecular ion makes the identification straightforward. The spectra of aromatic acids are characterised by intense ions at *m/z* $(M - 17)^+$ and $(M - 45)^+$ corresponding to $ArCO^+$ and Ar^+ ions. In the case of a mono-carboxylic aromatic acid the molecular ion is present in very high abundance, reflecting the high resonance stability of the benzoyl system.[43]

Component 1868 shows prominent ions at *m/z* 122, 105, and 77 in its mass spectrum (Fig. 2.98). On account of the molecular ion at *m/z* 122, the component was identified as benzoic acid. The fragmentation patterns observed in this mass spectrum are in perfect agreement with those reported for benzoic acid.

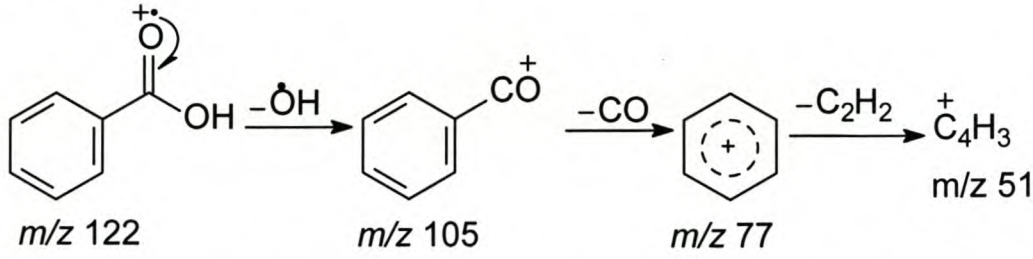

Deuterium labelling experiments[44] revealed that 18% of the abundance of the *m/z* 105 ion arises from loss of a hydroxyl ion containing a hydrogen atom from the ortho position. Thus the *m/z* 105 ion includes two isomeric species where the second isomer has the structure A which can be formed either by a concerted pathway or a two-step reaction sequence:

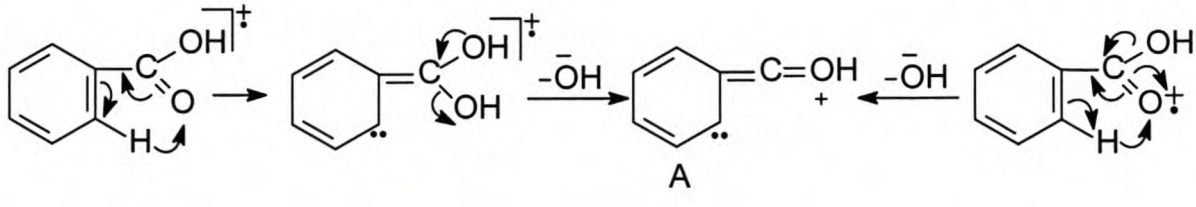

The mass spectrum of component 2179 (Fig. 2.99) is characterised by a base peak at *m/z* 91, which is the result of formation of a tropylium ion, and molecular ion at *m/z* 136. The *m/z* 91 ion is formed by loss of 45 amu from the parent ion indicating that the expelled fragment is definitely a COOH group. Therefore, component 2179 was identified as phenylacetic acid.

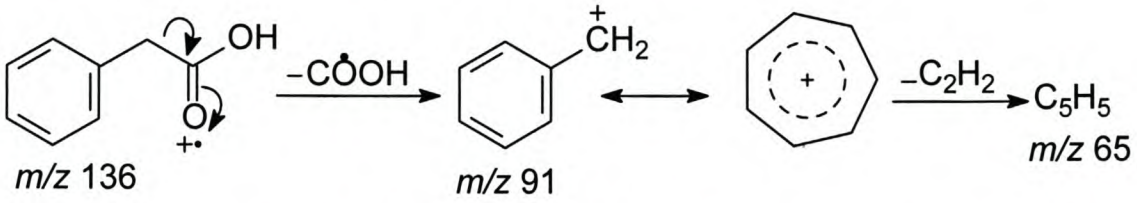

Similar to component 2179, the base peak at *m/z* 91, molecular ion peak at *m/z* 150 and other prominent ions at *m/z* 121, 105 and 65 in the mass spectrum of component 2496 (Fig. 2.100) suggest that the component could be 3-phenylpropanoic acid.

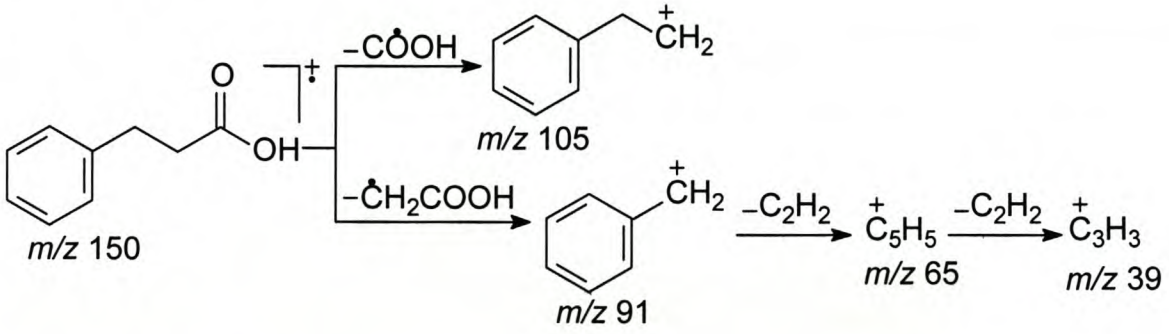

2.2.6 Methyl Esters

2.2.6.1 Aliphatic methyl esters

The mass spectra of methyl esters of short-chain fatty acids are characterised by molecular ions of relatively low abundance. The molecular ion is usually absent in the mass spectra of most branched methyl esters[45].

The main fragment ions in methyl esters are formed by alpha fission on the two sides of the carbonyl group giving primary ions R_1CO^+ and CH_3OCO^+. Other less intense ions are also formed by further fragmentation to give R_1^+ and CH_3O^+[46].

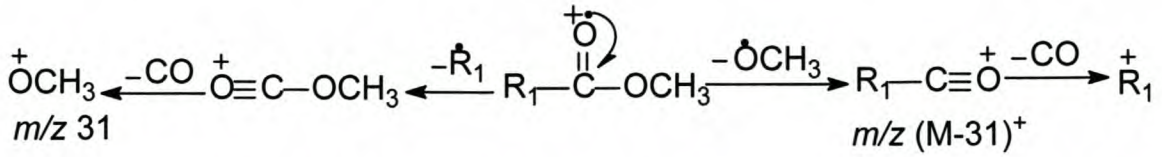

An ion at *m/z* 74 is typically present in the mass spectra of methyl esters that are unsubstituted at the alpha position. This ion is formed by a rearrangement in which a hydrogen atom is transferred from the gamma carbon atom to the ionized carbonyl oxygen, followed by alpha-beta bond fission[47].

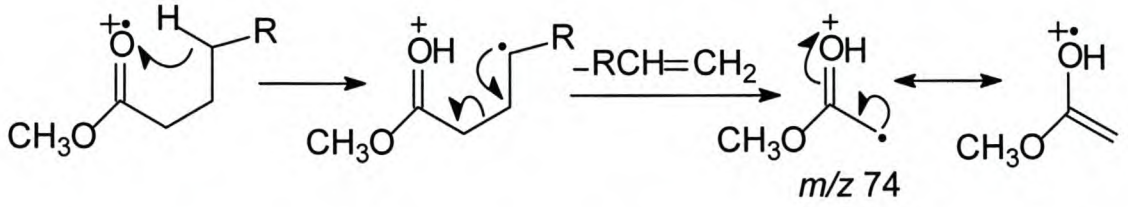

When the alpha carbon is substituted, the ion at *m/z* 74 is shifted to *m/z* 74 + 14n depending on the nature of the substituent on the alpha carbon.

The mass spectra of methyl esters of normal, long-chain carboxylic acids exhibit a series of intense ions (*m/z* 87, 143, 199,...,) corresponding to the ionized ion fragments of the general type $[(CH_2)_nOCOCH_3]^+$ with intact methoxycarbonyl group. Part of this ion series at *m/z* $(M - 43)^+$ is also found in straight chain methyl esters in which C2, C3 and C4 are expelled. The formation of these ions is similar to those found in straight-chain carboxylic acids.

When methyl branching exists, its position can be located by taking advantage of the existence of two prominent ions separated by 28 amu, with a weak ion 14 amu from these ions, because the corresponding fragment ion can only be formed by simultaneous breaking of two bonds and rearrangement of one hydrogen atom[48].

The mass spectrum of component 2441 (Fig. 2.101) has a base peak at *m/z* 57 and ions of diagnostic importance at *m/z* 59, 74, 113, 115, and 157. The ion at *m/z* 59 is derived from direct alpha cleavage, producing the CH_3OCO^+ ion. The *m/z* 74 ion which is the result of McLafferty rearrangement, indicates the absence of a substituent on the alpha carbon. The ions at *m/z* 87 and *m/z*

143 belong to the $[(CH_2)_nOCOCH_3]^+$ type of ions for which n = 2 and 4 respectively. The absence of M^+ and presence of *m/z* 157 can be considered to be because of methyl branching. The weak ion at *m/z* 101 relative to its neighbouring ions (*m/z* 87 and 115) indicates the position of branching at C4. Therefore component 2441 was identified as methyl 4-methyloctanoate.

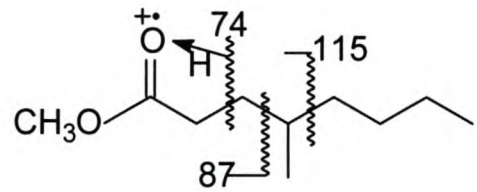

The absence of a molecular ion and interruption of the gradual decline in the intensity of the $[(CH_2)_nOCOCH_3]^+$ ion series in the mass spectrum of component 3566 (Fig. 2.103) indicate the presence of branching. The low abundance of *m/z* 101 and *m/z* 143 relative to their neighbouring ions (*m/z* 87 and 115, and *m/z* 129 and 157 respectively) indicates branching at C4 and C6. As a working hypothesis *m/z* 157 was taken as the $(M - 29)^+$ ion. The results of a computer library search were in good agreement with a thorough study of the mass spectrum, and the component was identified as methyl 4,6-dimethyloctanoate.

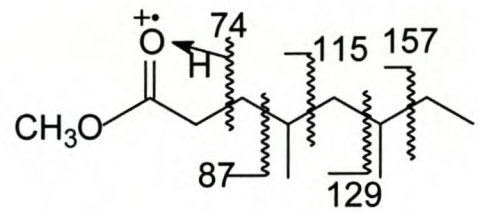

Close examination of the mass spectrum of component 3566 revealed a distinctive ion at the even mass *m/z* 124 $(M - 76)^+$ which is absent in the spectra of all the other methyl esters found in the secretion. Since this ion is absent in all methyl branched esters except in those with branching at C6, it must be characteristic of branched esters where the branching is at C6.

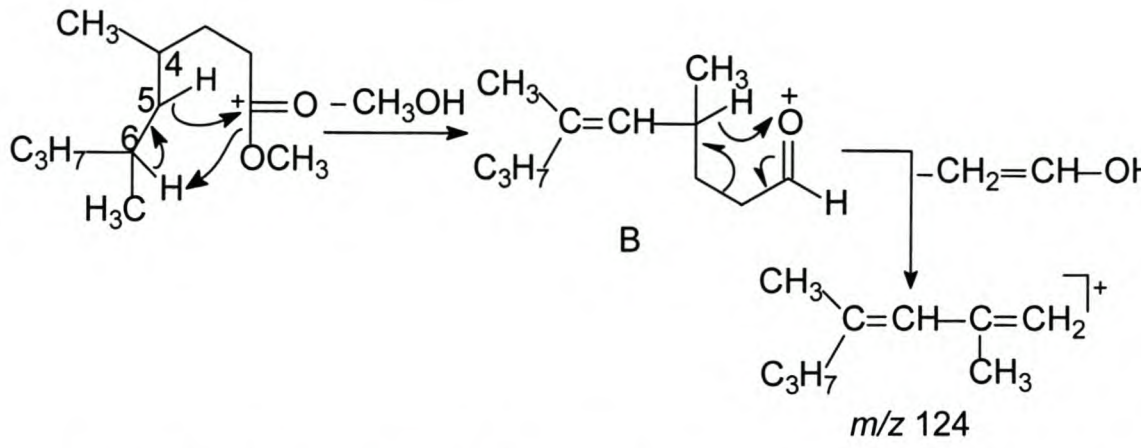

The driving force for the first step of this mechanism is furnished by the electron deficiency in the carbonyl group, assisted by the activated C-H bond in C6 and the second step is assisted by allylic activation of the C-H bond on C4 and by conjugation of the newly formed double bond with the π electron system already present in structure B[49].

Confirmation of the identity of the components 2441 and 3566 was obtained by the excellent agreement of their mass spectra with those of methyl 4-methyloctanoate and methyl 4,6-dimethyloctanoate present in the computer libraries.

Investigation of the relevant mass spectra (Fig. 2.102 and Fig. 2.104) and comparison with spectra of components 2441 and 3566 as well as library data, components 2766 and 4872 were identified as methyl 4-methylnonanoate and methyl 4-methylhexadecanoate respectively.

2.2.6.2 Aromatic esters

Unlike the mass spectra of aliphatic esters, prominent ions resulting from McLaffery rearrangement are not found in the mass spectra of aromatic esters. However, alpha fission and subsequent fragmentations are dominant in the mass spectra of aromatic esters.

The mass spectrum of component 3375 (Fig. 2.105) has a base peak at *m/z* 149. The ions at *m/z* 39, 51, 65, and 77 indicate the presence of a benzene ring. Component 3375 was identified as diethyl phthalate by computerised library search. This component is suspected to be an artefact possibly

introduced into the extract from a synthetic polymeric substance.

The ion at *m/z* 177 is formed by expulsion of an ethoxy radical through alpha fission.

Deuterium labelling experiments revealed that the base peak in ethyl and higher alkyl phthalates, which is usually the *m/z* 149 ion, is formed by non-selective transfer of alkyl hydrogens to the ionized oxygen. The formation of these and other ions follow the following routes[50]:

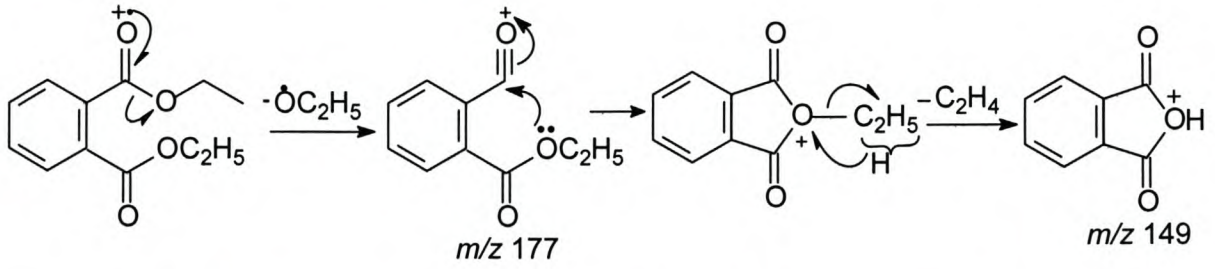

Further expulsion of a molecule of CO from the *m/z* 149 ion gives rise to the ion *m/z* 121[51].

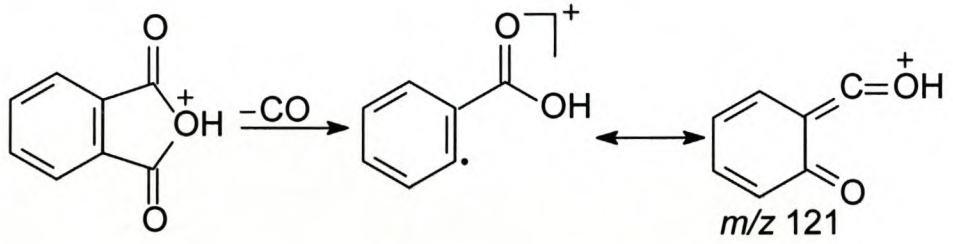

2.2.7 Amides

2.2.7.1 Aliphatic amides

Because of the presence of the carbonyl group, amides undergo similar fragmentations as aldehydes and ketones do. Preference for cleavage depends on the length of the acyl part and type and length of the substituents attached to the nitrogen atom.

Similar to aldehydes, α-cleavage is dominant for C_1-C_3 primary amides. This cleavage also occurs in long-chain amides giving rise to an *m/z* 44 ion of medium to low intensity[52].

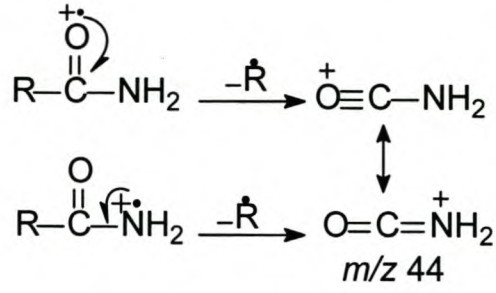

The base peak in straight chain amides higher than propionamide is formed by a McLafferty rearrangement which gives the *m/z* 59 ion[53] (because of the presence of an odd number of nitrogen atoms the *m/z* value is odd).

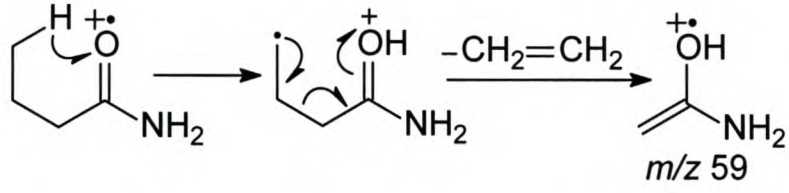

The presence of alkyl substituents at the α-position shifts the base peak to *m/z* 73 or *m/z* (73 + 14n) depending on the type of the substituents on the α-carbon.

Primary amides higher than propionamide usually give a moderately abundant *m/z* 86 ion as a result of formation of a five-membered ring. The reason for the relatively high abundance of this ion, which forms as follows, is the stability afforded by the ring system[54].

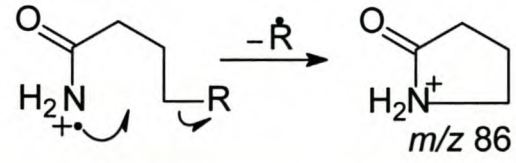

Secondary and tertiary amides, similar to tertiary amines, undergo double cleavage with hydrogen rearrangement. This cleavage of a C-C bond beta to the nitrogen atom followed by carbonyl C-N bond fission and hydrogen rearrangement, leads to the formation of the *m/z* 30 or (30 + 14n) ion.

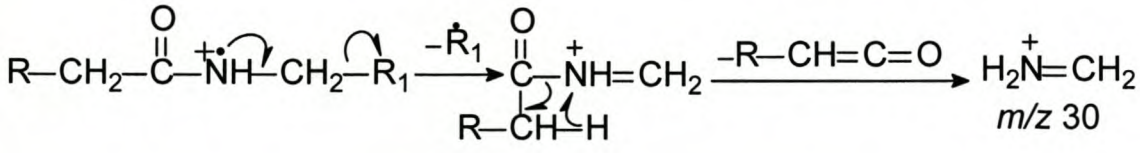

Deuterium labelling experiments with butylacetamide[55] showed that the source of hydrogen atom is usually the acetyl carbon, but as the chain-length of the acyl part of the amide increases, the hydrogen is randomly abstracted via either a 4-membered or a 6-membered ring transition state with the former dominating over the latter[56].

Component 1016 with a molecular ion at *m/z* 101 and base peak at *m/z* 59 in its mass spectrum (Fig. 2.106) was identified as pentanamide. The base peak is because of McLafferty rearrangement accompanied by "McLafferty + 13" rearranged ion at *m/z* 72. The ions at *m/z* 44 and 86 are formed by simple α-cleavage and five-membered ring formation respectively.

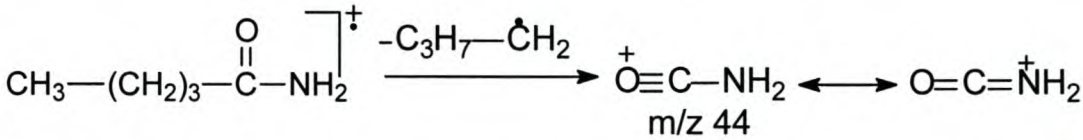

The mass spectrum of component 1552 (Fig. 2.107), which was identified as N-pentylacetamide, has *m/z* 129 as its molecular ion. The base peak at *m/z* 30 is because of C-C fission next to the nitrogen atom followed by hydrogen rearrangement from the acyl part. The formation of the ions at *m/z* 43 and *m/z* 72 can be ascribed to α-cleavage with respect to the carbonyl group and nitrogen atom respectively.

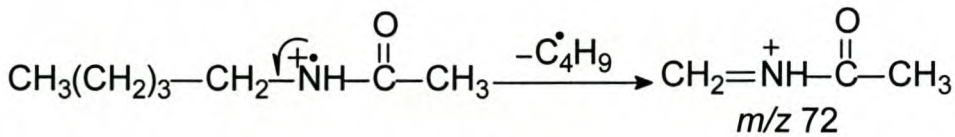

The ion at *m/z* 60 (CH_3-C·OH-NH_2) is probably due to a double McLafferty rearrangement with *m/z* 73 as "McLafferty + 13" rearranged ion. The *m/z* 44 ion is formed as a result of the inductive effect of the electron-deficient nitrogen atom in the *m/z* 86 ion and is made energetically favourable by the formation of a three-membered ring[57].

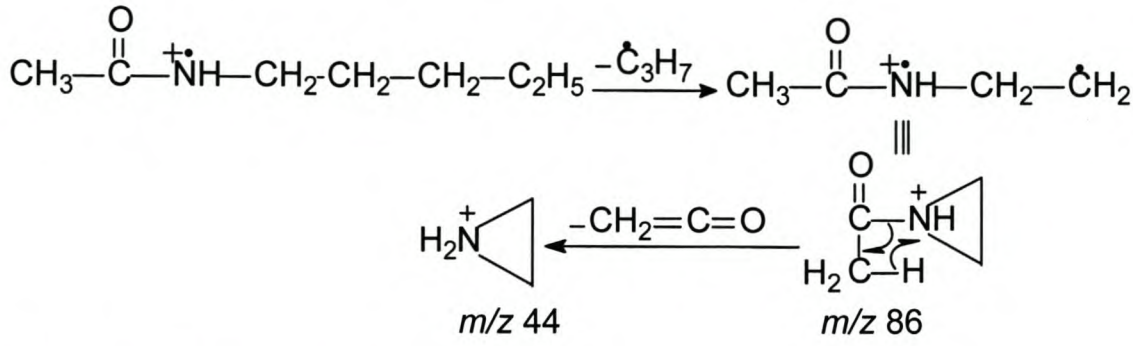

2.2.7.2 Aromatic amides

The mass spectrum of component 2503 (Fig. 2.108) is characterised by prominent ions at *m/z* 51 and 77, which are indicative of the presence of an aromatic ring, and *m/z* 105 and 121. The molecular ion at an odd mass of *m/z* 121 indicates the presence of an odd number of nitrogen atoms in the component. The only aromatic amide with such a molecular ion at *m/z* 121 is unsubstituted benzamide. Component 2503 was therefore identified as benzamide.

The base peak at *m/z* 105 in the spectrum of this compound is because of the benzoyl ion which is the result of the expulsion of an amine radical through α-fission[58]. Subsequent ejection of CO from the benzoyl ion gives the $C_6H_5^+$ ion (*m/z* 77). The ion at *m/z* 51 is the result of loss of C_2H_2 from $C_6H_5^+$.

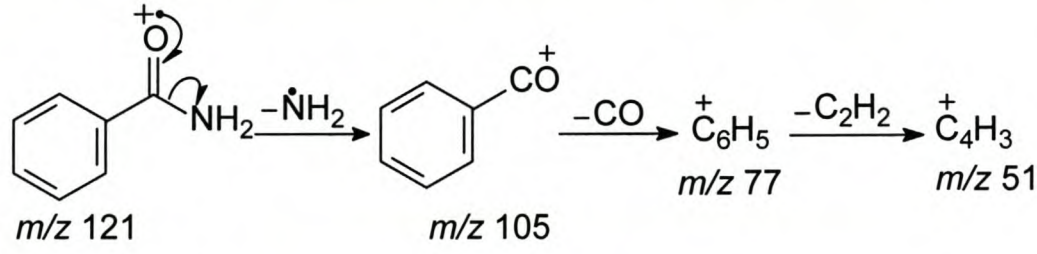

The ion at *m/z* 44 is derived from α-fission resulting in the expulsion of a phenyl radical:

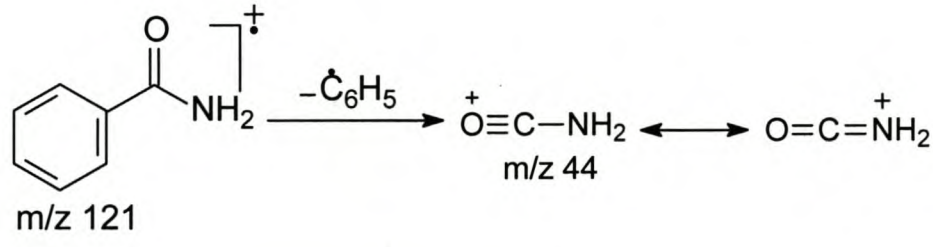

When the injection port is too hot, benzamide sometimes undergoes pyrolytic dehydration prior to ionization to give an abundant ion at *m/z* 103. This ion was found to arise because of the thermal formation of benzonitrile which in turn loses HCN to give an abundant ion at *m/z* 76 $(C_6H_4)^+$ [59].

$$C_6H_5CO{-}NH_2 \longrightarrow C_6H_5C{\equiv}N^+ + H_2O$$

$$\underset{m/z\ 103}{C_6H_5C{\equiv}N^+} \longrightarrow \underset{m/z\ 76}{C_6H_4^+} + HCN$$

The mass spectrum of component 3102 (Fig. 2.109) has the *m/z* 104 and 163 ions as its base peak and molecular ion peak respectively. The odd numbered molecular ion together with the *m/z* 30 ion indicates the component to be either an amine or amide. However the presence of a moderately abundant *m/z* 43 ion together with the ion at *m/z* 30 confines the possible structure of the component to that of a secondary amide. Besides, ions at *m/z* 91, 65, 51 and 39 are those formed from a benzyl group. Therefore thi

s component was identified as *N*-(2-phenylethyl) acetamide on account of its mass spectrum and a computer library search.

The base peak is formed by hydrogen rearrangement followed by expulsion of an acetamide molecule via a 4-membered transition state. The high abundance of this ion is because of higher stability of its conjugated system.

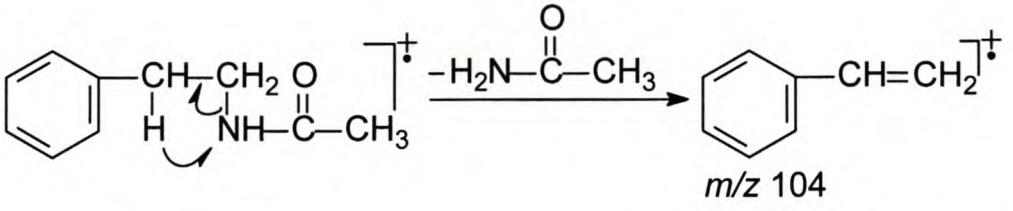

m/z 104

While the *m/z* 59 ion is formed by McLafferty rearrangement, the *m/z* 72 ion in which the charge remains with the nitrogen atom is due to α-cleavage triggered by the nitrogen atom.

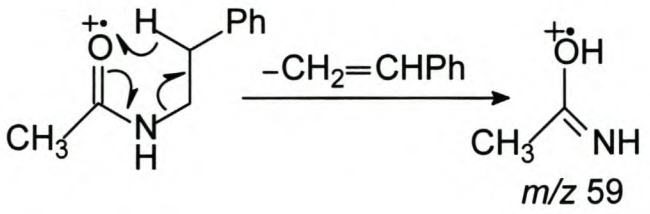

m/z 59

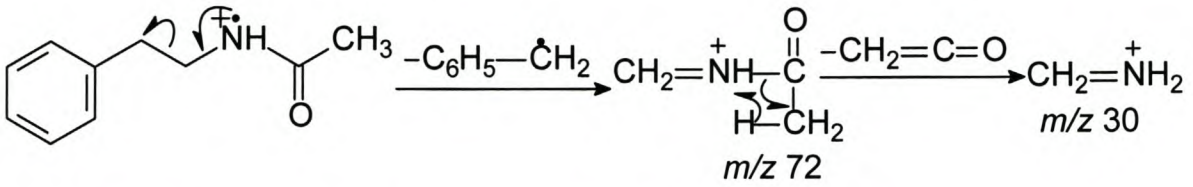

m/z 72 *m/z* 30

The mass spectrum of component 3128 (Fig. 2.110) is characterised by an abundant molecular ion at *m/z* 186. The high abundance of the molecular ion together with the *m/z* 91, 77, 65, 51, and 39 ions indicates the presence of an aromatic ring. On account of a computer library search component 3128 was tentatively identified as *N*-1-isoquinolinylacetamide.

While the *m/z* 185 ion is the $(M - 1)^+$ ion, the highly abundant ion at *m/z* 171 is formed through the removal of a methyl radical by α-fission with respect to the carbonyl group.

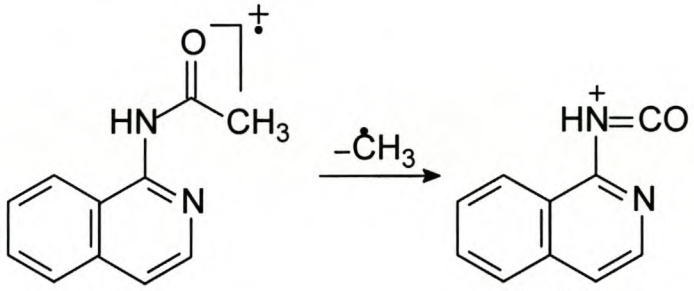

m/z 186 m/z 171

The ions at *m/z* 144 and *m/z* 117 are most probably formed via the following mechanism:

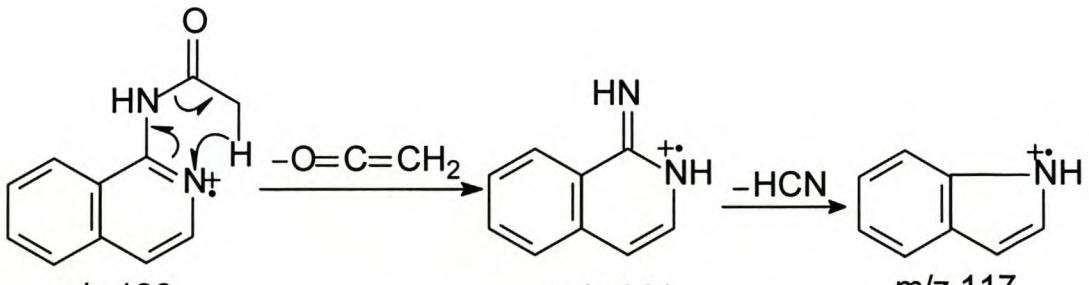

m/z 186 m/z 144 m/z 117

2.2.8 Amines

2.2.8.1 Aliphatic amines

As a result of the nitrogen rule, a compound containing an odd number of nitrogen atoms can easily be identified if the molecular ion is visible, since it occurs at an odd *m/z* value.

As in the case of other heteroatom-containing compounds (especially alcohols and sulfides), fragmentation is induced by the removal of one of the unbonded electrons of the nitrogen atom. Fragmentation is usually brought about by C-C bond fission between the α and β carbon atoms[60].

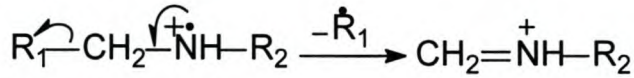

The fragmentation pathway shown above gives the most abundant ions in the spectra of primary, secondary and tertiary amines with preferential discharge of the largest alkyl group. In a situation in which no other alternative exists apart from the removal of a hydrogen atom, a prominent ion at *m/z* $(M - 1)^+$ is usually formed, as in the spectrum of methylamine[61].

Although α-fission that gives rise to the base peak at *m/z* 30 is dominant in primary amines, β- and γ-cleavages usually give more intense ions as the chain length of the amines increases. Unlike alcohols and thiols in which the ion resulting from δ-cleavage is more intense than those from β- and γ-cleavages because of the formation of a stable five-membered ring, primary amines give prominent ions because of fission at the ε-position, suggesting that for amines the formation of a six-membered ring is more favourable than that of a five-membered ring[62].

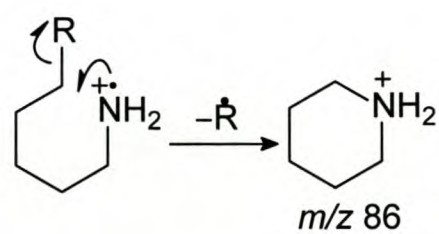

m/z 86

In straight-chain alkyl secondary and tertiary amines an ion with *m/z* (30 + 14n) is usually observed. Since this ion is formed as a result of a rearrangement, it is not as intense as the corresponding one found in primary amines. In α-substituted secondary and tertiary amines, however, it is observed as the most abundant ion[63]. In this process α-fission and subsequent cleavage of an N-C bond on the opposite side occurs with hydrogen rearrangement to give an immonium ion. Deuterium labelling experiments[64] showed that there is random selection for hydrogen rearrangement whenever alternatives exist.

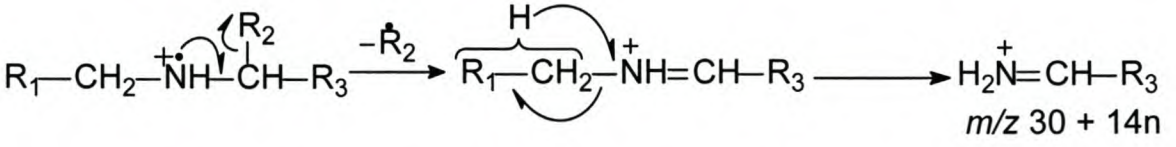

Component 41, having a base peak at *m/z* 58 and molecular ion peak at *m/z* 59 in its mass spectrum (Fig. 2.111), was identified as trimethylamine. Since there is no C-C bond adjacent to the nitrogen atom the only possibility is cleavage of a C-H bond, which in fact gives the base peak at *m/z* 58. The moderately abundant ion at *m/z* 42 is derived from $(C_2H_4N)^+$ and the ion at *m/z* 30 to the rearranged $(CH_2{=}NH_2)^+$ ion.

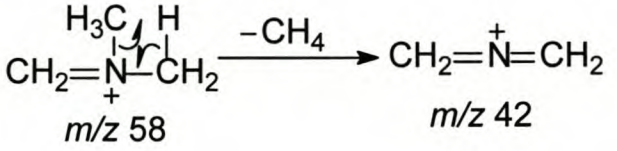

2.2.8.2 Aromatic Amines

The presence of a molecular ion at *m/z* 119 and base peak at *m/z* 118 in the mass spectrum of component 1090 (Fig. 2.112) reveals the existence of a stable $(M-1)^+$ ion. The ions at *m/z* 39, 51, 65, 77, and 91 indicate the presence of an aromatic ring in this compound. Therefore *N*-(benzylidene)methyl imine, as proposed by a computer library search, was considered a likely structure for component 1090.

The formation of the more abundant ions in this spectrum most likely occurs through the following fragmentation:

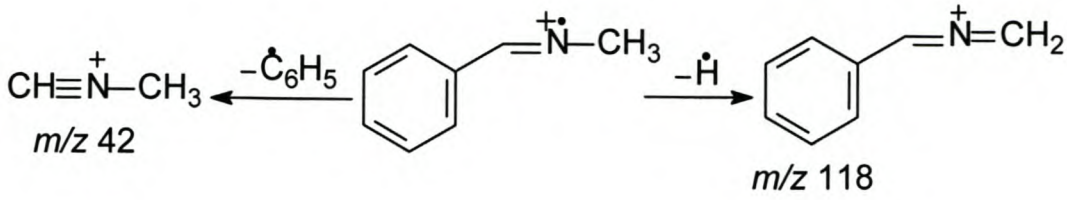

The rearrangement of a hydrogen atom through a 4- or 6-membered ring transition state, followed by β-fission with respect to the ring, is assumed to be the source of the *m/z* 91 ion:

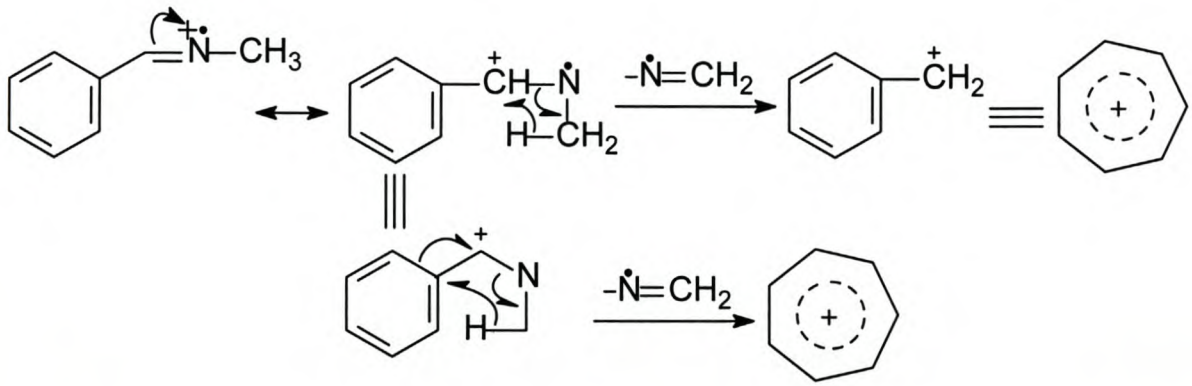

The presence of ions at *m/z* 65 and *m/z* 39 supports the generation of the tropylium ion in the above reaction mechanism[65].

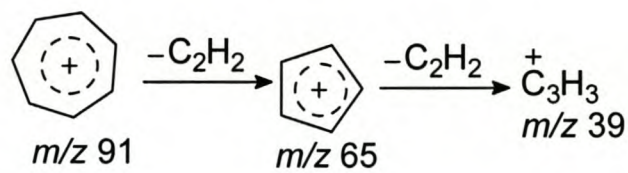

2.2.9 Nitriles

2.2.9.1 Aliphatic nitriles

In this class of compounds, with the exception of the first two members, the molecular ion is very weak but readily discernible. Frequently the molecular ion for a nitrile is surrounded by the more intense *m/z* $(M + 1)^+$ and $(M - 1)^+$ ions suggesting higher stability of the paired-electron ions over their unpaired-electron counterparts[66].

Because of the similarity between the dissociation energy of a hydrogen atom at C2 of nitriles and allylically or benzylically bound hydrogen, the $(M - 1)^+$

ion can be represented as a hybrid of two resonance forms[67]:

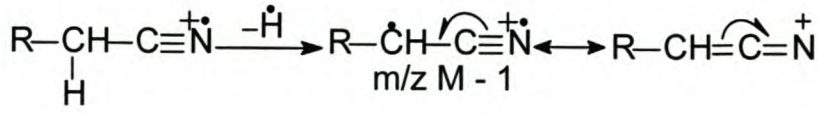

Another characteristic ion in the spectra of aliphatic nitriles is the pressure-dependent ion at *m/z* $(M+1)^+$. Since this ion is produced through capture of a hydrogen atom by the molecular ion in the course of ion–molecule interaction, its presence can be confirmed by injection of a relatively higher proportion of a sample.

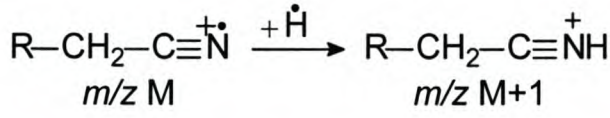

Like other unsaturated heteroatom-containing compounds, such as aldehydes, the mass spectra of aliphatic nitriles show similar fragmentation patterns with respect to β-fission and hydrogen rearrangement but α-fission is virtually absent in the nitriles.

The base peak in the spectra of unbranched alkyl nitriles in the range of C_4-C_{11} occurs at *m/z* 41. This ion arises from β-bond cleavage relative to the nitrogen atom following transfer of a single hydrogen atom. Since this process does not occur in propanenitrile, the rearranged hydrogen atom must come from the γ-carbon atom, most likely through a six-membered transition state[68].

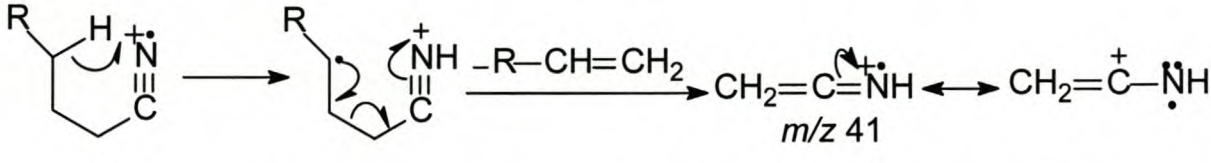

This *m/z* 41 ion and its homologues $[(C_nH_{2n+1})CN]^+$ (*m/z* 55, 69, 83, ...,) are intense ions that are formed by expulsion of an olefin. As the length of the alkyl chain increases, loss of an alkyl group without rearrangement of a hydrogen atom dominates, which leads to the formation of fragment ions having the general formula $[(CH_2)_nCN]^+$ with n values 5, 6, or 7 as the most abundant ones. This series of ions is terminated at M - 1[69].

Aliphatic nitriles give characteristic ions at $(M - 28)^+$ arising from the

expulsion of an ethylene molecule. Labelling experiments showed that the expelled carbon atoms are either C2 and C3 through a 4-membered transition state or C3 and C4 through a 6-membered transition state. When the expelled ethylene is from C3 and C4 the molecular ion must exist as a mesomeric form in order to satisfy the spatial requirements for the commencement of the expulsion[70].

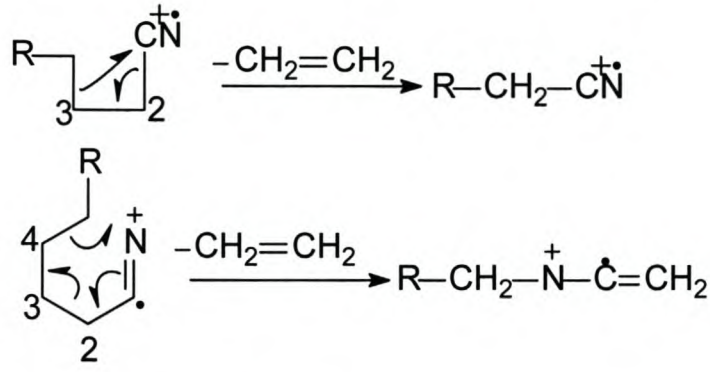

Expulsion of C_2H_4 reaches its maximum in hexanenitrile whereupon elimination of higher olefins dominate, leading to production of an *m/z* 97 ion. This characteristic ion which sometimes is the base peak for C_{10} or higher nitriles, is formed in a process involving a six-membered cyclic transition state. The driving force for this fragmentation is assumed to be the ejection of a stable olefin molecule coupled with stabilization of the unpaired-electron species through cyclization[71].

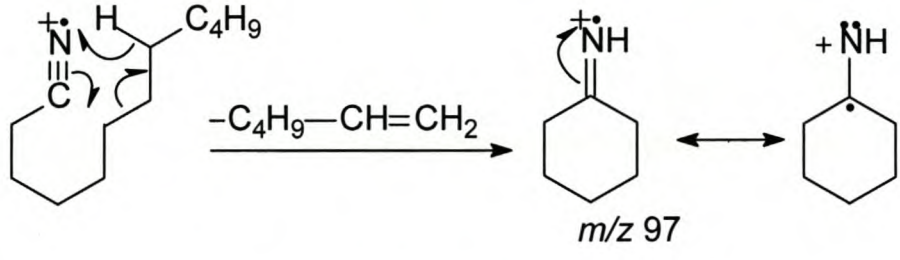

The mass spectrum of component 94 (Fig. 2.113) has a molecular ion peak at *m/z* 69. On account of a computer library search this component was identified as 2-methylpropanenitrile. The abundant *m/z* 68 and *m/z* 54 ions are formed as a result of loss of respectively a hydrogen atom and methyl radical from the molecular ion.

The base peak at *m/z* 42 is formed by the loss of a molecule of HCN

whereas the *m/z* 41 ion is the result of a McLafferty rearrangement.

In the EI mass spectrum of component 4113 (Fig. 2.117), to which the structure undecanenitrile was assigned, the *m/z* 181 ion is the molecular ion accompanied by *m/z* 180 and *m/z* 182 as $(M - 1)^+$ and $(M + 1)^+$ ions respectively. The ions at *m/z* 40, 54, 68, ..., 180 belong to the $[(CH_2)_nCN]^+$ series.

A study of the mass spectra of components 181, 479 and 1696 (Fig. 2.114 - 2.116) resulted in the identification of these components as pentanenitrile, hexanenitrile, and nonanenitrile respectively and this was confirmed by spectral library data.

2.2.9.2 Aromatic nitriles

The mass spectrum of component 832 (Fig. 2.118) is characterised by a molecular ion at *m/z* 103 which is also the base peak. The presence of *m/z* 77 and 51 ions together with the molecular ion led to the identification of component 832 as benzonitrile. This was confirmed by a computer library search.

The abundant *m/z* 76 ion is formed by expulsion of a molecule of HCN. Further expulsion of an acetylene molecule from the *m/z* 76 ion produces the ion at *m/z* 50.

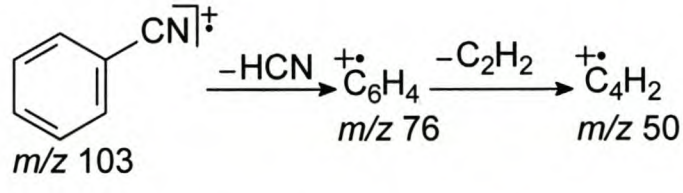

Component 1488 has a base peak at *m/z* 117 in its mass spectrum (Fig. 2.119). The *m/z* 90 and 91 ions which are most likely formed by loss of HCN and a CN radical respectively, support the identification of the component as an aromatic nitrile. Although phenylacetonitrile and the three isomers of methylbenzonitrile (*o*-, *m*-, and *p*- isomers) have the same fragmentation pattern in their mass spectra, phenylacetonitrile was considered to be the most likely structure in the light of the other aromatic acids identified in the secretion

(section 2.2.5).

2.2.10 Sulfur-containing compounds

2.2.10.1 Hydrogen sulfide

The presence of a sulfur atom in a compound can easily be deduced from its mass spectrum by considering the contribution of the natural ^{34}S-isotope (4.4%) to the intensity of $(M + 2)^+$ and fragment ions containing a sulfur atom[72]. The abundance of the molecular ions of sulfur-containing compounds is much higher than those of oxygen-containing analogues because of lower electronegativity of the sulfur atom.

Similarities in chemical properties between oxygen and sulfur atoms are manifested in the identical fragmentation modes of their respective compounds. A notable exception is the expulsion of SH (sulfhydryl) from the parent ion of sulfur containing compounds. Bond fission occurs predominantly at the β-position relative to the sulfur atom and rearrangement ions are usually observed.

From its simple mass spectrum (Fig. 2.120) component 28, having both its base peak and molecular ion peak at *m/z* 34, was identified as hydrogen sulfide and this was in excellent agreement with a computer library search. The ions at *m/z* 36, 33, and 32 are ascribed to $(M + 2)^+$, $(M - H)^+$ and $(M - 2H)^+$ respectively.

2.2.10.2 Thiols

In primary thiols C-C bond fission beta to the sulfur atom occurs leading to the formation of an *m/z* 47 ion having the composition CH_3S^+[73].

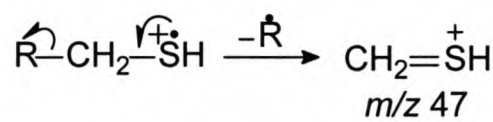

When there is no available β-carbon, as in methanethiol (R = H), expulsion of hydrogen would be the only alternative for the formation of this ion.

The ion at *m/z* 47 is normally accompanied by a homologous ion at *m/z*

61 because of the high probability of γ-cleavage[74].

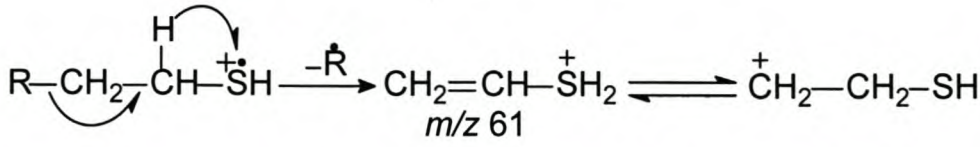

Another unique fragmentation pattern for primary thiols is loss of H_2S similar to the elimination of water from alcohols. Isotope labelling experiments using pentanethiol showed that, unlike alcohols in which predominantly 1,4-eliminations occur, in thiols both 1,4- and 1,3-eliminations occur with comparable probabilities[75], viz 60% and 40% respectively, without any contribution from the hydrogen atoms on the α- or δ-carbon atoms.

Some of the patterns mentioned above are observed in the mass spectrum of component 37 (Fig 2.121), which was identified as methanethiol. The high abundance (4.61%) of the *m/z* 50 ion $[(M + 2)^+]$ relative to the molecular ion at *m/z* 48, revealed that this compound contains one sulfur atom. The *m/z* 47 ion is formed by β-hydrogen fission. The ions at *m/z* 46 and *m/z* 45 are formed by consecutive removal of one and two hydrogen atoms from the *m/z* 47 ion.

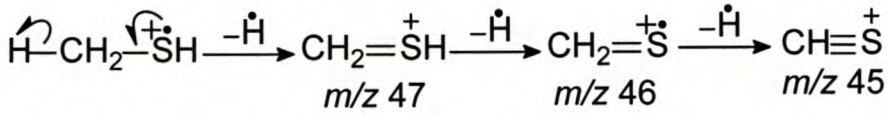

The formation of the ion at *m/z* 33 is derived by expulsion of a methyl radical from the molecular ion.

2.2.10.3 Disulfides

In disulfides the base peak is formed by fission of a C-S bond with expulsion of an olefin[76].

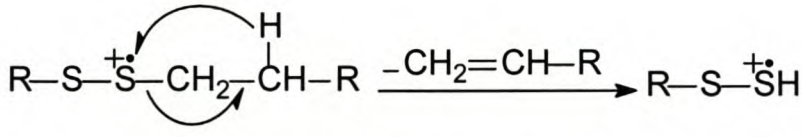

Dimethyl disulfide is an exception in that it cannot undergo such fission to expel an olefin. Instead it undergoes fragmentation in such a way that H_2S, SH,

and CH_3 radicals are readily lost.

The mass spectrum of component 202 (Fig. 2.122), which was identified as dimethyl disulfide, shows a molecular ion and $(M + 2)^+$ ion at *m/z* 94 and *m/z* 96 respectively. The high percentage abundance (8.74%) of the $(M + 2)^+$ ion relative to the base peak is a positive confirmation for the presence of two sulfur atoms. The *m/z* 79 ion is formed by loss of a methyl radical following the rearrangement of a hydrogen atom and a methyl group. Ions at *m/z* 64 (S_2^+) and *m/z* 61 ($C_2H_5S^+$) are derived from loss of two methyl groups and SH respectively. The formation of some of these ions can be formulated as follows[77]:

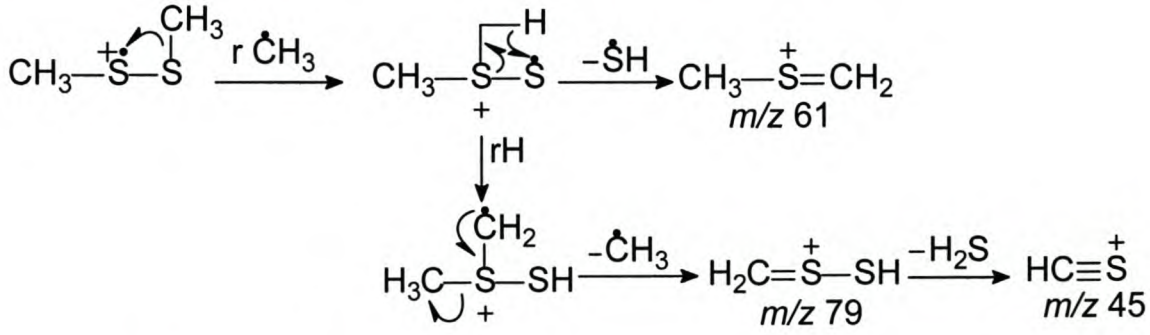

The ions at *m/z* 47 and *m/z* 46 are ascribed to CH_2SH^+ and CH_2S^+:

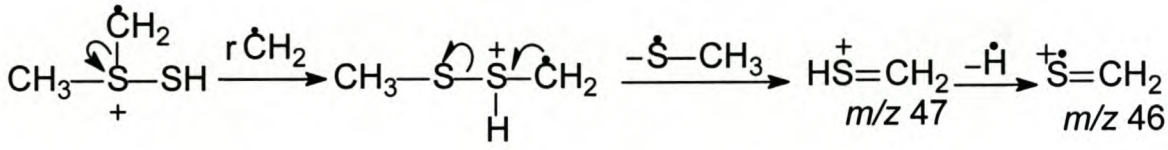

2.2.10.4 Trisulfide

Component 767 has an abundant $(M + 2)^+$ ion at *m/z* 128 in its mass spectrum (Fig. 2.123).This relatively high abundance (13.84% relative to the base peak) can only be accounted for by the presence of three sulfur atoms. The subtraction of 96 amu corresponding to three sulfur atoms from the molecular ion indicates the presence of two terminal methyl groups which is in good agreement with the identification of the compound by a computer spectral library search as dimethyl trisulfide.

At the high mass end of the spectrum the ions at *m/z* 126 and *m/z* 128 represent the molecular and $(M + 2)^+$ ions respectively. The *m/z* 111 ion is

derived from the loss of a methyl radical from the molecular ion. The prominent ions at *m/z* 79 and *m/z* 45 are ascribed to $CH_3S_2^+$ and CHS^+ respectively.

The generation of these fragment ions is likely to occur according the following pathways:

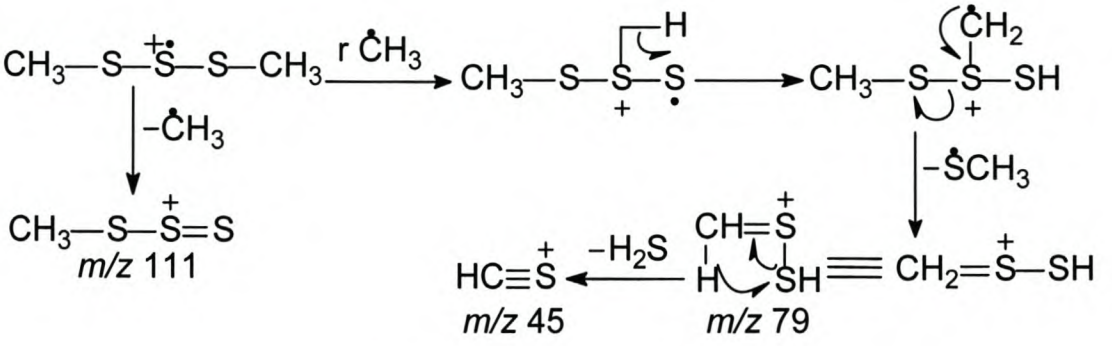

2.2.11 Miscellaneous

2.2.11.1 Lactones

The mass spectrum of component 632, which was identified as 2-dihydrofuranone has a base peak at *m/z* 42 and molecular ion at *m/z* 86 (Fig. 2.124). With the exception of the $(M - 1)^+$ ion where the charge is retained by the ring oxygen, other prominent fragment ions are formed as a result of bond fission triggered by the carbonyl oxygen.

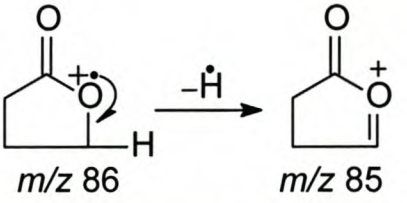

Experiments with isotope labelled carbonyl oxygen revealed that the ion at *m/z* 56 contains the carbonyl oxygen which clearly indicates two consecutive bond ruptures (5 and 3)[78].

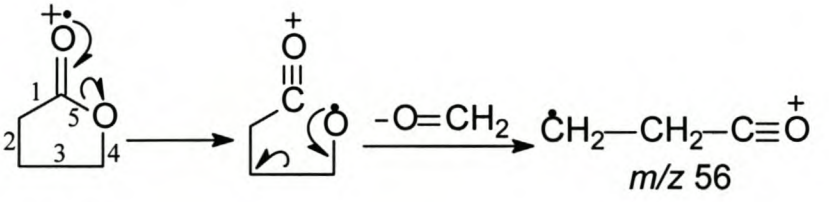

The formation of the base peak at *m/z* 42 ($C_3H_6^+$) indicates a high probability for consecutive 1 and 4 bond ruptures. The ions at *m/z* 41, 40, and 39 are formed by further dissociation of the *m/z* 42 ion[79].

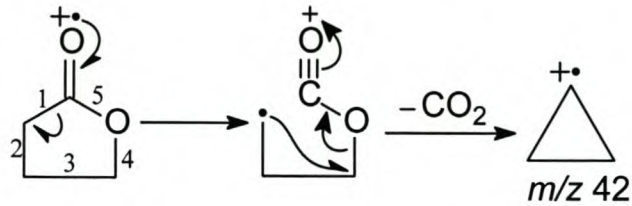

The high abundance of the *m/z* 28 ion can be accounted for by the presence of a number of pathways for its formation. It can be formed either by consecutive 1 and 3 bond ruptures or by expulsion of a molecule of CO from the *m/z* 56 ion.

Since γ-C_5 lactones have mass spectra similar to those of δ-C_5 lactones, component 779 was identified as either one of these two compounds. But the presence of less abundant ion pairs at *m/z* 70 and 71, together with the base peak at *m/z* 42 in the mass spectrum of this component (Fig. 2.125), characteristic for δ-C_5 lactones[80], ruled out the possibility of the component representing a γ-C_5 lactone.

The ions at *m/z* 70 and 71 are most probably formed by expulsion of CHO and CO respectively from the ion at *m/z* 99.The ion at *m/z* 42, which is known to contain the carbonyl oxygen[78], is formed by rupture of two bonds of the ring.

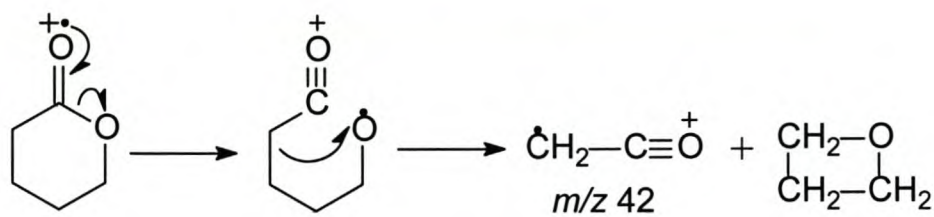

A moderately abundant ion which cannot be formed directly from the δ-C_5 lactone is found at *m/z* 85. This ion is formed due to facile rearrangement of the molecular ion of the δ-C_5 lactone to the γ-C_5 lactone from which a methyl radical is easily lost.

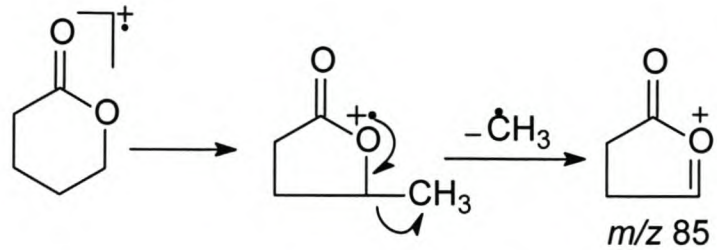

Component 779 was therefore assigned the structure 5-pentanolide.

2.2.11.2 Lactams

2-Piperidones which are unsubstituted at the nitrogen atom are characterised by prominent molecular ions accompanied by $(M - 1)^+$ ions resulting from the removal of a hydrogen radical. The presence of a ring in these compounds, which contributes to the stabilization of the ion through cyclization, leads to these M^+ ions normally appearing as base peaks.

In the mass spectrum of component 1743 (Fig. 2.129) the molecular ion is present at *m/z* 99 with the $(M - 1)^+$ ion at *m/z* 98. This component was tentatively identified as 2-piperidone on account of the molecular ion at *m/z* 99.

Analogous to 2-pyrrolidone where the hydrogen atom attached to C5 is lost in the formation of the $(M - 1)^+$ ion, the $(M - 1)^+$ ion in 2-piperidone is similarly formed by removal of a hydrogen atom from C6, the charge remaining on the nitrogen atom:

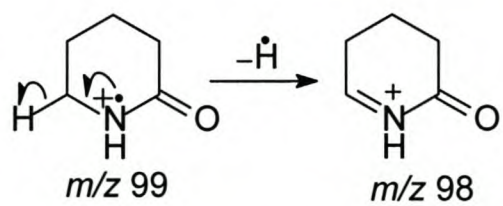

The most characteristic and abundant ions of diagnostic importance are observed at *m/z* 30, 41, 42, 43, 70, and 71. The formation of some of these ions is known to occur in the following manner[81]:

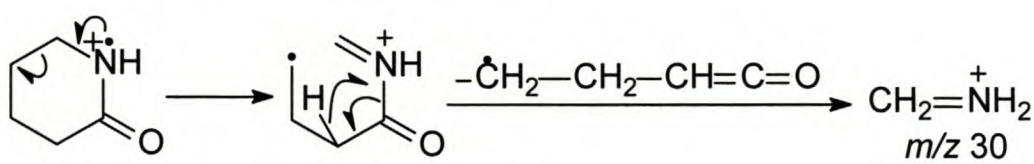

Isotope labelling experiments showed that C3 and C4 are expelled from

the molecular ion as ethylene in the formation of the *m/z* 71 ion. Further expulsion of a molecule of CO produces the *m/z* 43 ion.

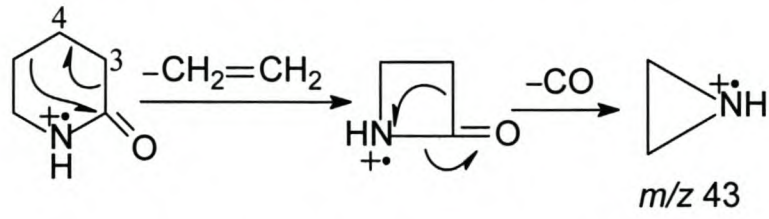

The *m/z* 70 ion which is produced by loss of 29 amu was found to have different compositions which are formed by three different mechanisms to produce the ions $C_4H_6O^+$ (84%), $C_4H_8N^+$ (14%) and $C_3H_4NO^+$ (2%) having the following structures:

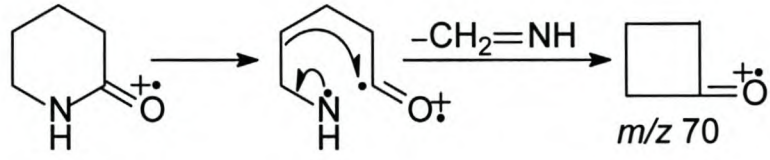

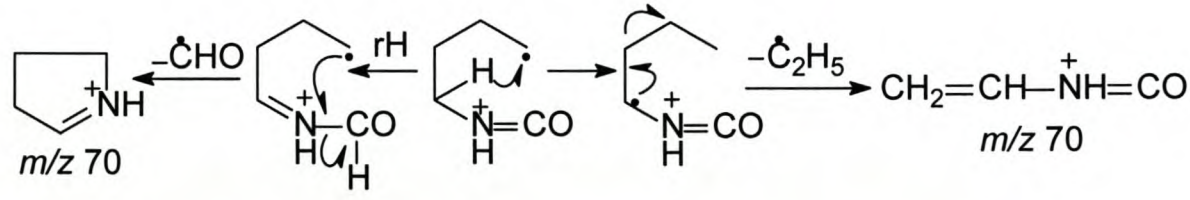

The formation of the ion at *m/z* 55 can be ascribed to transfer of a hydrogen atom from C3 followed by homolytic cleavage of the C4 - C5 bond to give the resonance stabilized ion $C_3H_3O^+$.

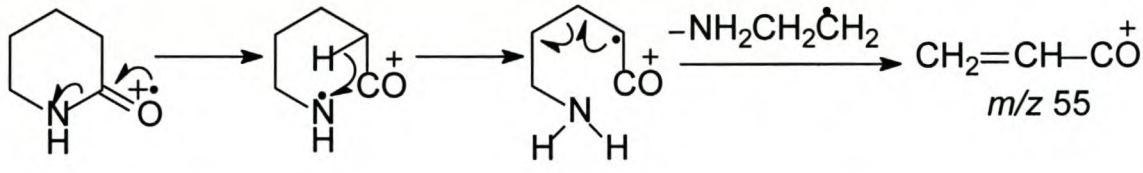

On account of its mass spectrum and excellent agreement with spectral library data, component 1743 was identified as 2-piperidone.

2.2.11.3 Pyrroles

Apart from the ambiguity arising from the presence of isobaric hydrocarbon fragments in their mass spectra, pyrroles give a simple

fragmentation pattern. If high-resolution mass spectral data are available, the assignment of structures to the ions in these spectra is relatively easy.

The mass spectrum of component 233 (Fig. 2.127), which was identified as 1H-pyrrole on account of the presence of a molecular ion at *m/z* 67 and the results of a computerised library search, has prominent ions at *m/z* 39, *m/z* 41 and *m/z* 40

According to high-resolution data the *m/z* 39 ion represents mainly $C_3H_3^+$ with a trace contribution from C_2HN^+, while the ion at *m/z* 41 is solely ascribed to $C_2H_3N^+$ which is formed as a result of the expulsion of acetylene. The ions $C_3H_4^+$ and $C_2H_2N^+$ both contribute to the ion at *m/z* 40[82].

The route for the generation of some of these ions can be formulated as follows:

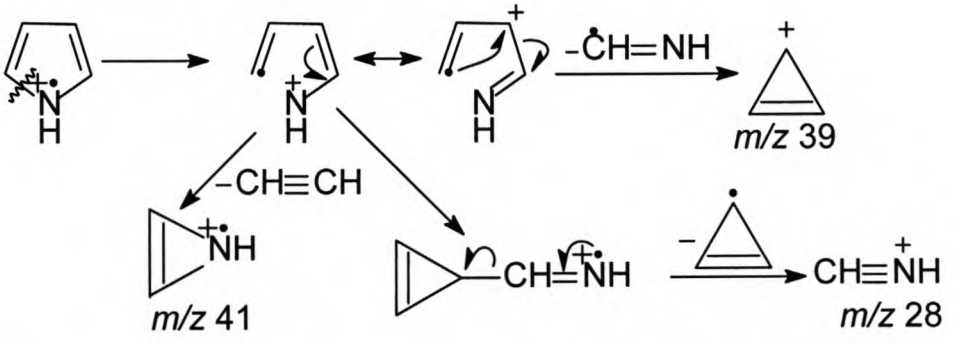

The mass spectrum of component 198 (Fig. 2.126) differs from that of component 233 in two respects. Instead of abundant ions at *m/z* 28 and 41 corresponding to $(HC{\equiv}NH)^+$ and $(C_2H_2\text{-}NH)^+$, there are ions at *m/z* 42 and 55, probably from $(HC{\equiv}NCH_3)^+$ and $(C_2H_2\text{-}NCH_3)^+$ respectively.

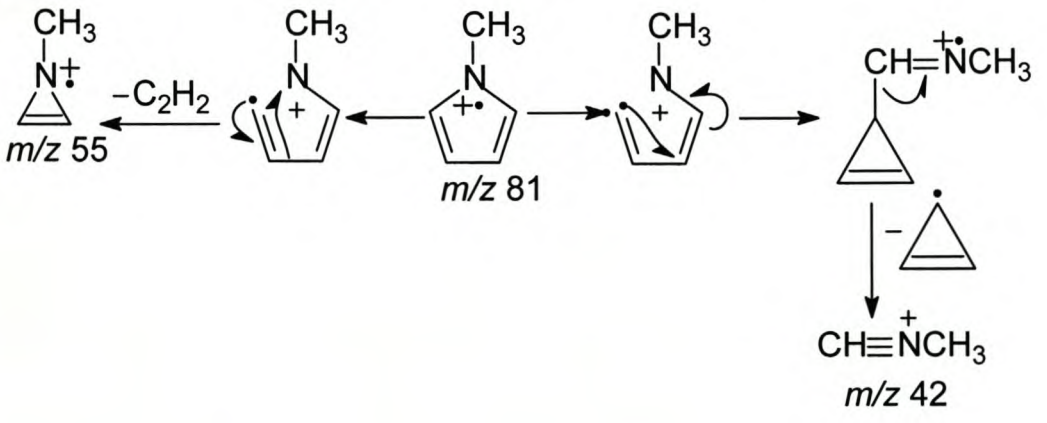

There is also an abundant ion at *m/z* 80 in the mass spectrum of component 198 which arises from the expulsion of a hydrogen atom. This ion is assumed to have the structure of the pyridinium cation, because the ring expansion is similar to the formation of the tropylium ion from toluene[83].

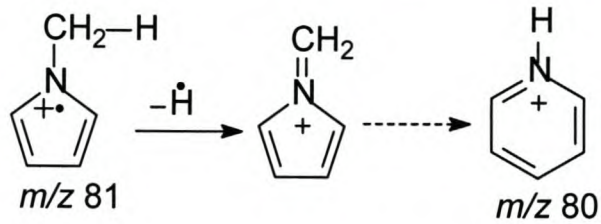

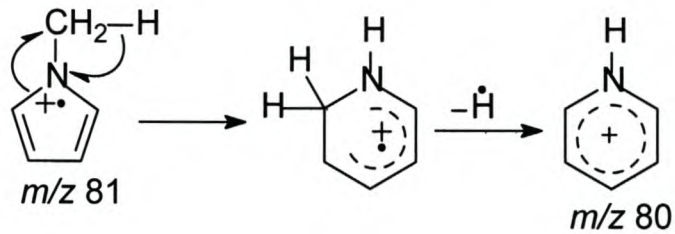

Component 198 with its molecular ion at *m/z* 81, was therefore identified as 1-methylpyrrole.

The base peak at *m/z* 94, which is the result of $(M - 1)^+$ in the mass spectrum of component 454 (Fig. 2.128), is characteristic for C-methylated pyrroles. A computer library search confirmed this component to be 2,4-dimethylpyrrole.

Unlike xylenes, which exhibit a greater tendency to lose a methyl group than a hydrogen atom, the loss of a hydrogen atom in C-methylated pyrroles far exceeds the loss of a methyl group. As a result, pyrroles, which are methyl substituted at the carbon atom have their base peak at $(M - 1)^+$ which is usually stabilized by ring expansion or resonance involving the ring.

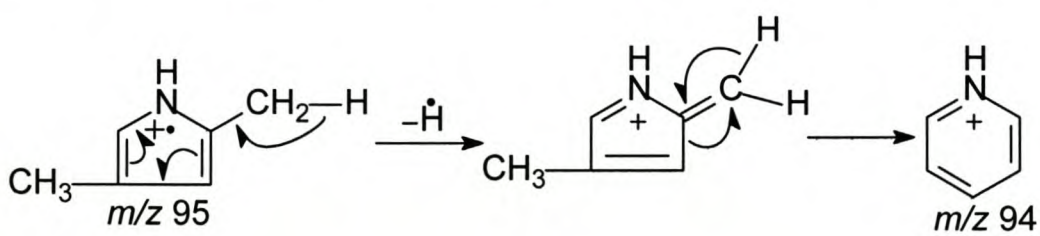

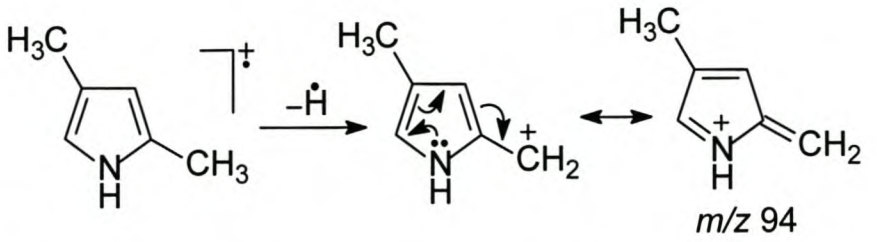

With respect to fragmentation patterns, C-methylated pyrroles follow similar routes as those of pyrroles and N-methylated pyrroles.

2.2.11.4 Indole

The molecular ion at an odd mass (*m/z* 117) in the mass spectrum of component 2219 (Fig. 2.130) indicates the presence of an odd number of nitrogen atoms. The ions at *m/z* 39, 50-52, and 63 which are typical of a benzene ring, indicate that the nitrogen atom is not incorporated in the benzene ring as a heteroatom. This component was tentatively identified as indole on account of the results of a computer library search[84].

The *m/z* 90 ion is produced by the loss of a molecule of HCN from the molecular ion[85]:

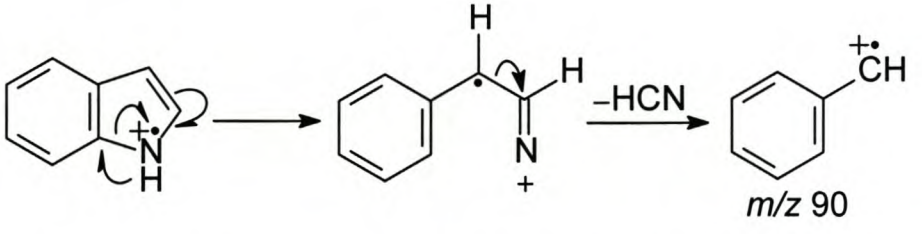

The presence of the ions at *m/z* 91, 64, and 38 is likely to favour the following mechanism:

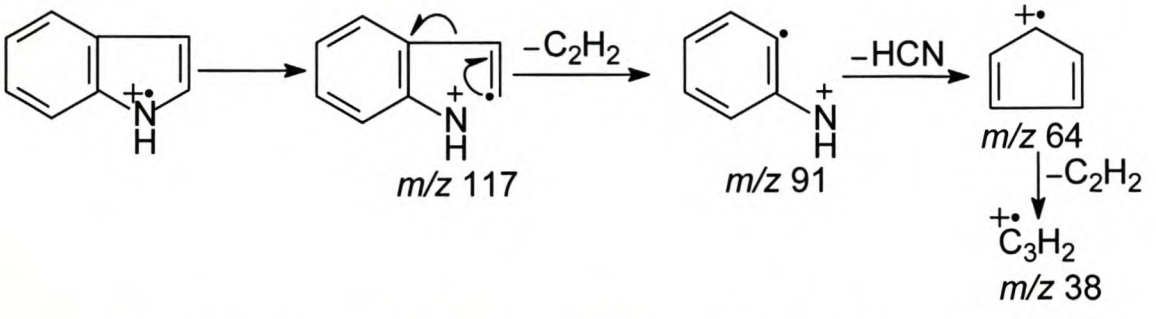

The moderately abundant ion at *m/z* 89 is most probably formed by expulsion of a molecule of HCN from the $(M - 1)^+$ ion. Further loss of a molecule

of acetylene from the *m/z* 89 ion gives rise to the *m/z* 63 ion. This mass spectrometric evidence confirms the identification of component 2219 as 1H-indole.

2.2.11.5 Quinoxaline

On account of the results of a computer library search, component 1925 with *m/z* 130 as the molecular ion in its mass spectrum (Fig. 2.131), was tentatively identified as quinoxaline. The relatively abundant *m/z* 103 and 76 ions are formed by sequential removal of a molecule of HCN from the molecular ion[86]. The formation of these ions together with the ion at *m/z* 50 is assumed to occur through the following mechanism:

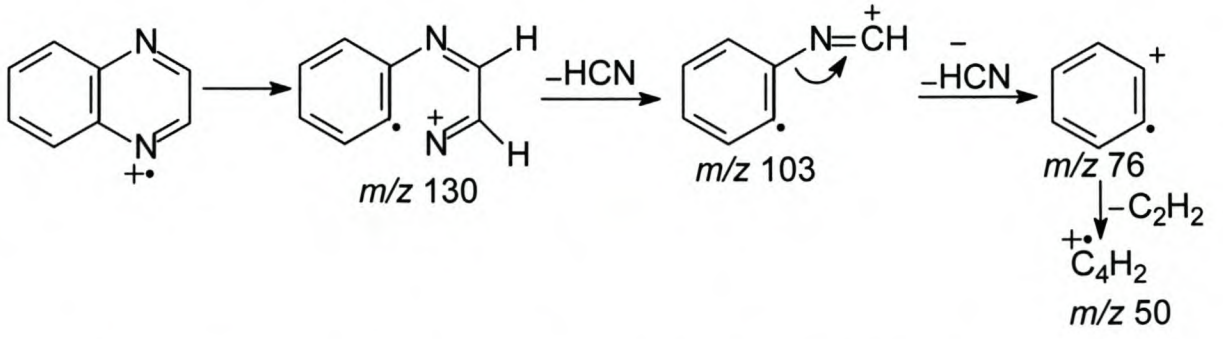

The mass spectrum of component 2356 (Fig. 2.132) differs slightly from the spectrum of component 1925 in that it has its molecular ion at *m/z* 144, i.e. at *m/z* 130 + 14 amu, and additional ions at *m/z* 117 and 129. A computer library search confirmed the identification of component 2356 as 4-methylquinazoline.

The *m/z* 129 ion is formed by fission alpha with respect to the ionized nitrogen atom, which results in the expulsion of a methyl radical. The formation of the ion at *m/z* 103 is most likely formed either by sequential loss of a methyl radical and a cyanide radical or direct elimination of methyl cyanide from the molecular ion:

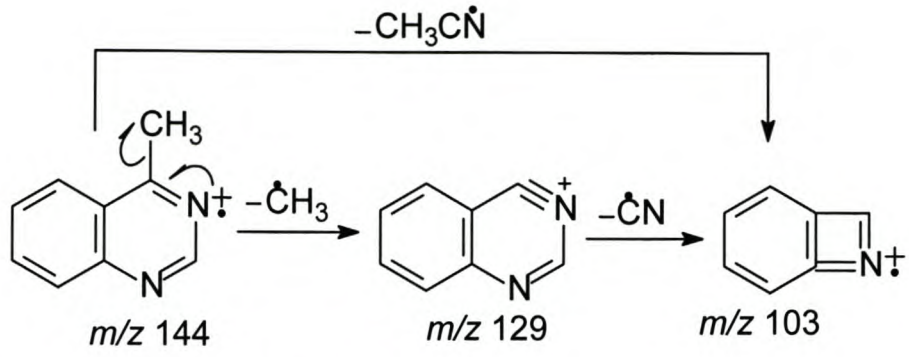

The ion at *m/z* 117 is formed by direct loss of a molecule of HCN from the molecular ion. The formation of this and some other fragment ions is assumed to occur through the following mechanism:

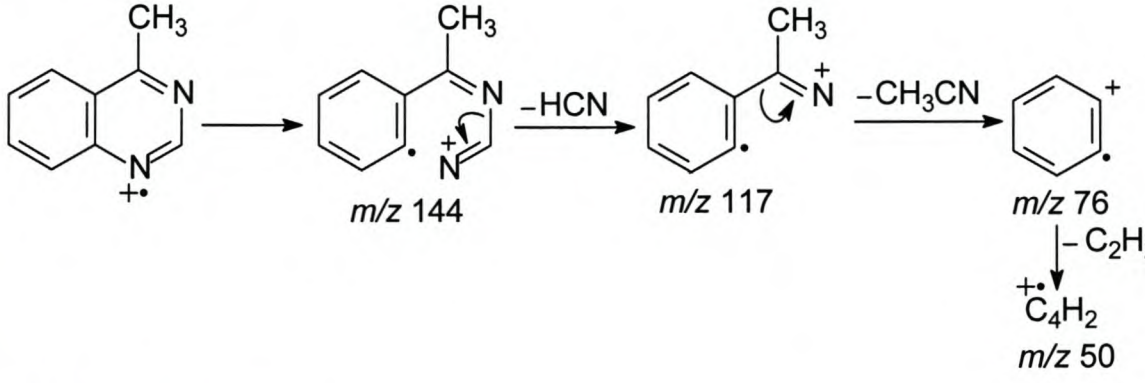

2.2.11.6 Bipyridine

On account of a study of its mass spectrum (Fig. 2.133), component 2697 was identified as bipyridine. Beta fission with respect to the ring nucleus in substituted pyridine produces less abundant ions if side chains are present at the C2 or C4 positions. Since C3 is electron rich, an abundant ion can be expected if branching is at position C3[87]. However, the low abundance of the *m/z* 78 ion restricts the possible candidate structures to 2,2'- or 4,4'- bipyridine. In good agreement with this, the computer library search suggested the component to be 4,4'- bipyridine.

The ions at *m/z* 156 and 155 represent the molecular ion and $(M-1)^+$. The *m/z* 129 and 130 ions are formed by expulsion of a molecule of HCN and C_2H_2 respectively from the molecular ion. The ion at *m/z* 103 can be formed from either of the above ions. It is most likely that the formation of these ions together with the *m/z* 78 ion favours the following mechanism:

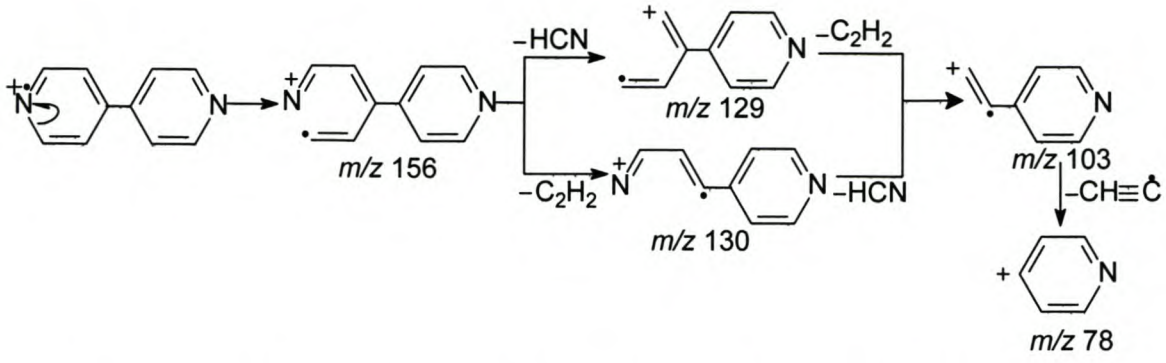

Sequential expulsion of a molecule of HCN and C_2H_2 from the *m/z* 103 ion furnishes the ions at *m/z* 76 and 50.

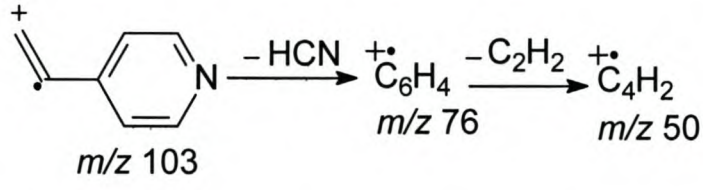

2.2.11.7 3,4-Dihydro-2-*H*-pyran

On account of a computer library search component 268 was considered to be 3,4-dihydro-2-*H*-pyran. The *m/z* 56 and *m/z* 28 ions in the mass spectrum of this component (Fig. 2.134) are formed by retro-Diels-Alder decomposition.

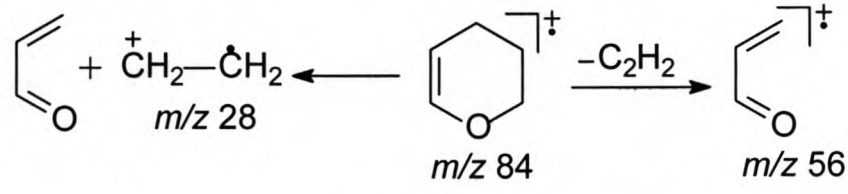

High resolution data revealed that these peaks are composed of two different ions: the *m/z* 56 peak is composed of $C_4H_8^+$ (75%) and $C_3H_4O^+$ (25%) and the *m/z* 28 peak of CO^+ (10%) and $C_2H_4^+$ (90%)[88].

The mass spectrum of this component is dominated by odd mass hydrocarbon fragment ions of which the *m/z* 55 is the most prevalent and sometimes the base peak. This ion is formed by the following mechanism[89]:

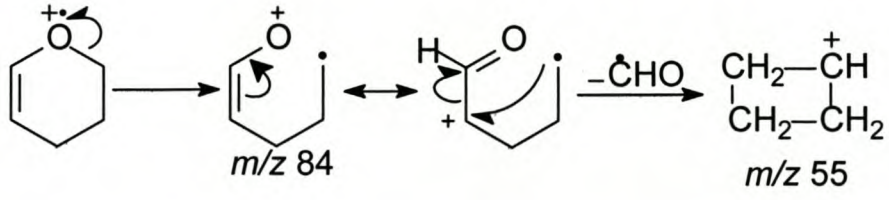

2.2.12 Wax esters

In ethyl and higher esters, the MacLafferty rearrangement can take place at either side of the functional group. In esters of long-chain fatty acids with short alcohol moieties, the acid unit is involved in the rearrangement, yielding an alkene fragment and the intense ketene hemiacetal fragment at *m/z* 74 or 88 for methyl and ethyl esters respectively. In contrast, acetates or propanoates of long chain alcohols yield an alkene fragment from the alcohol side and weak but characteristic signals indicating the protonated acid at *m/z* 61 or *m/z* 75, respectively. The fragmentation of typical saturated wax-type esters is similar; the MacLafferty rearrangement takes place at the alcohol unit. Key characteristics in the spectra of wax esters are a pronounced signal representing the protonated acid, accompanied by a much weaker signal representing the corresponding acylium ion and a clearly visible alkene fragment which is usually observed as the only even mass ion in the upper mass region apart from the molecular ion, which may be of low intensity.

The formation of the protonated acid and deprotonated alcohol in long chain esters takes place according to the following mechanisms[90]:

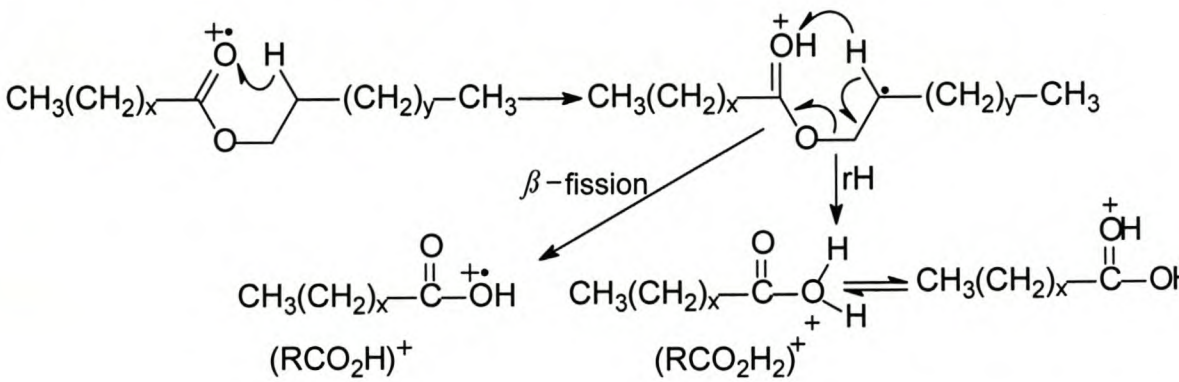

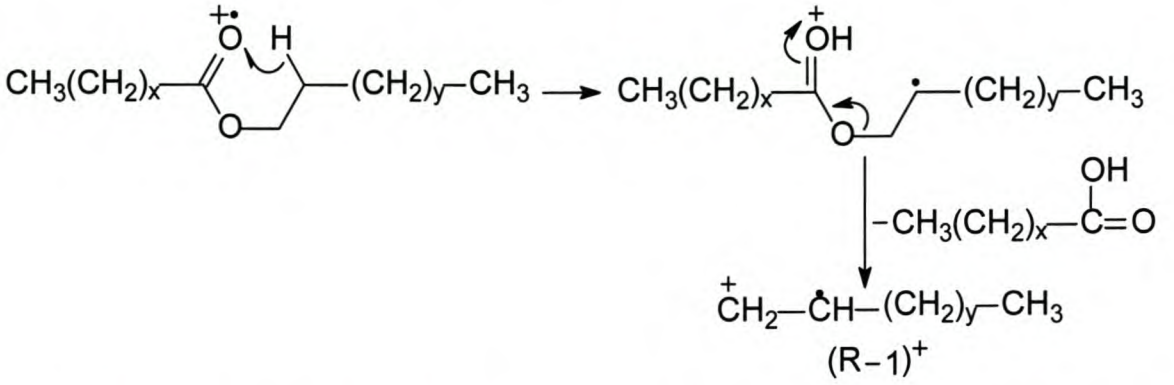

As a control for the correct interpretation of the spectrum, addition of the mass of the alkene fragment and that of the acid must give the molecular mass. Using these simple rules, mixtures of isomeric wax-type isomers which, although inseparable by GC, can easily be analyzed with respect to both qualitative (mass fragments) and quantitative (intensities of signals of protonated acid) composition, even when the compounds are not amenable to separation by GC. When the fatty acid is esterified with a secondary alcohol the relative intensities of the signals for the protonated acid and the acylium ion in the mass spectrum may be characteristically different[91].

Other important ions that are useful for structural characterisation of long-chain esters are formed by alpha fission on either side of the carbonyl group with the one in the acid unit being more intense than the one at the alcohol moiety.

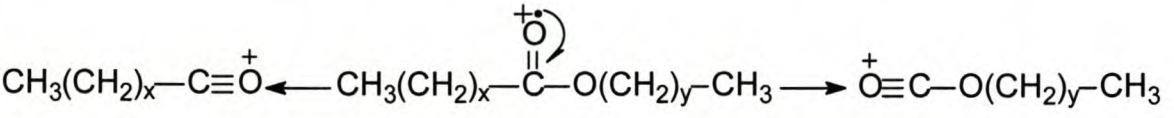

The comparatively easy cleavage of bonds attached to a tertiary carbon atom carrying a methyl side-chain, usually gives rise to two abundant ions corresponding to ions A and B which differ by 28 amu. The intermediate methoxy carbonyl ion separated by 14 amu from each of these ions is usually very small or absent, as the ion responsible for it can be formed only by a process involving double cleavage and rearrangement. The position of the methyl side chain can therefore be determined from the position of these characteristic ions in the mass spectrum[92].

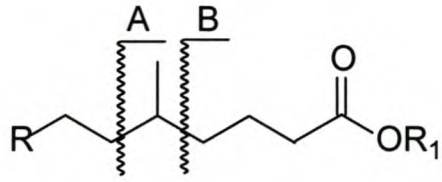

The anteiso isomers are an apparent exception, in that the abundance of the $(M - 43)^+$ ion is much higher than those of the $(M - 29)^+$ and $(M - 57)^+$ ions, suggesting that the $(M - 43)^+$ ion, which is the next most abundant ion in the high mass range, is not formed by simple cleavage involving the loss of the propyl end group of the chain. The formation of this ion is identical to those ions found in long-chain carboxylic acids[93].

Component 6834 will be discussed as a representative of the wax esters present in the secretion.

The mass spectrum of component 6834 (Fig. 2.145) has *m/z* 410 as its molecular ion and *m/z* 159 as the base peak. The *m/z* 159 ion is produced by a rearrangement of two hydrogen atoms from the alcohol chain to the acid chain to give a protonated nonanoic acid.

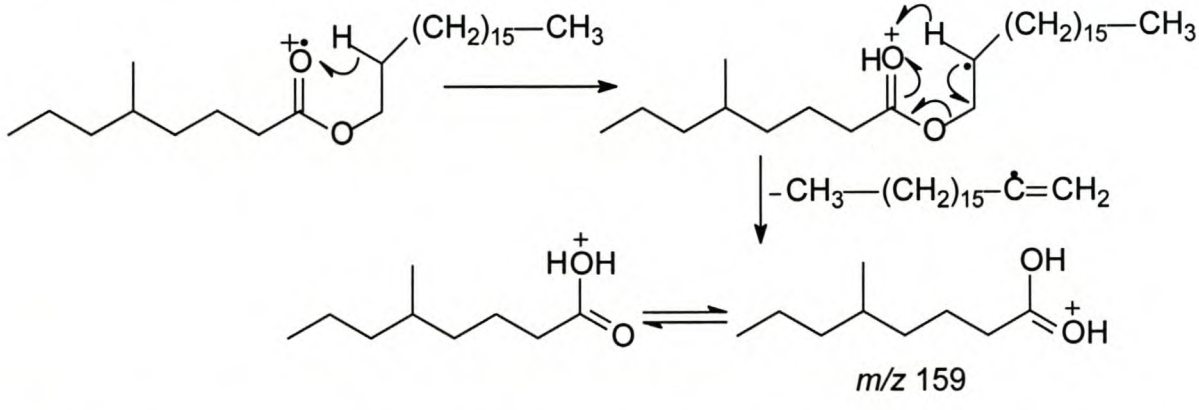

The base peak gives the number of carbon atoms in the acid moiety, k = (*m/z*-33)/14, and the molecular ion gives the total number of carbon atoms, N = (M-32)/14[94]. Hence component 6834 is an ester of nonanoic acid esterified with octadecanol [27(9;18)].

The *m/z* 252 ion represents a deprotonated alkyl moiety

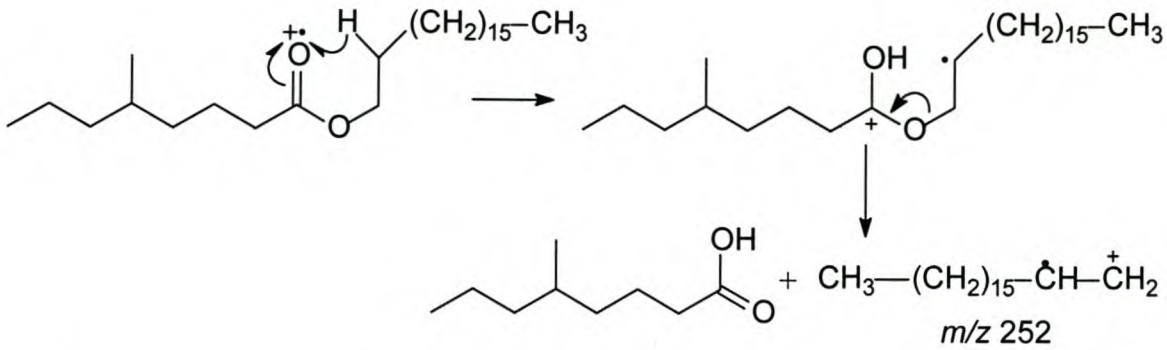

Alpha cleavage with the expulsion of the alkyl group gives a moderately intense ion at *m/z* 297.

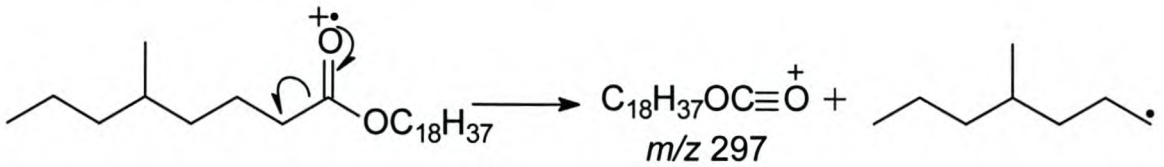

The absence of *m/z* 325 and low abundant ion at *m/z* 311 in comparison to *m/z* 326 indicates hydrogen rearrangement from the acid moiety to the alcohol moiety, followed by expulsion of an alkyl radical, is favoured instead of simple C3 - C4 bond cleavage.

The relatively facile cleavage at a tertiary carbon atom gives abundant ions at *m/z* 339 and *m/z* 367. The absence of *m/z* 353 in this component shows that methyl branching is found at C5 in the acid moiety. This is also further confirmed by the presence of *m/z* 395 which is the result of $(M\text{-}CH_3)^+$.

Other common ion fragments resulting from the saturated hydrocarbon series $(C_nH_{2n+1})^+$ are observed at *m/z* 57, 71, 85,…,

Sometimes a single peak in the TIC can represent a number of esters, having the same molecular ion. The EI spectra of saturated wax esters (R^1COOR^2) from such peaks contain a single molecular ion and a set of dominant $(R^1CO_2H_2)^+$ ions which might show a difference of 14n amu and lead to the conclusion that the individual GC peaks contain wax ester isomers with the same carbon number but different composition of the ester moiety within the wax ester because of different chain lengths of the acid and alcohol components or to different substitution patterns. Further evidence of this observation can be obtained from the $(R^2\text{-}H)^+$ ions and the acylium ions

$(R^1CO)^+$. Because of the high abundance of these ions the identification of individual wax ester isomers is possible[95].

Only one molecular ion at *m/z* 424 is present in component 6859 in the TIC of the secretion (Fig. 2.148) indicating that one or more esters containing 28 carbon atoms is present at this position in the TIC. The presence of ions at *m/z* 201 and *m/z* 187 shows the ester consists of two acid moieties; dodecanoic acid and undecanoic acid. The presence of ions at *m/z* 183 and 169, because of alpha fission, and deprotonated alcohol ions at *m/z* 224 and 238 led to the conclusion that two isomeric esters having the same number of carbon atoms but different acid and alcohol moieties are co-eluted as one peak numbered 6859 in the TIC.

The moderately intense *m/z* 311 and 339 ions, which differ by 28 amu, show the presence of methyl branching at C5 in the acid moiety. This is also further supported by the presence of an *m/z* 409 ion which is the result of expulsion of a methyl radical from the molecular ion.

Hence component 6859 is known to consist of two isomers namely 28 (12/16) and 28 (11/17) both with methyl branching at C5 in the acid moiety.

A similar approach in the interpretation of the mass spectra of other wax ester compounds present in the uropygial secretion, led to the identification of the esters as listed in Table 2.2.

Of all the esters found in the uropygial gland secretion, only component 7269 was found to be an unsaturated ester. The presence of *m/z* 201 in the mass spectrum of this component (Fig. 2.160) shows the acid moiety to be dodecanoic acid. The molecular ion at *m/z* 450 and deprotonated alcohol ion at *m/z* 250 indicate that this component is a monounsaturated ester in which the alkene functionality is found in the alcohol moiety. Further evidence for this is also obtained from the presence of ions at *m/z* 309 and 323 which otherwise are found at *m/z* 311 and 325 for all saturated long-chain esters. The high abundance of ions *m/z* 337 and *m/z* 365 relative to *m/z* 351 shows methyl branching to be present at C5 in the acid moiety.

Hence component 7269 was finally identified as an octadecenyl 7-methylundecanoate.

2.3 Conclusion

A total of 179 compounds have so far been identified in the uropygial gland secretion of the Scimitar-billed woodhoopoe. These compounds comprise both highly volatile odourous compounds and higher molecular weight hydrocarbons and wax esters as listed in Tables 2.1 and 2.2. For the wax esters the abbreviated representation for the total carbon atoms, acid moieties and alcohol moieties are used instead of the actual names.

In the reported EI mass spectra (Fig. 2.2-2.179) of these compounds the name *Phoeniculus cyanomelas*, which is the previous name for the Scimitar-billed woodhoopoe is used.

Table 2.1: Compounds identified in the secretion of the uropygial gland of the Scimitar-billed woodhoopoe.

EI mass spectrum	Component	Compound
Fig. 2.2	2264	Tridecane
Fig. 2.3	2682	Tetradecane
Fig. 2.4	3080	Pentadecane
Fig. 2.5	3460	Hexadecane
Fig. 2.6	3827	Heptadecane
Fig. 2.7	4169	Octadecane
Fig. 2.8	4525	Nonadecane
Fig. 2.9	4819	Eicosane
Fig. 2.10	5178	Heneicosane
Fig. 2.11	5458	Docosane
Fig. 2.12	5749	Tricosane
Fig. 2.13	6014	Tetracosane
Fig. 2.14	6268	Pentacosane
Fig. 2.15	6479	Hexacosane
Fig. 2.16	579	2,4-Dimethylhexane
Fig. 2.17	1151	3-Ethylpentane
Fig. 2.18	3692	2-Methylhexadecane
Fig. 2.19	3981	7-Methylheptadecane
Fig. 2.20	4070	3-Methylheptadecane
Fig. 2.21	4667	5-Methylnonadecane
Fig. 2.22	5258	7-Methylheneicosane
Fig. 2.23	5854	11-Methyltricosane
Fig. 2.24	6413	3-Methylpentacosane
Fig. 2.25	3733	Heptadecene*
Fig. 2.26	3755	Heptadecene
Fig. 2.27	4409	Nonadecene
Fig. 2.28	4427	Nonadecene
Fig. 2.29	4455	Nonadecene
Fig. 2.30	4477	Nonadecene
Fig. 2.31	4743	Eicosene
Fig. 2.32	5039	Heneicosene
Fig. 2.33	5075	Heneicosene
Fig. 2.34	5090	Heneicosene
Fig. 2.35	5346	Docosene
Fig. 2.36	5367	Docosene
Fig. 2.37	5929	Tetracosene
Fig. 2.38	5945	Tetracosene
Fig. 2.39	5970	Tetracosene
Fig. 2.40	6152	Pentacosene
Fig. 2.41	6174	Pentacosene
Fig. 2.42	6193	Pentacosene
Fig. 2.43	5862	Methyltricosene
Fig. 2.44	5010	Heneicosyne*
Fig. 2.45	5279	Docosyne
Fig. 2.46	5560	Tricosyne
Fig. 2.47	5874	Tetracosyne
Fig. 2.48	6099	Pentacosyne
Fig. 2.49	4304	1-Hexadecanol
Fig. 2.50	4959	1-Octadecanol
Fig. 2.51	5248	1-Nonadecanol
Fig. 2.52	5385	1-Docosanol
Fig. 2.53	3769	12-Methyl-1-tridecanol
Fig. 2.54	3963	13-Methyl-1-tetradecanol
Fig. 2.55	2127	3-Nonanol
Fig. 2.56	500	2-Furanylmethanol
Fig. 2.57	972	Phenol
Fig. 2.58	47	Propanal
Fig. 2.59	63	2-Methylpropanal
Fig. 2.60	77	Butanal
Fig. 2.61	113	3-Methylbutanal
Fig. 2.62	120	2-Methylbutanal
Fig. 2.63	148	Pentanal
Fig. 2.64	227	2-Methylpentanal
Fig. 2.65	292	Hexanal
Fig. 2.66	555	5-Methylhexanal
Fig. 2.67	929	Octanal
Fig. 2.68	1361	Nonanal
Fig. 2.69	3331	Nonanal *o*-methyloxime
Fig. 2.70	743	Benzaldehyde
Fig. 2.71	276	2-Hexanone
Fig. 2.72	525	2-Heptanone
Fig. 2.73	1311	5-Methyl-2-heptanone
Fig. 2.74	1600	6-Methyl-2-octanone
Fig. 2.75	1759	8-Methyl-2-nonanone
Fig. 2.76	2602	3-Dodecanone
Fig. 2.77	2200	2-Decanone
Fig. 2.78	3010	3-Tridecanone
Fig. 2.79	3030	2-Tridecanone

Fig. 2.80	3789	13-Methyl-2-tetradecanone
Fig. 2.81	4357	2-Heptadecanone
Fig. 2.82	404	4-Chloro-2-cyclopentene-1-one
Fig. 2.83	2664	Diphenylethanedione
Fig. 2.84	239	Propanoic acid
Fig. 2.85	340	2-Methylpropanoic acid
Fig. 2.86	487	3-Methylbutanoic acid
Fig. 2.87	520	2-Methylbutanoic acid
Fig. 2.88	610	Pentanoic acid
Fig. 2.89	894	4-Methylpentanoic acid
Fig. 2.90	961	Hexanoic acid
Fig. 2.91	1817	2-Ethylheptanoic acid
Fig. 2.92	1260	4-Methylheptanoic acid
Fig. 2.93	2388	4-Methyloctanoic acid
Fig. 2.94	2582	Nonanoic acid
Fig. 2.95	4044	Tetradecanoic acid
Fig. 2.96	4704	Hexadecanoic acid
Fig. 2.97	5887	Eicosanoic acid
Fig. 2.98	1868	Benzoic acid
Fig. 2.99	2179	Phenylacetic acid
Fig. 2.100	2496	3-Phenypropanoic acid
Fig. 2.101	2441	Methyl 4-methyloctanoate
Fig. 2.102	2766	Methyl 4-methylnonanoate
Fig. 2.103	3566	Methyl 2,6-dimethyloctanoate
Fig. 2.104	4872	Methyl 4-methylhexadecanoate
Fig. 2.105	3375	Diethylphthalate
Fig. 2.106	1016	Pentaneamide
Fig. 2.107	1552	Pentaneacetamide

Fig. 2.108	2503	Benzamide
Fig. 2.109	3102	N-(2-Phenylethyl)-acetamide
Fig. 2.110	3128	N-1-Isoquinolinyl acetamide
Fig. 2.111	41	N,N,N-Trimethylamine
Fig. 2.112	1090	*N*-(benzylidene)methyl imine
Fig. 2.113	94	2-Methylpropanenitrile
Fig. 2.114	181	Pentanenitrile
Fig. 2.115	479	Hexanenitrile
Fig. 2.116	1696	Nonanenitrile
Fig. 2.117	4113	Undecanenitrile
Fig. 2.118	832	Benzonitrile
Fig. 2.119	1488	Phenylacetonitrile
Fig. 2.120	28	Hydrogen sulfide
Fig. 2.121	37	Methanethiol
Fig. 2.122	202	Dimethyl disulfide
Fig. 2.123	767	Trimethyl disulfide
Fig. 2.124	632	2-Dihydrofuranone
Fig. 2.125	779	5-Pentanolide
Fig. 2.126	198	1-Methyl-1H-pyrrole
Fig. 2.127	233	1H-Pyrrole
Fig. 2.128	454	2,4-Dimethyl-1H-pyrrole
Fig. 2.129	1743	2-Piperidone
Fig. 2.130	2219	1H-Indole
Fig. 2.131	1925	Quinoxaline
Fig. 2.132	2356	4-Methylquinazoline
Fig. 2.133	2697	4,4-Bipyridine
Fig. 2.134	268	3,4-Dihydro-2-*H*-pyran

* In all the alkenes and alkynes the position of the double bond or triple bond was not determined.

Table 2.2: Wax esters identified in the uropygial secretion of the scimitar-billed woodhoopoe

Fig. No	Component	C-atoms	M^+	Acid;Alcohol	$(RCO_2H_2)^+$	$(RCO)^+$	$(R - 1)^+$
Fig. 2.135	6331	25	382	9;16	159	141	224
Fig. 2.136	6381			8;17	145	127	238
Fig. 2.137	6430	26	396	9;17	159	141	238
Fig. 2.138	6452			9;17	159	141	238
Fig. 2.139	6507			9;17	159	141	238
Fig. 2.140	6572			9;17	159	141	238
Fig. 2.141	6628			8;18	145	127	252
Fig. 2.142	6650	27	(410)*	9;18	159	141	252
Fig. 2.143	6678		410	11;16	187	169	224
Fig. 2.144	6705		(410)	8;19	145	127	266
Fig. 2.145	6834		410	9;18	159	141	252
Fig. 2.146	6776	28	424	11;17	187	169	238
Fig. 2.147	6798			11;17	187	169	238
Fig. 2.148	6859			12;16	201	183	224
				11;17	187	169	238
Fig. 2.149	6898			9;19	159	141	266
Fig. 2.150	6923			11;17	187	169	238
Fig. 2.151	6934			9;19	159	141	266
Fig. 2.152	6987			9;19	159	141	266
				11;17	187	169	238
Fig. 2.153	6949	29	438	12;17	201	183	238
Fig. 2.154	6972			12;17	201	183	238
Fig. 2.155	7023			12;17	201	183	238
				11;18	187	169	252
				10;19	173	155	266
Fig. 2.156	7089			12;17	201	183	238
Fig. 2.157	7189			11;18	187	169	252
Fig. 2.158	7244	30	452	11;19	187	169	266
Fig. 2.159	7382			12;18	201	183	252
Fig. 2.160	7269		450	12;18	201	183	250
Fig. 2.161	7393	31	467**	12;19	201	183	266
Fig. 2.162	7445		466	12;19	201	183	266
Fig. 2.163	7455		467	12;19	201	183	266
				13;18	215	197	252
Fig. 2.164	7473			12;19	201	183	266
Fig. 2.165	7485			11;20	187	169	280
Fig. 2.166	7529			12;19	201	183	266
Fig. 2.167	7600			12;19	201	183	266
Fig. 2.168	7645			13;18	215	197	252

Fig. 2.169	7543	32	481	12;20	201	183	280
Fig. 2.170	7685		480	12;20	201	183	280
Fig. 2.171	7713		481	14;18	229	211	252
Fig. 2.172	7899		481	14;18	229	211	252
Fig. 2.173	7801	33	495	14;19	229	211	266
Fig. 2.174	7946		495	15;18	243	225	252
Fig. 2.175	7999		(495)	14;19	229	211	266
Fig. 2.176	8021		(495)	12;21	201	183	294
Fig. 2.177	8047	34	(509)	15;19	243	225	266
Fig. 2.178	8135	34	(509)	15;19	243	225	266
Fig. 2.179	8346	35	(523)	15;20	243	225	280

* Molecular ions in brackets are not visible in the mass spectrum.

** Molecular ions are not protonated. As the number of carbon atoms increases the value of the molecular ion is rounded up to the next higher value.

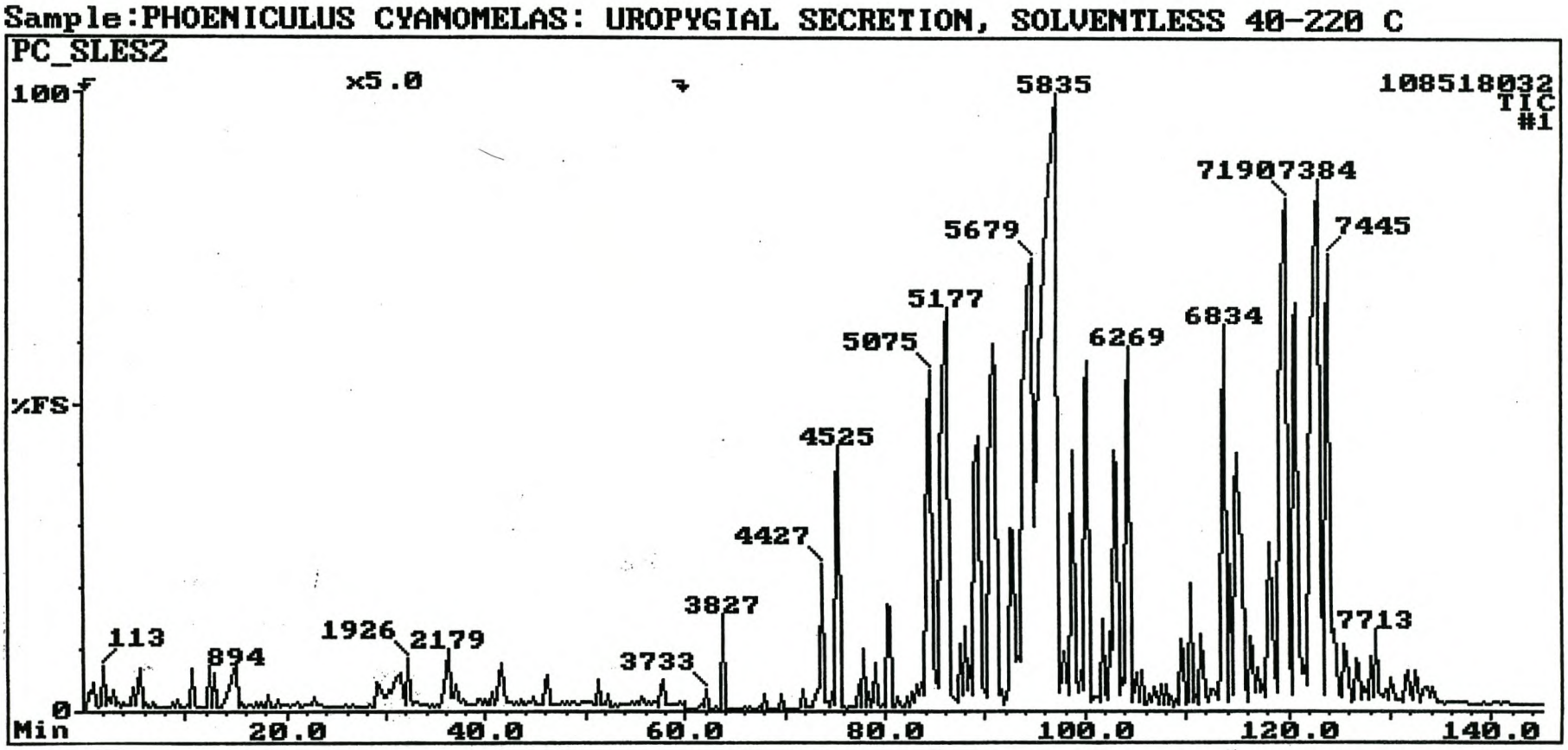

Fig. 2.1 Total ion chromatogram of the secretion obtained from the uropygial gland of the Scimitar-billed woodhoopoe.

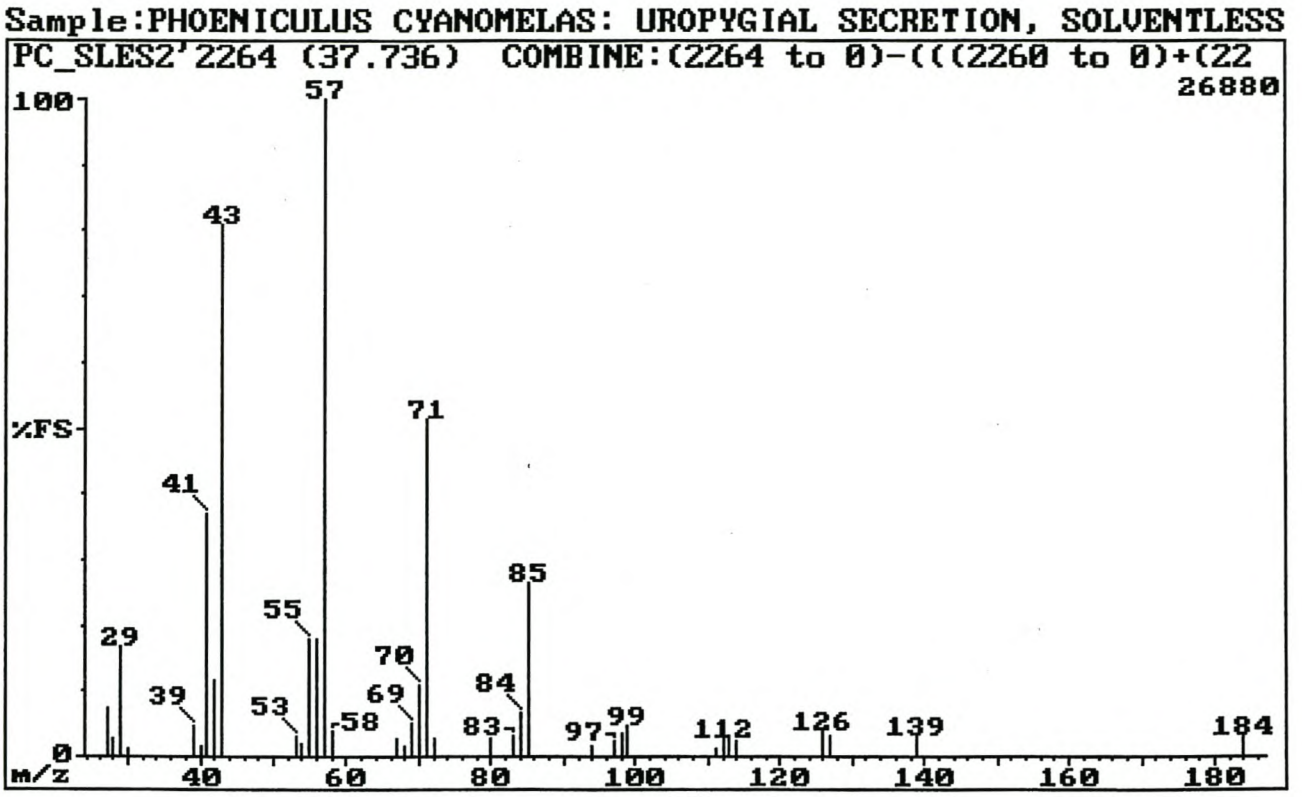

Fig. 2.2: EI mass spectrum of component 2264 (tridecane)

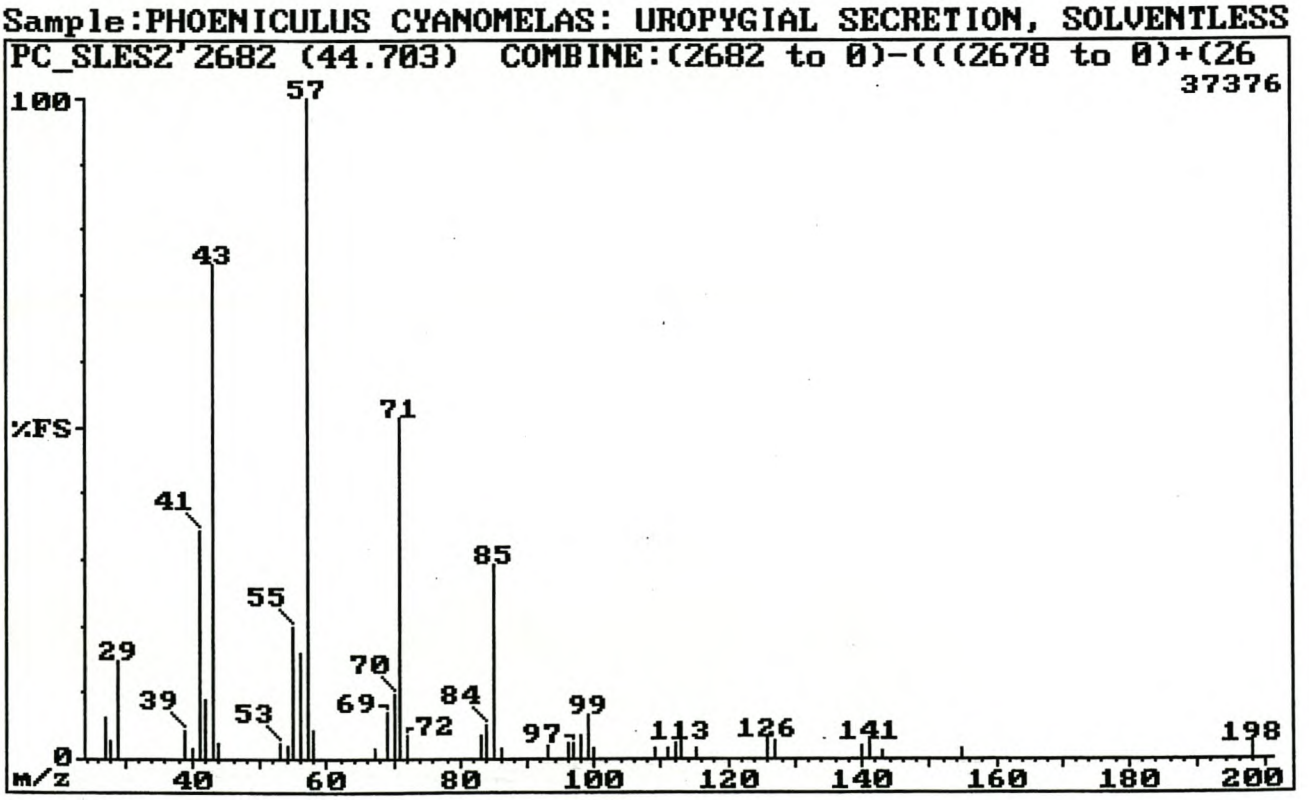

Fig. 2.3: EI mass spectrum of component 2682 (tetradecane)

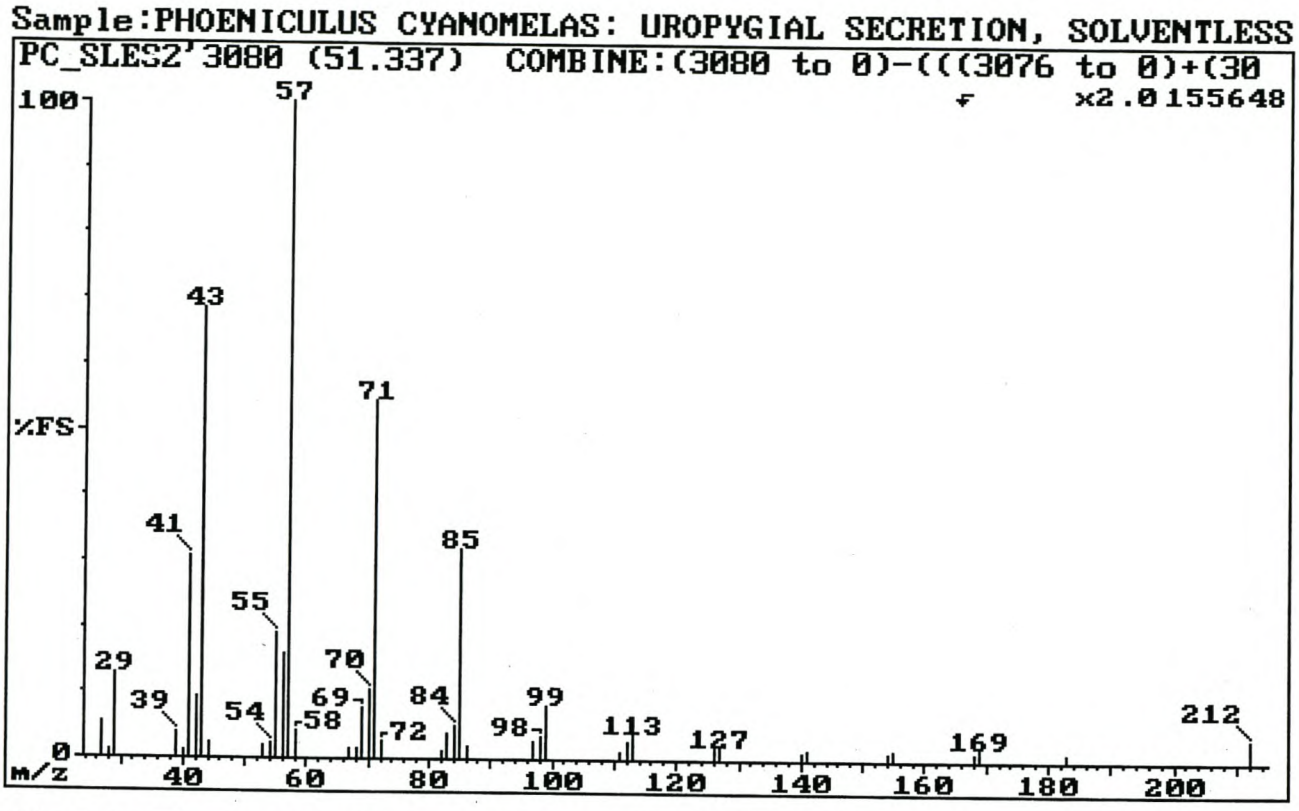

Fig. 2.4: EI mass spectrum of component 3080 (pentadecane)

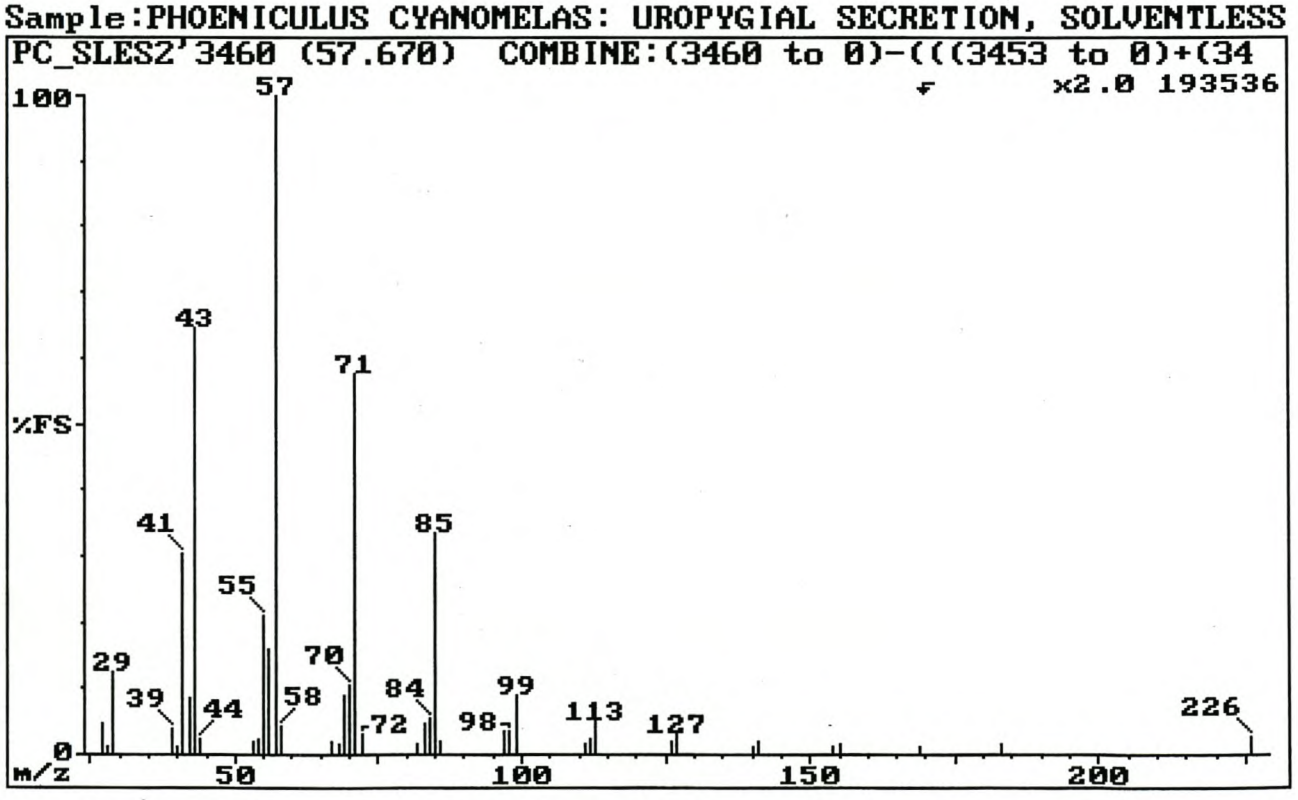

Fig. 2.5: EI mass spectrum of component 3460 (hexadecane)

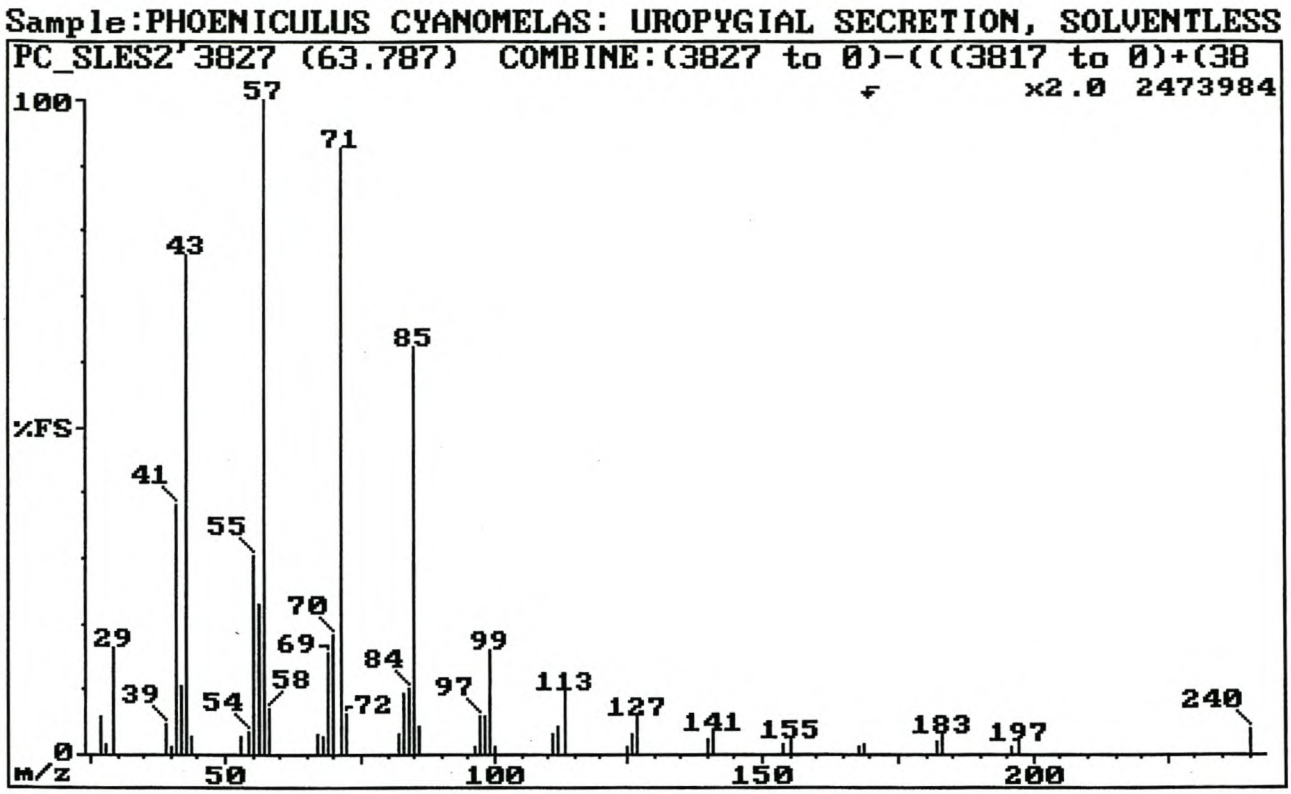

Fig 2.6: EI mass spectrum of component 3827 (heptadecane)

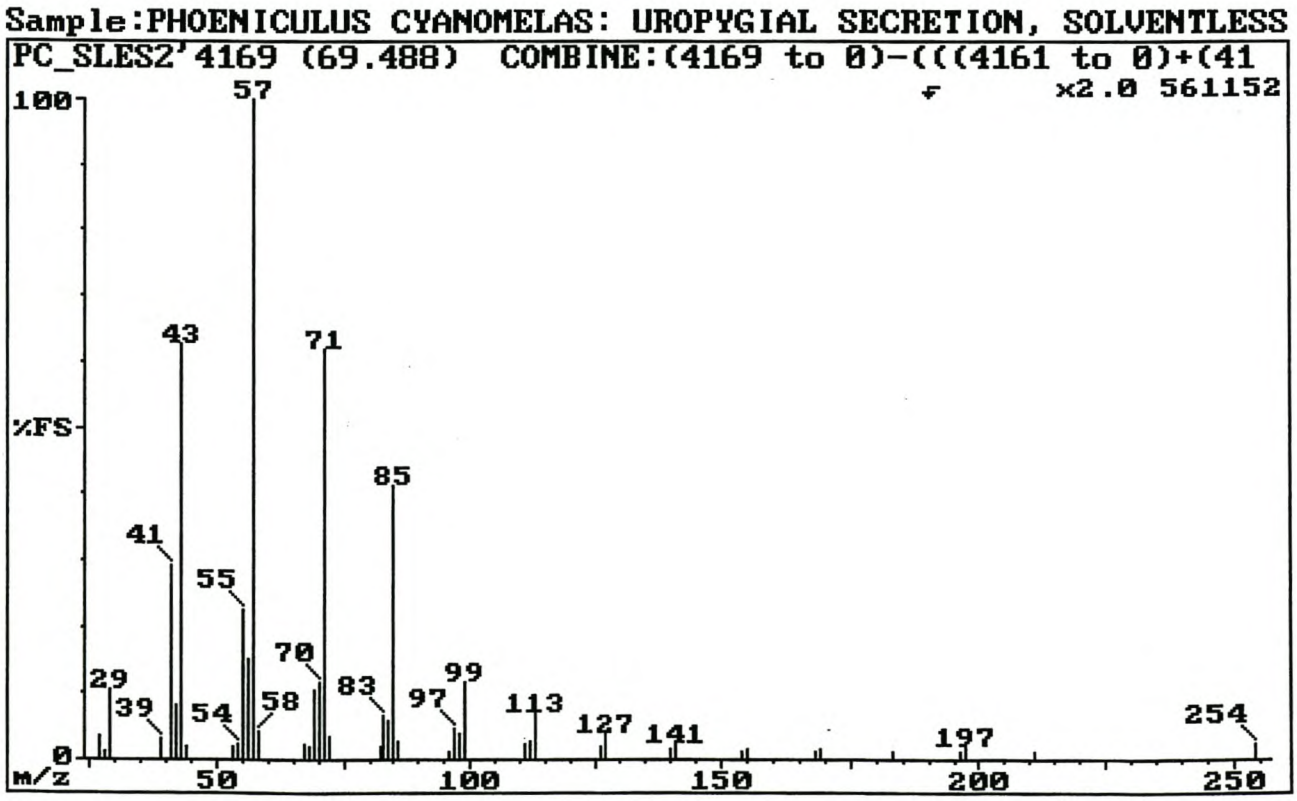

Fig 2.7: EI mass spectrum of component 4169 (octadecane)

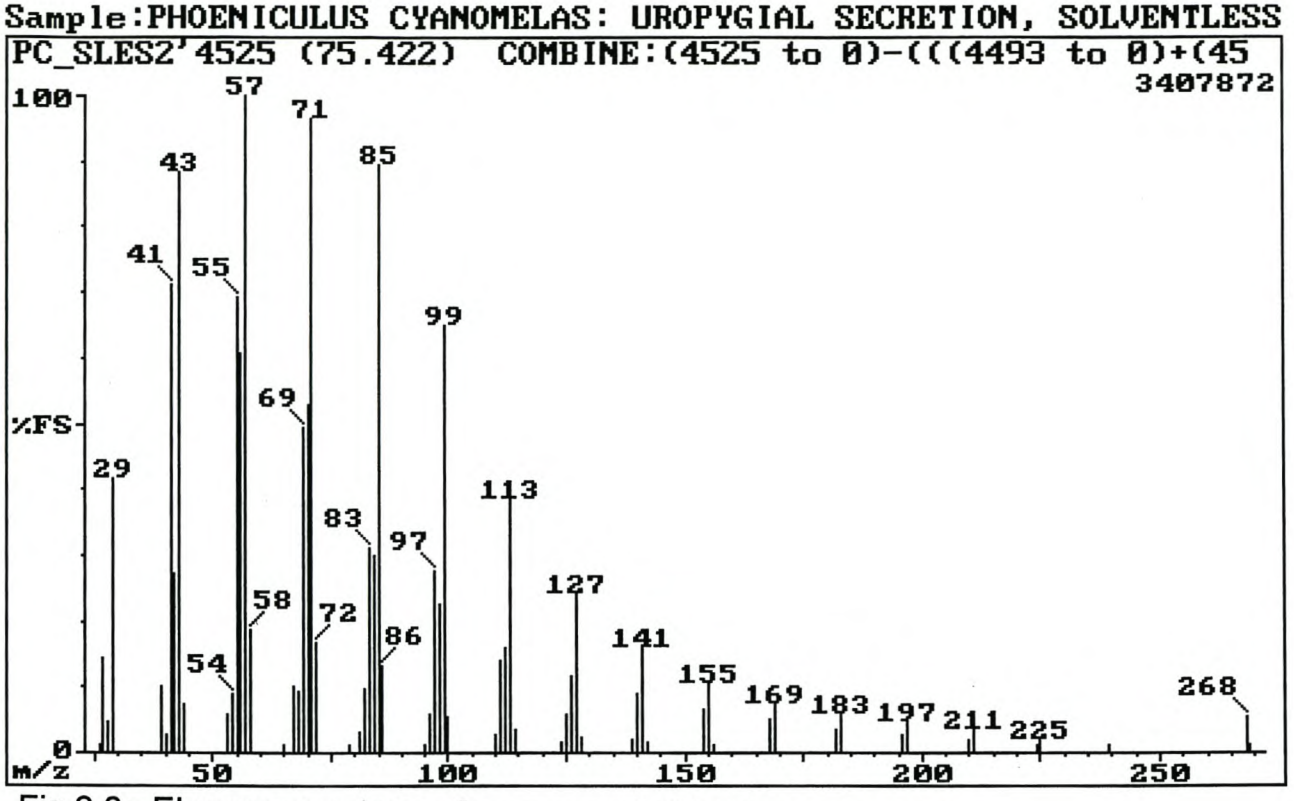

Fig.2.8: EI mass spectrum of component 4525 (nonadecane)

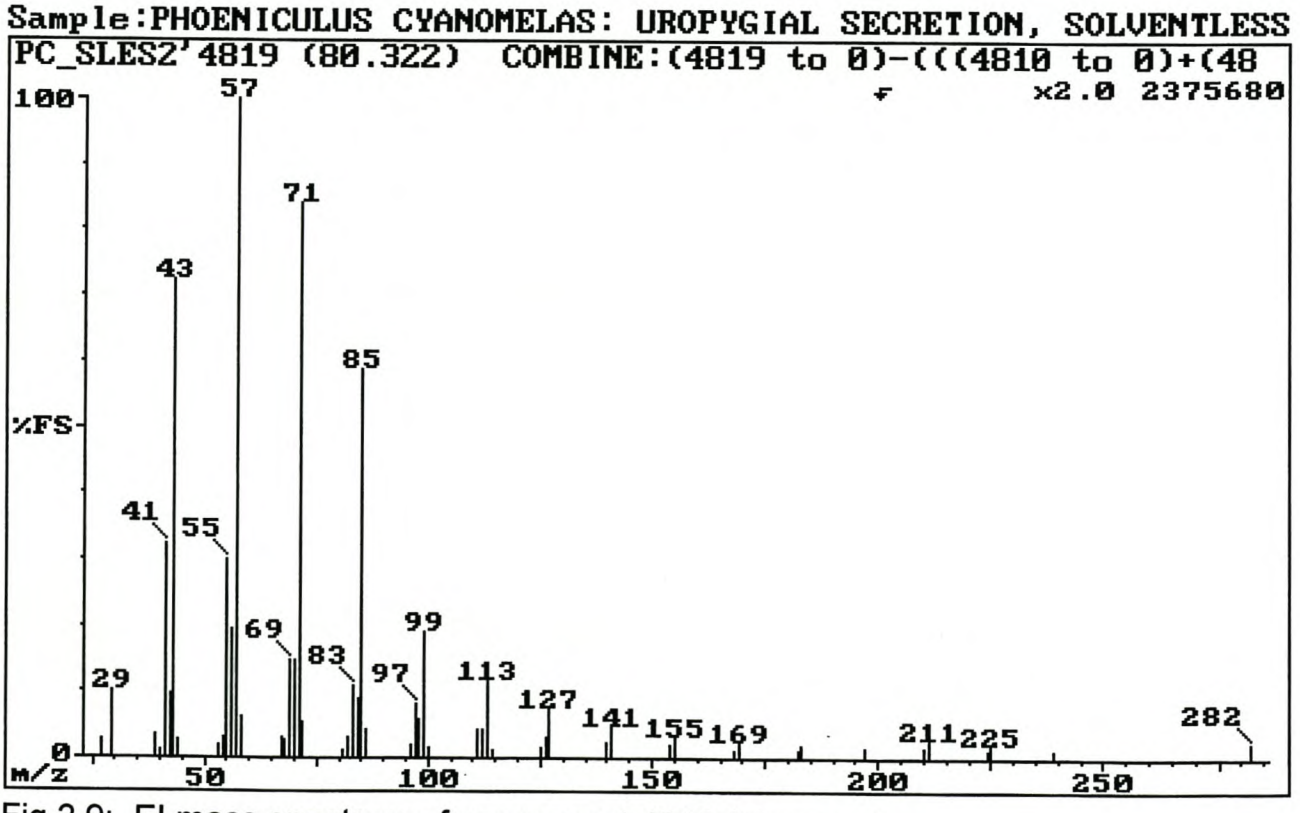

Fig.2.9: EI mass spectrum of component 4819 (eicosane)

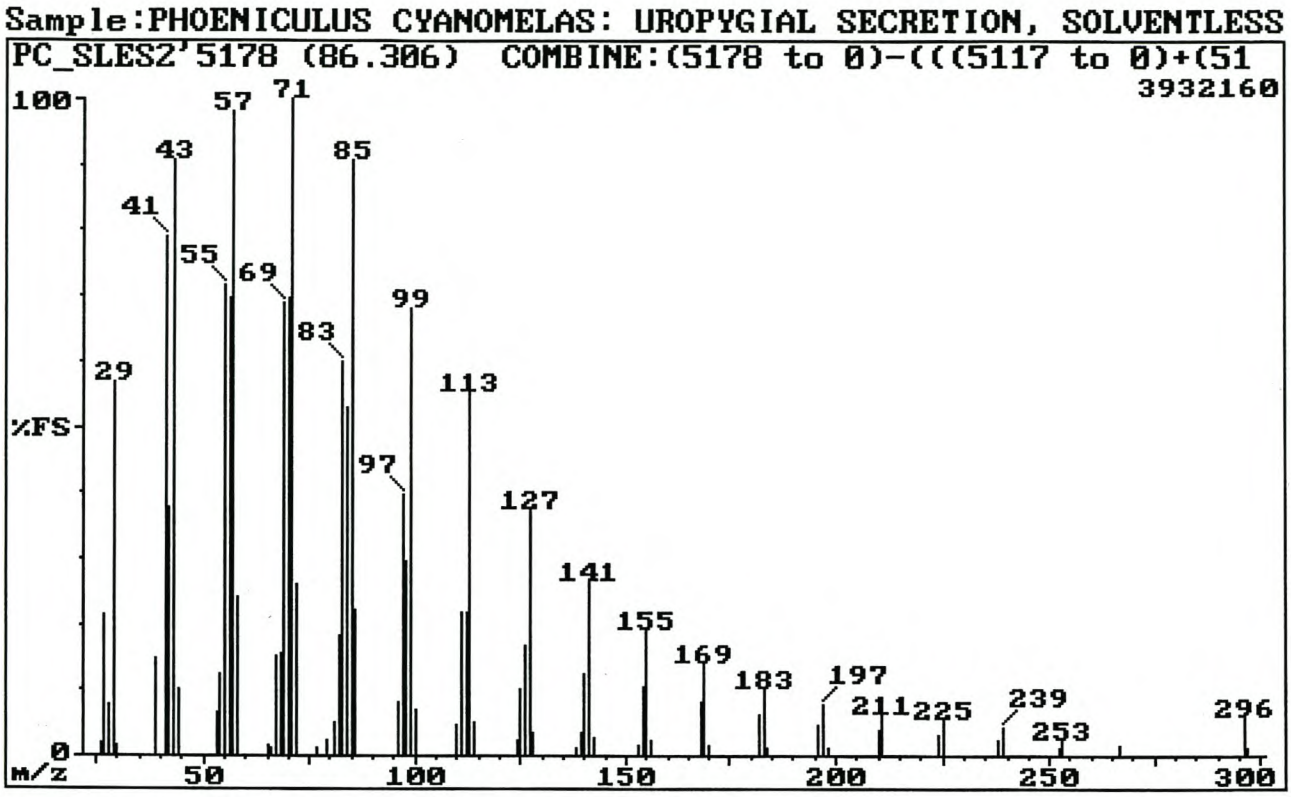

Fig.2.10: EI mass spectrum of component 5178 (heneicosane)

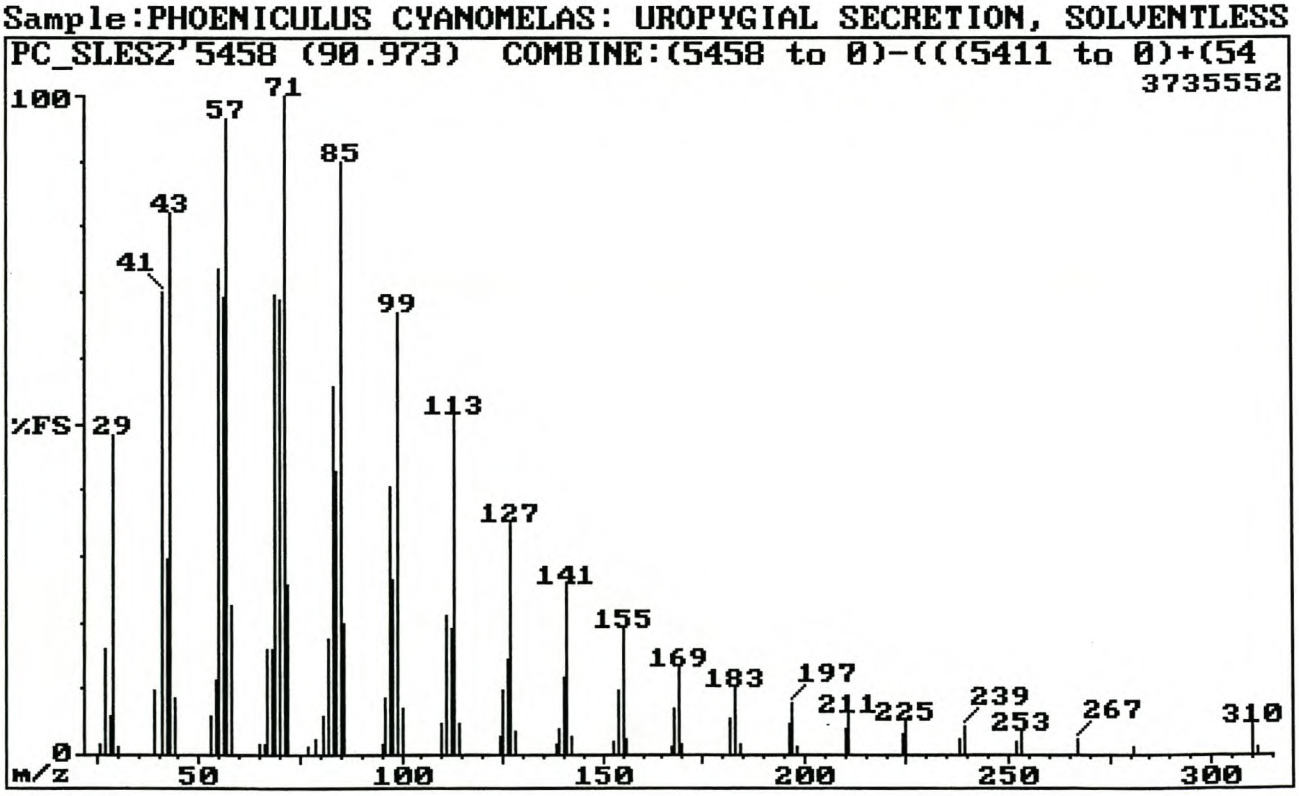

Fig.2.11: EI mass spectrum of component 5458 (docosane)

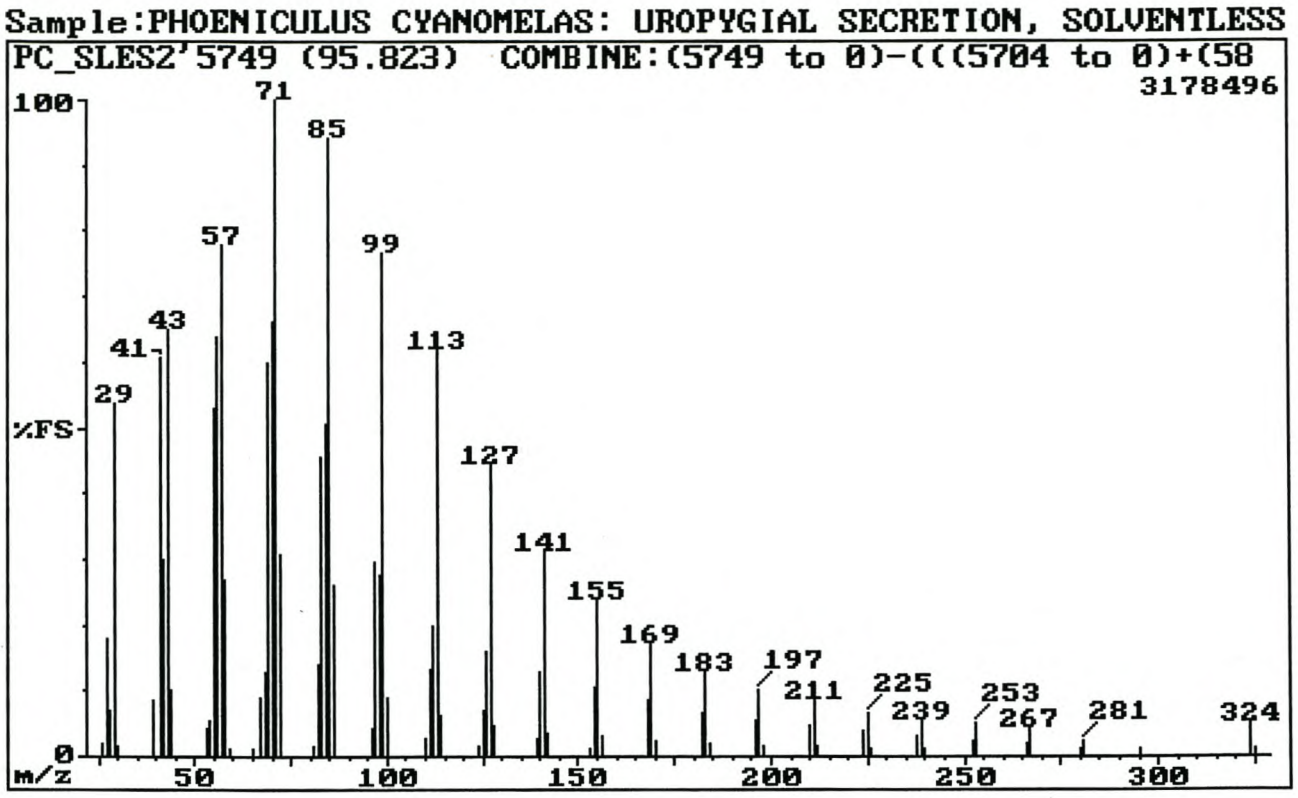

Fig.2.12: EI mass spectrum of component 5749 (tricosane)

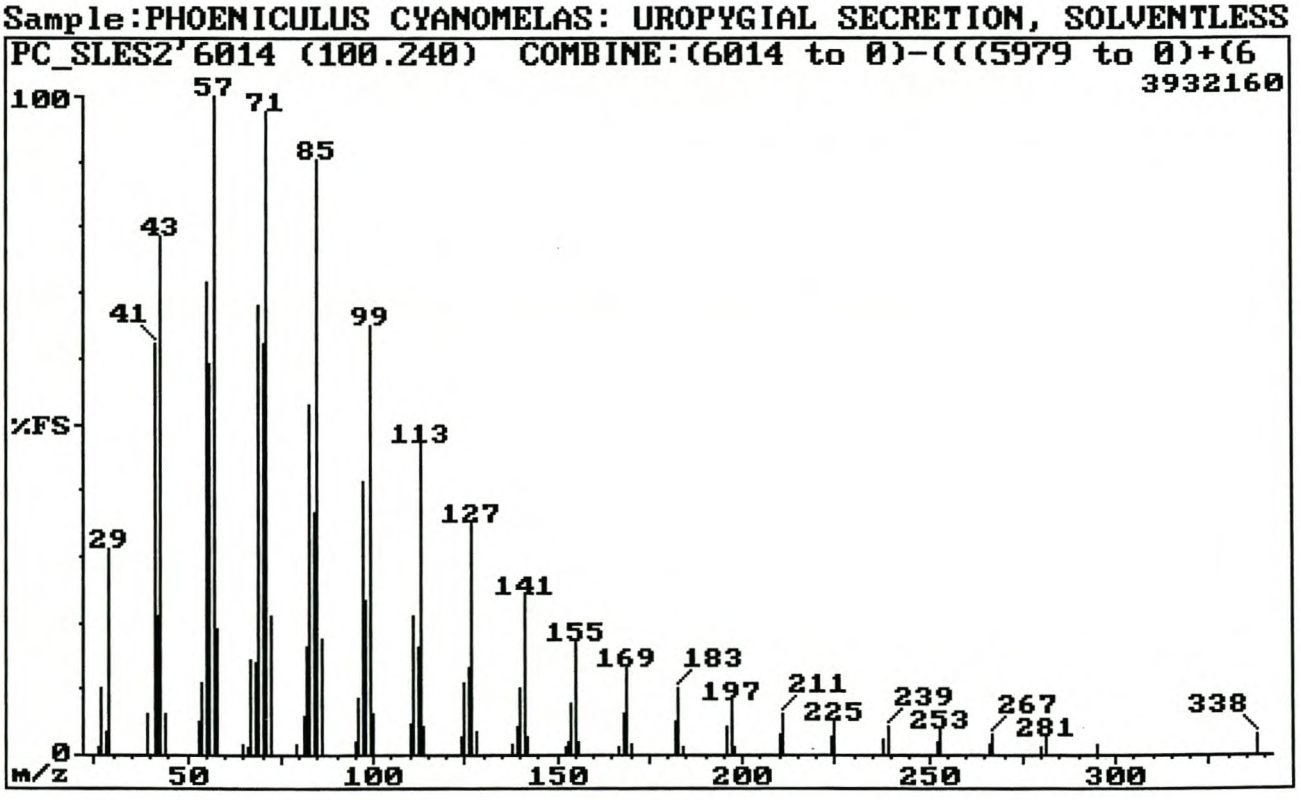

Fig.2.13: EI mass spectrum of component 6014 (tetracosane)

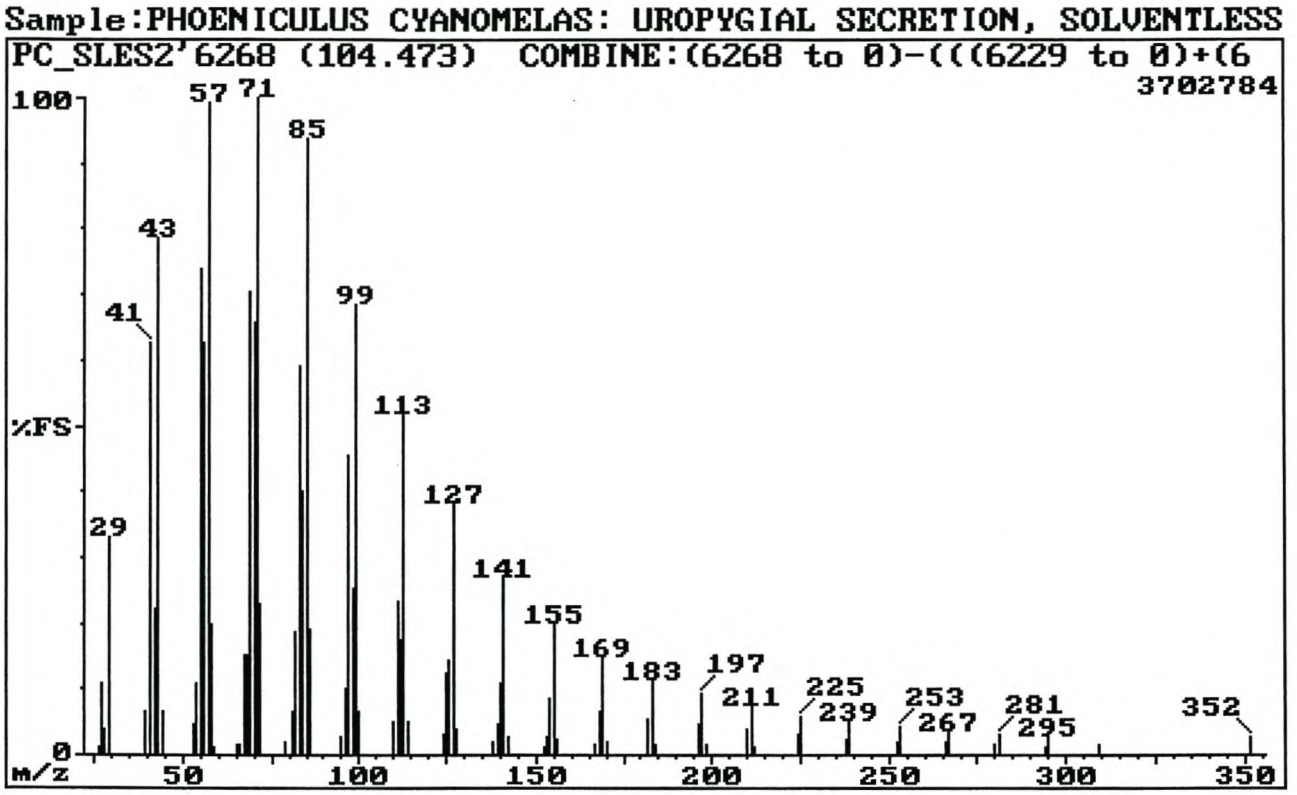

Fig.2.14: EI mass spectrum of component 6268 (pentacosane)

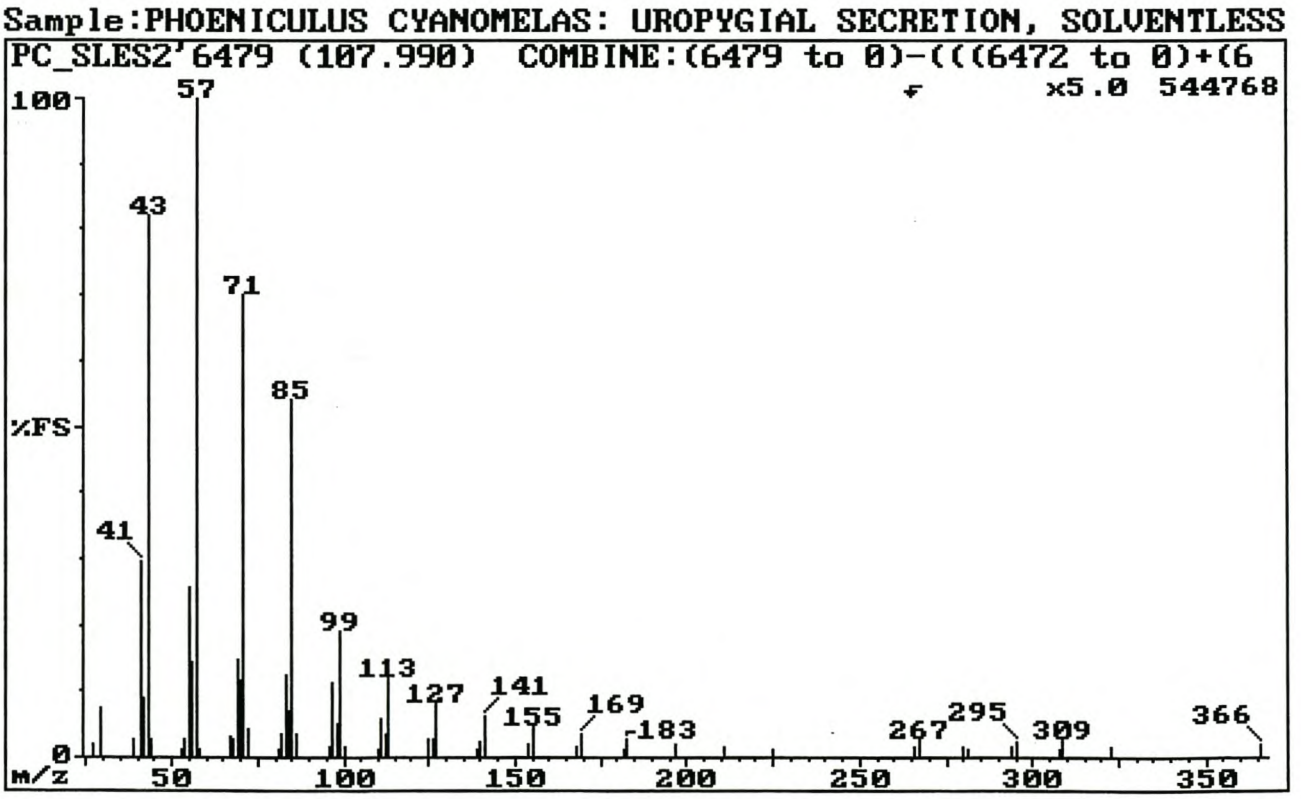

Fig.2.15: EI mass spectrum of component 6479 (hexacosane)

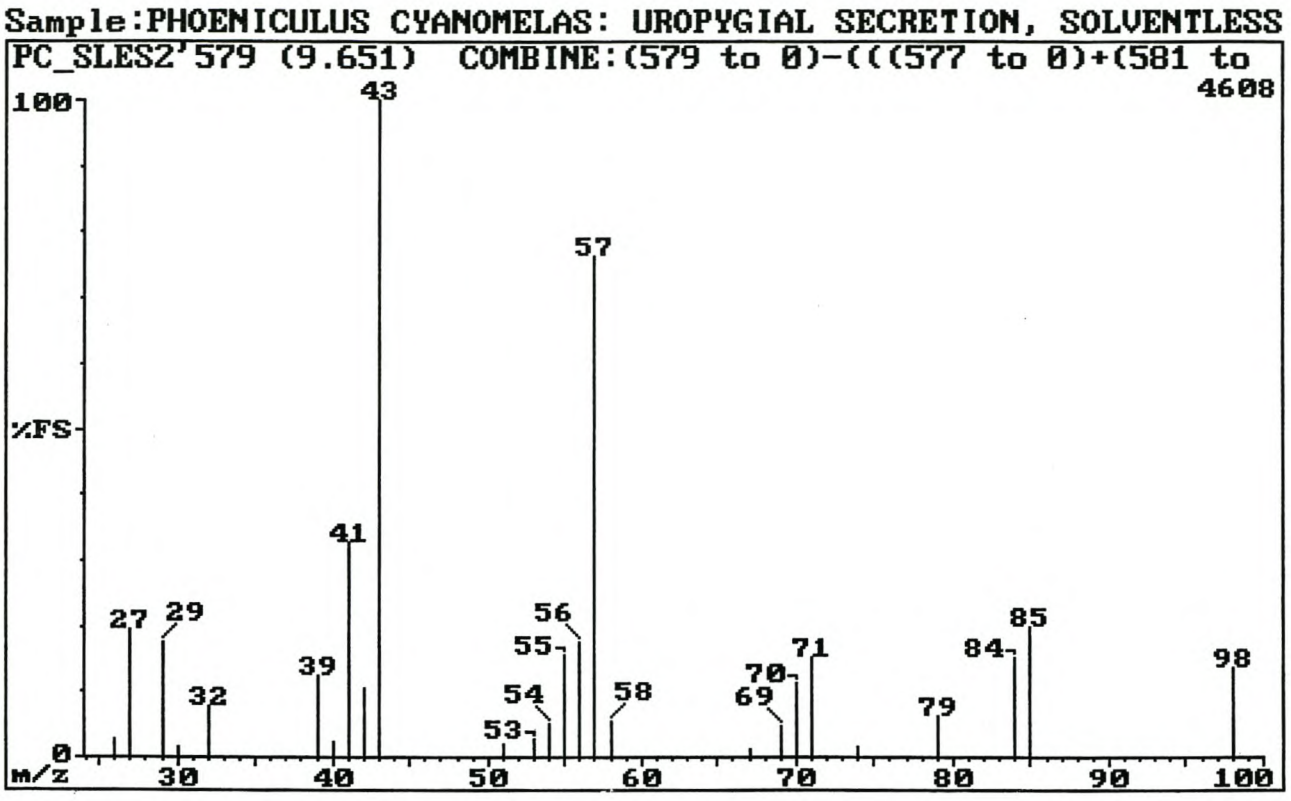

Fig.2.16: EI mass spectrum of component 579 (2,4-dimethylhexane)

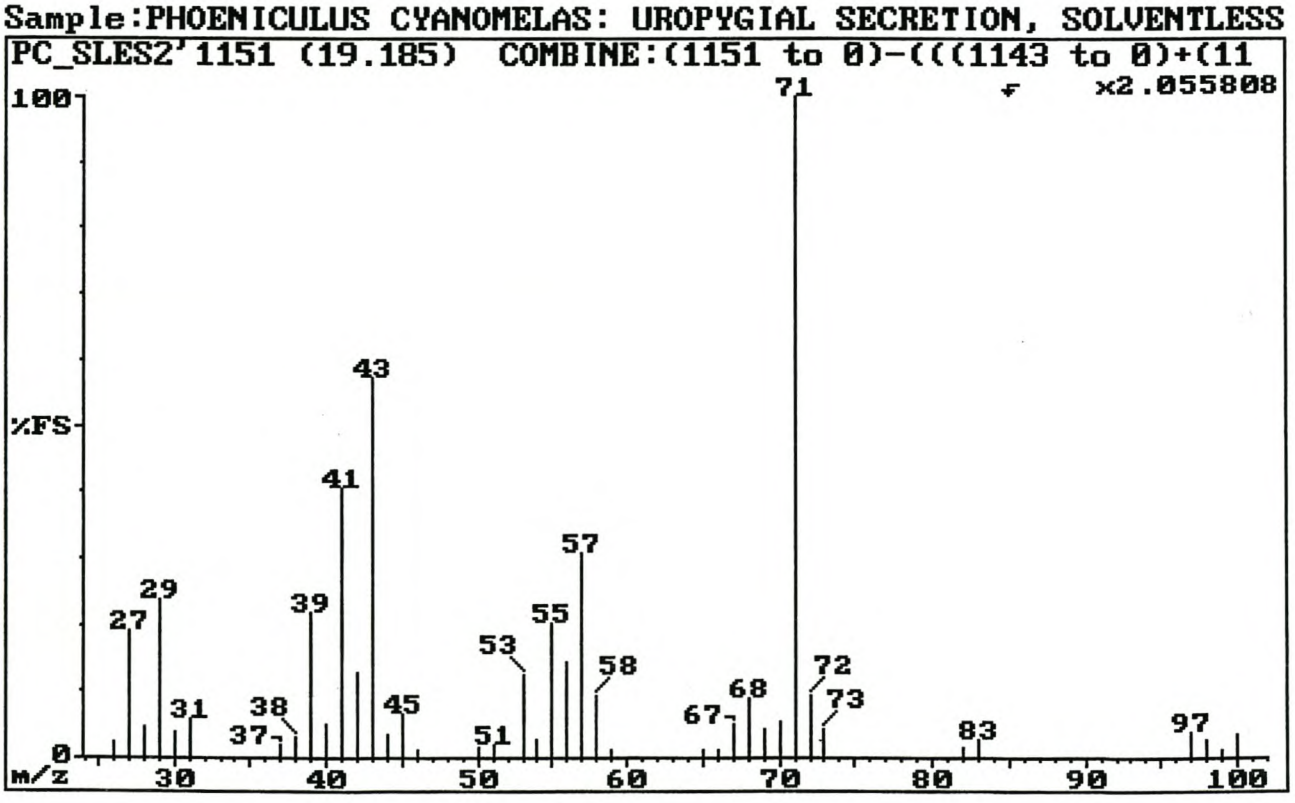

Fig.2.17: EI mass spectrum of component 1151 (3-ethylpentane)

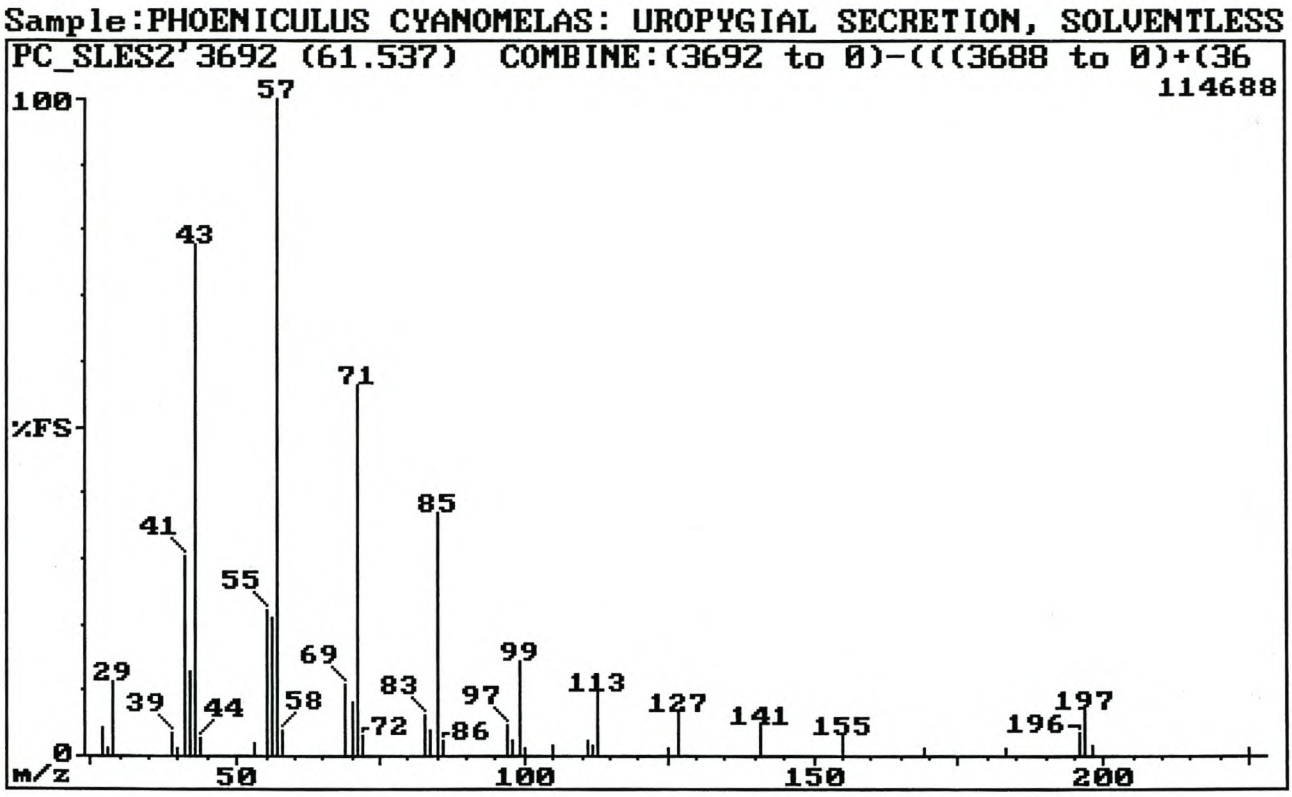

Fig.2.18: EI mass spectrum of component 3692 (2-methylhexadecane)

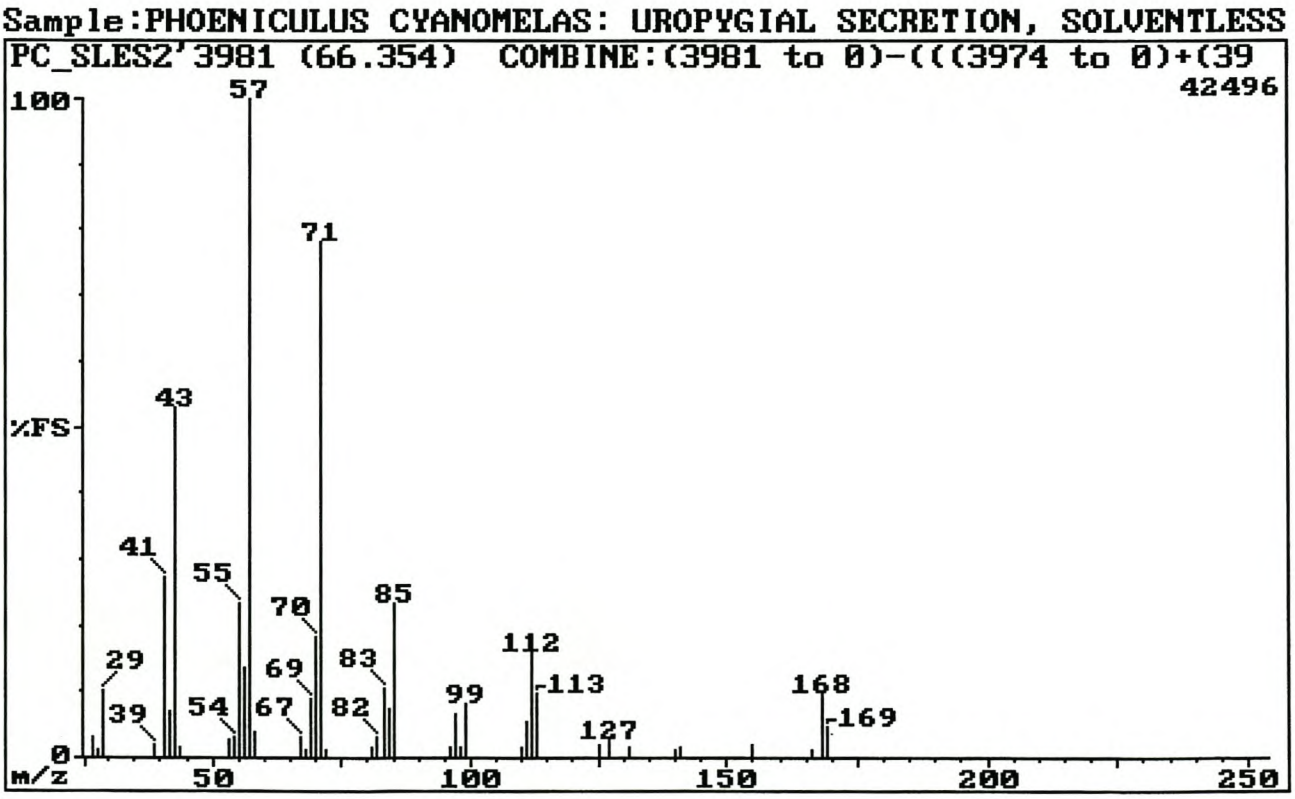

Fig.2.19: EI mass spectrum of component 3981 (7-methylheptadecane)

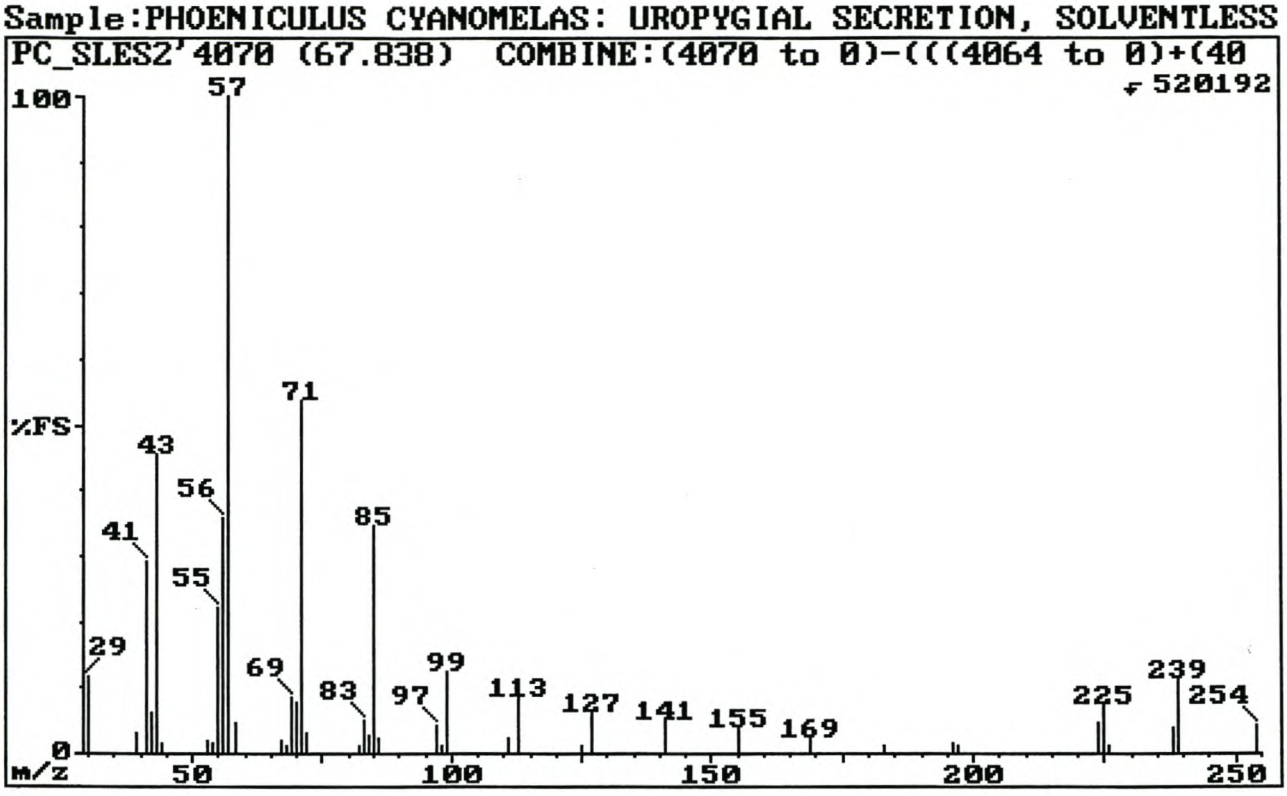

Fig 2.20: EI mass spectrum of component 4070 (3-methylheptadecane)

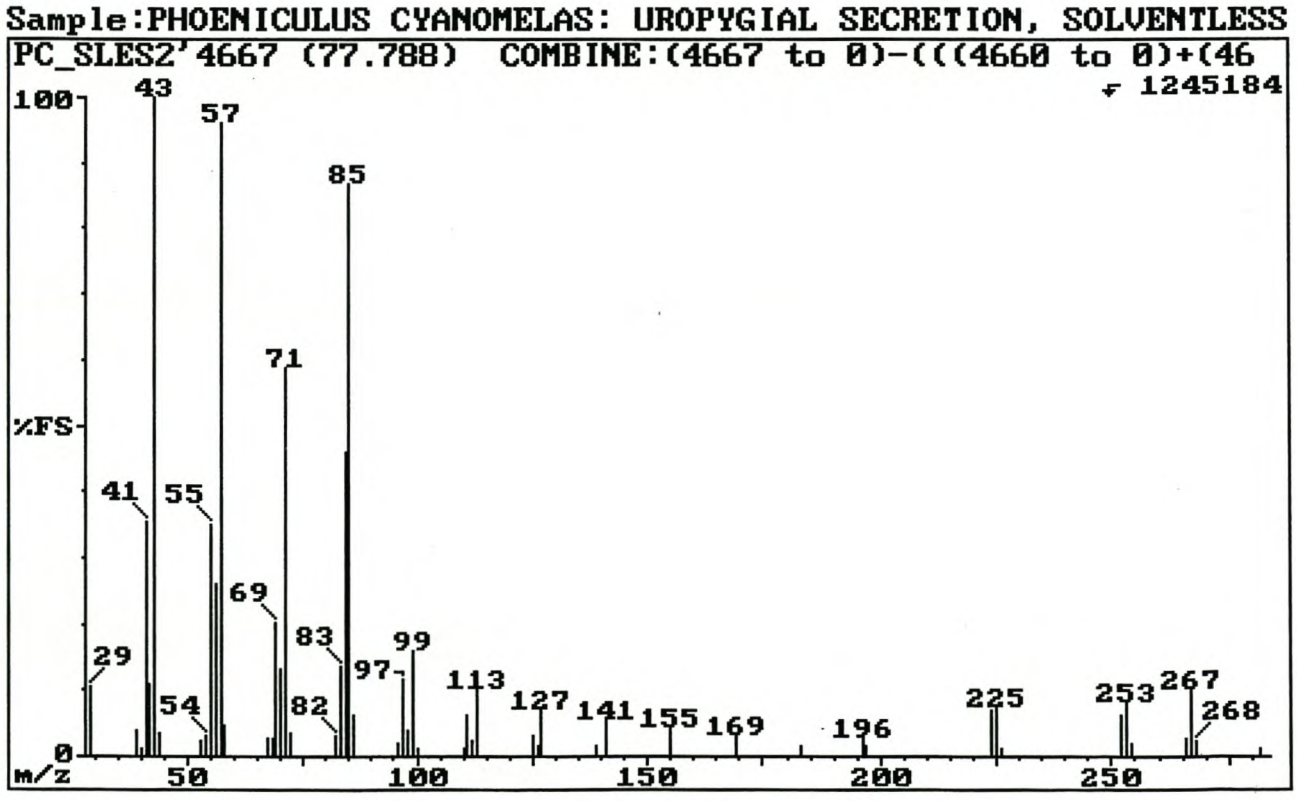

Fig 2.21: EI mass spectrum of component 4667 (5-methylnonadecane)

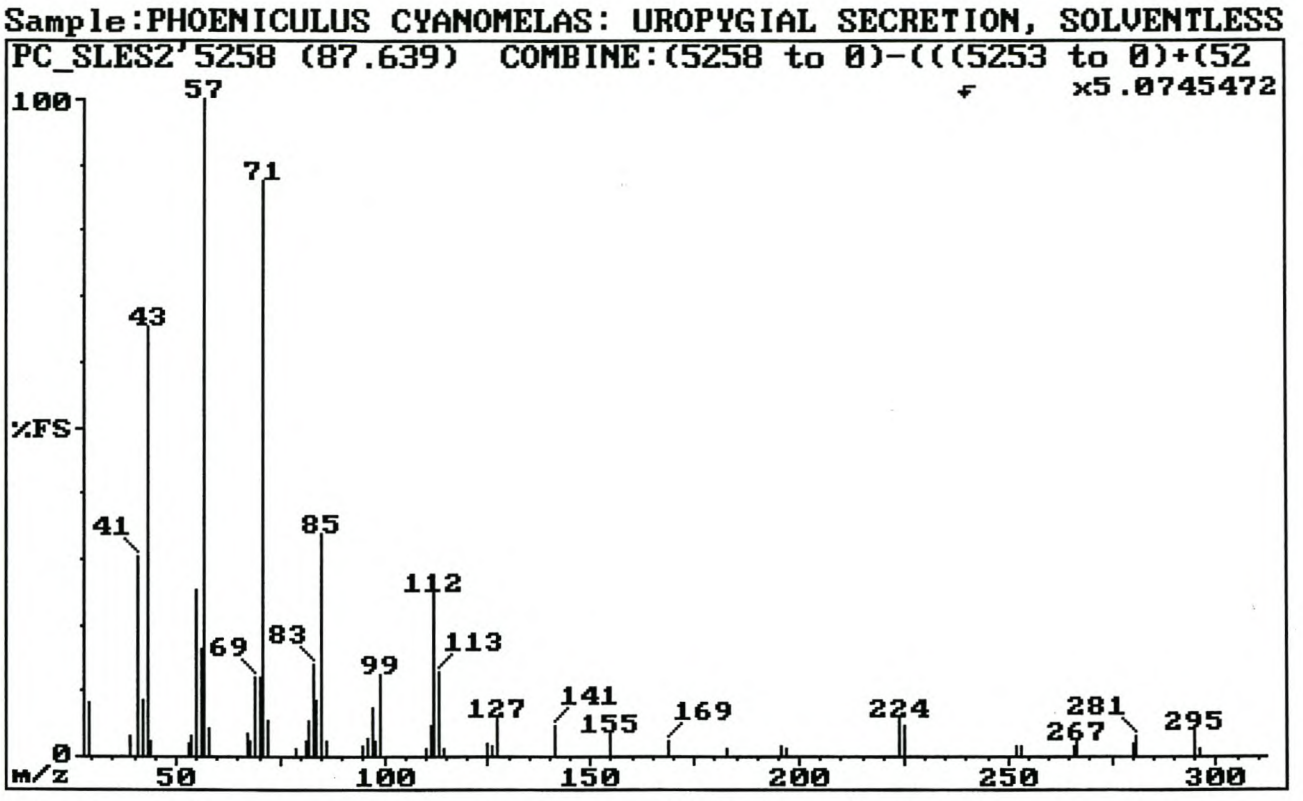

Fig 2.22: EI mass spectrum of component 5258 (7-methylheneicosane)

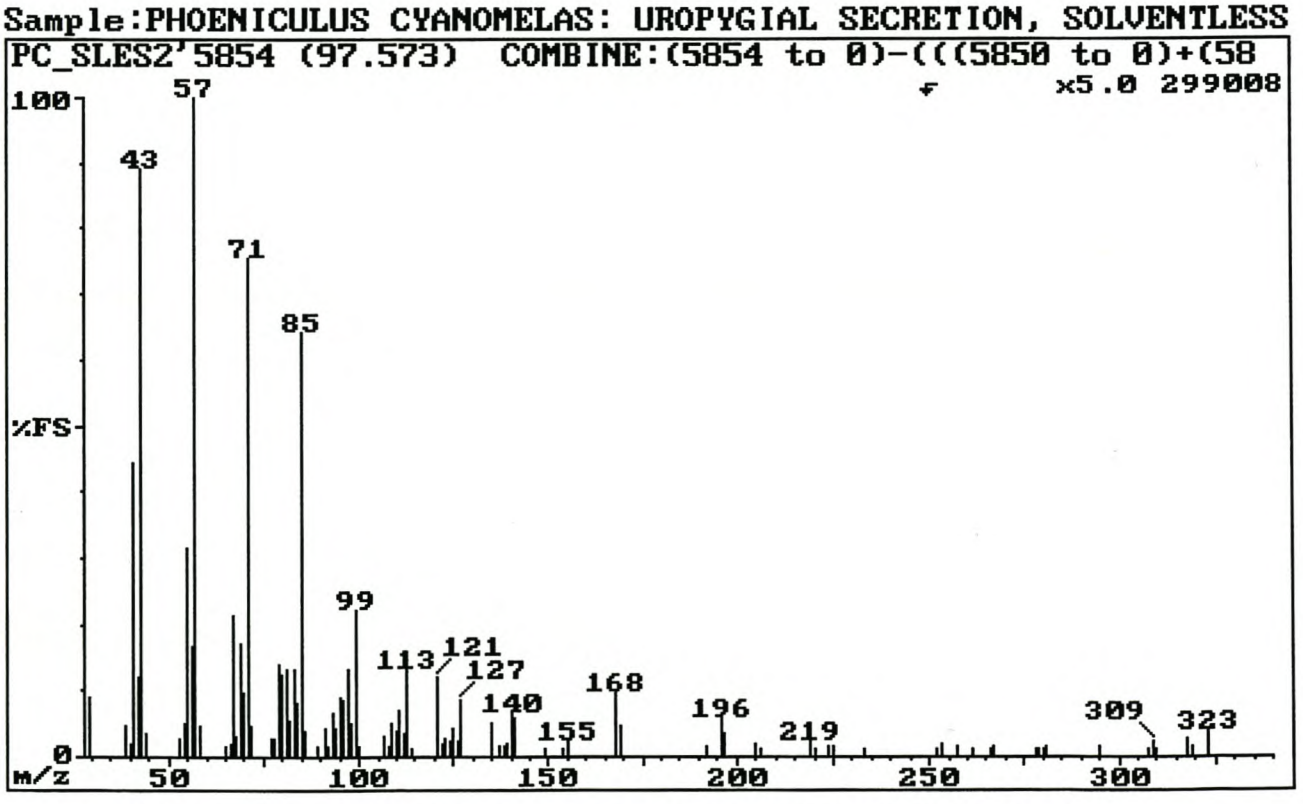

Fig 2.23: EI mass spectrum of component 5854 (11-methyltricosane)

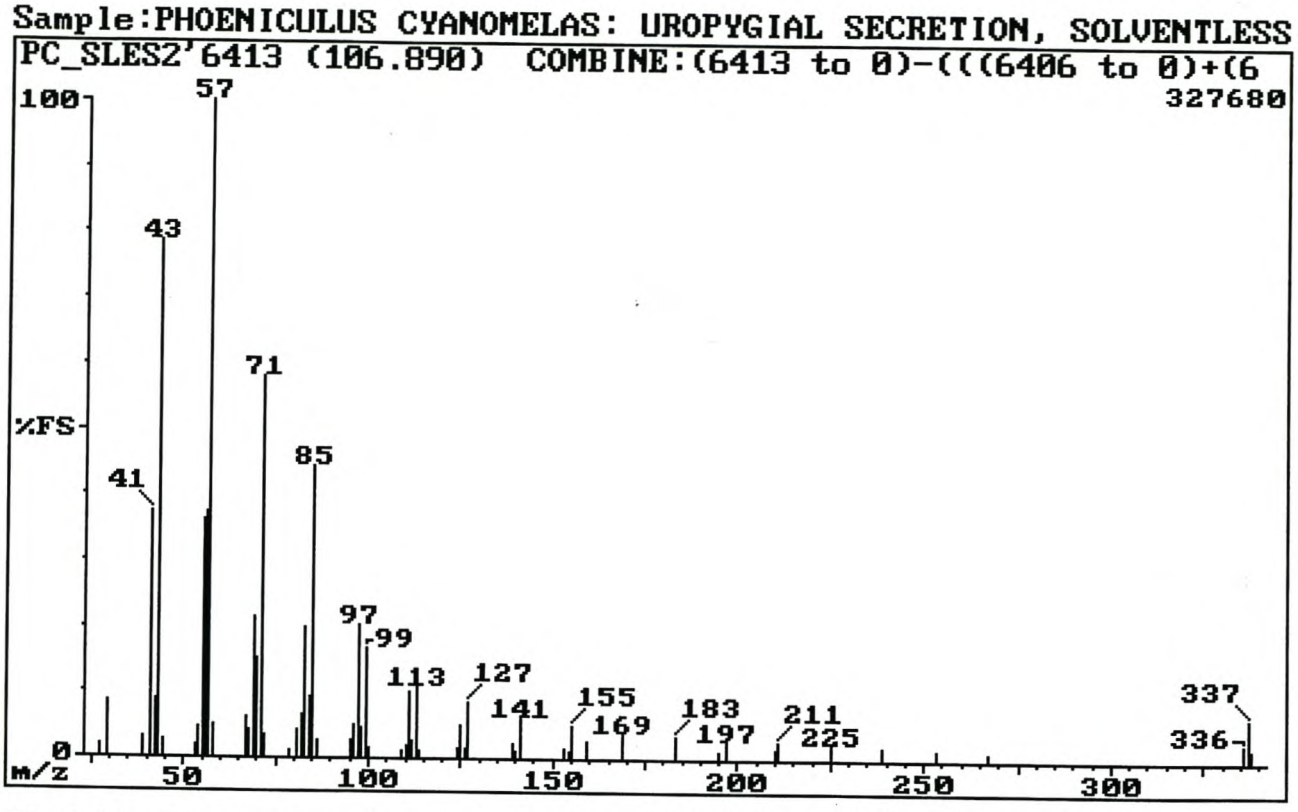

Fig 2.24: EI mass spectrum of component 6413 (3-methylpentacosane)

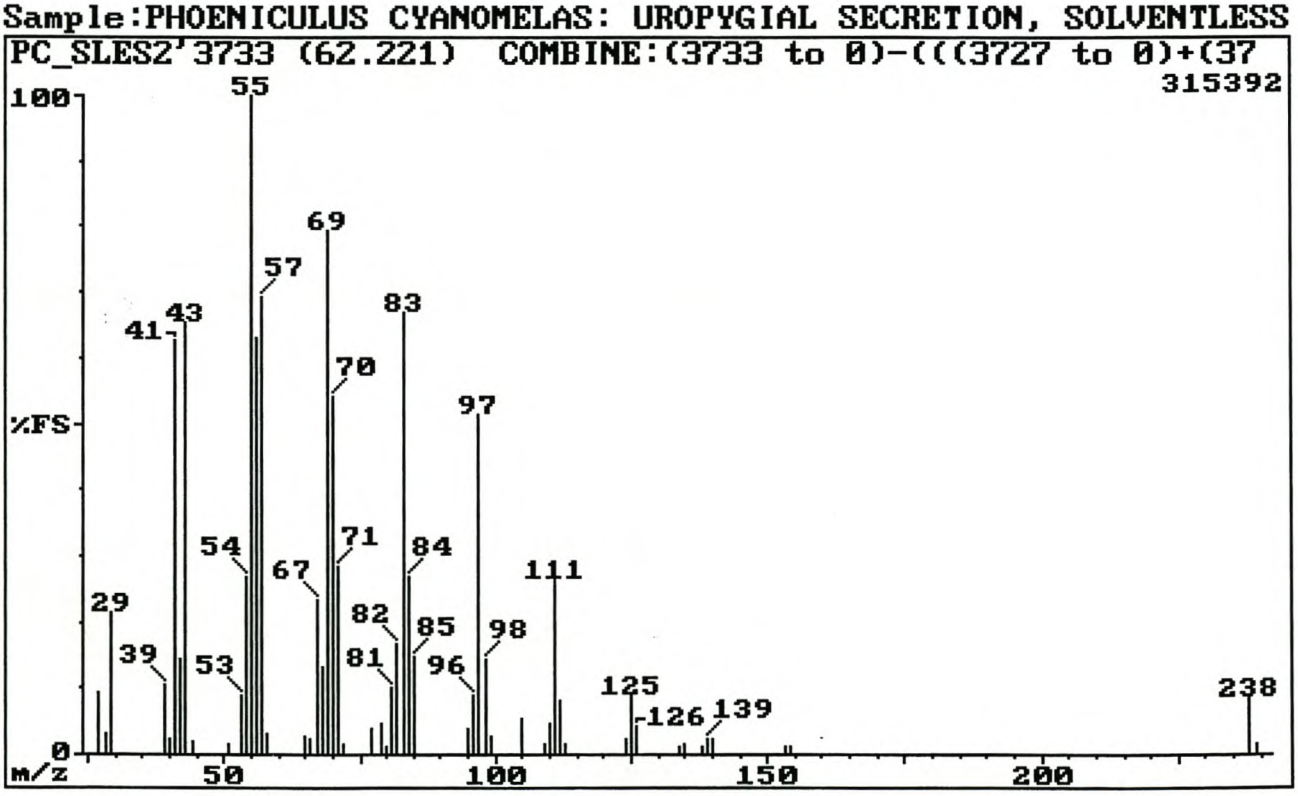

Fig 2.25: EI mass spectrum of component 3733 (heptadecene)

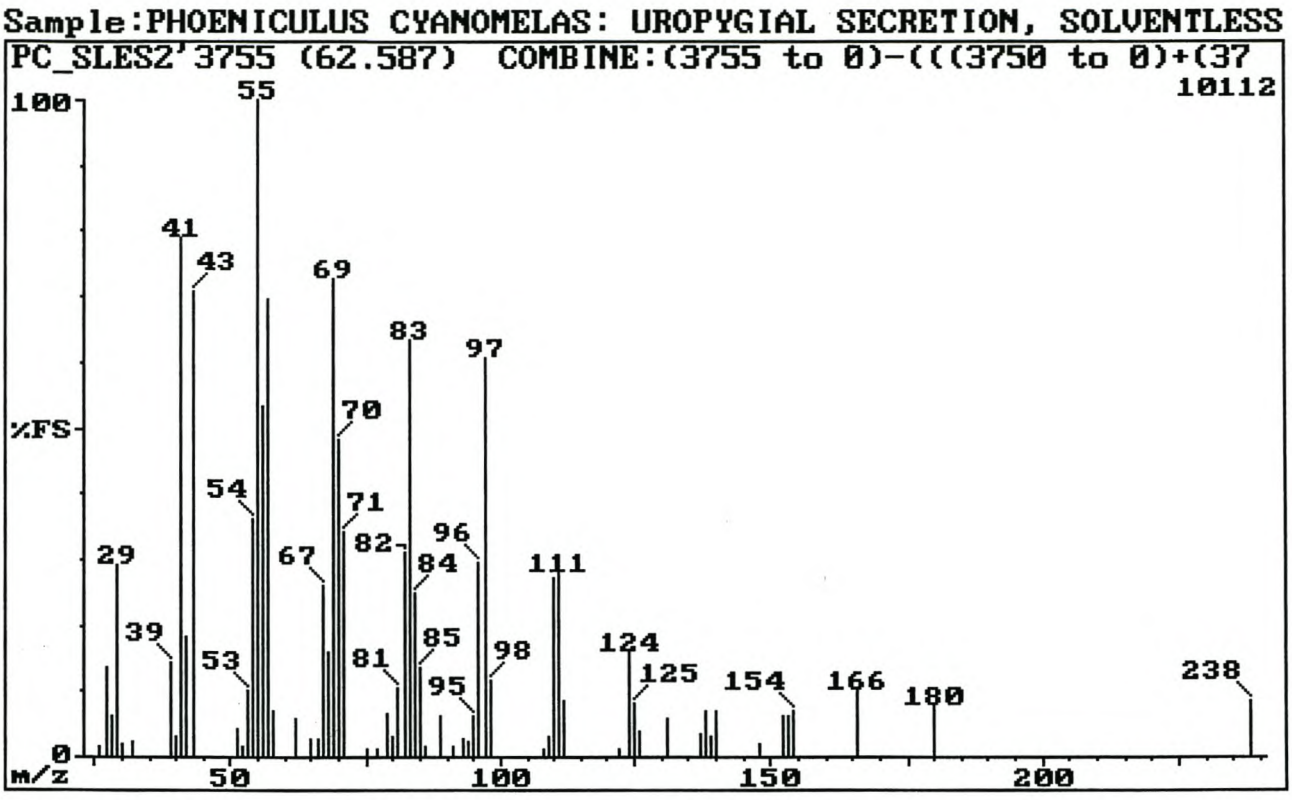

Fig 2.26: EI mass spectrum of component 3755 (heptadecene)

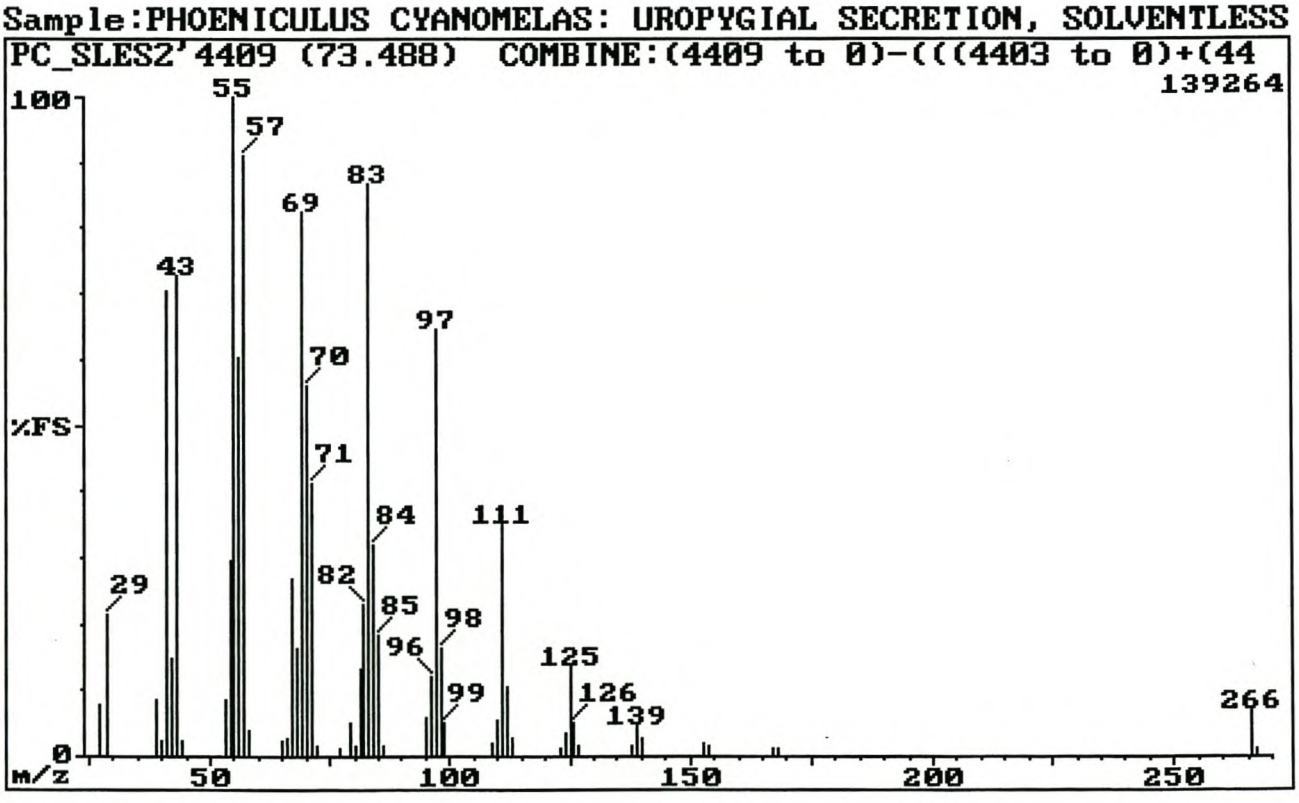

Fig 2.27: EI mass spectrum of component 4409 (nonadecene)

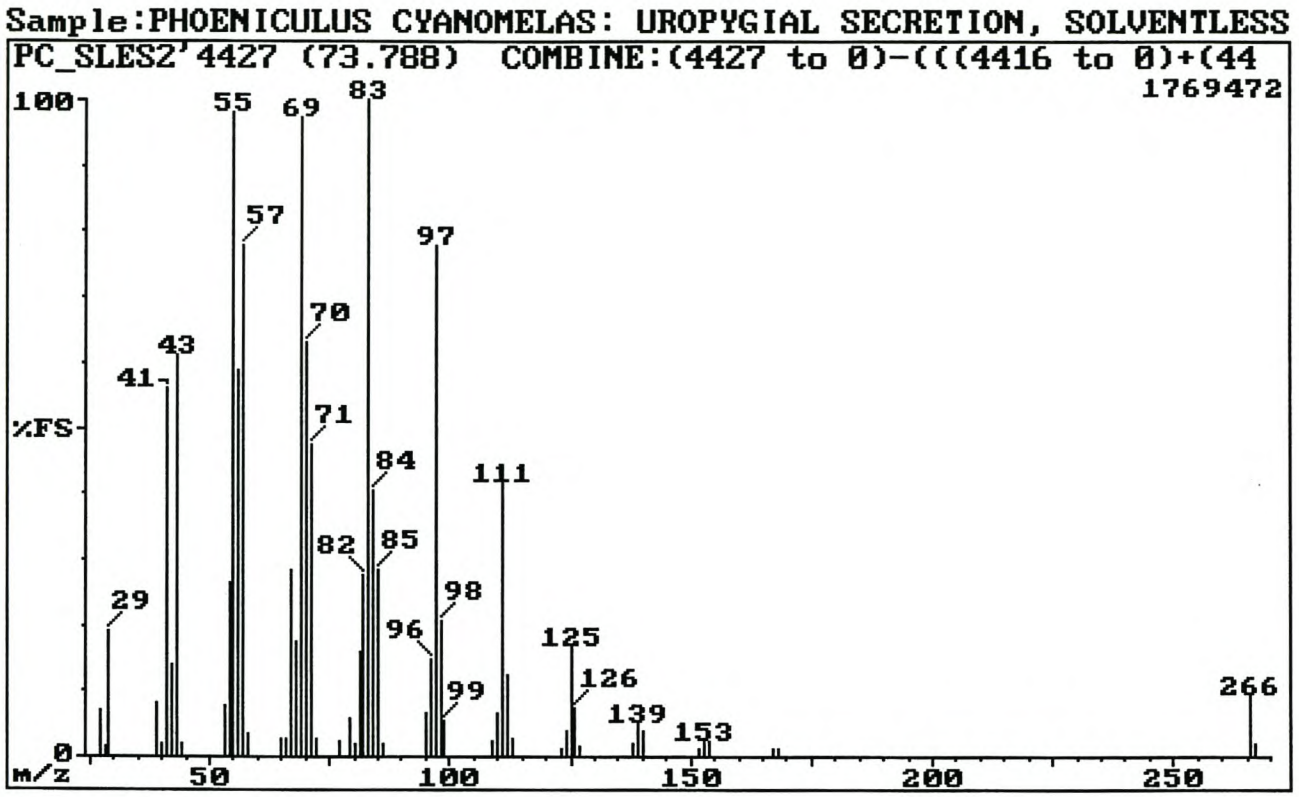

Fig 2.28: EI mass spectrum of component 4427 (nonadecene)

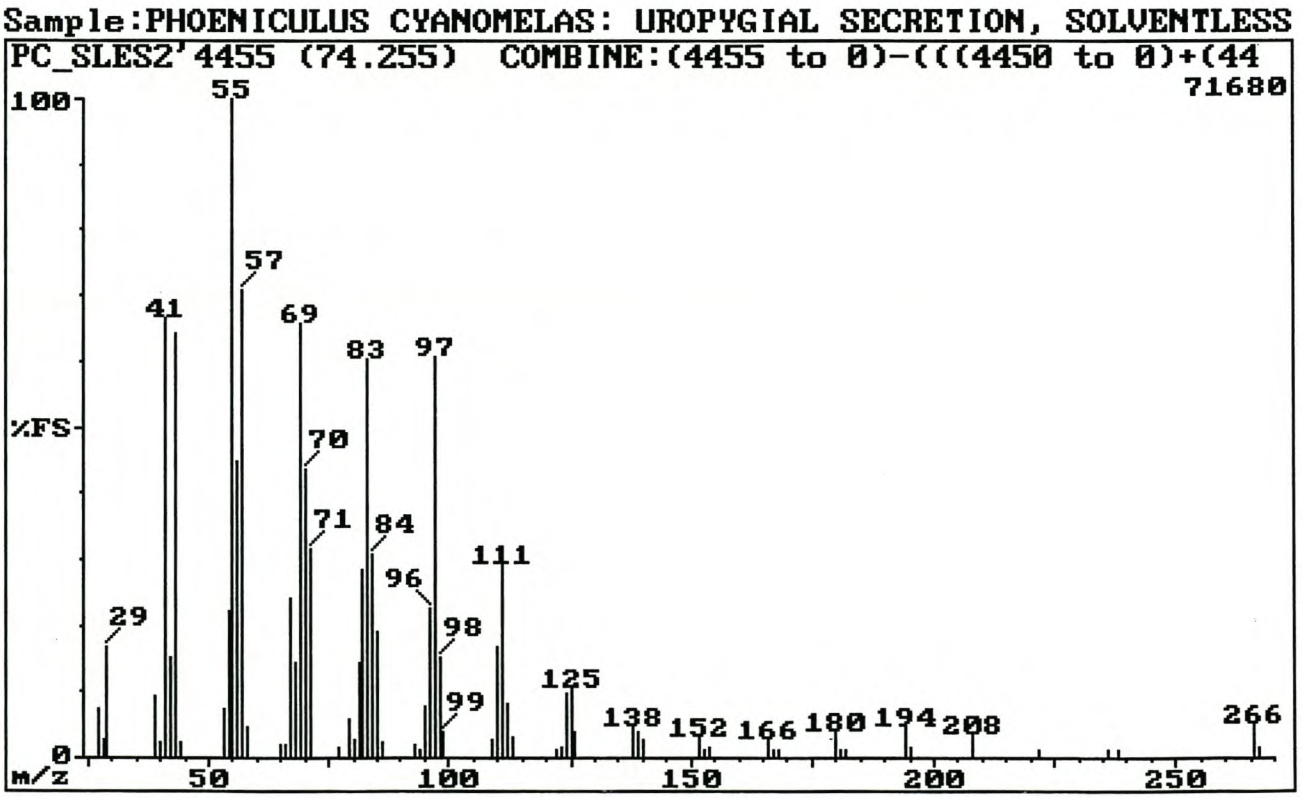

Fig 2.29: EI mass spectrum of component 4455 (nonadecene)

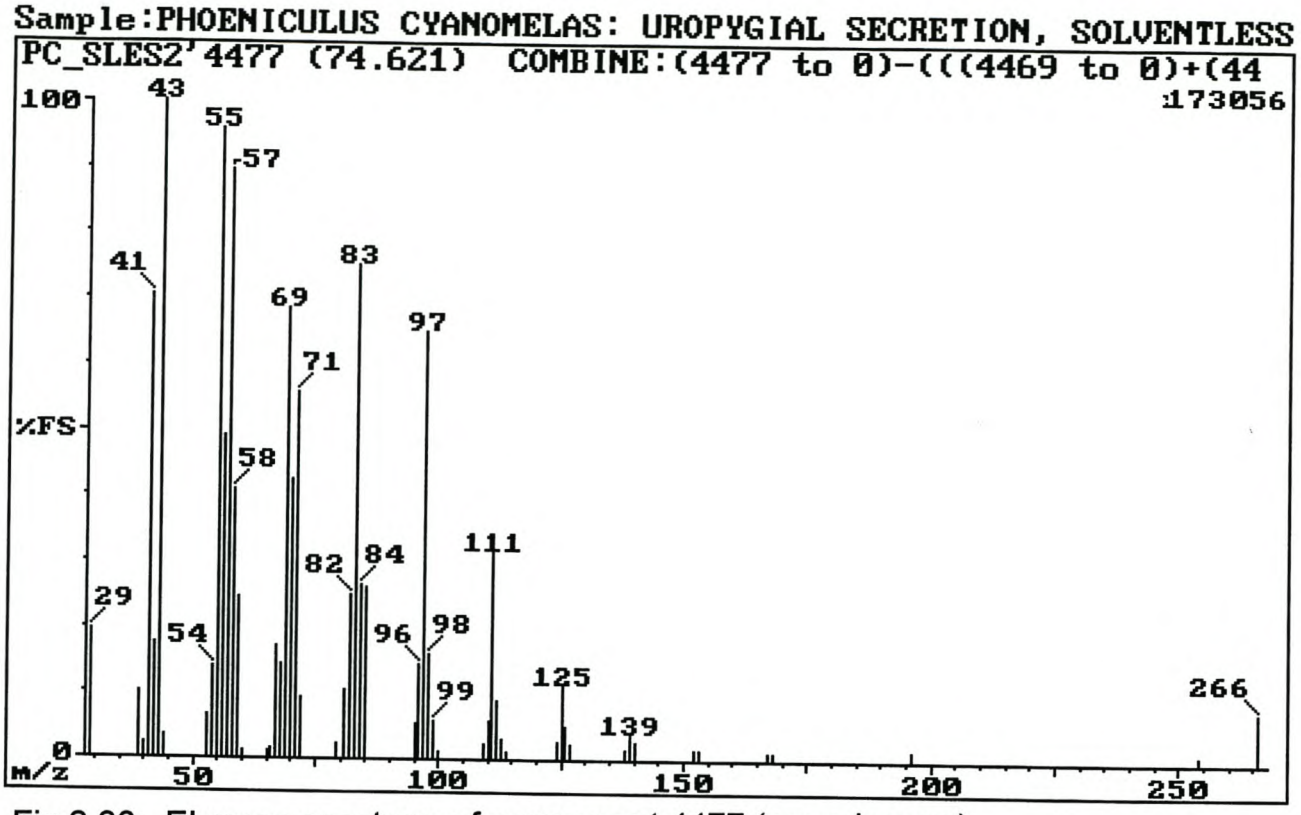

Fig 2.30: EI mass spectrum of component 4477 (nonadecene)

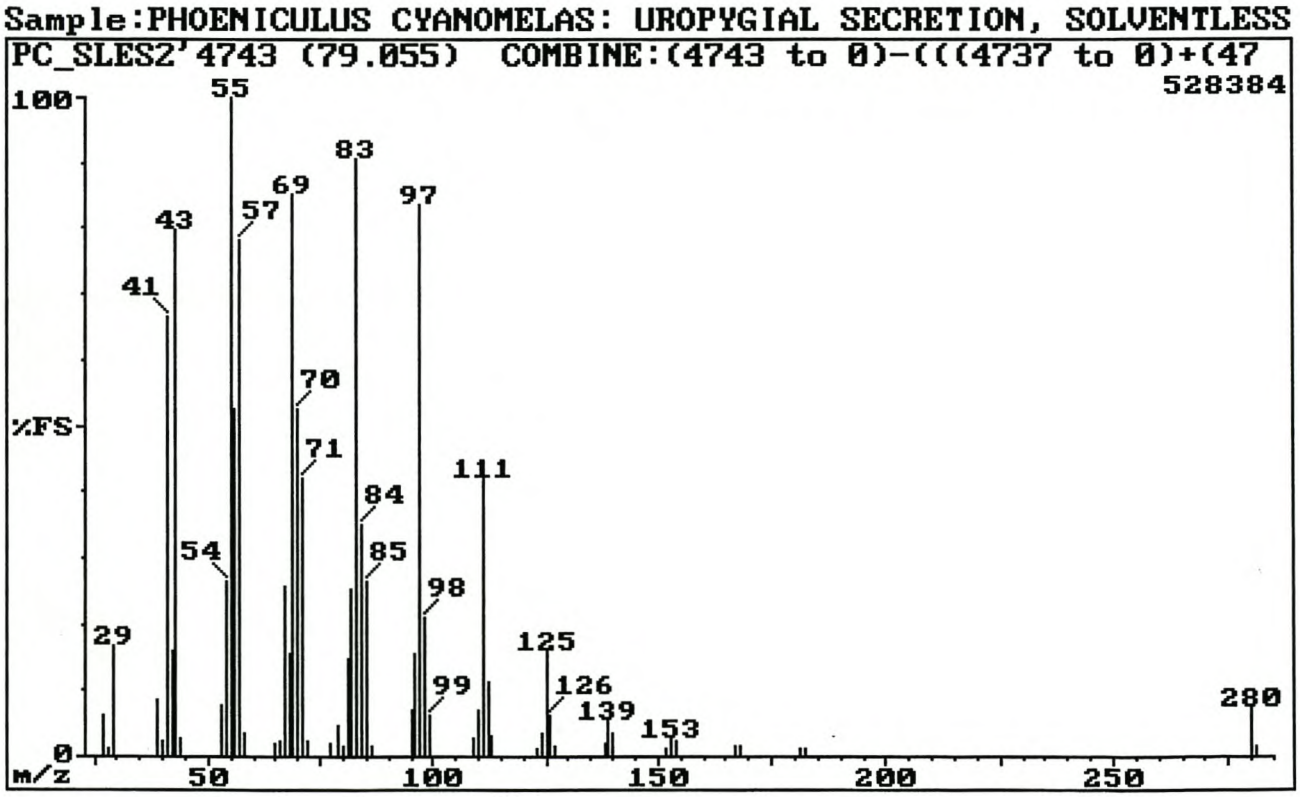

Fig 2.31: EI mass spectrum of component 4743 (eicosene)

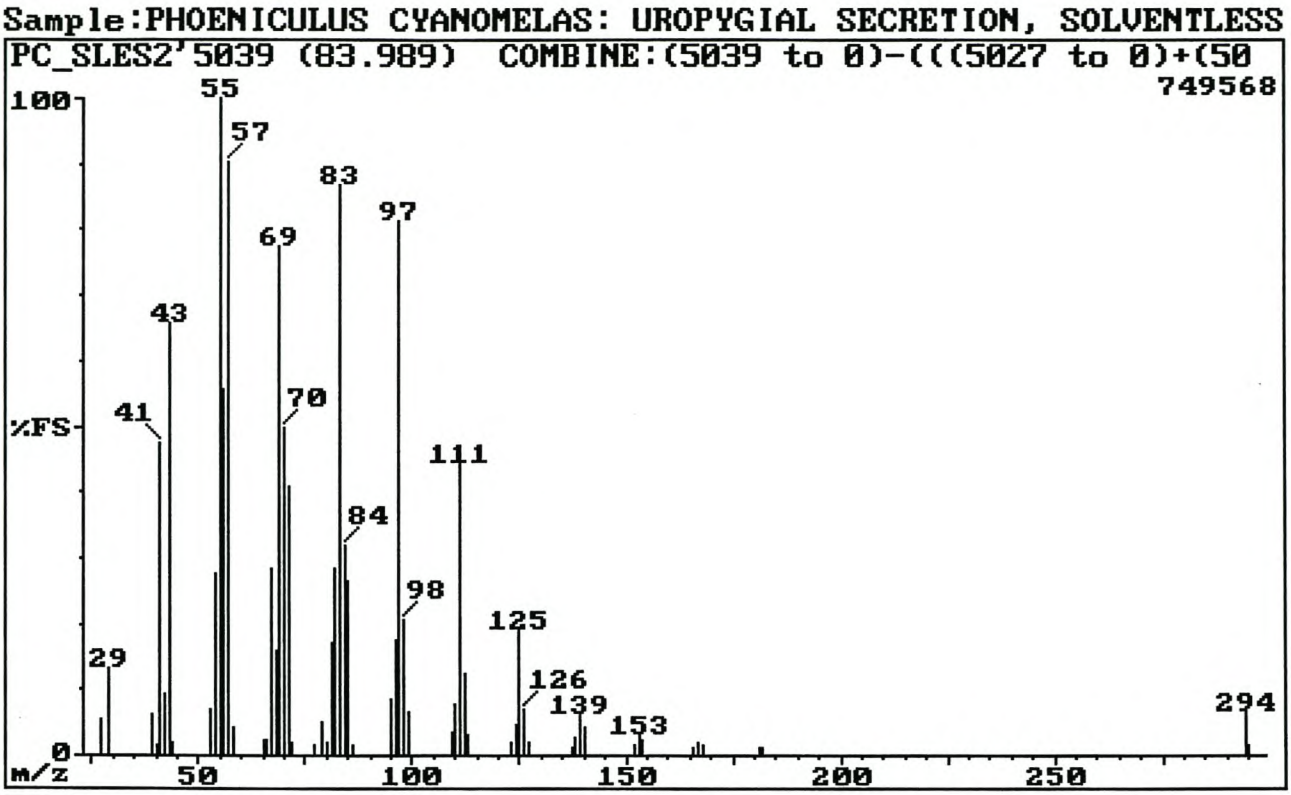

Fig 2.32: EI mass spectrum of component 5039 (heneicosene)

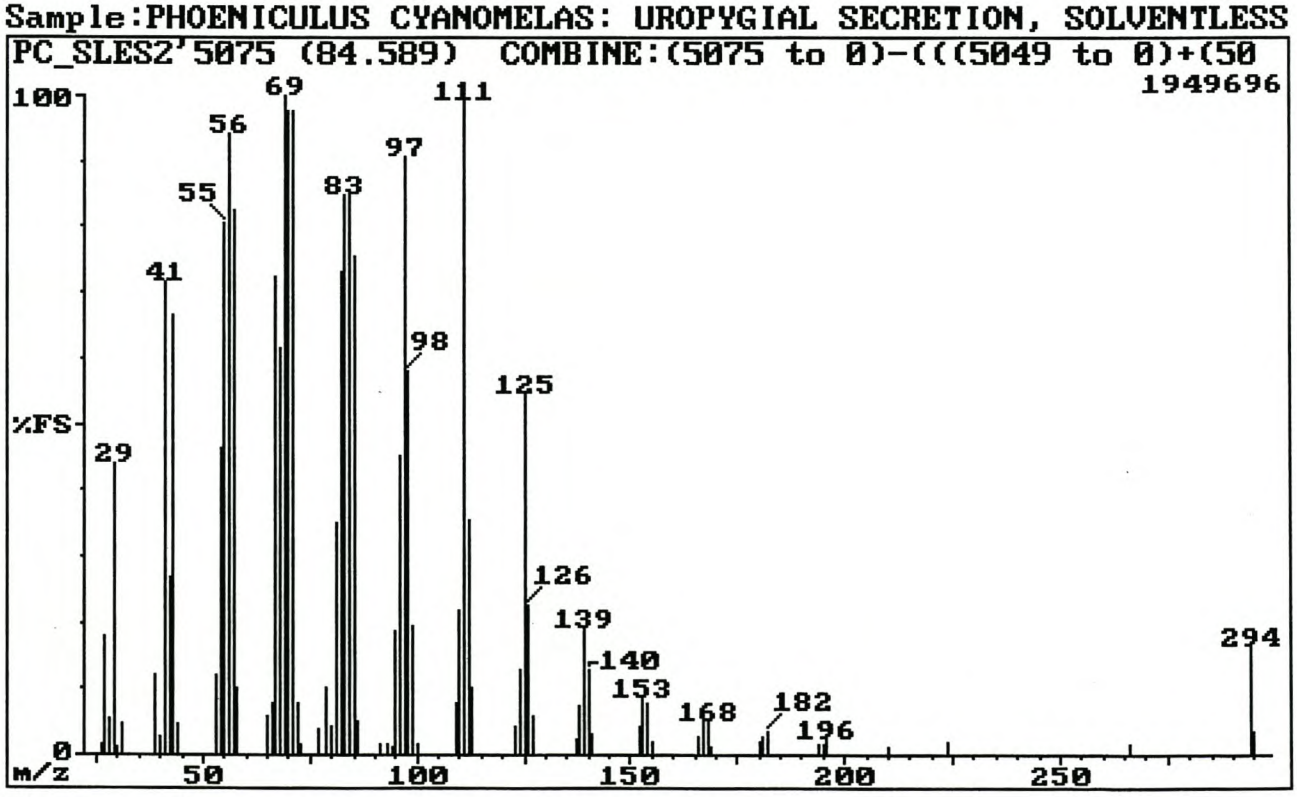

Fig 2.33: EI mass spectrum of component 5075 (heneicosene)

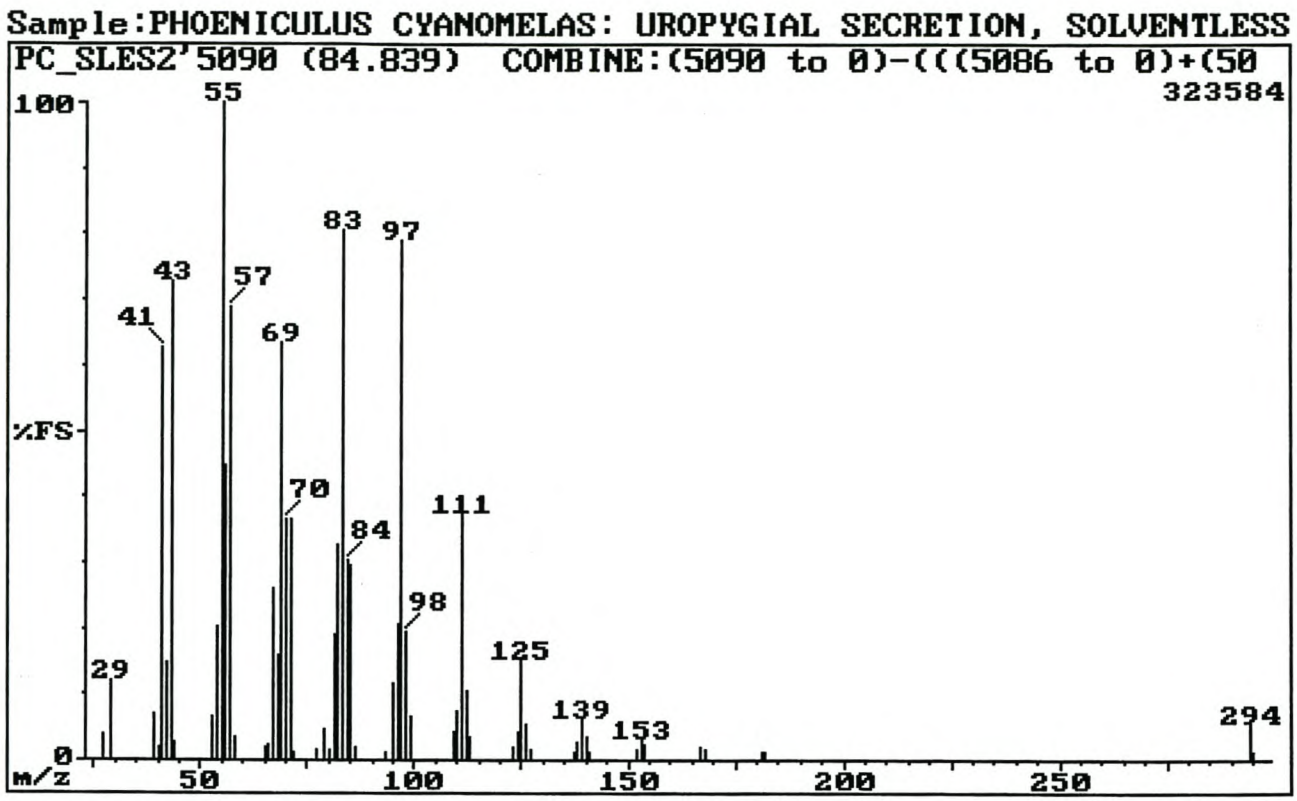

Fig 2.34: EI mass spectrum of component 5090 (heneicosene)

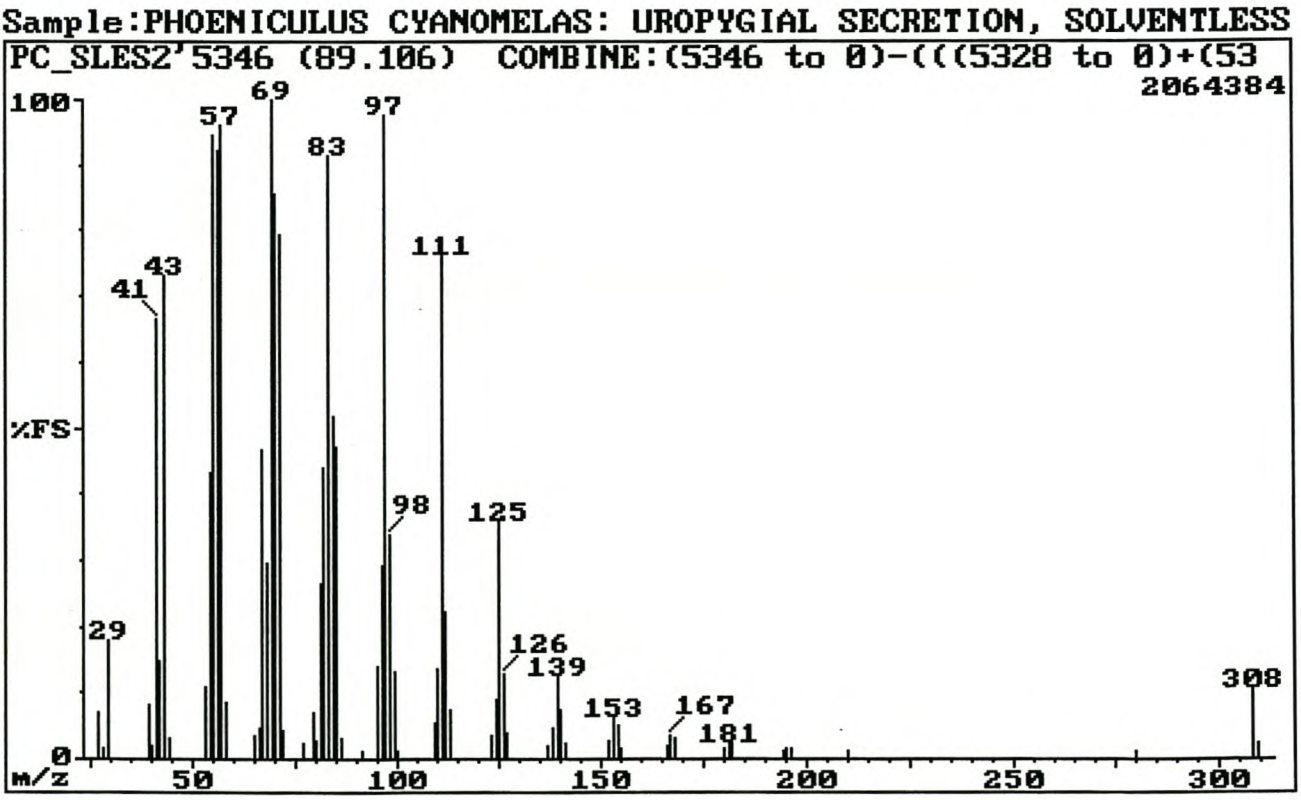

Fig 2.35: EI mass spectrum of component 5346 (docosene)

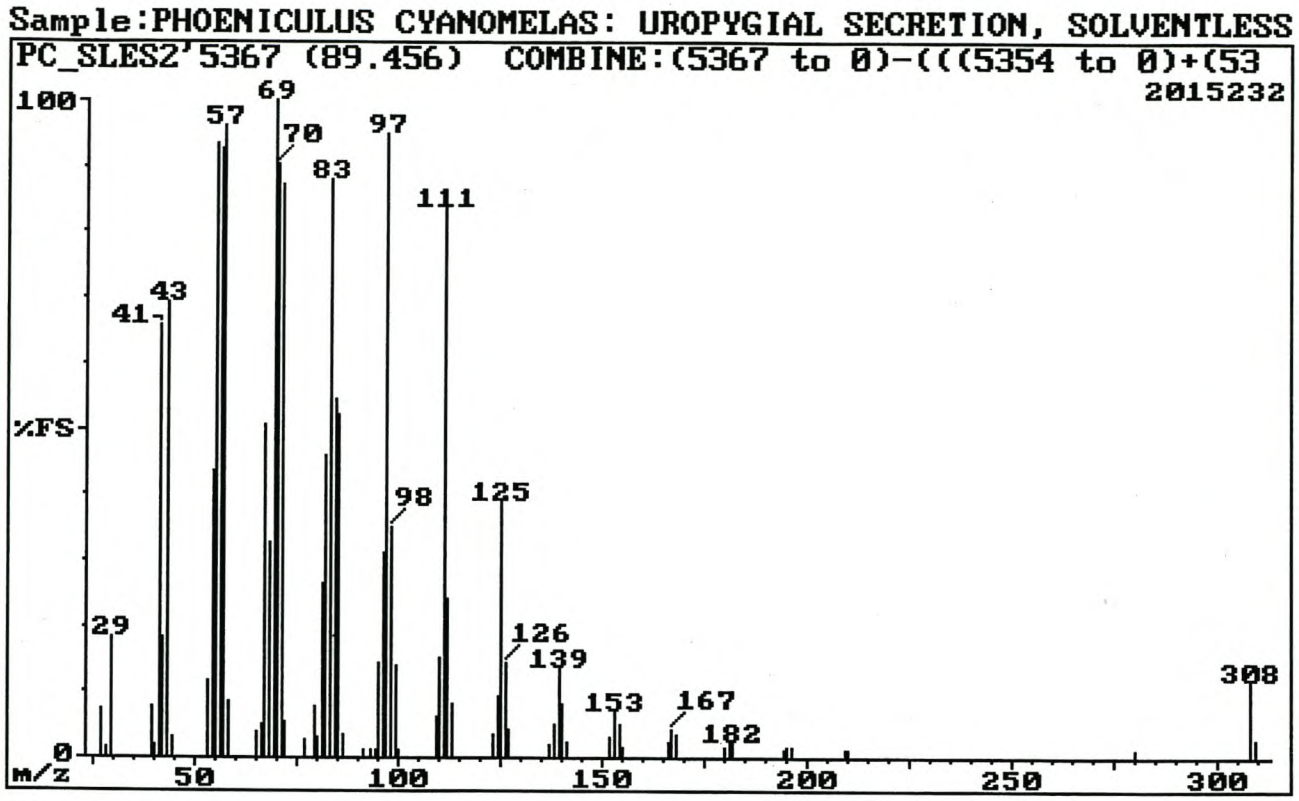

Fig 2.36: EI mass spectrum of component 5367 (docosene)

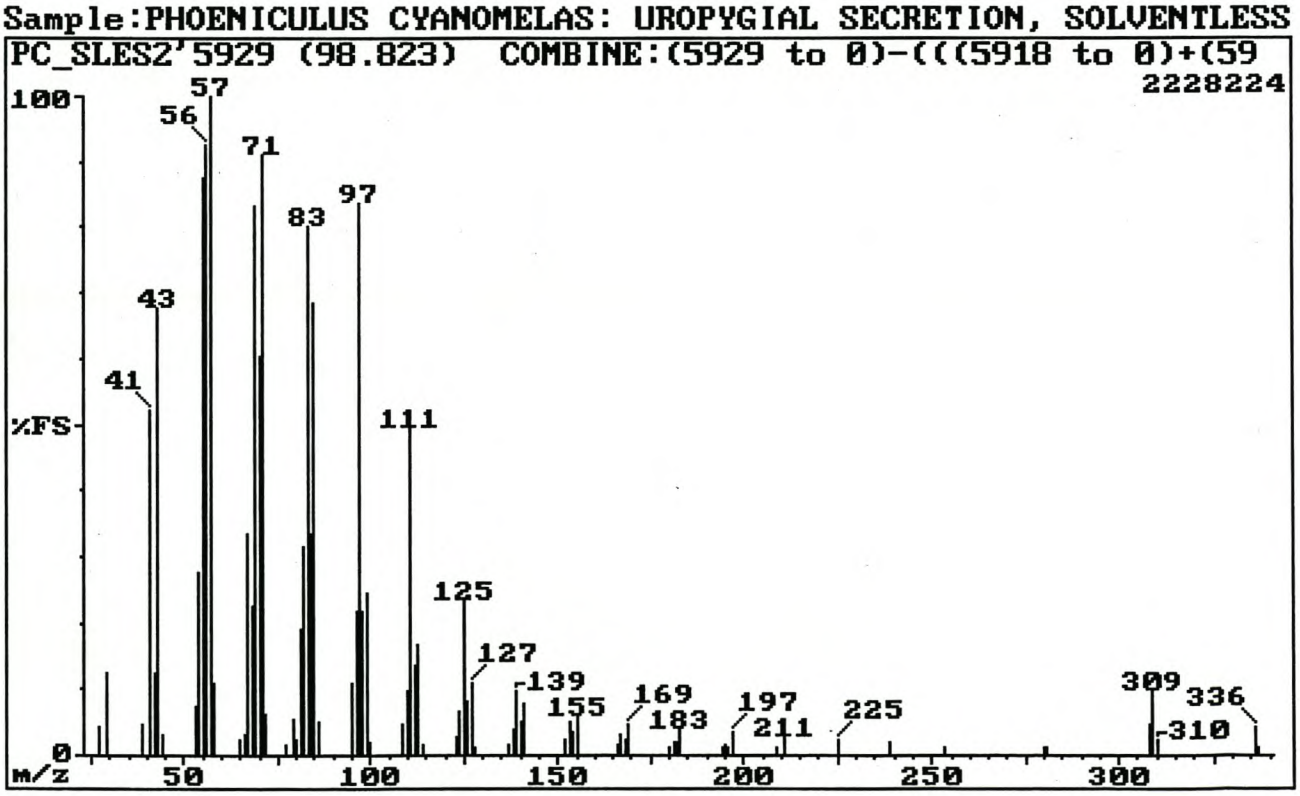

Fig 2.37: EI mass spectrum of component 5929 (tetracosene)

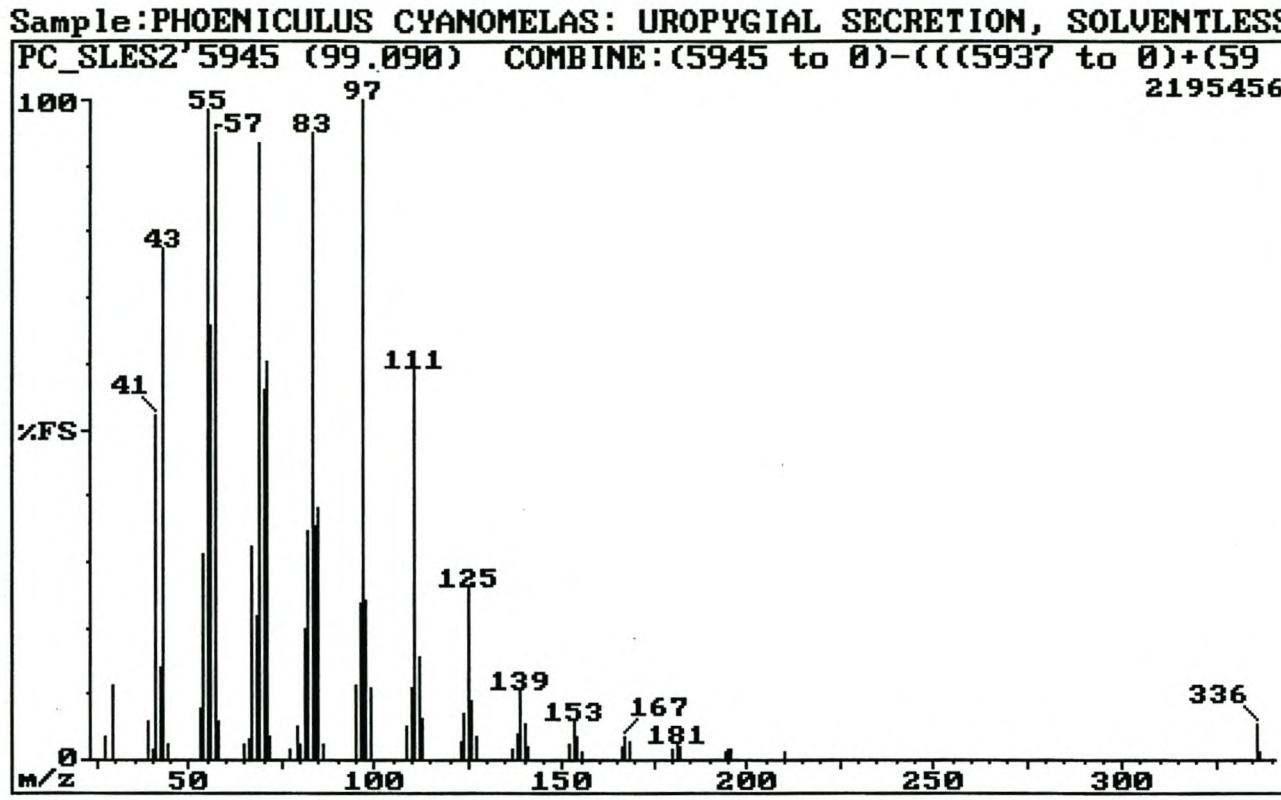

Fig 2.38: EI mass spectrum of component 5945 (tetracosene)

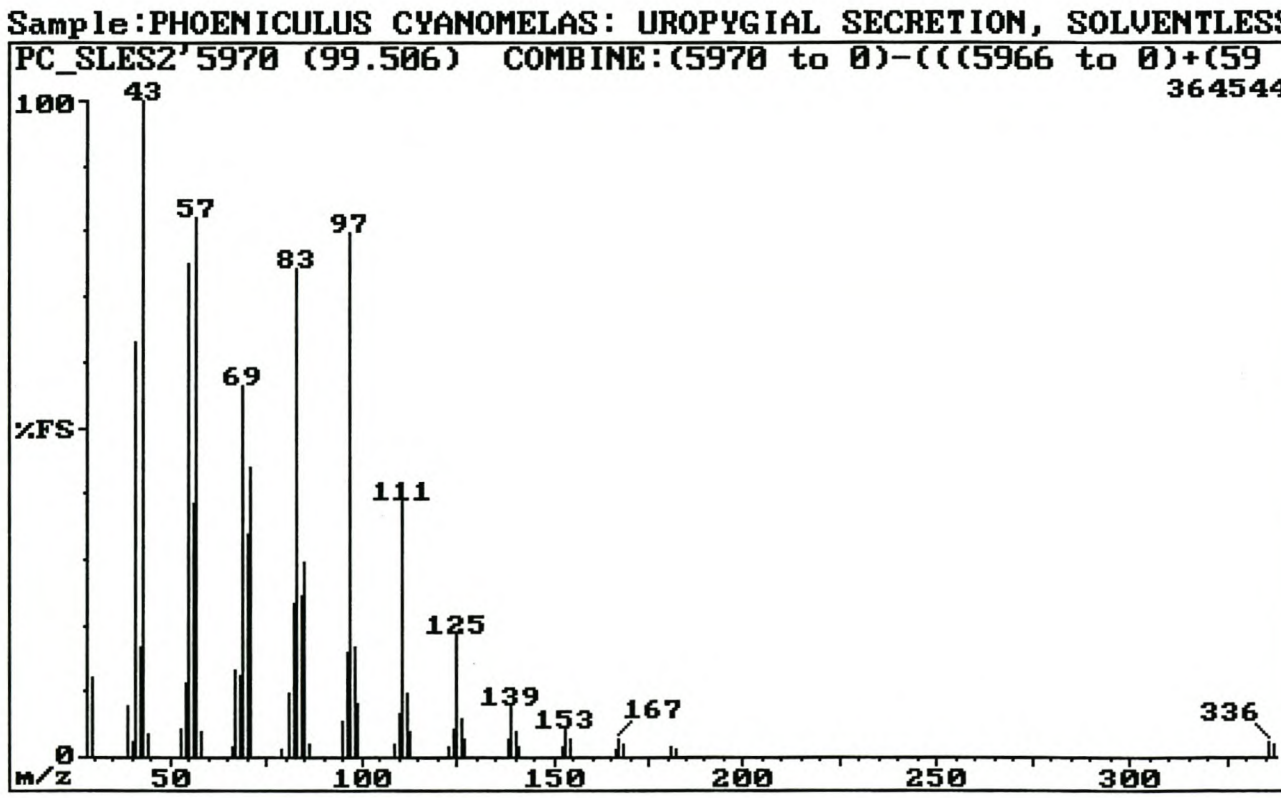

Fig 2.39: EI mass spectrum of component 5970 (tetracosene)

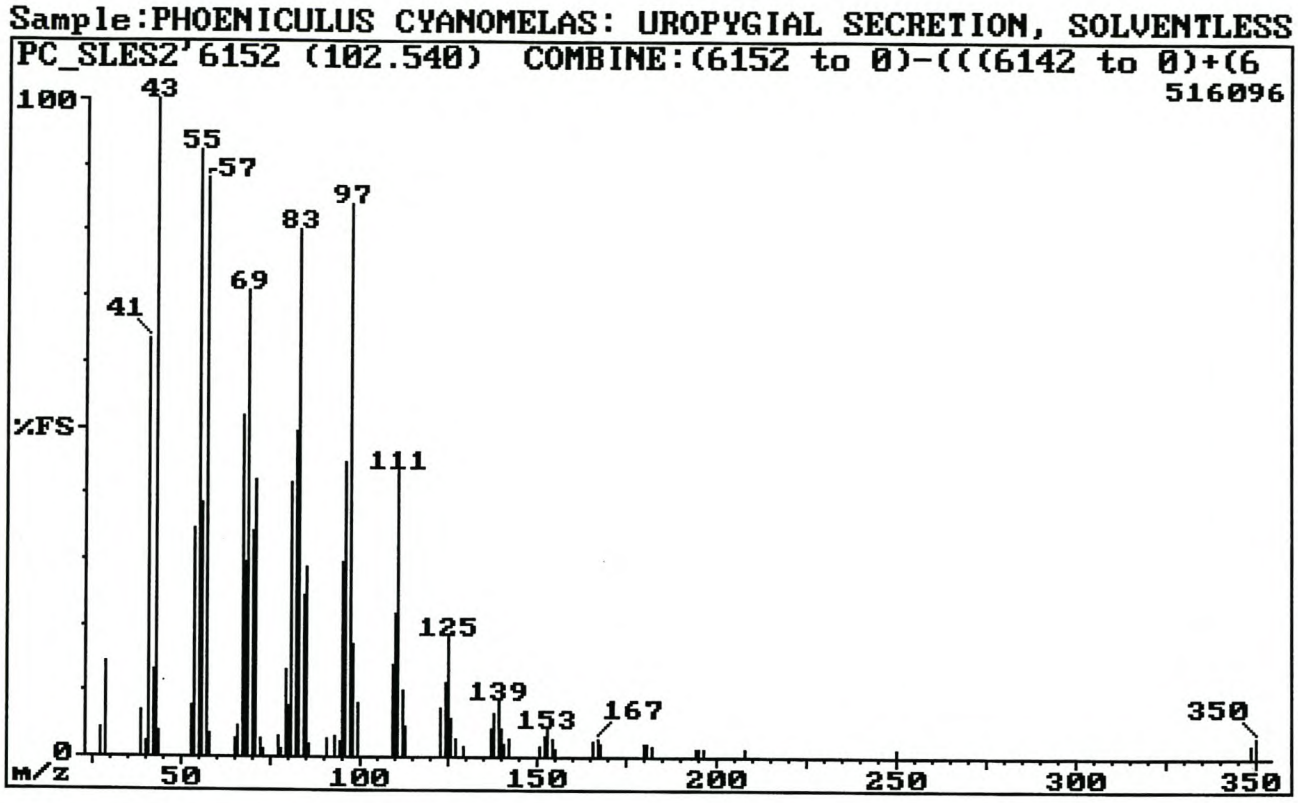

Fig 2.40: EI mass spectrum of component 6152 (pentacosene)

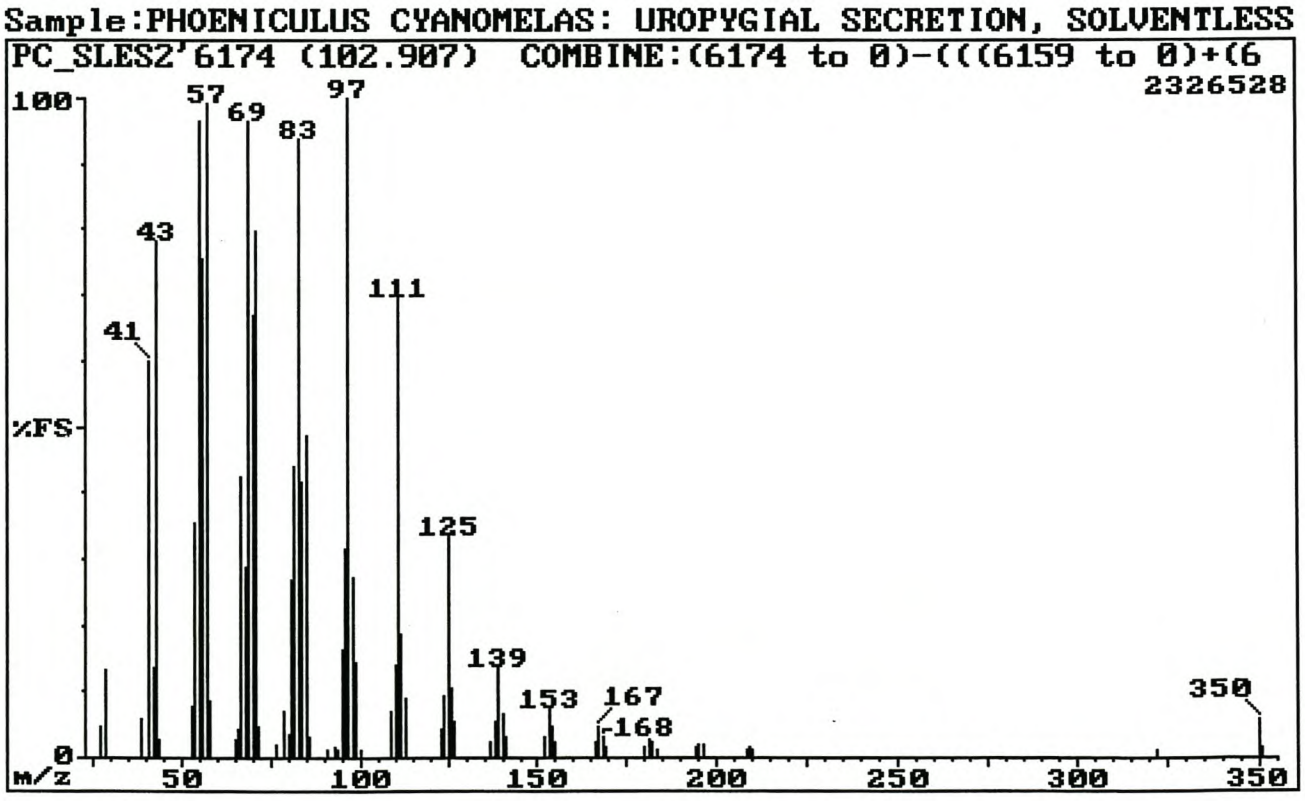

Fig 2.41: EI mass spectrum of component 6174 (pentacosene)

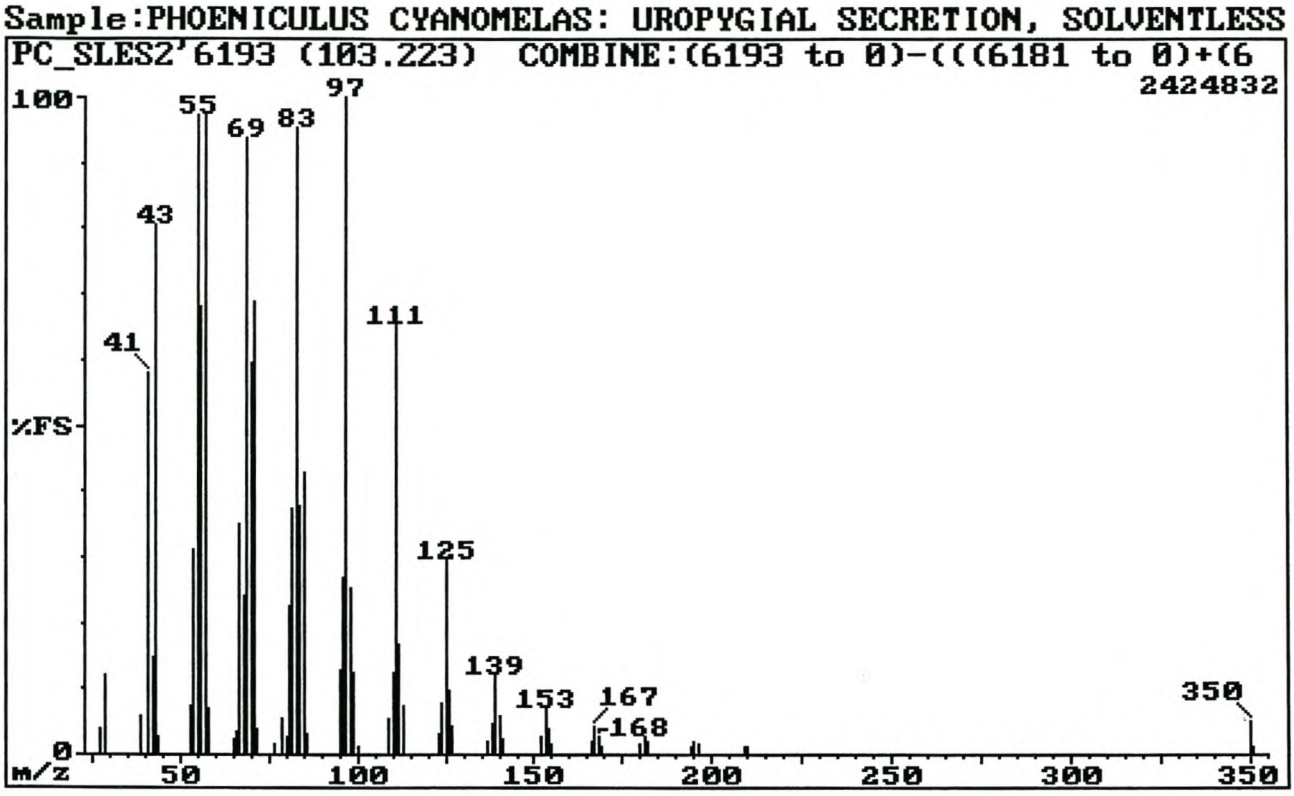

Fig 2.42: EI mass spectrum of component 6193 (pentacosene)

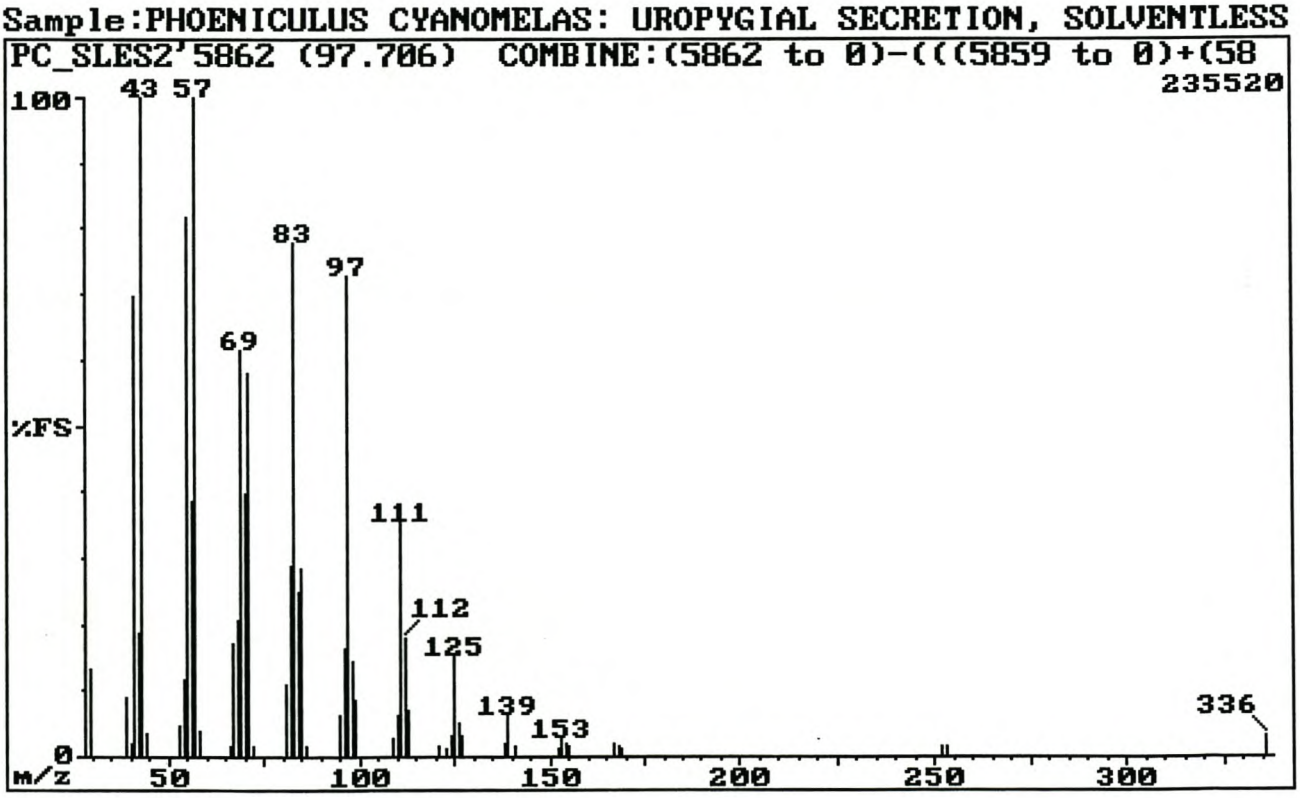

Fig 2.43: EI mass spectrum of component 5862 (methyltricosene)

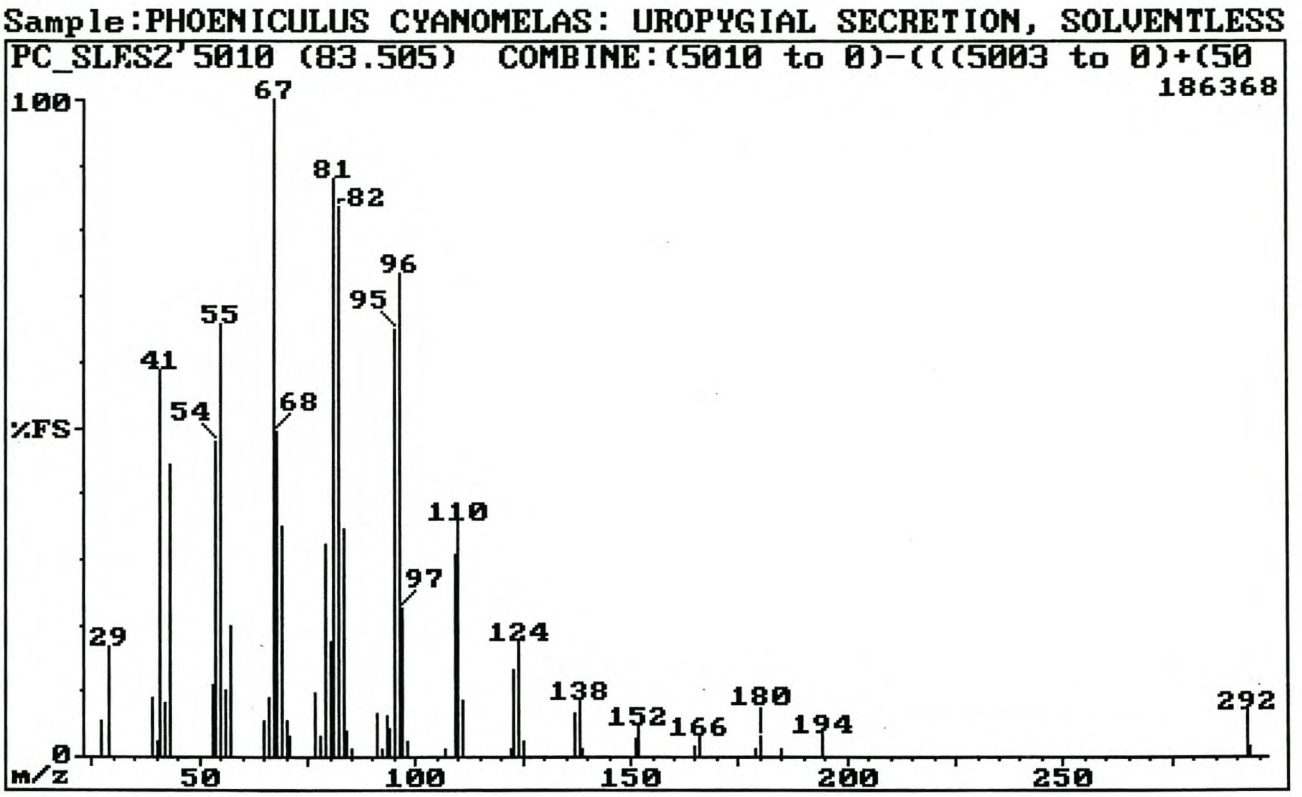

Fig 2.44: EI mass spectrum of component 5010 (heneicosyne)

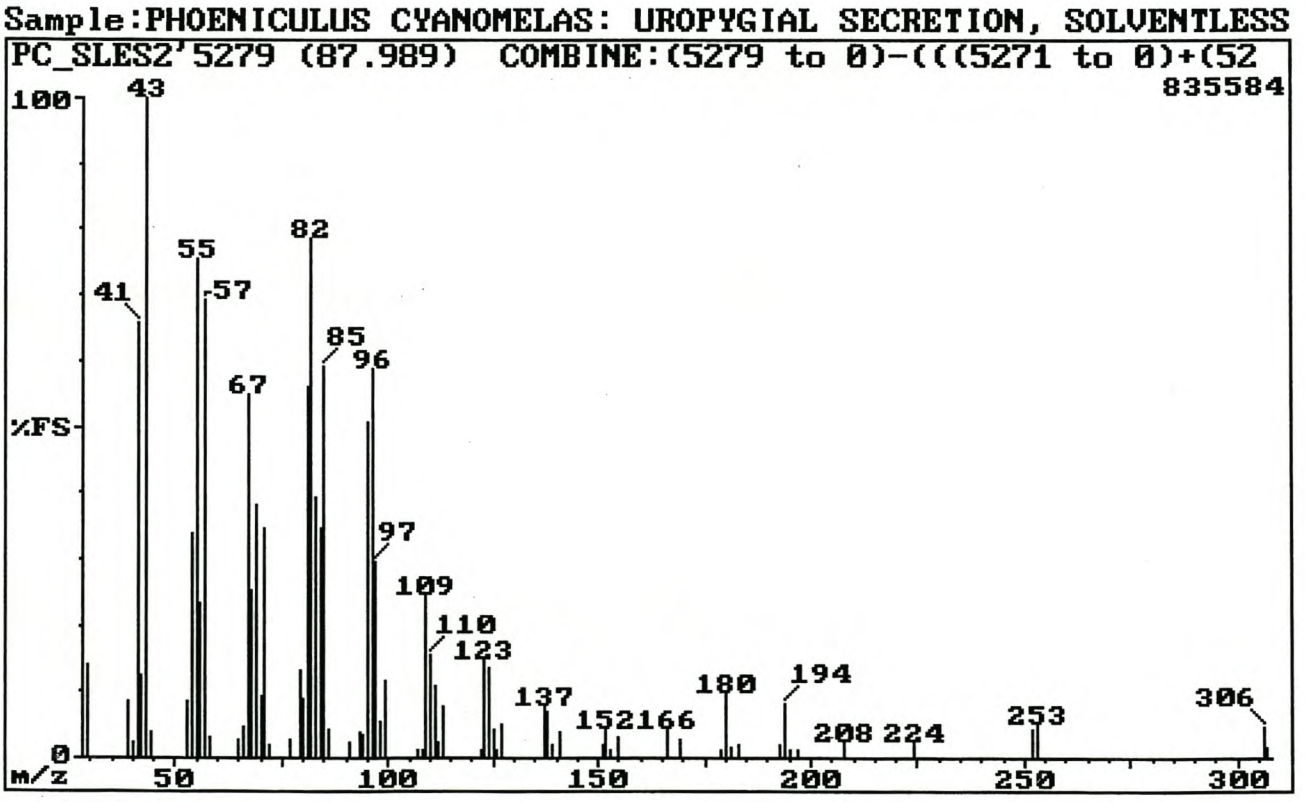

Fig 2.45: EI mass spectrum of component 5279 (docosyne)

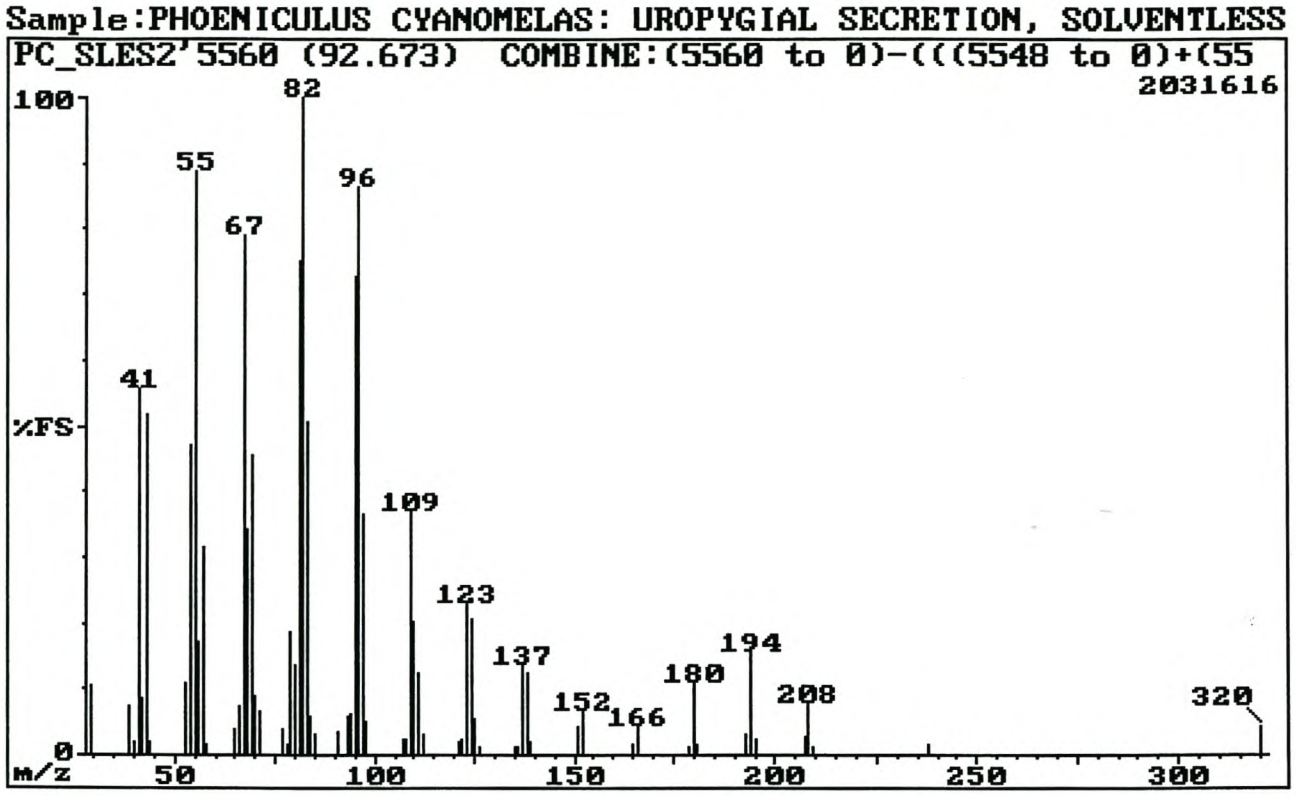

Fig 2.46: EI mass spectrum of component 5560 (tricosyne)

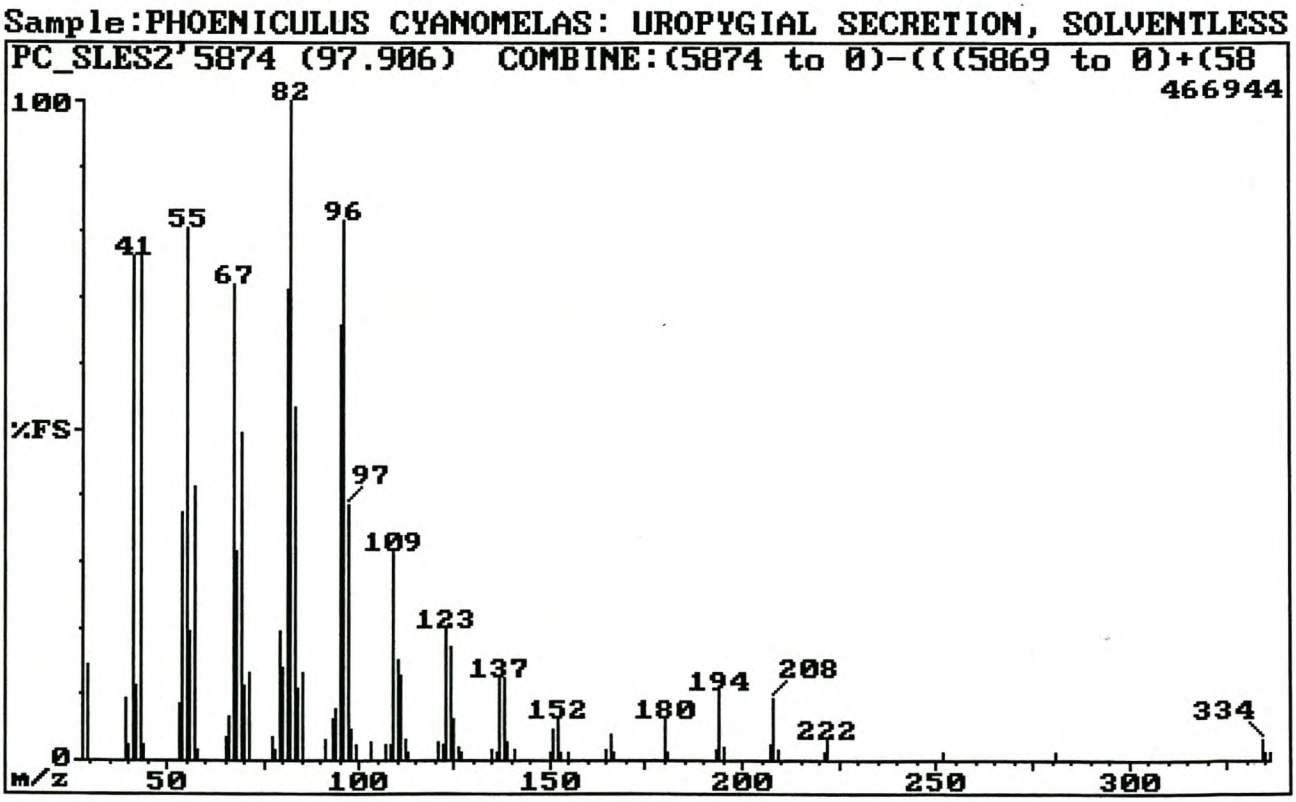

Fig 2.47: EI mass spectrum of component 5874 (tetracosyne)

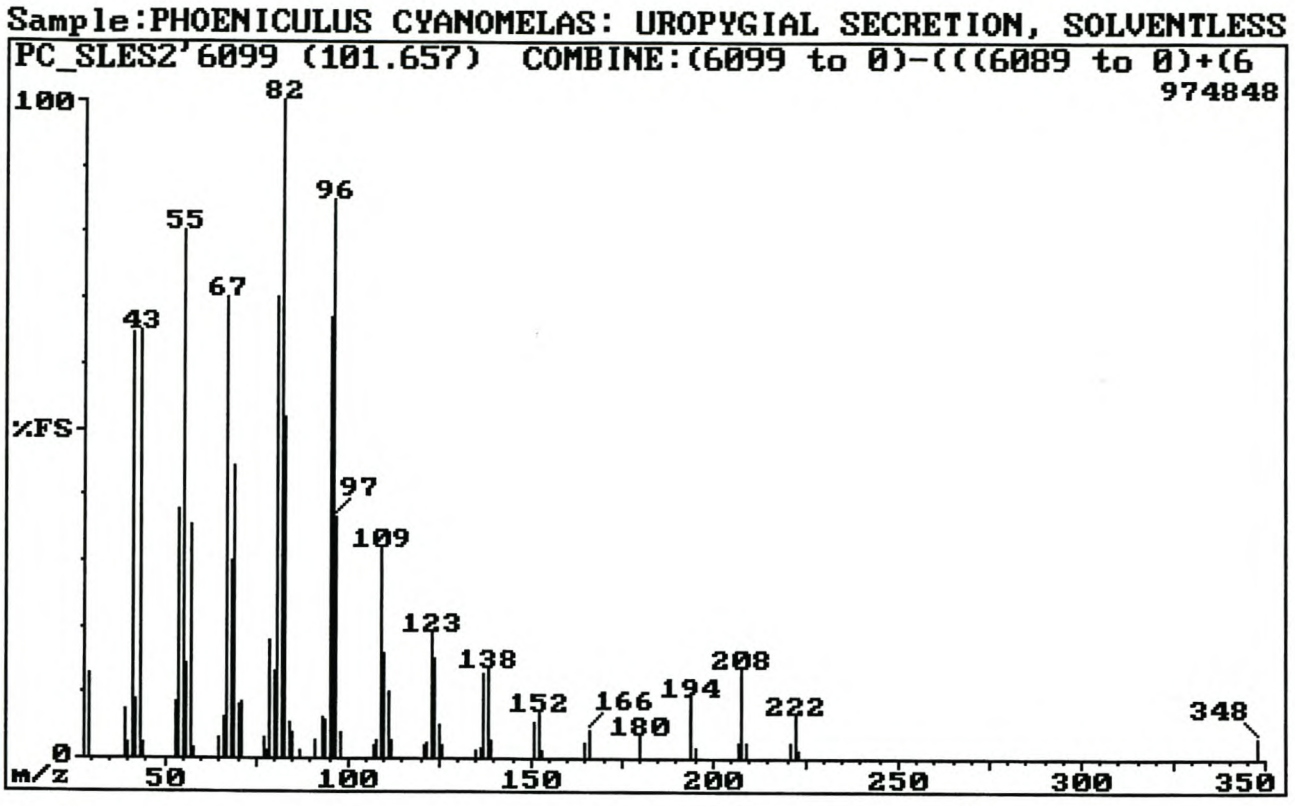

Fig 2.48: EI mass spectrum of component 6099 (pentacosyne)

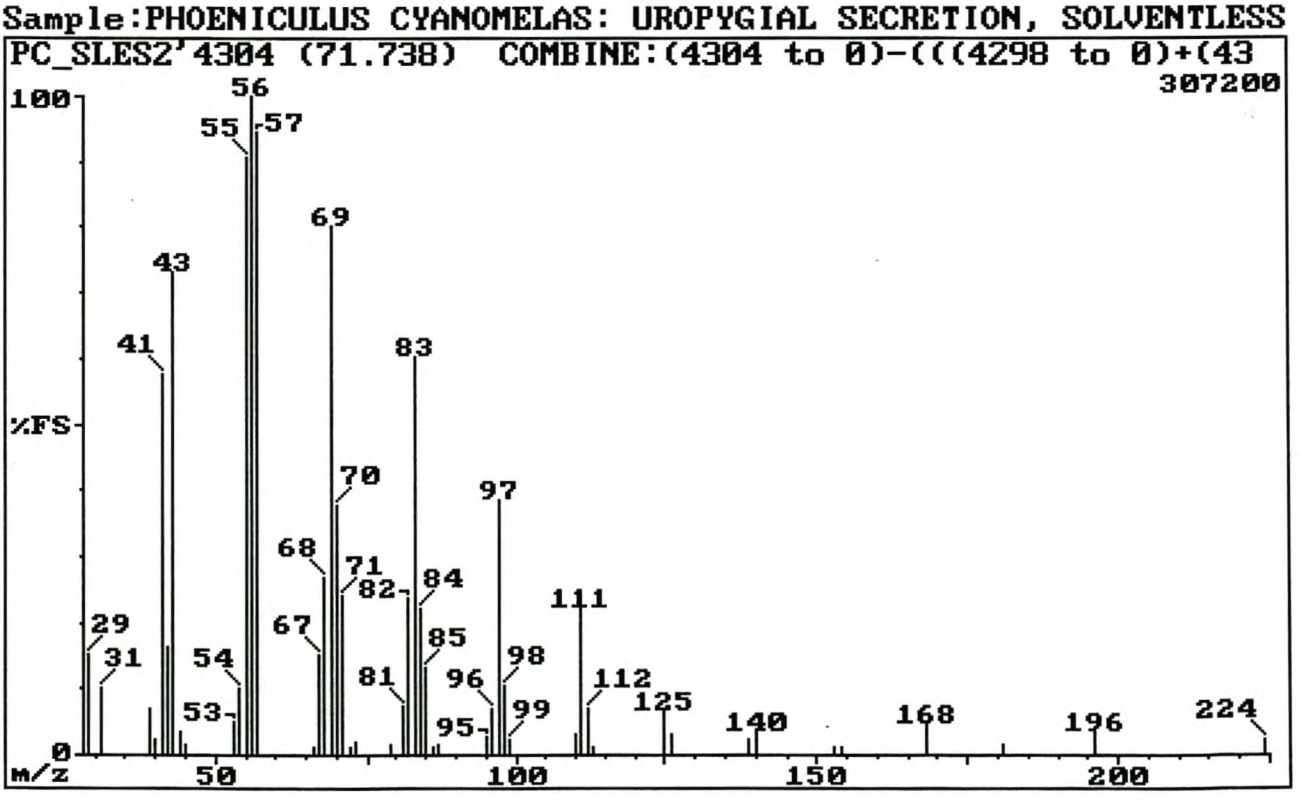

Fig 2.49: EI mass spectrum of component 4304 (1-hexadecanol)

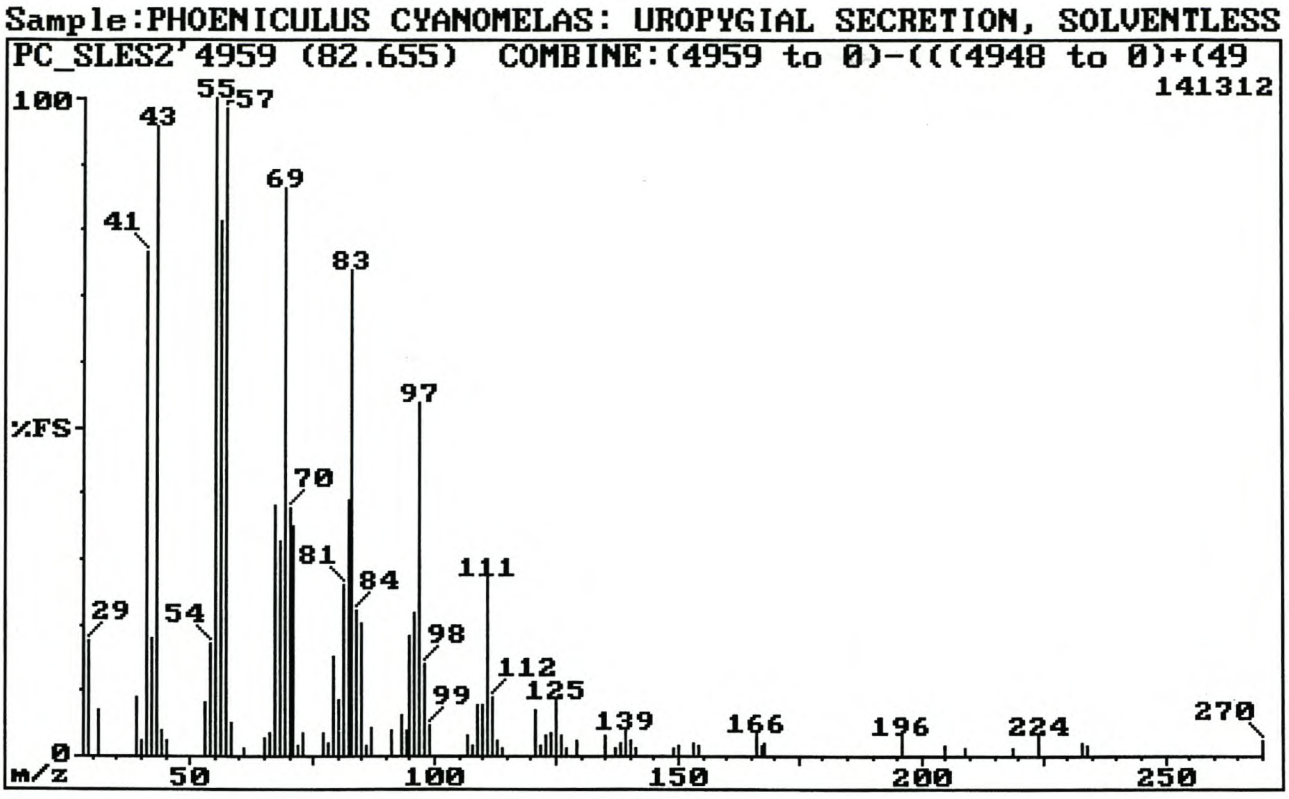

Fig 2.50: EI mass spectrum of component 4959 (1-octadecanol)

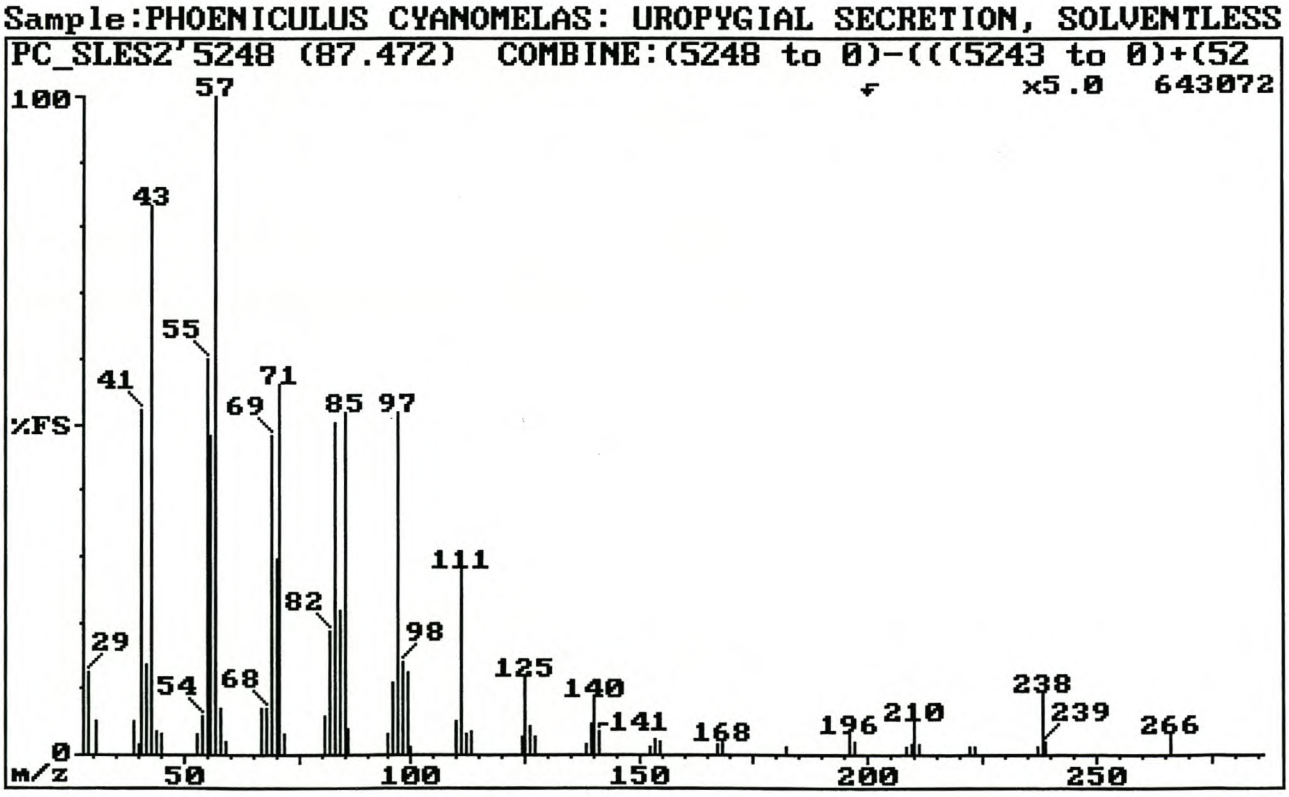

Fig 2.51: EI mass spectrum of component 5248 (1-nonadecanol)

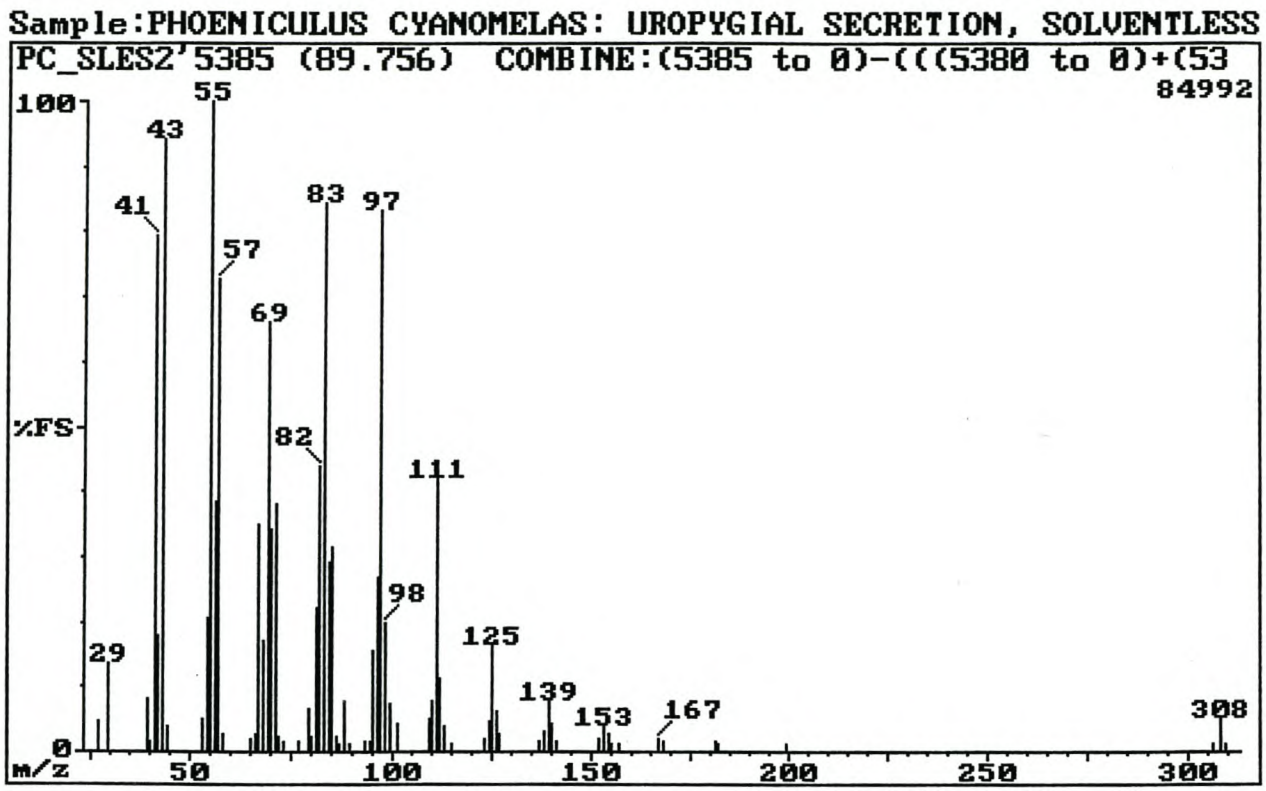

Fig 2.52: EI mass spectrum of component 5385 (1-docosanol)

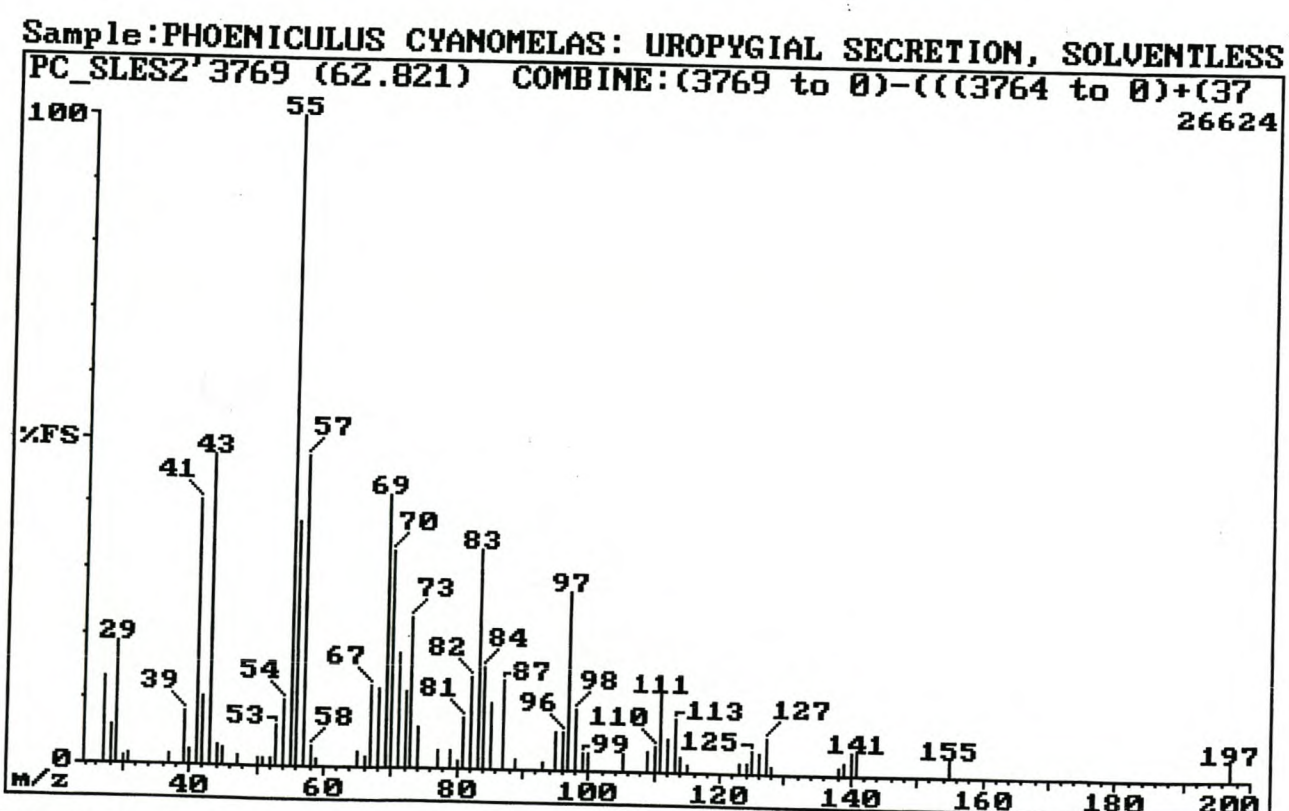

Fig 2.53: EI mass spectrum of component 3769 (12-methyl-1-tridecanol)

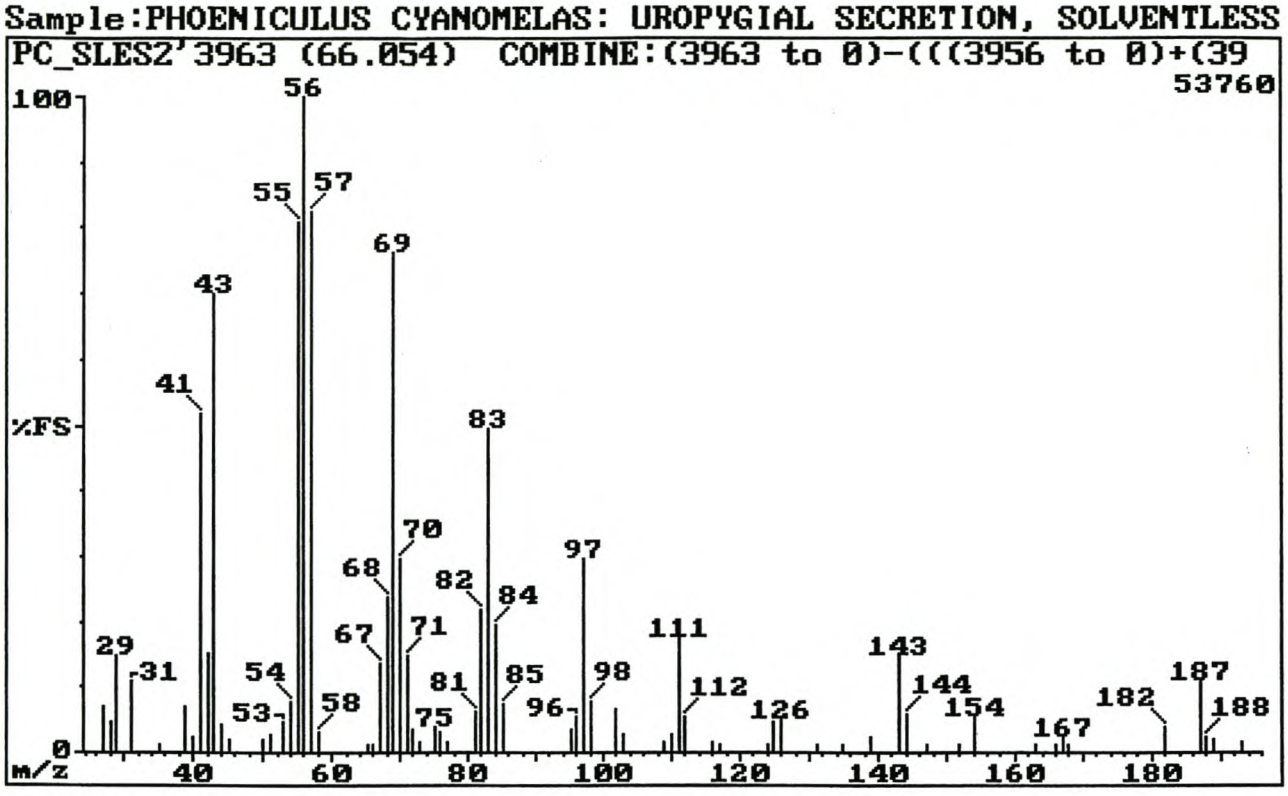

Fig 2.54: EI mass spectrum of component 3963 (13-methyl-1-tetradecanol)

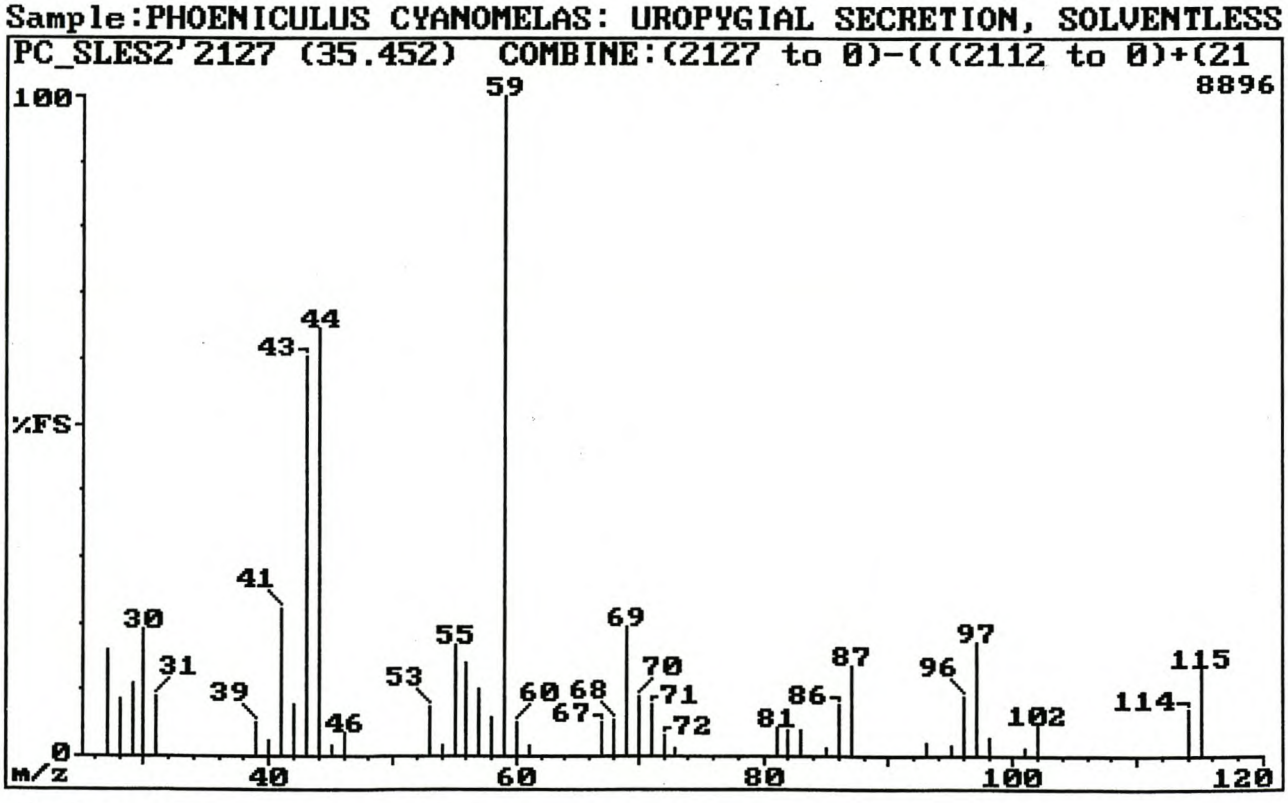

Fig 2.55: EI mass spectrum of component 2127 (3-nonanol)

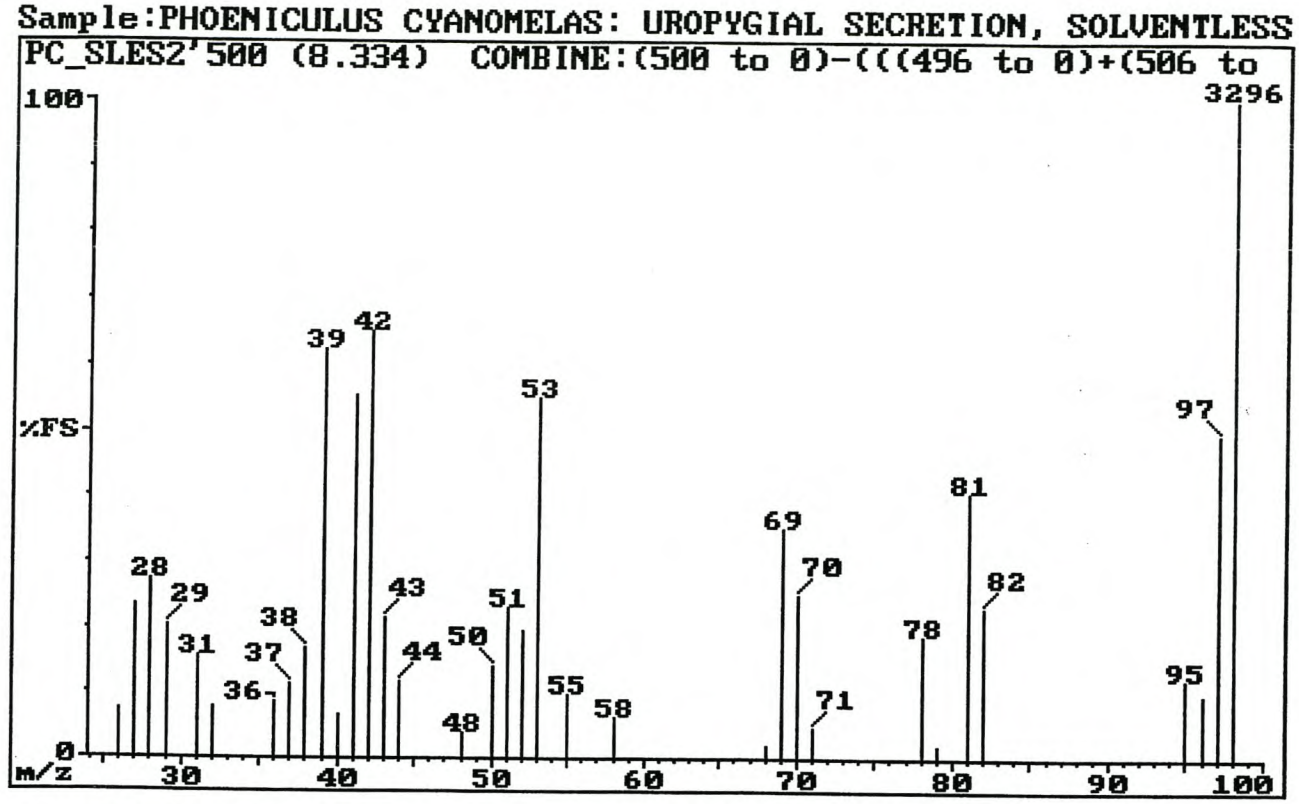

Fig 2.56: EI mass spectrum of component 500 (2-furanylmethanol)

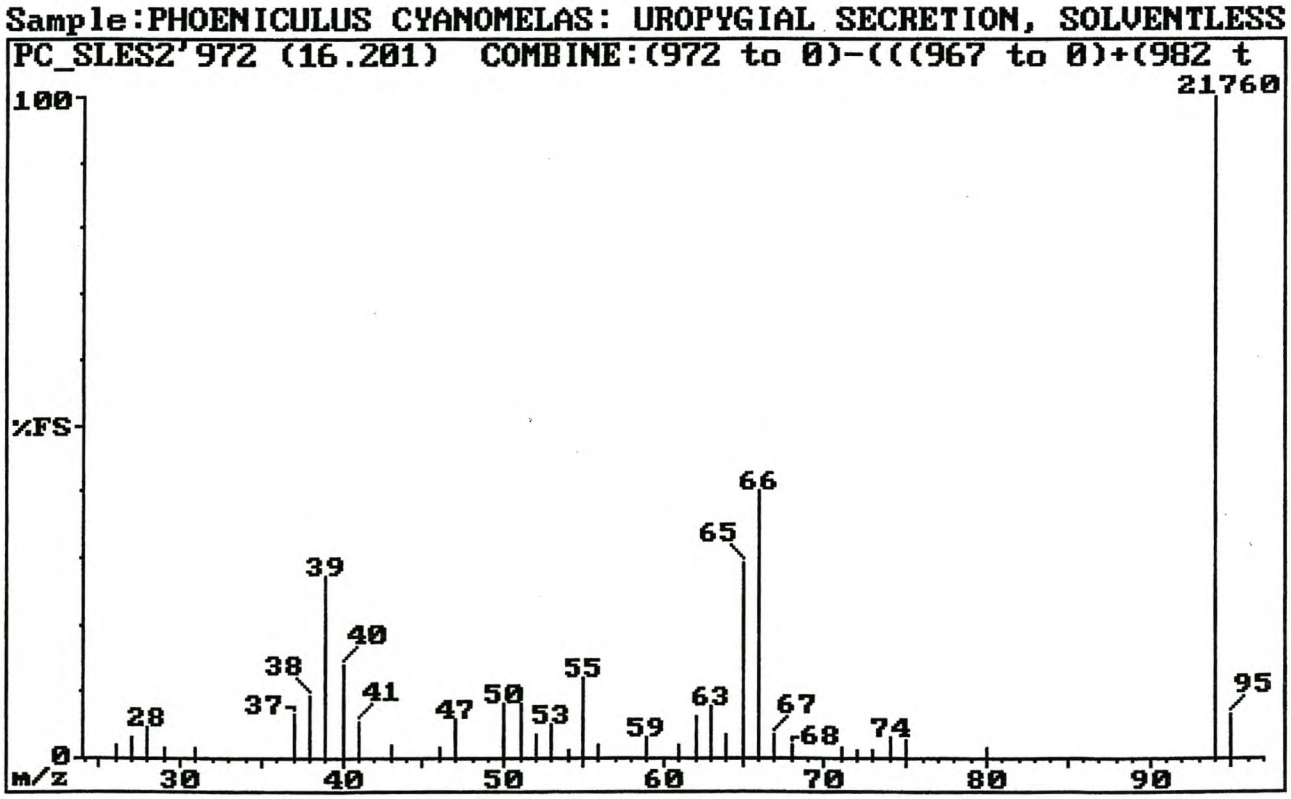

Fig 2.57: EI mass spectrum of component 972 (phenol)

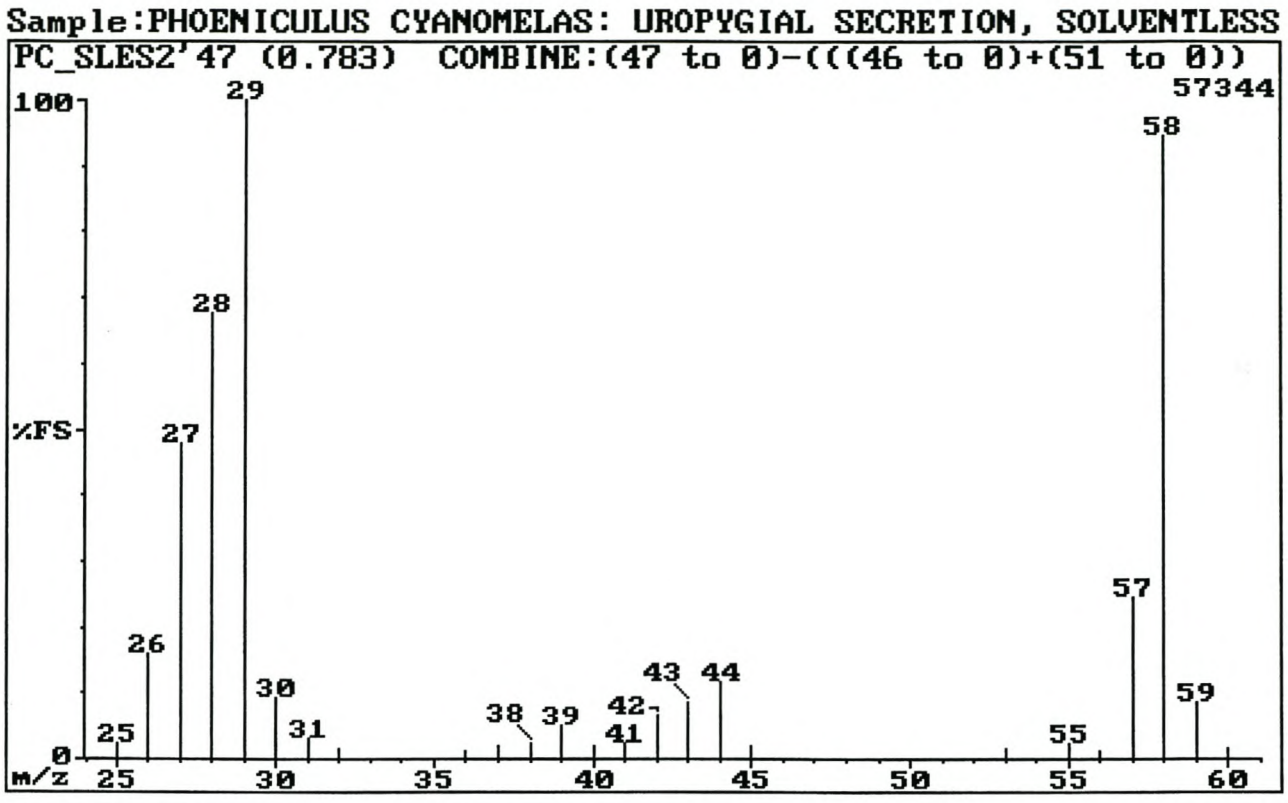

Fig 2.58: EI mass spectrum of component 47 (propanal)

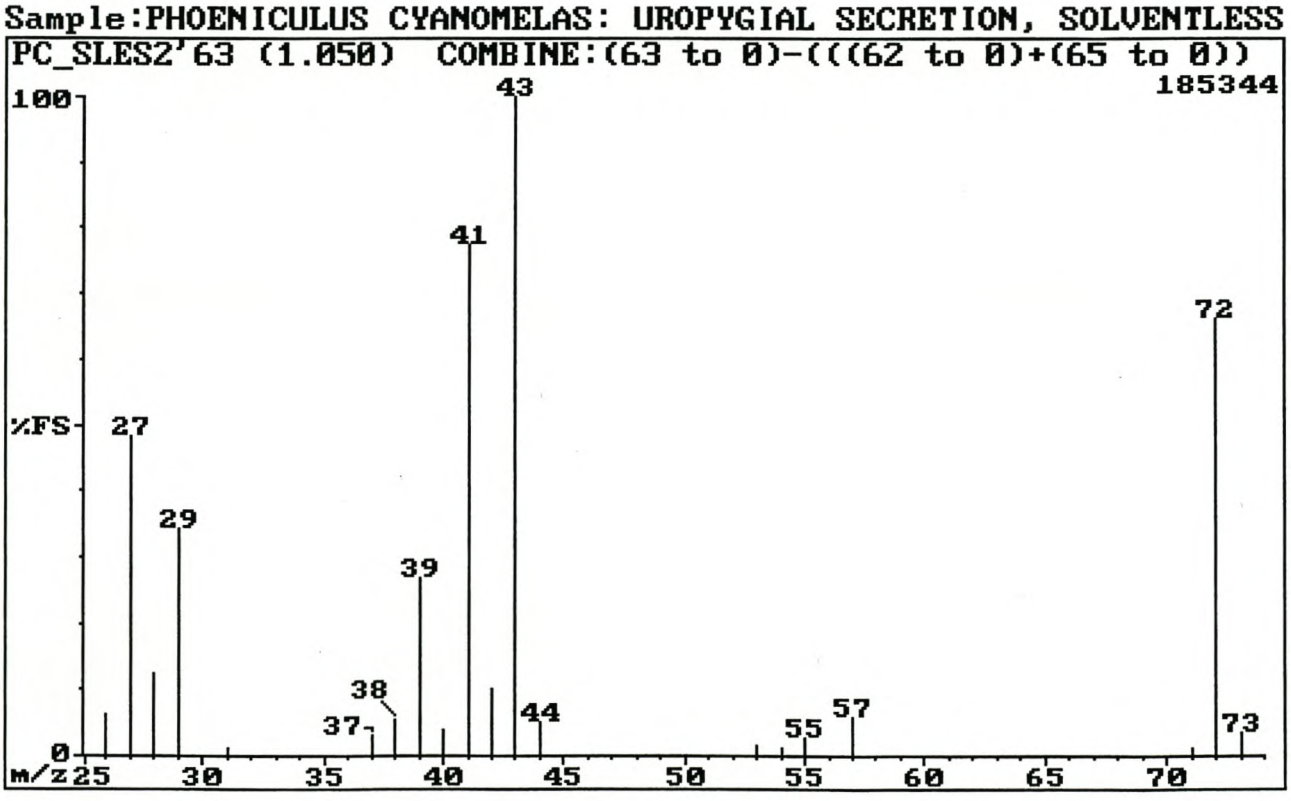

Fig 2.59: EI mass spectrum of component 63 (2-methylpropanal)

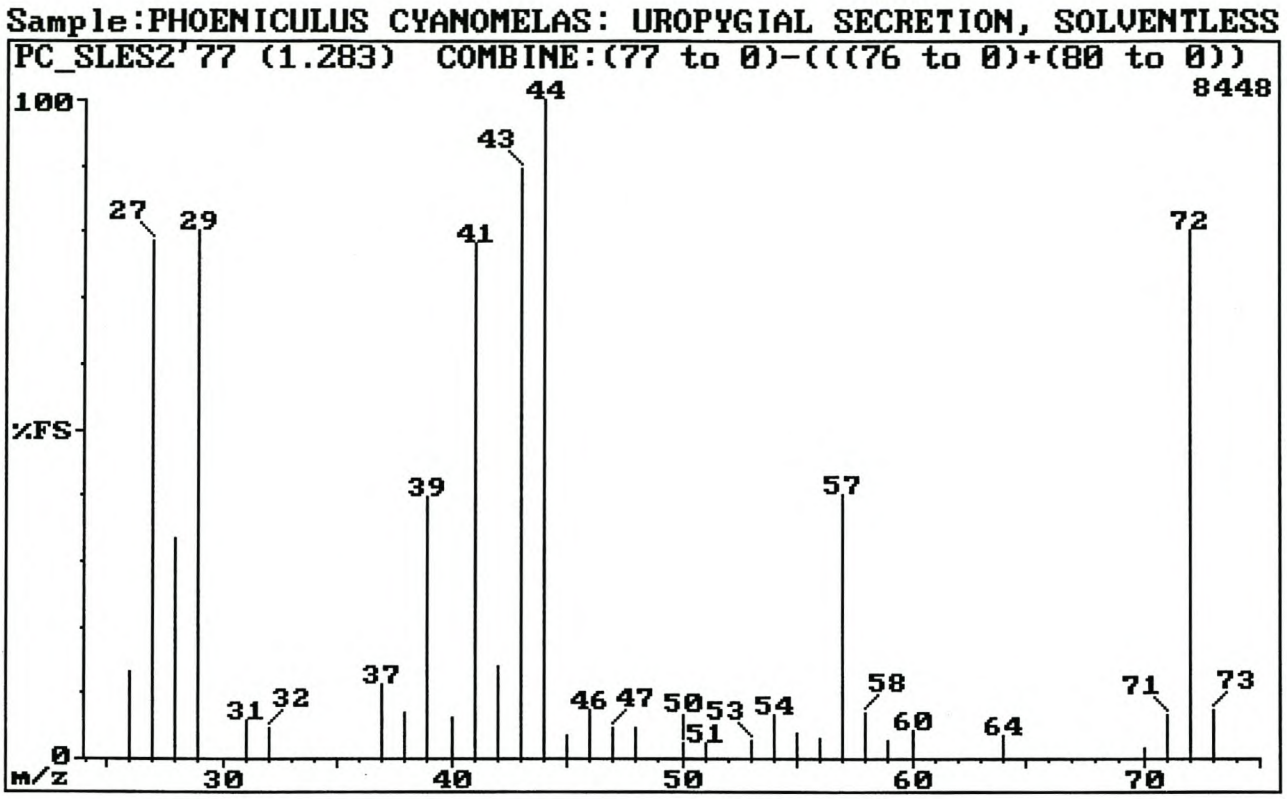

Fig 2.60: EI mass spectrum of component 77 (butanal)

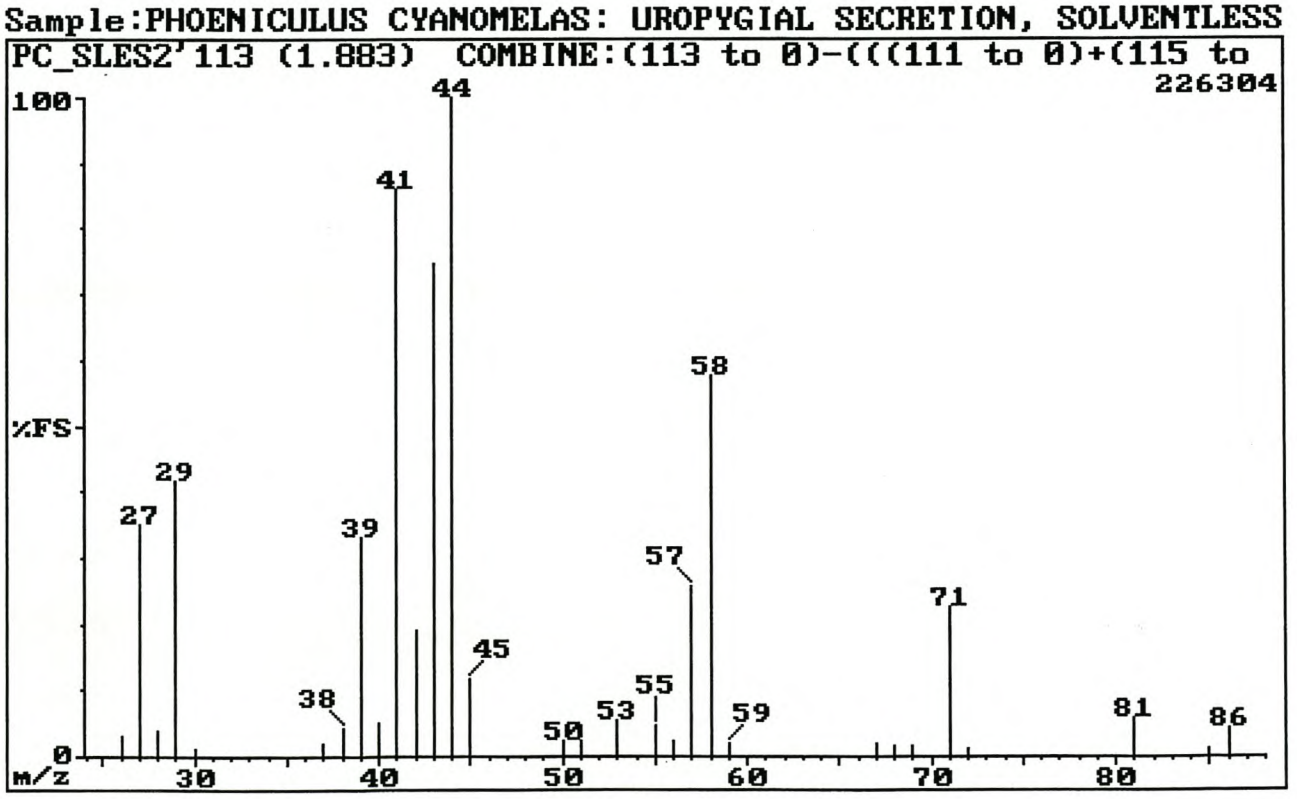

Fig 2.61: EI mass spectrum of component 113 (3-methylbutanal)

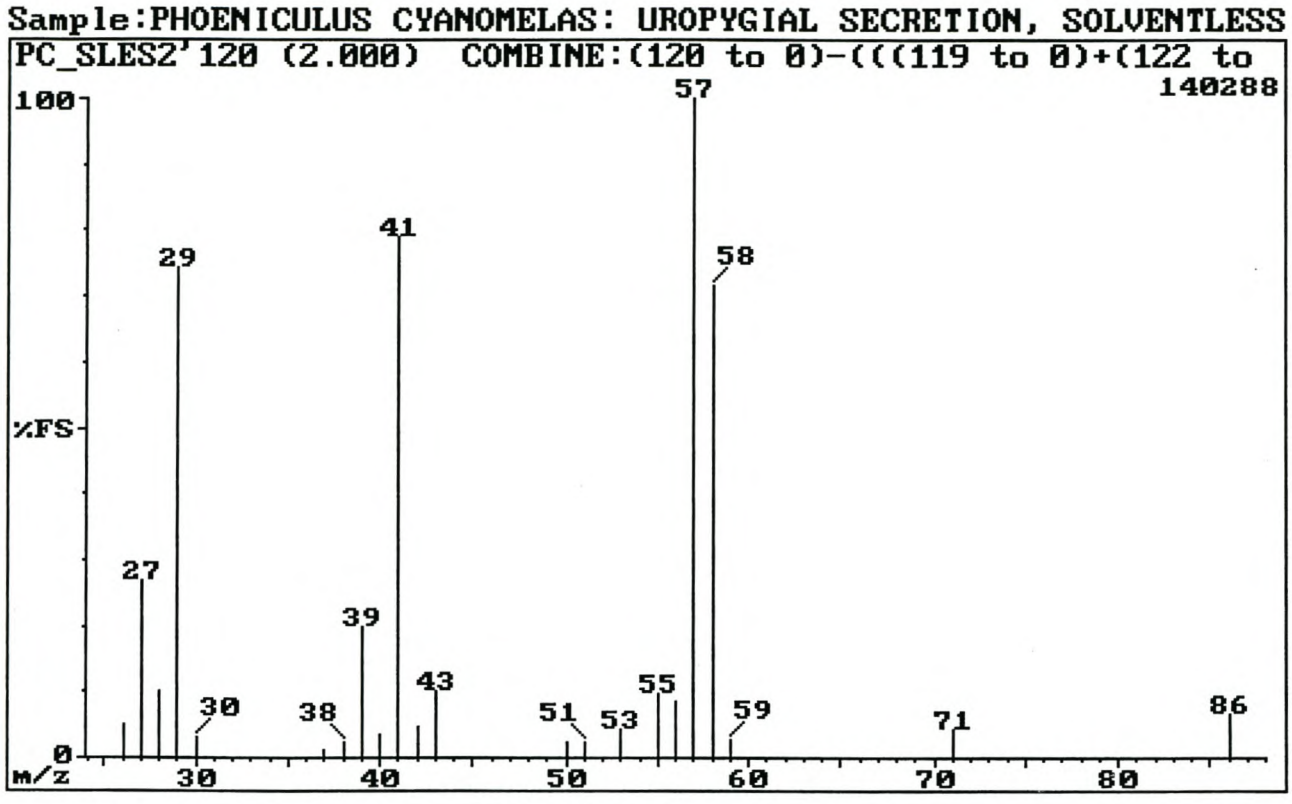

Fig 2.62: EI mass spectrum of component 120 (2-methylbutanal)

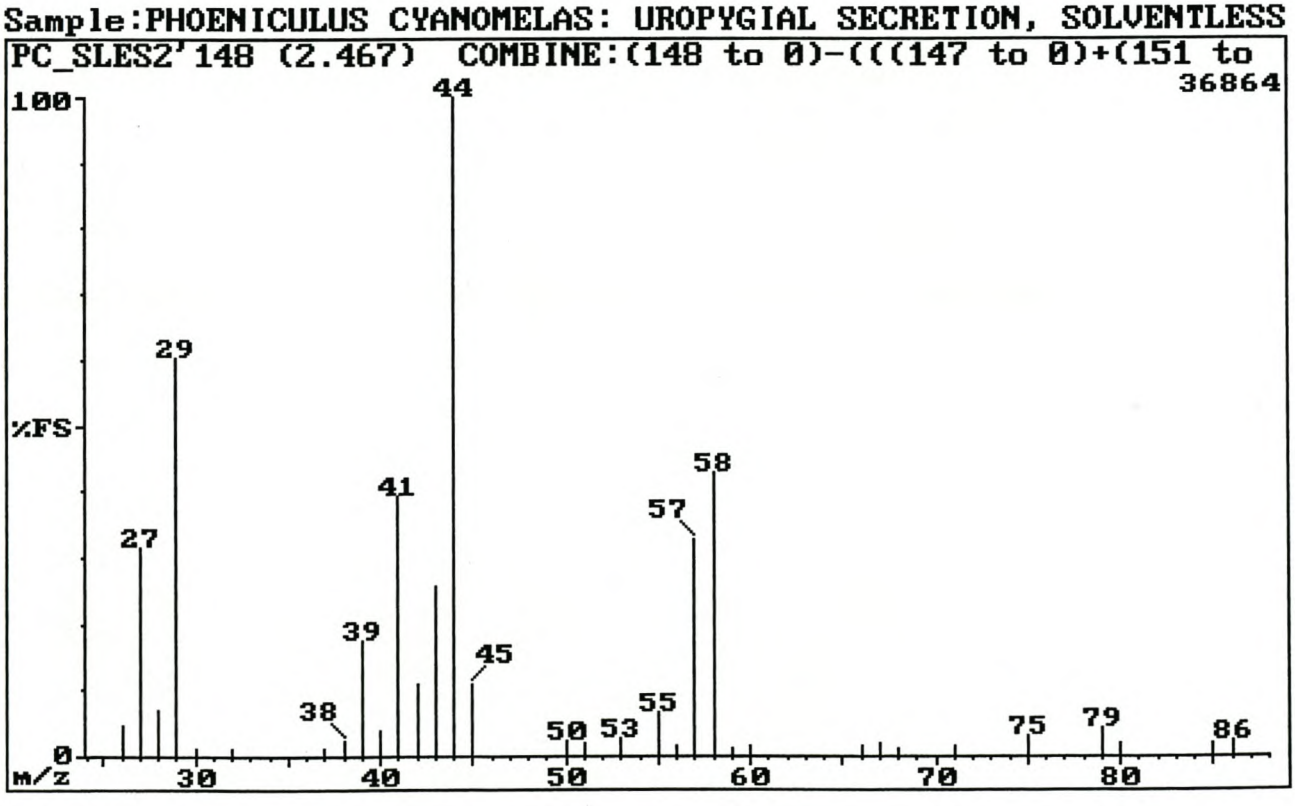

Fig 2.63: EI mass spectrum of component 148 (pentanal)

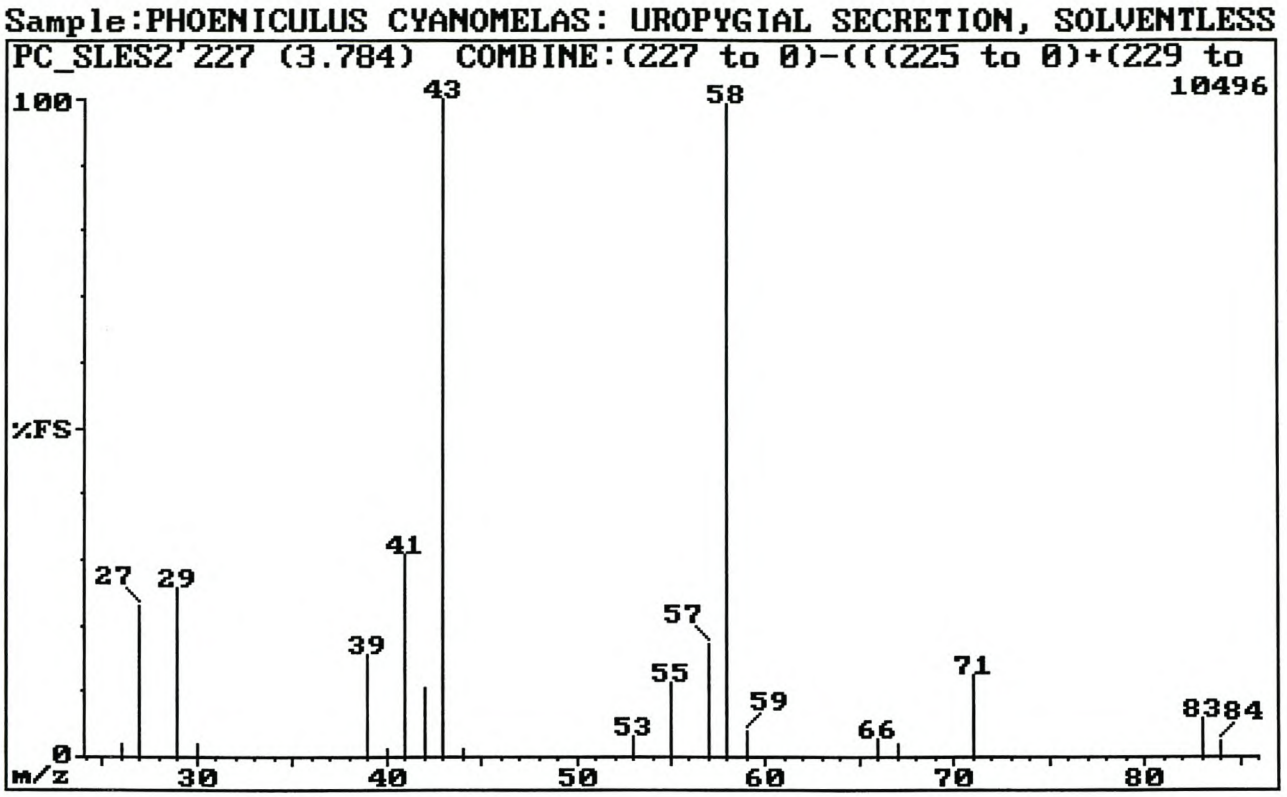

Fig 2.64: EI mass spectrum of component 227 (2-methylpentanal)

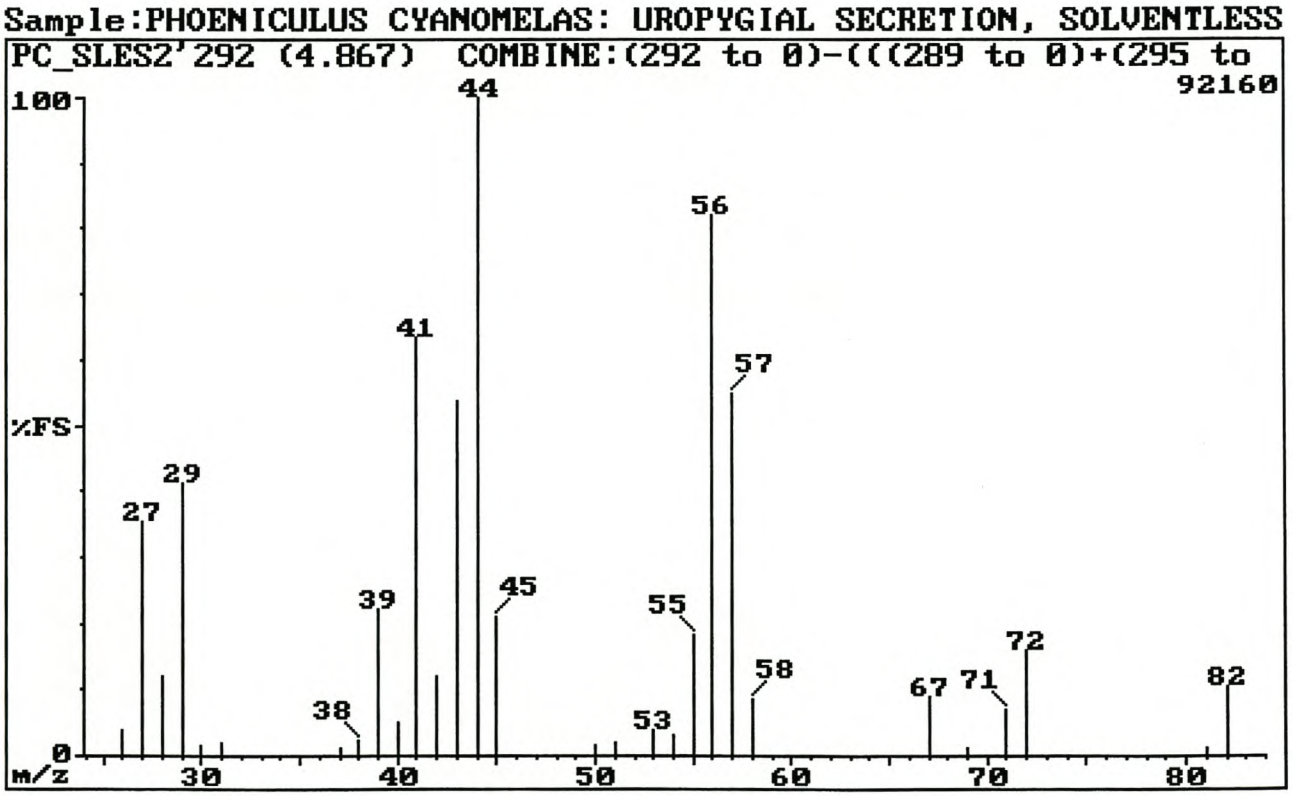

Fig 2.65: EI mass spectrum of component 292 (hexanal)

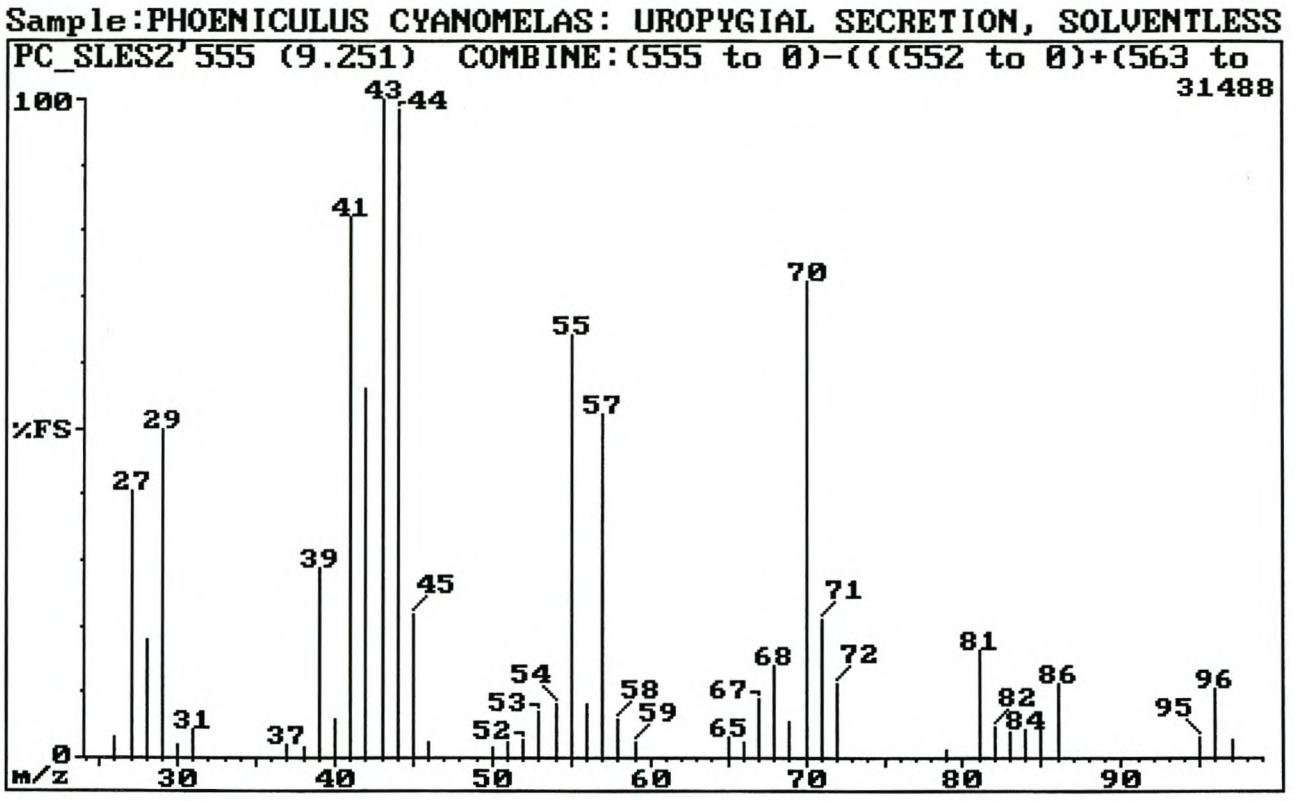

Fig 2.66: EI mass spectrum of component 555 (5-methylhexanal)

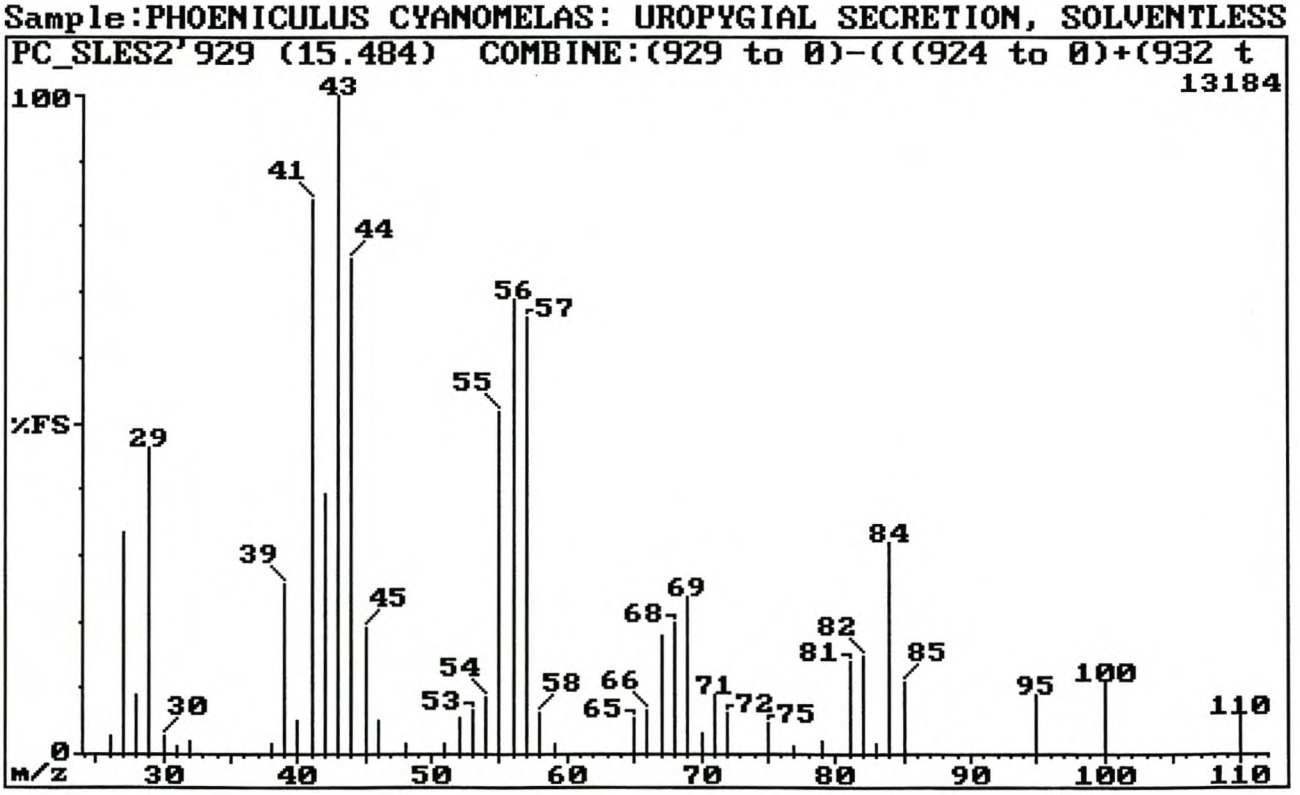

Fig 2.67: EI mass spectrum of component 929 (octanal)

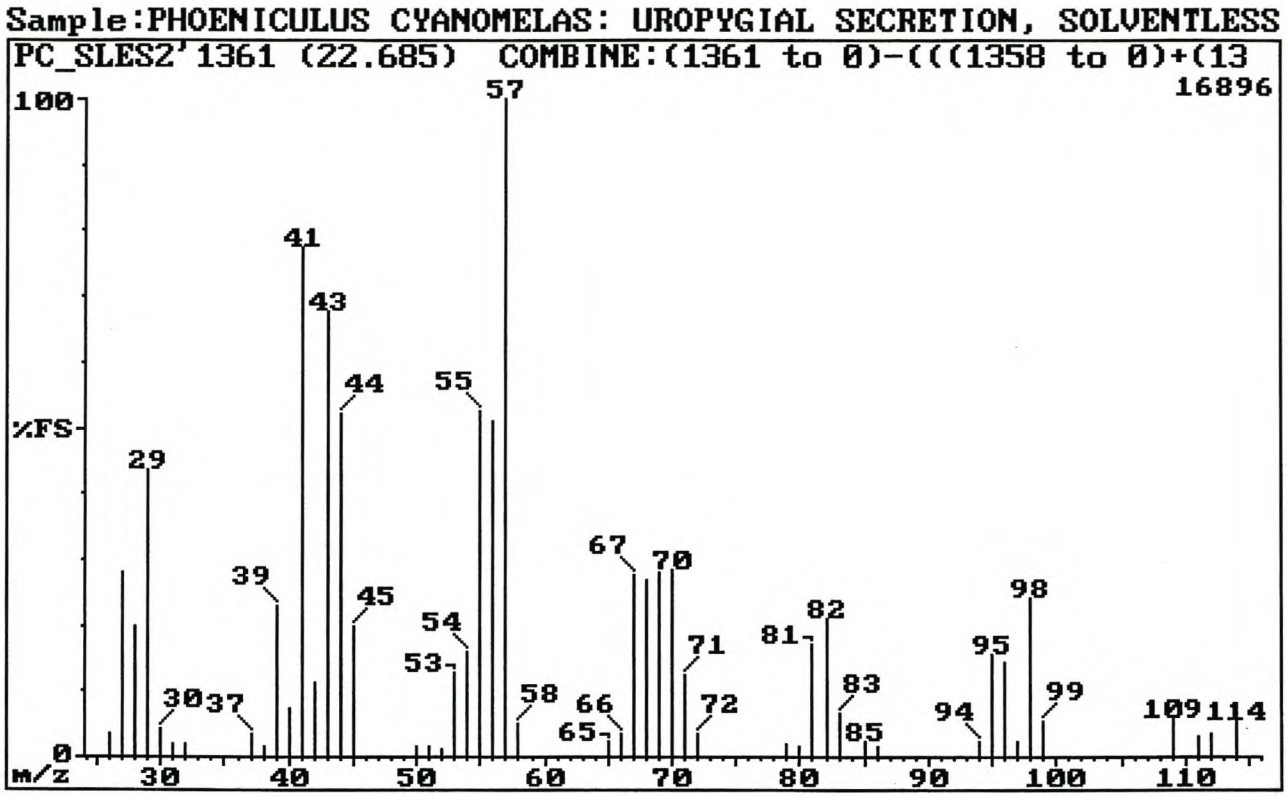

Fig 2.68: EI mass spectrum of component 1361 (nonanal)

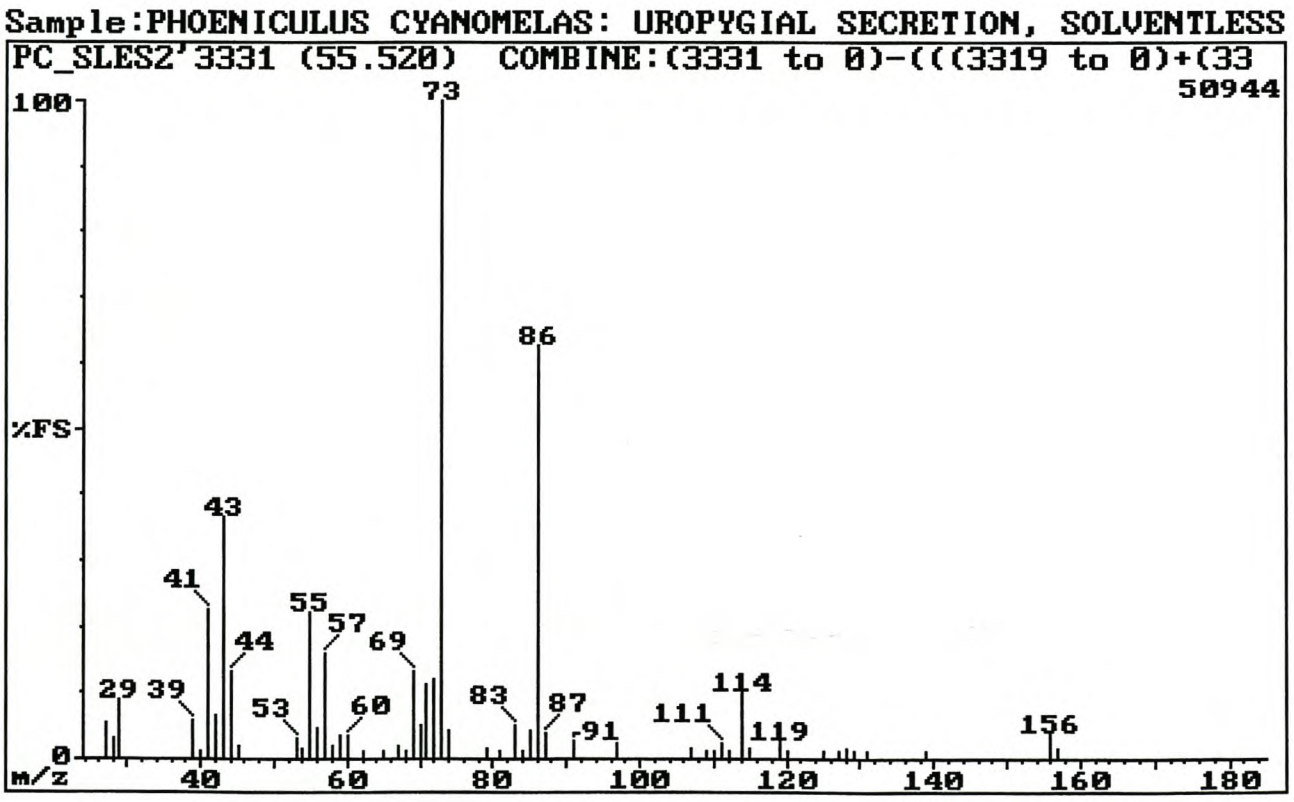

Fig 2.69: EI mass spectrum of component 3331 (nonanal *o*-methyloxime)

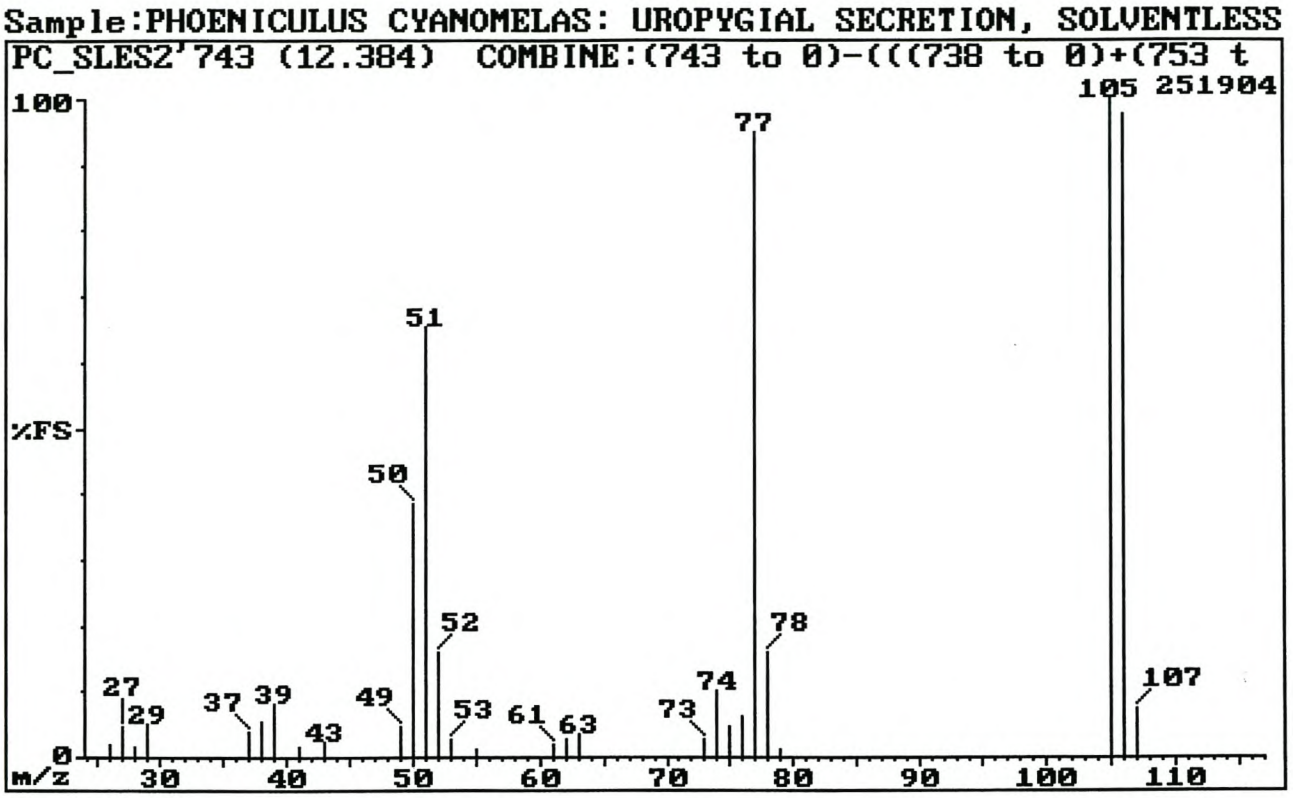

Fig 2.70: EI mass spectrum of component 743 (benzaldehyde)

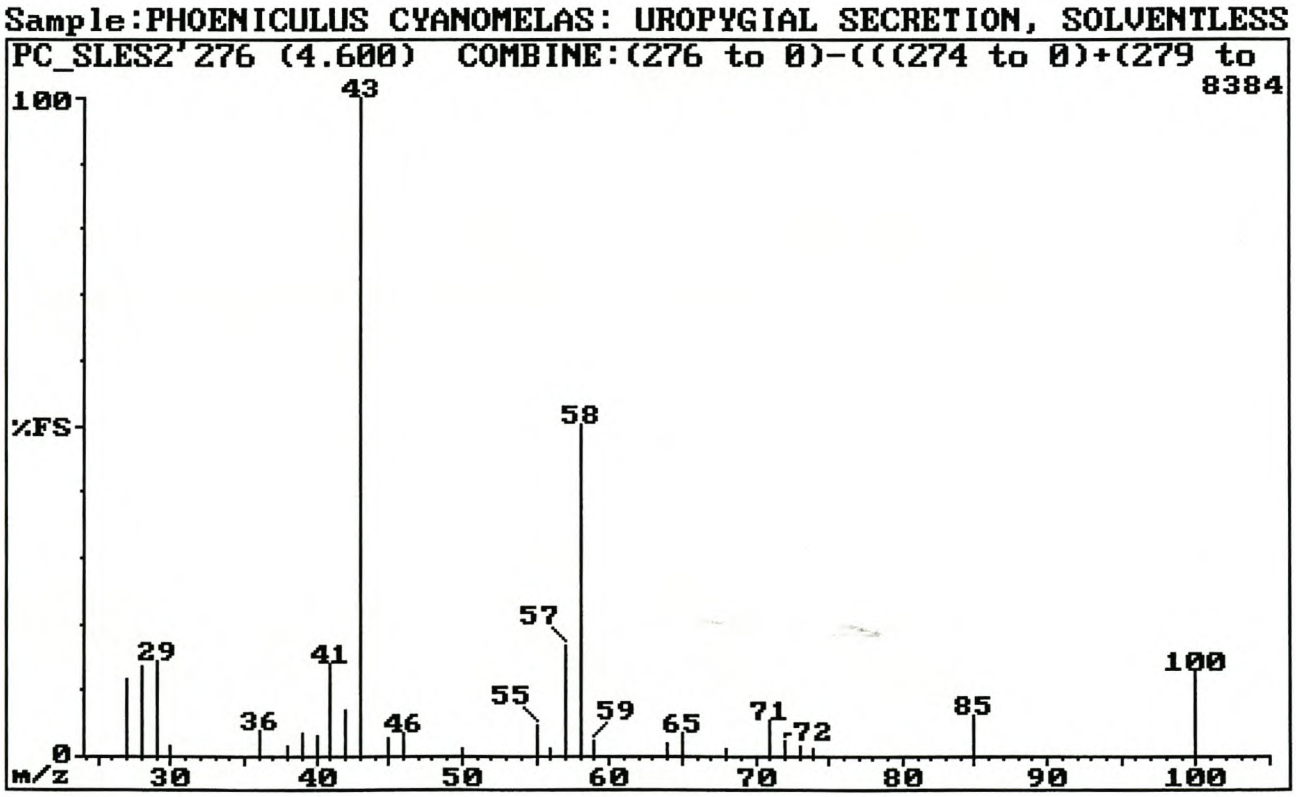

Fig 2.71: EI mass spectrum of component 276 (2-hexanone)

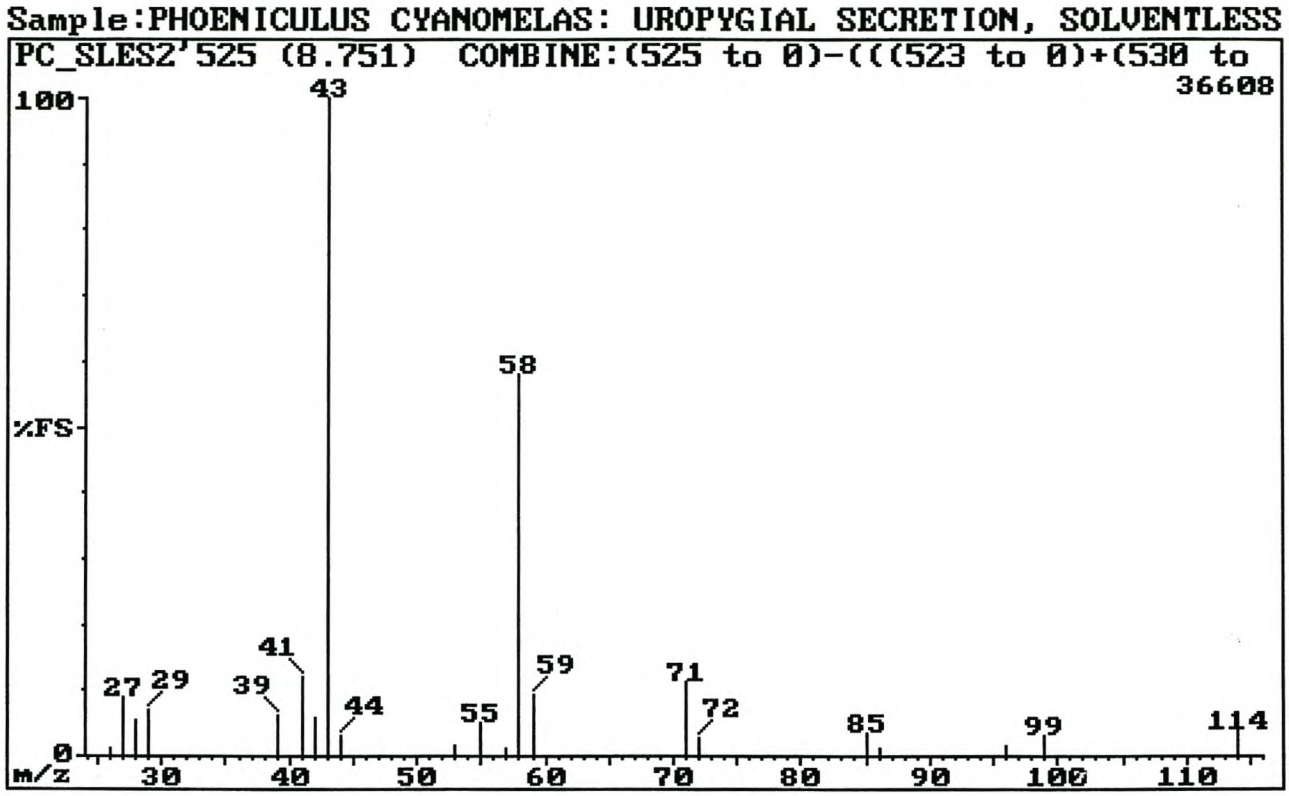

Fig 2.72: EI mass spectrum of component 525 (2-heptanone)

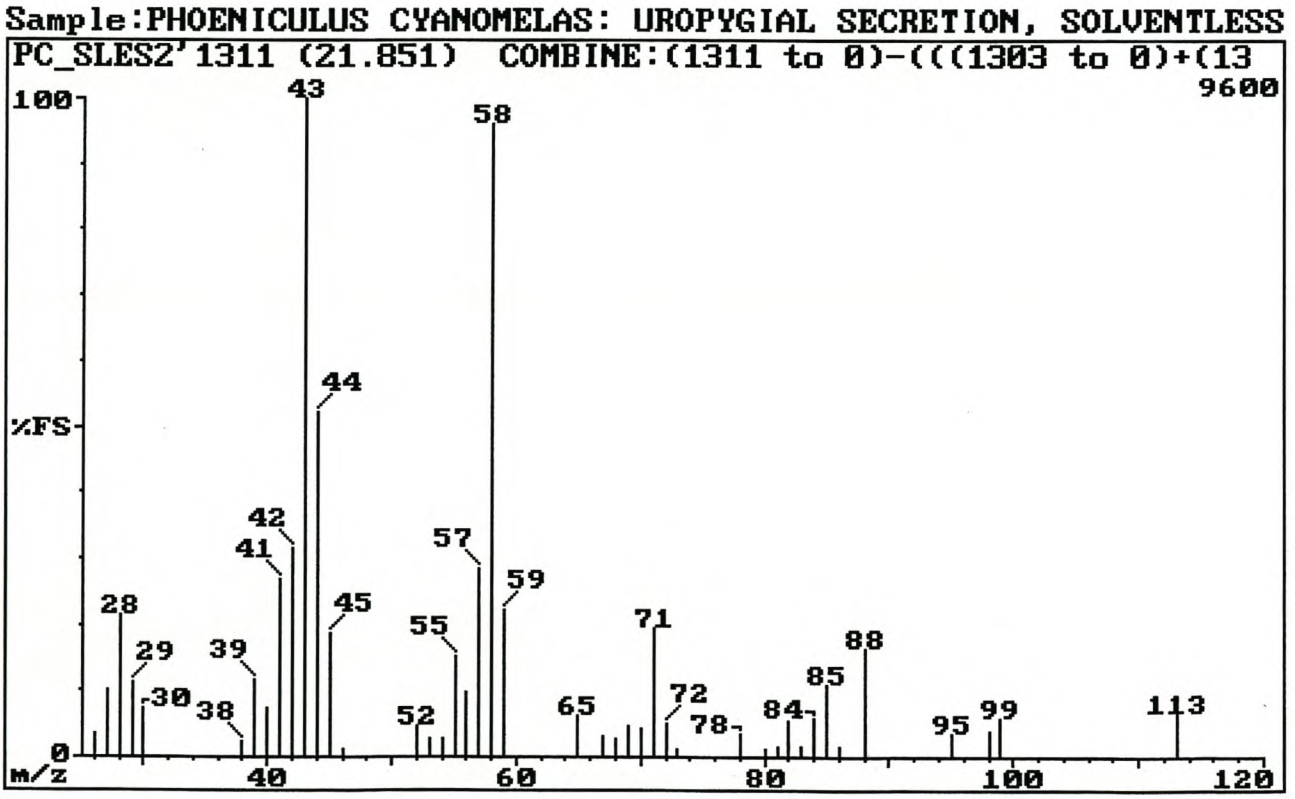

Fig 2.73: EI mass spectrum of component 1311 (5-methyl-2-heptanone)

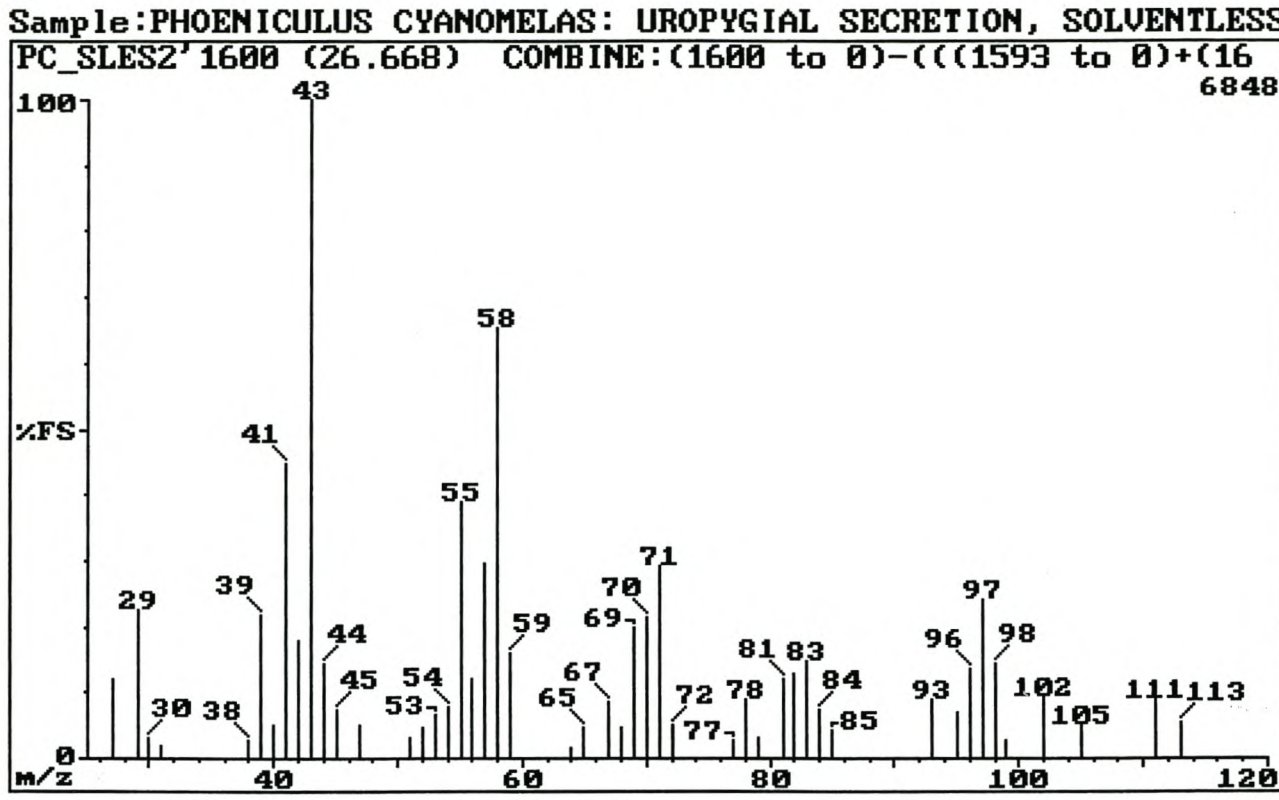

Fig 2.74: EI mass spectrum of component 1600 (6-methyl-2-octanone)

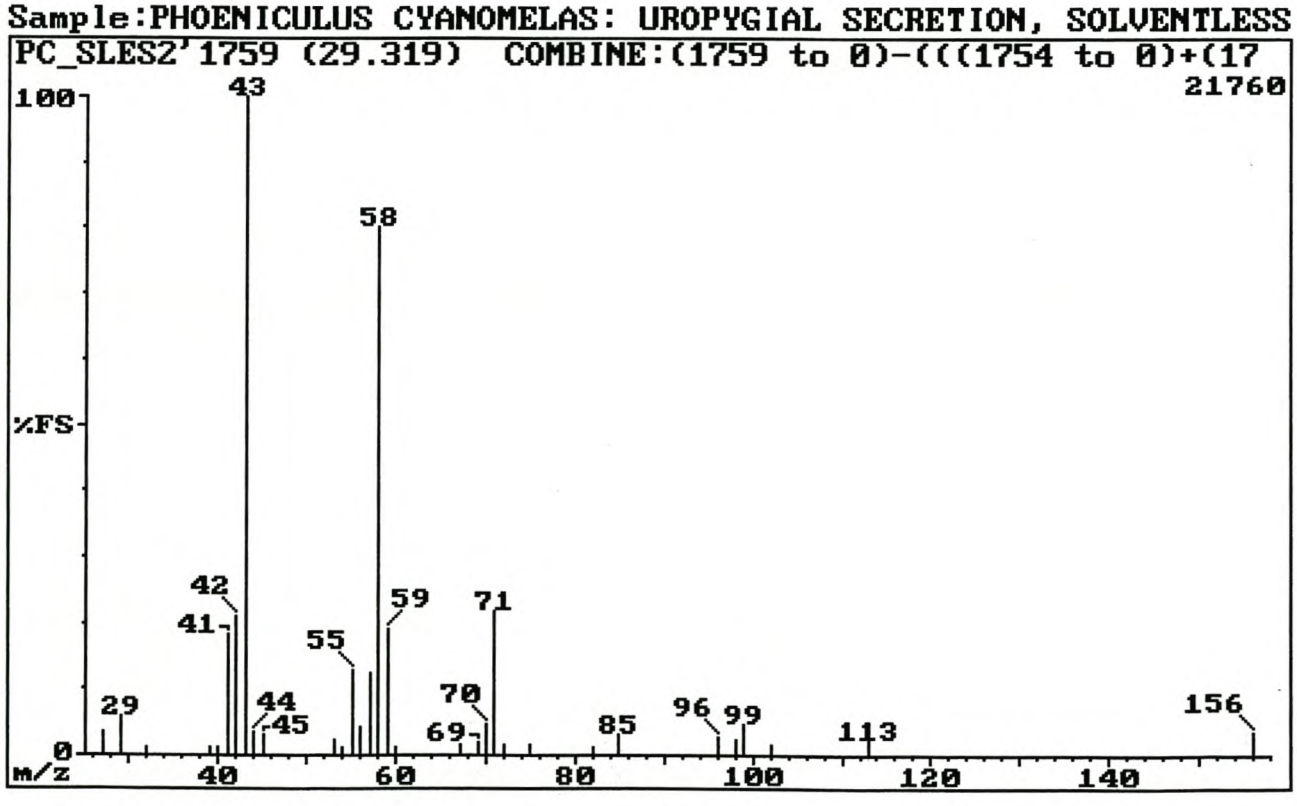

Fig 2.75: EI mass spectrum of component 1759 (8-methyl-2-nonanone)

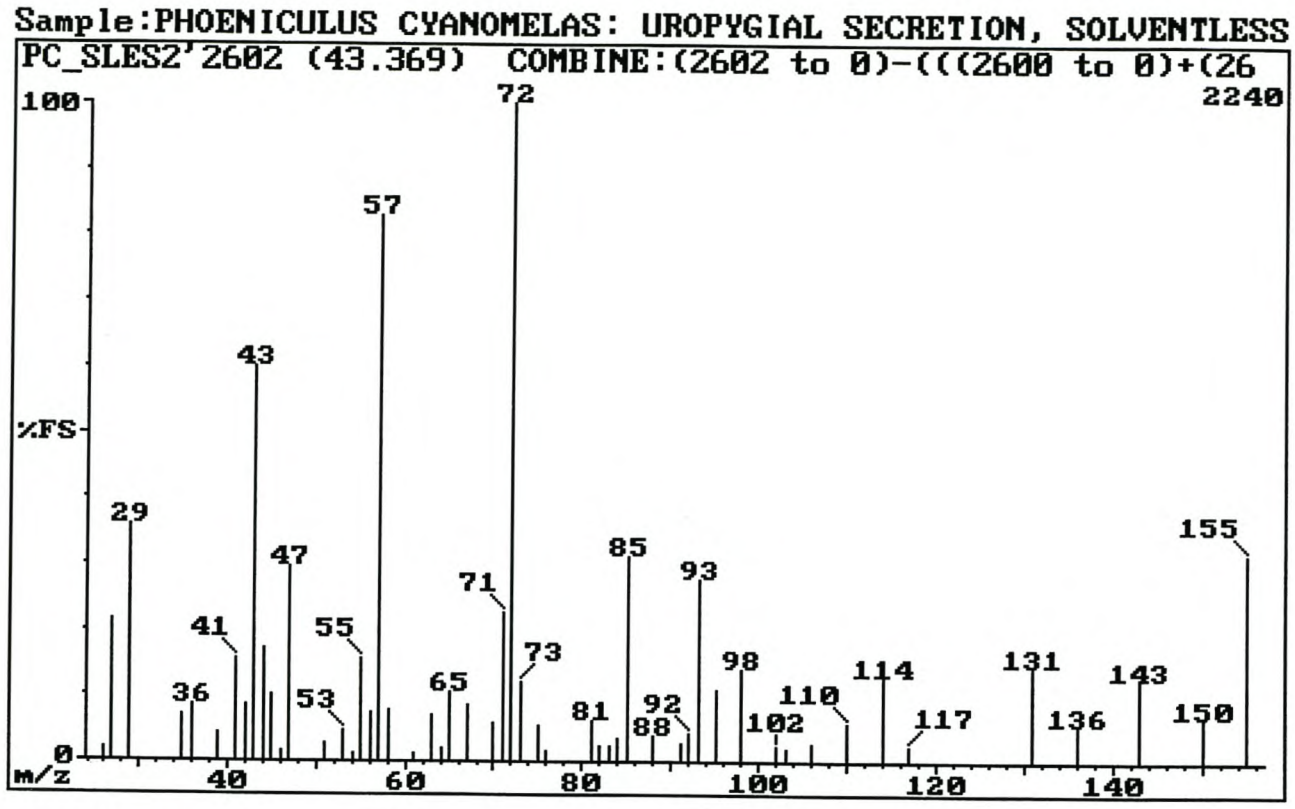

Fig 2.76: EI mass spectrum of component 2602 (3-dodecanone)

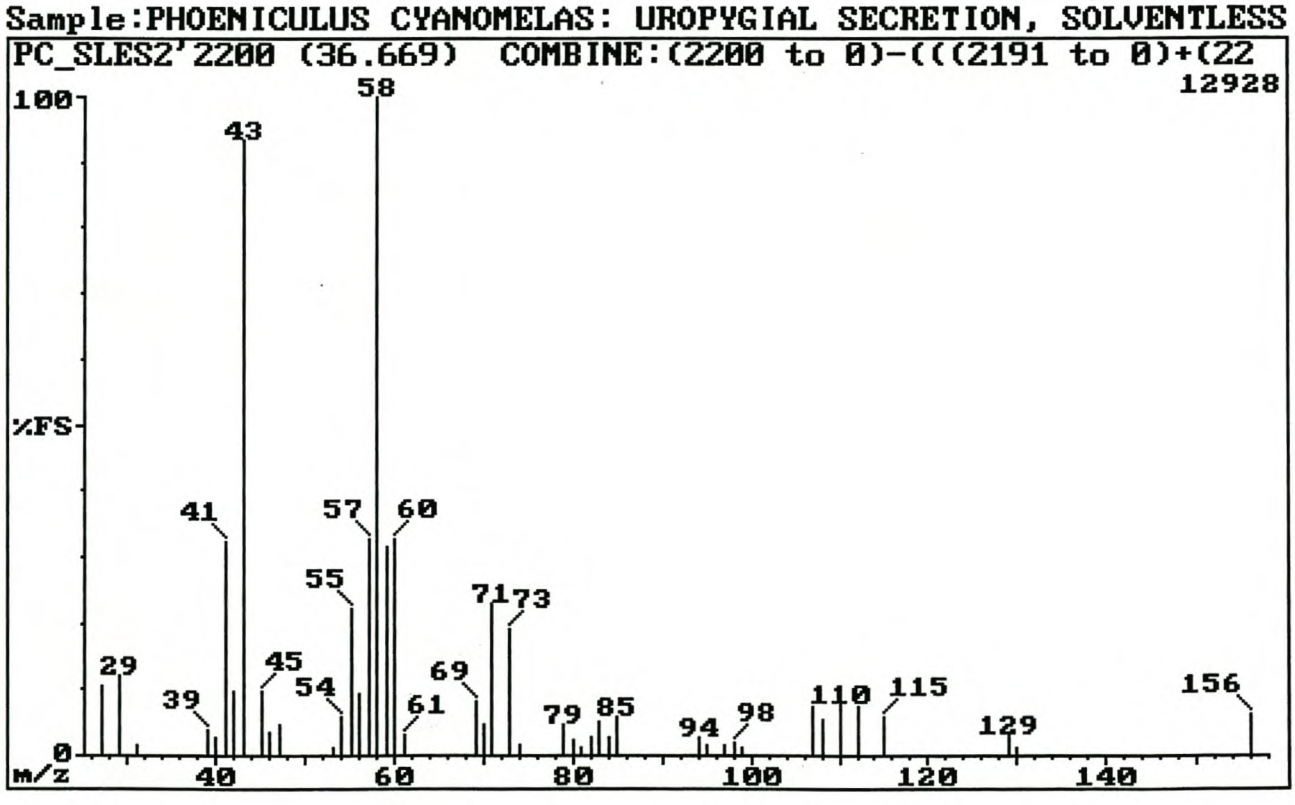

Fig 2.77: EI mass spectrum of component 2200 (2-decanone)

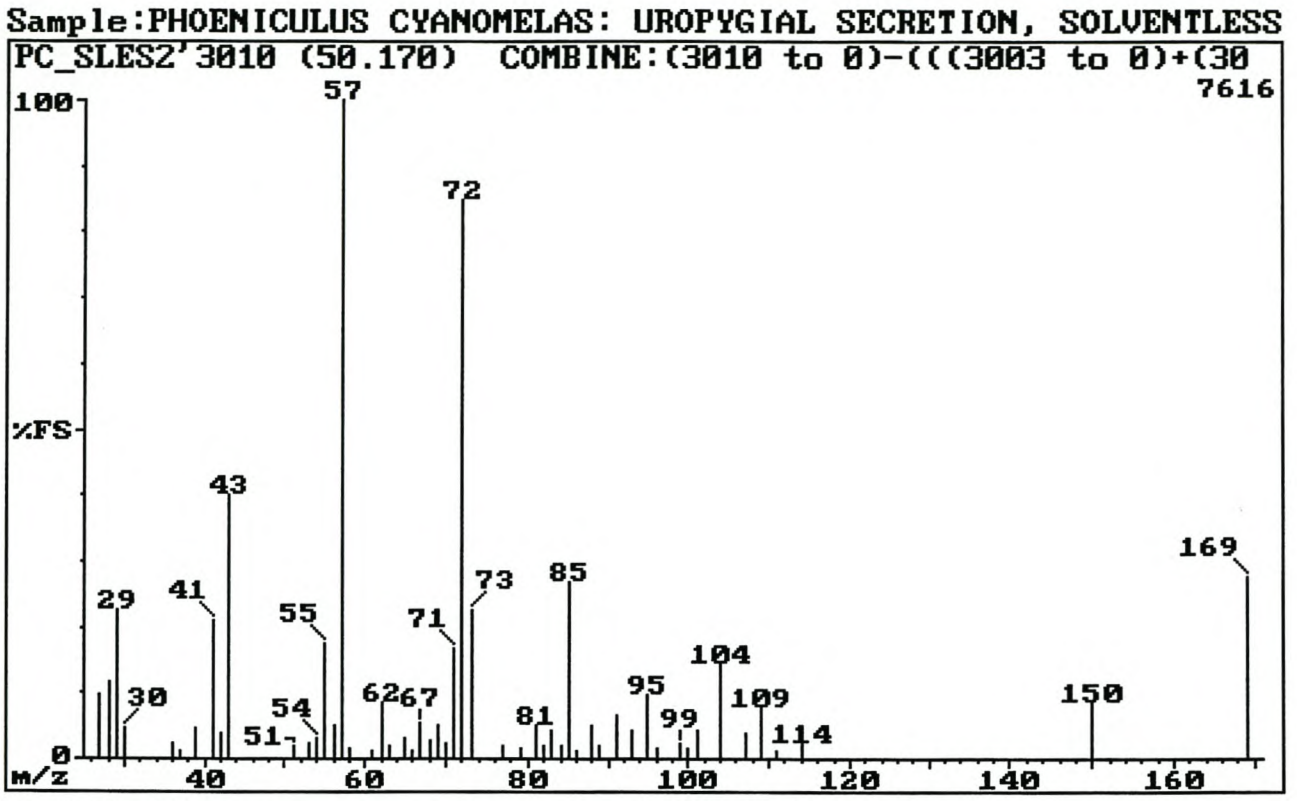

Fig 2.78: EI mass spectrum of component 3010 (3-tridecanone)

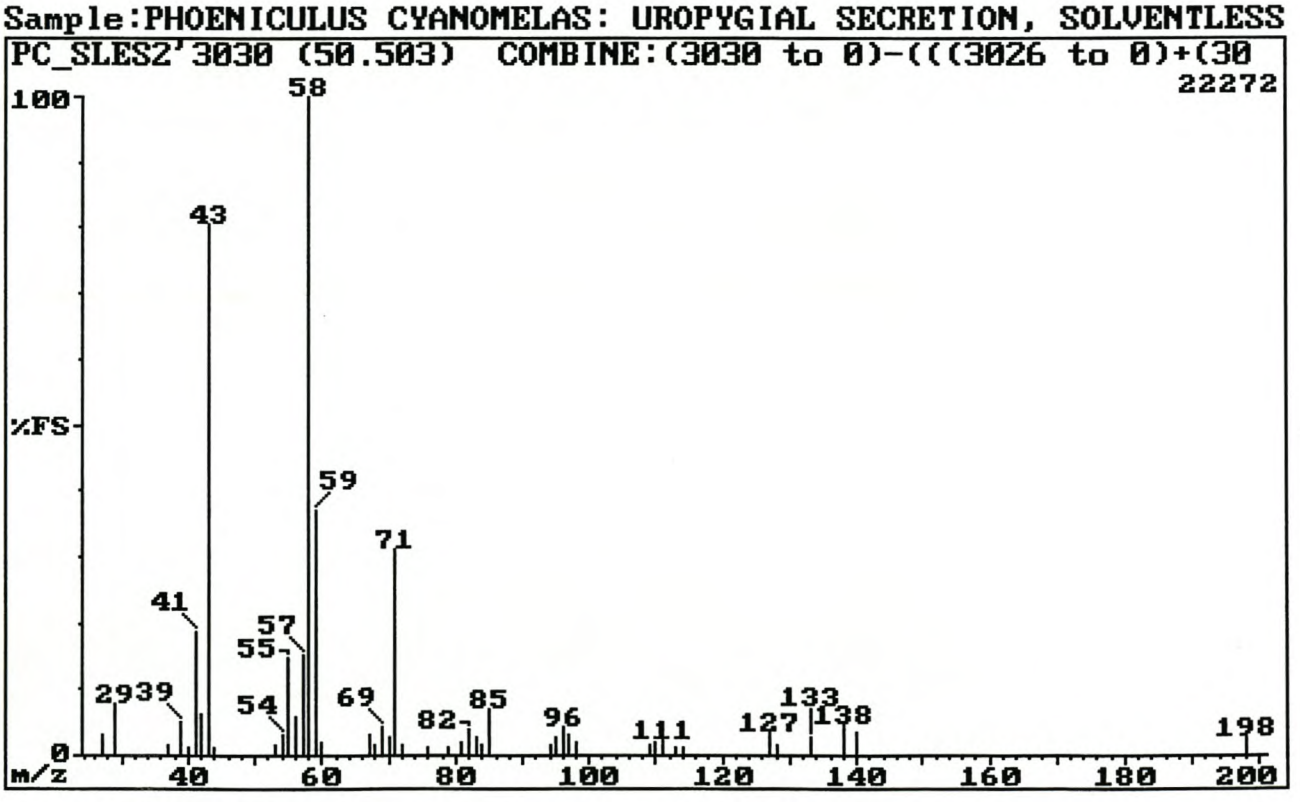

Fig 2.79: EI mass spectrum of component 3030 (2-tridecanone)

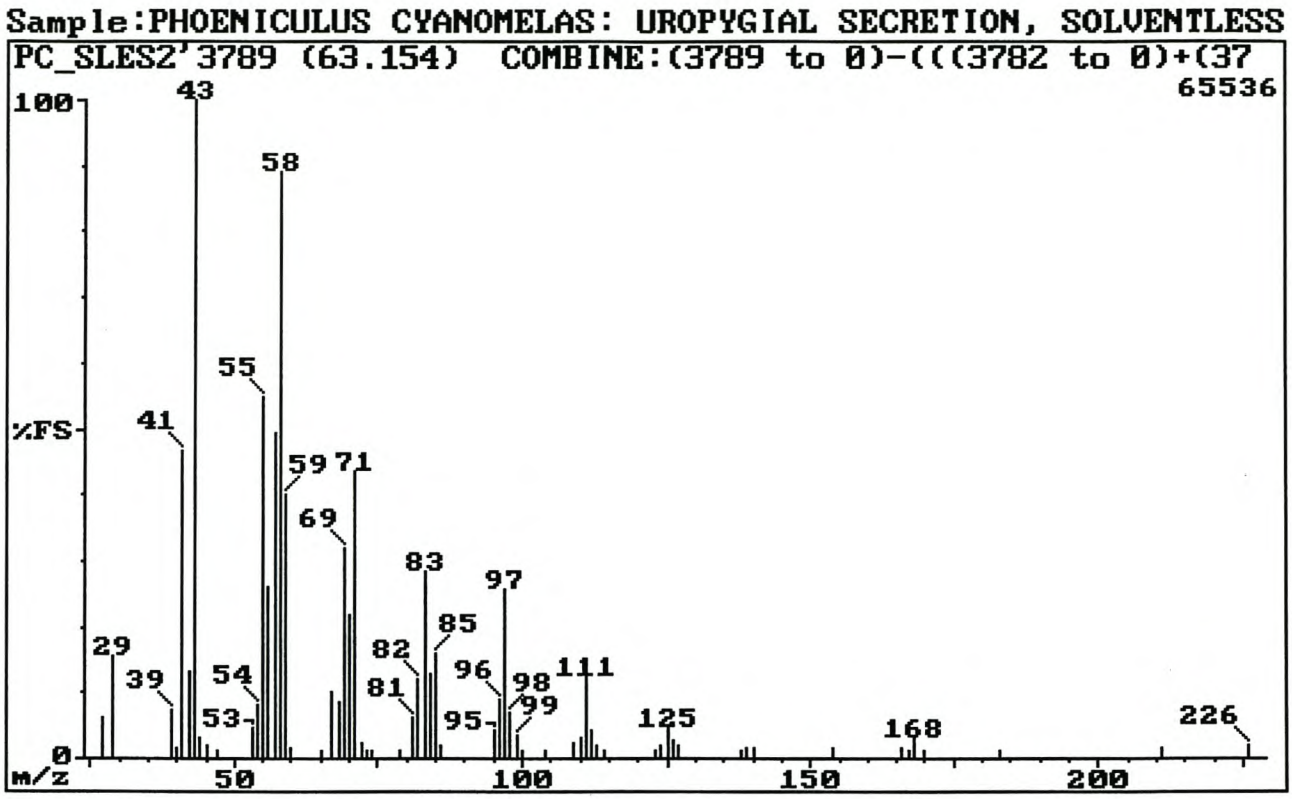

Fig 2.80: EI mass spectrum of component 3789 (13-methyl-2-tetradecanone)

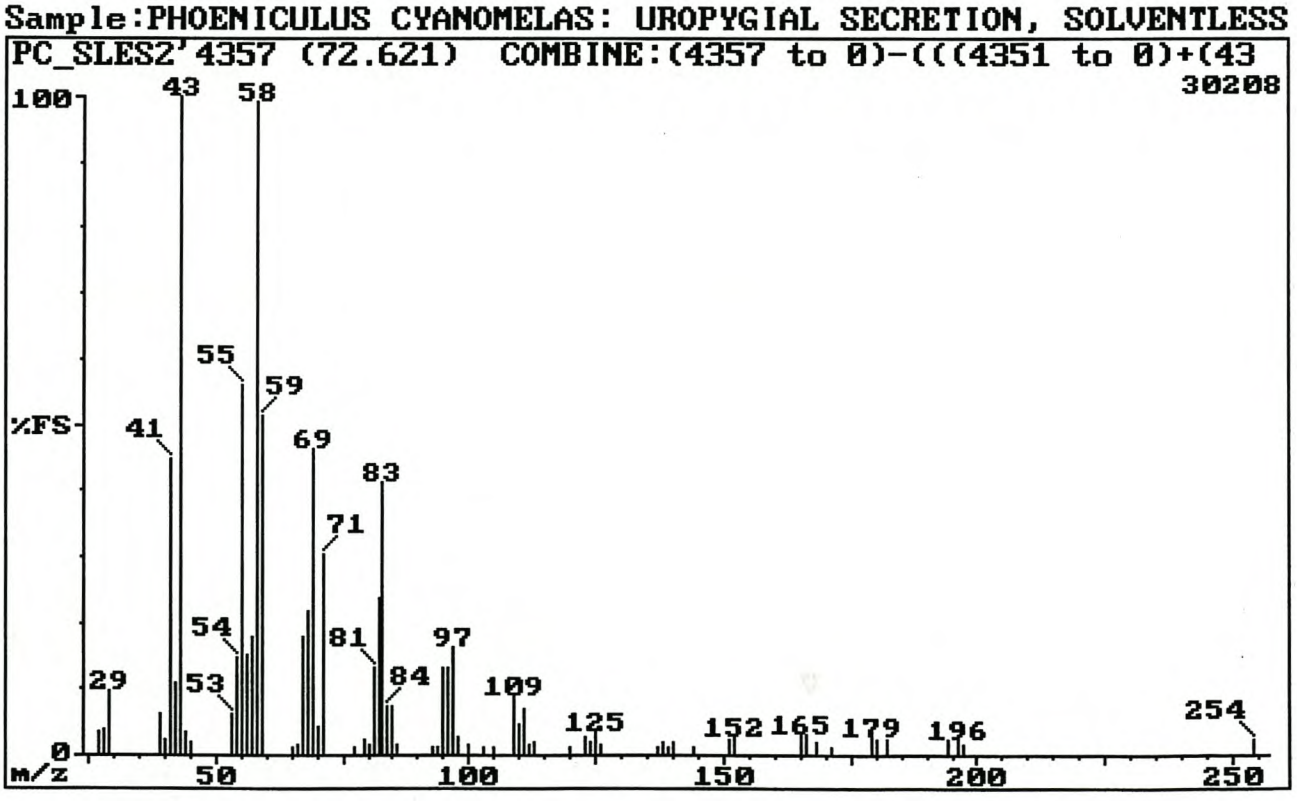

Fig 2.81: EI mass spectrum of component 4357 (2-heptadecanone)

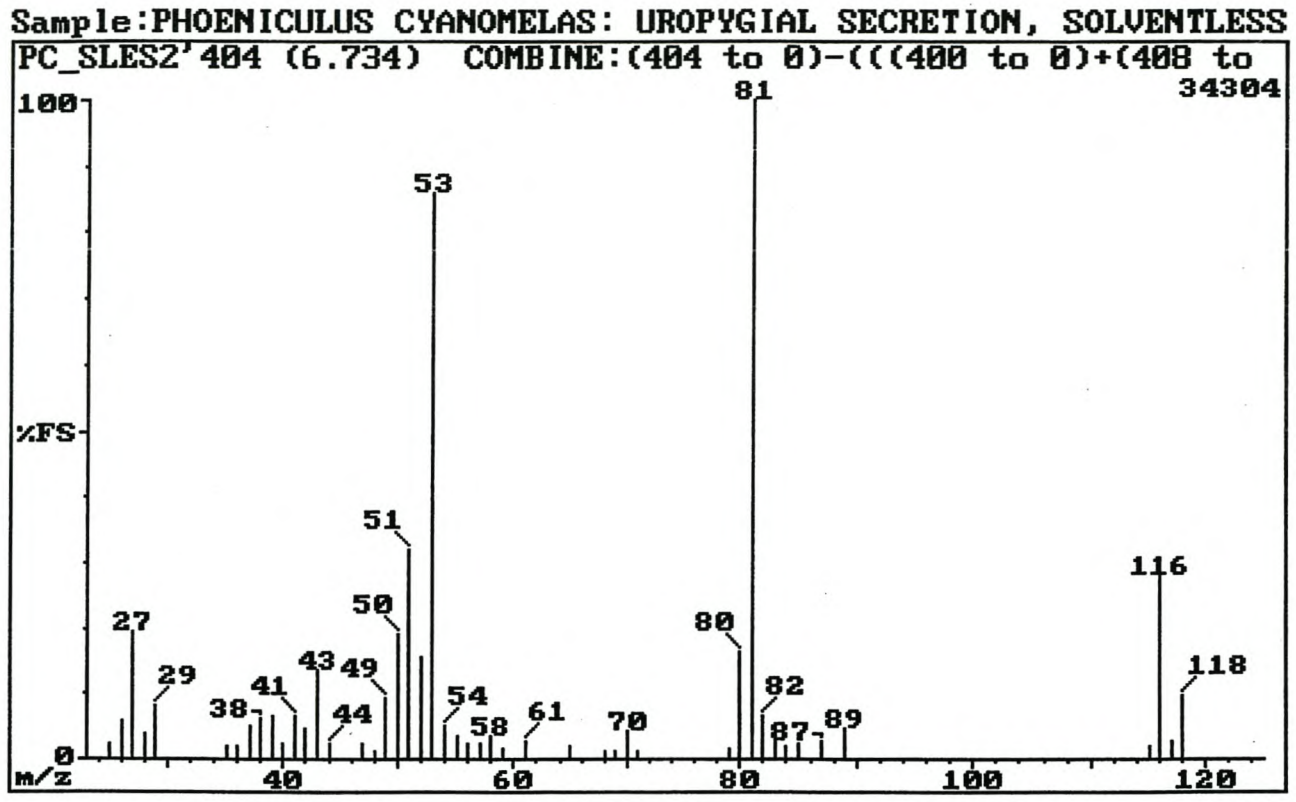

Fig 2.82: EI mass spectrum of component 404 (4-chloro-2-cyclopentene-1-one)

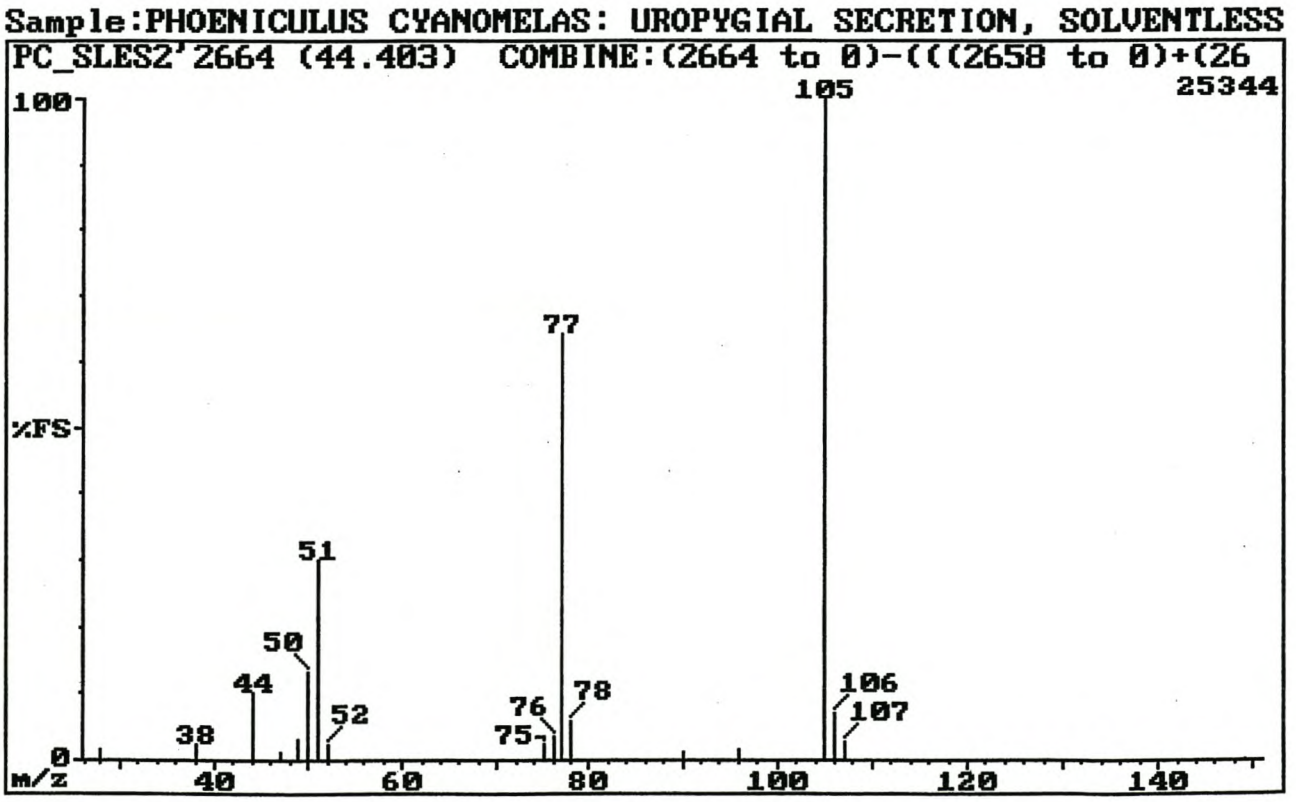

Fig 2.83: EI mass spectrum of component 2664 (diphenylethanedione)

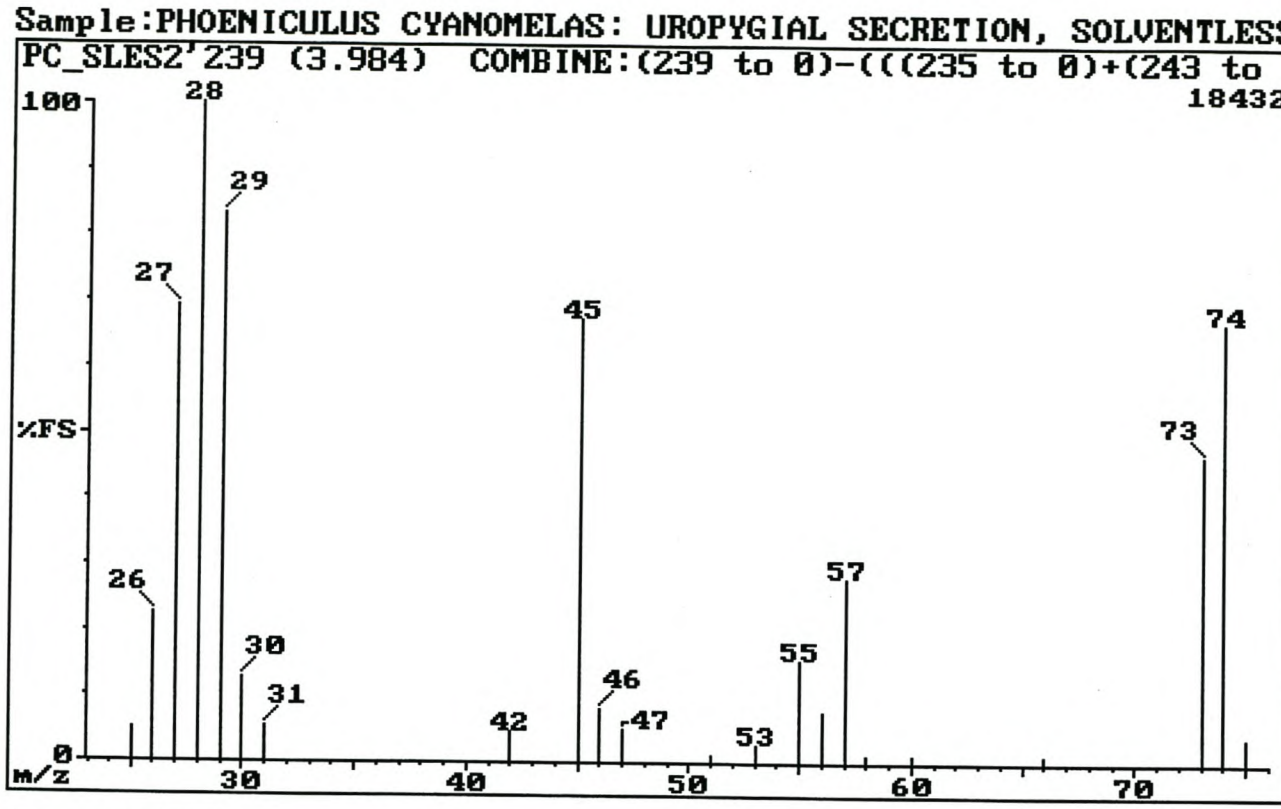

Fig 2.84: EI mass spectrum of component 239 (propanoic acid)

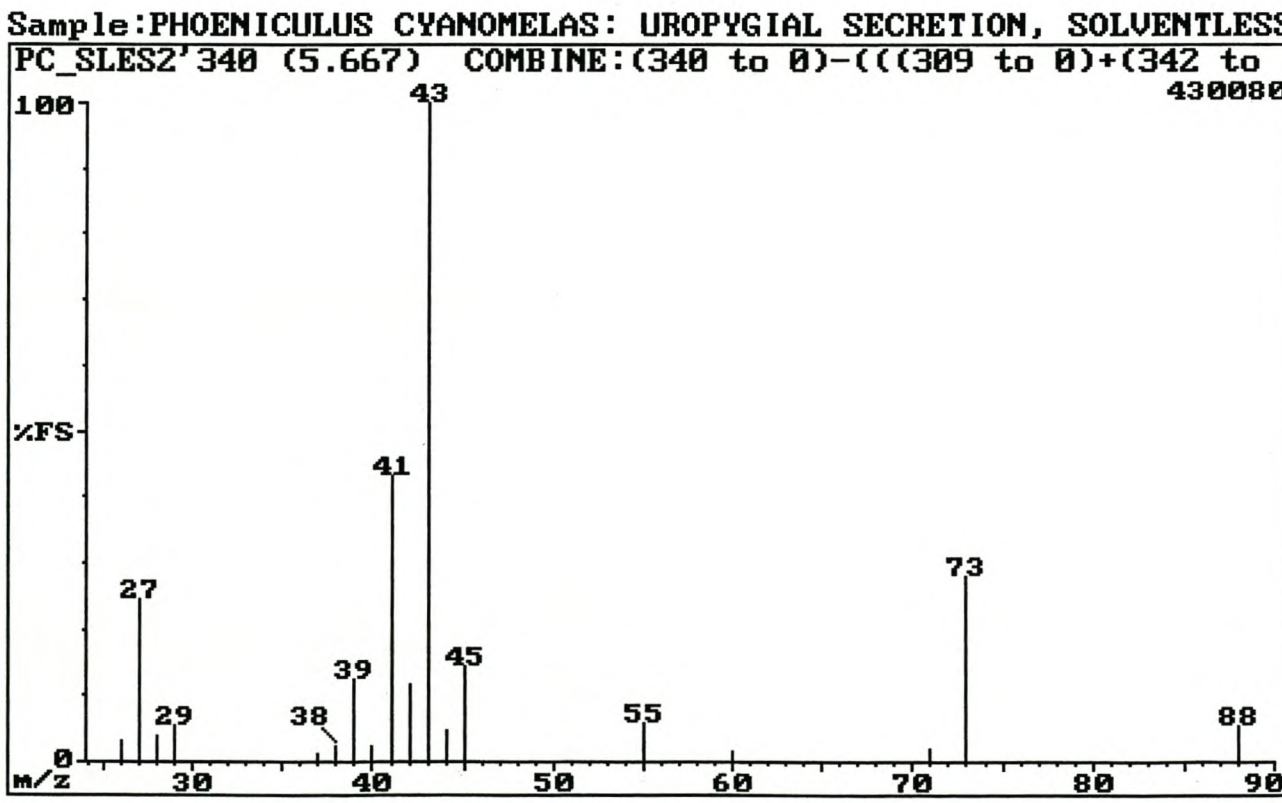

Fig 2.85: EI mass spectrum of component 340 (2-methylpropanoic acid)

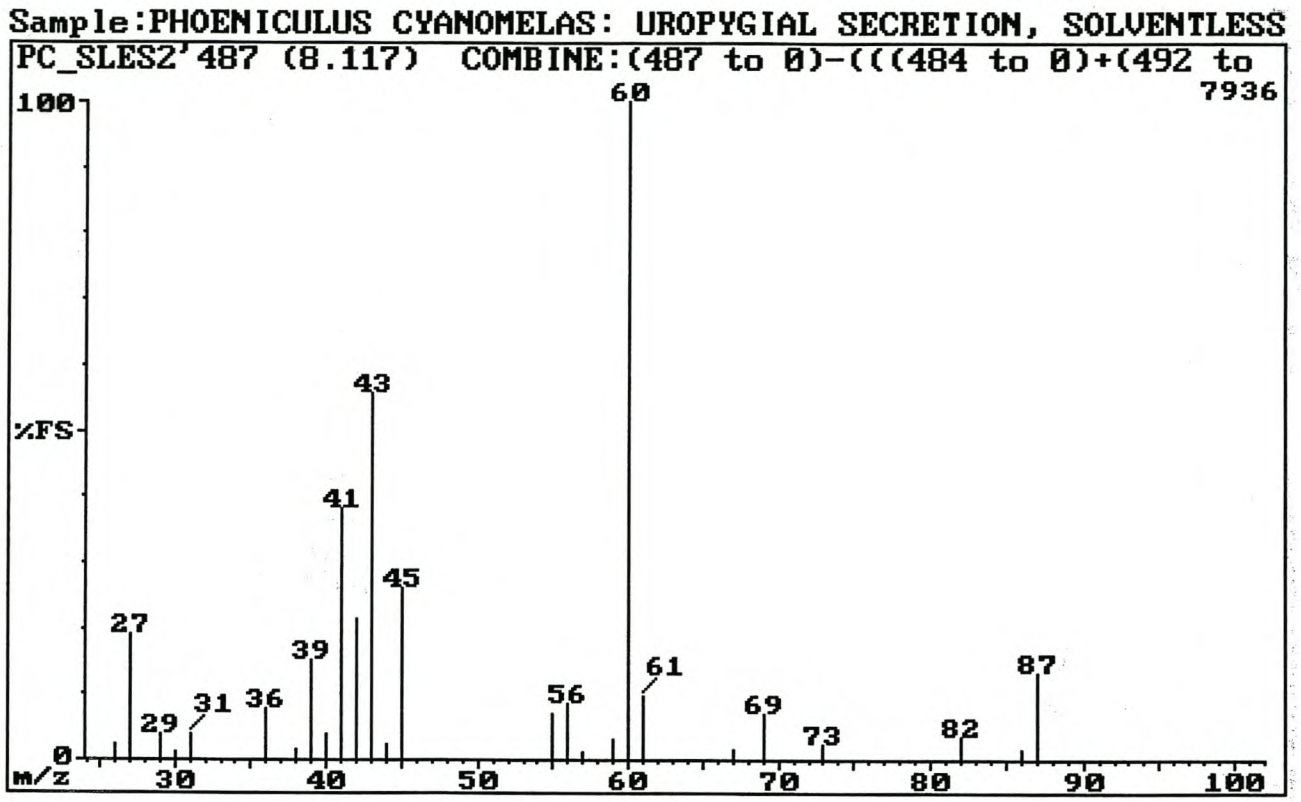

Fig 2.86: EI mass spectrum of component 487 (3-methylbutanoic acid)

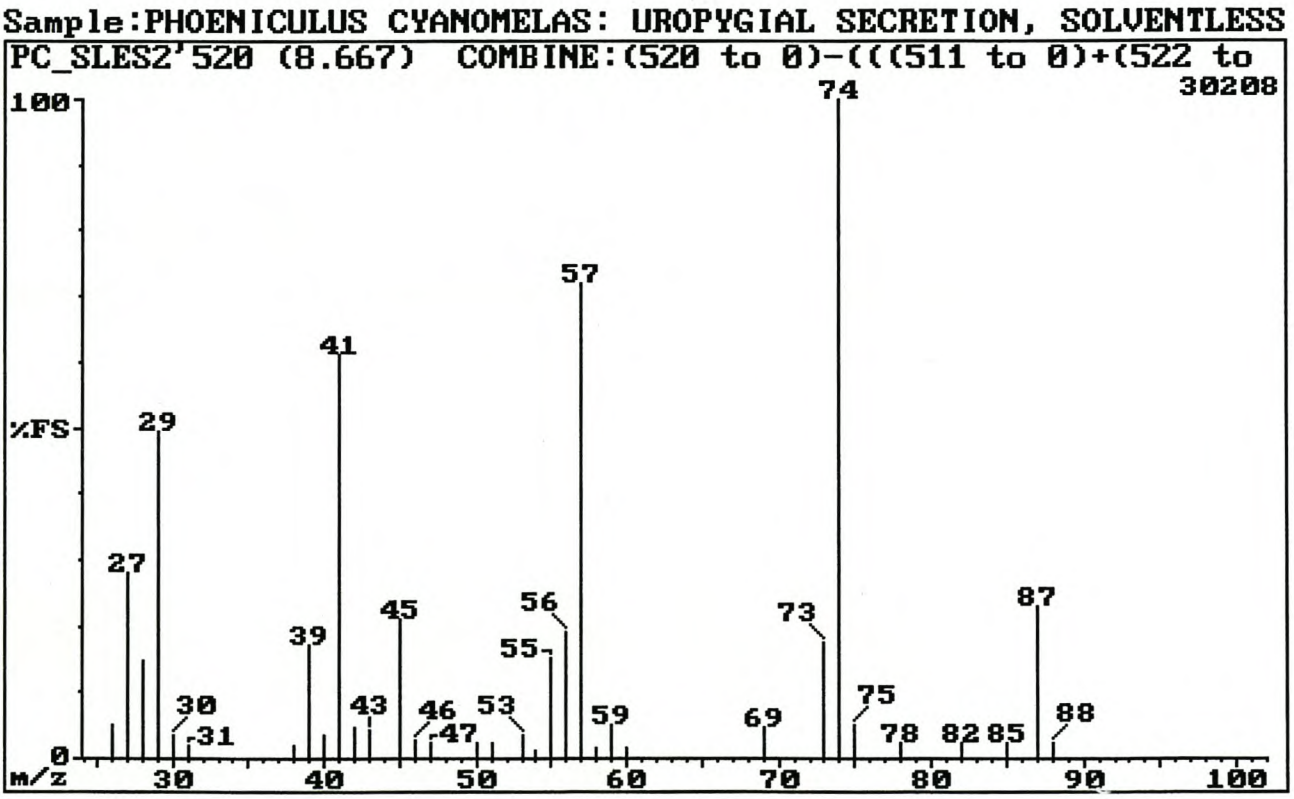

Fig 2.87: EI mass spectrum of component 520 (2-methylbutanoic acid)

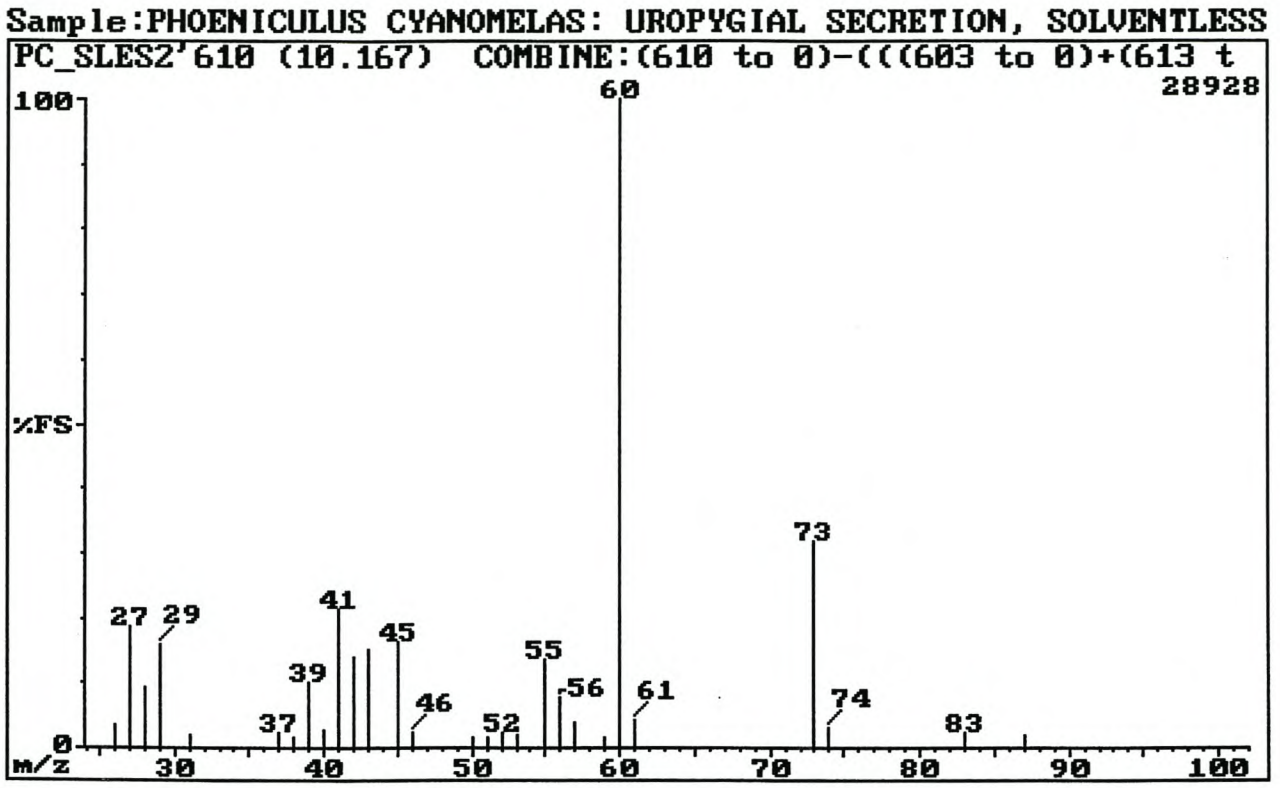

Fig 2.88: EI mass spectrum of component 610 (pentanoic acid)

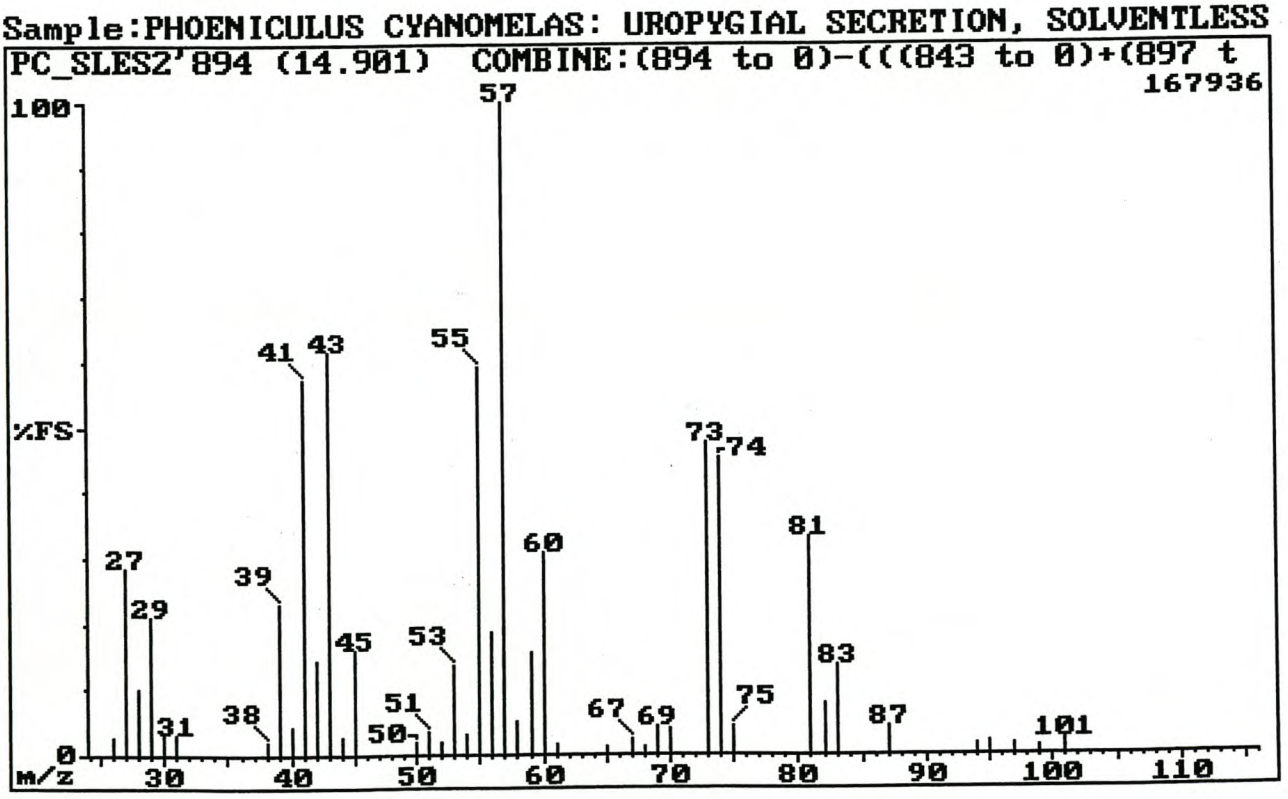

Fig 2.89: EI mass spectrum of component 894 (4-methylpentanoic acid)

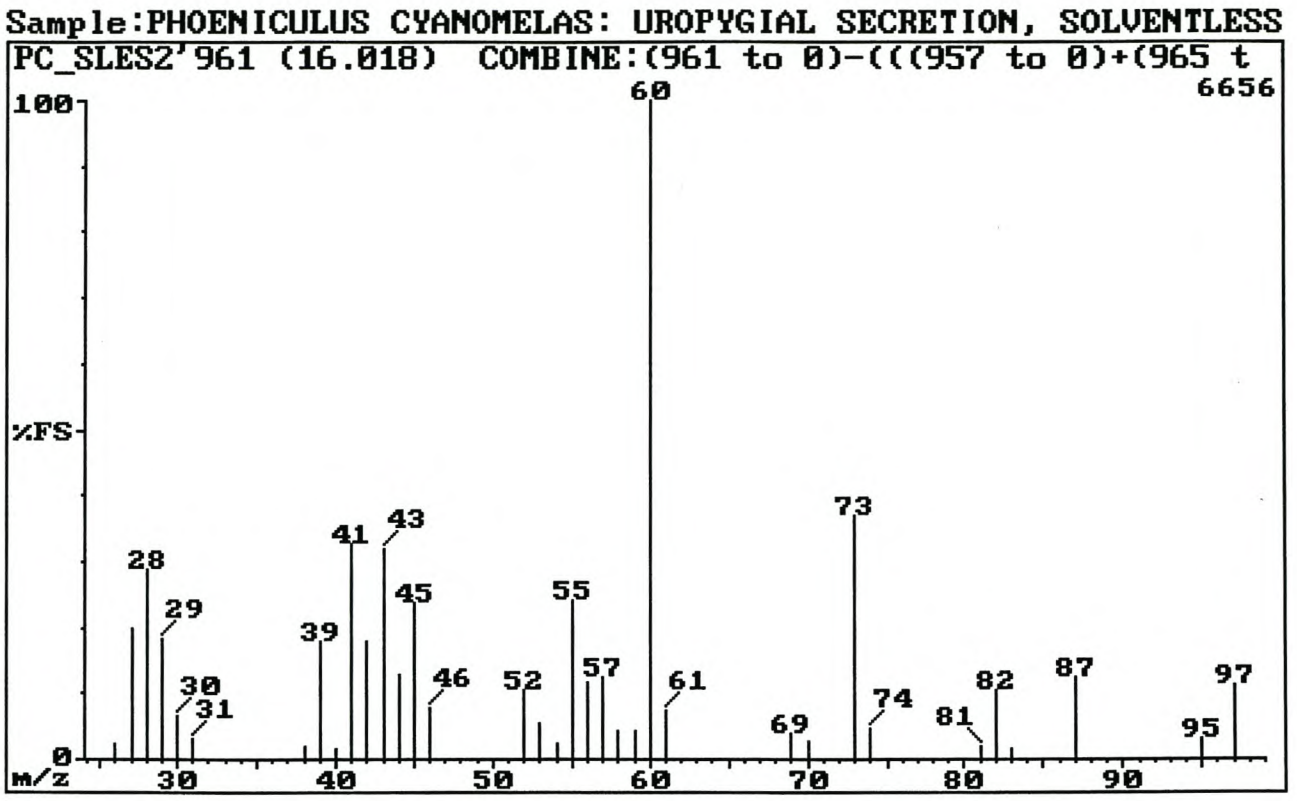

Fig 2.90: EI mass spectrum of component 961 (hexanoic acid)

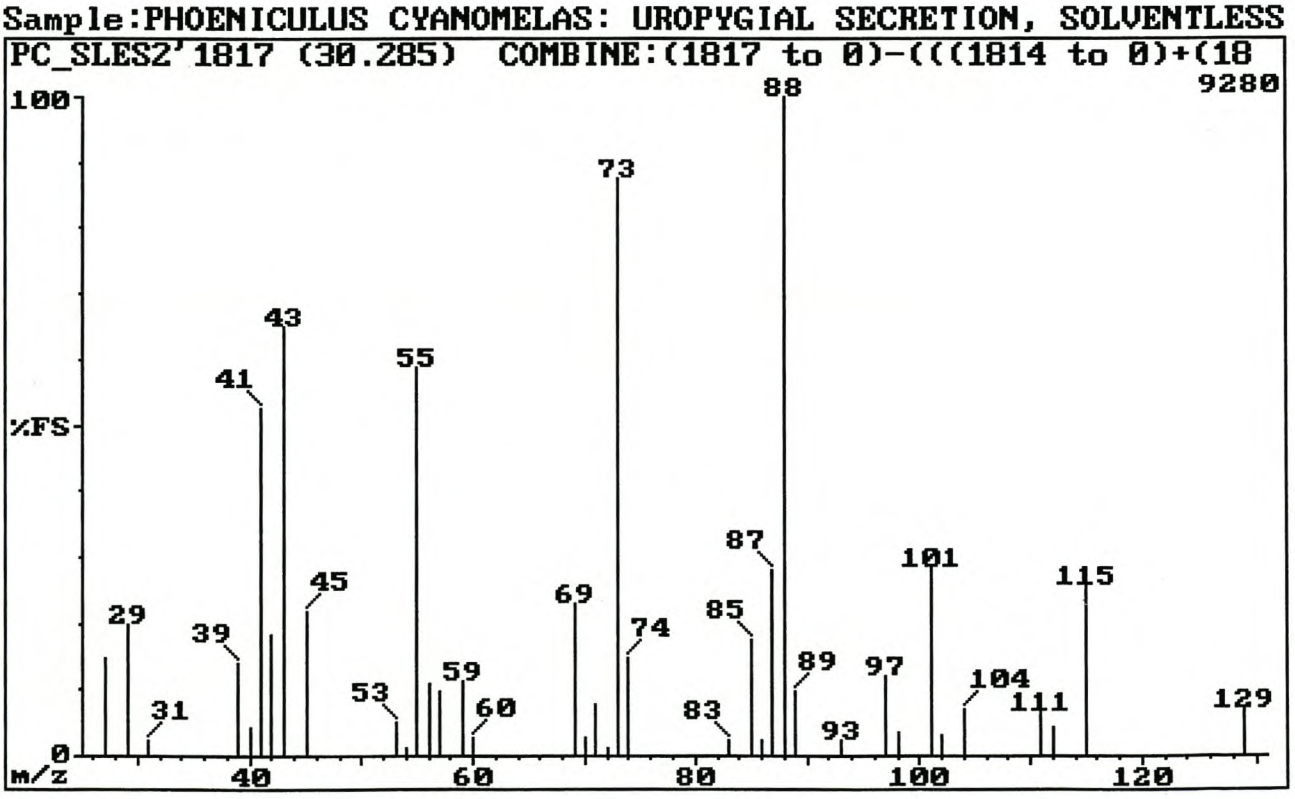

Fig 2.91: EI mass spectrum of component 1817 (2-ethylheptanoic acid)

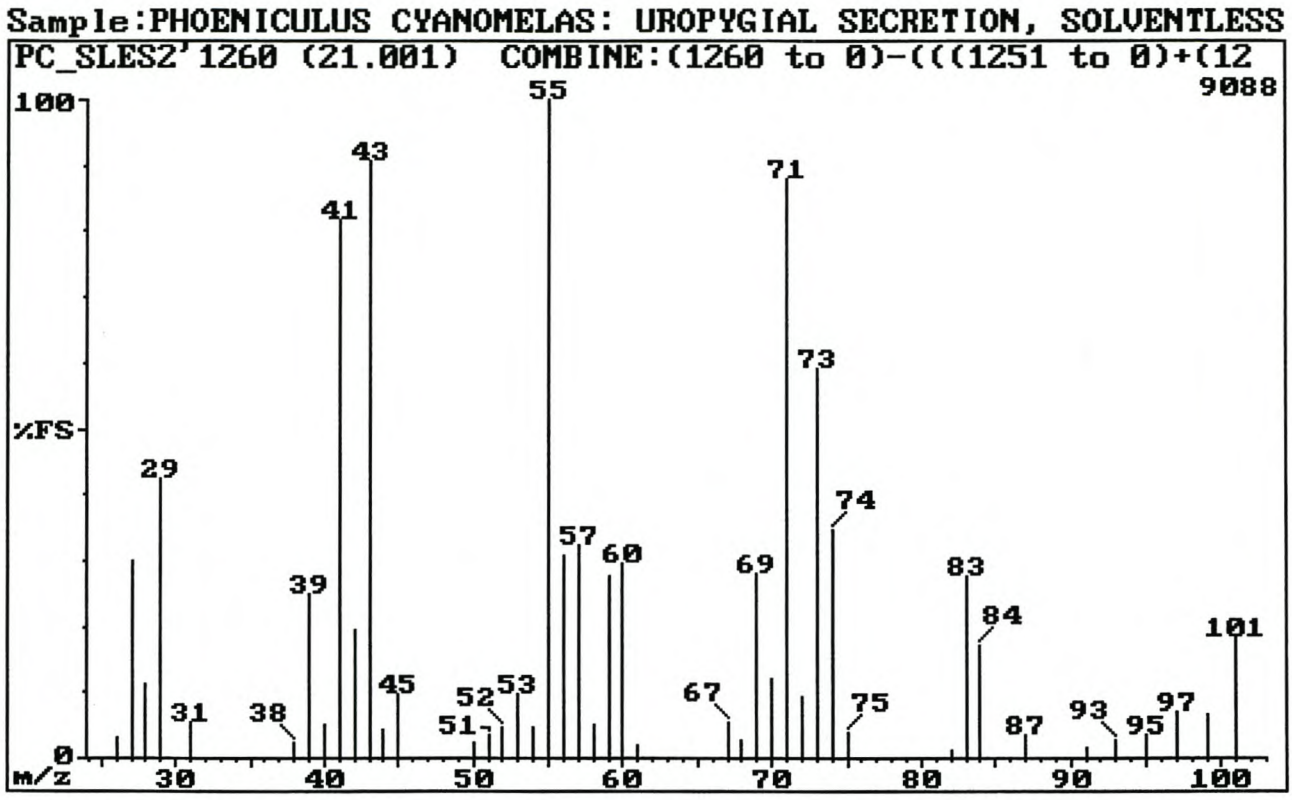

Fig 2.92: EI mass spectrum of component 1260 (4-methylheptanoic acid)

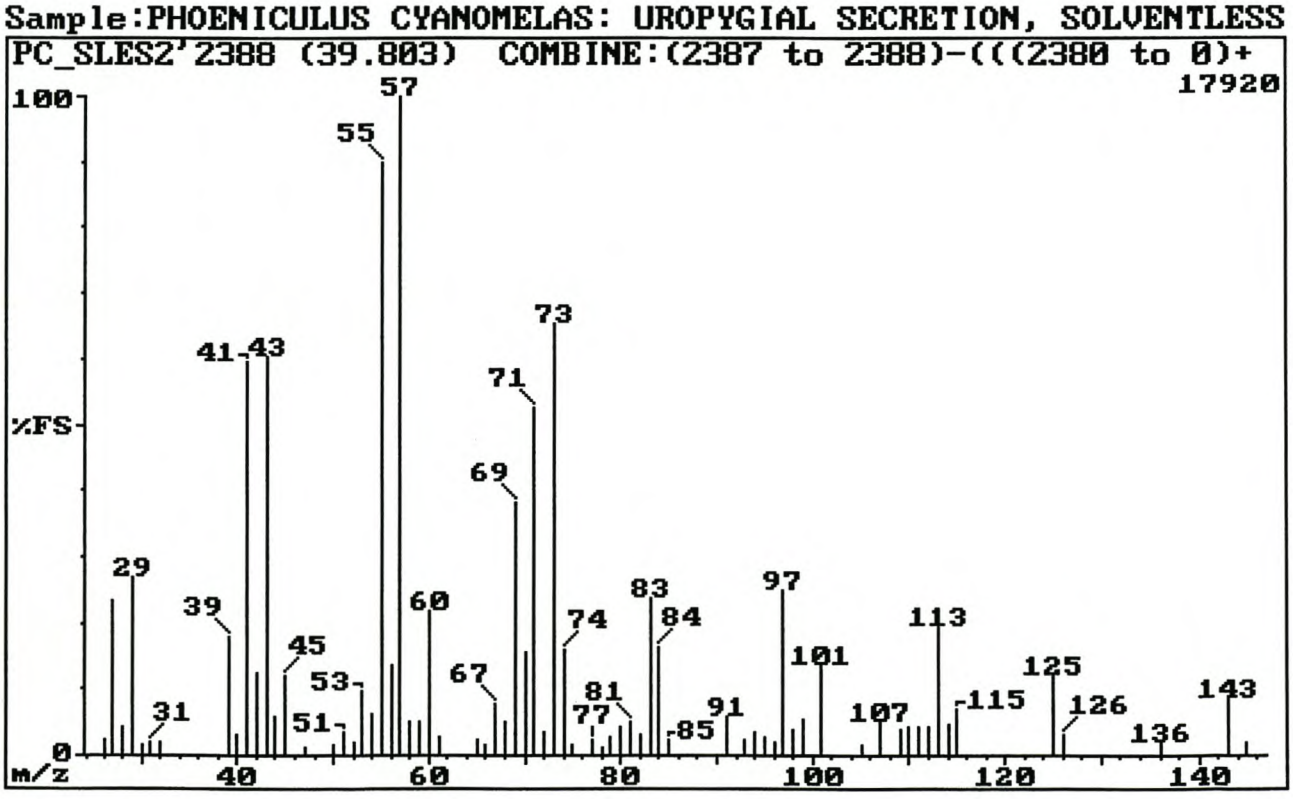

Fig 2.93: EI mass spectrum of component 2388 (4-methyloctanoic acid)

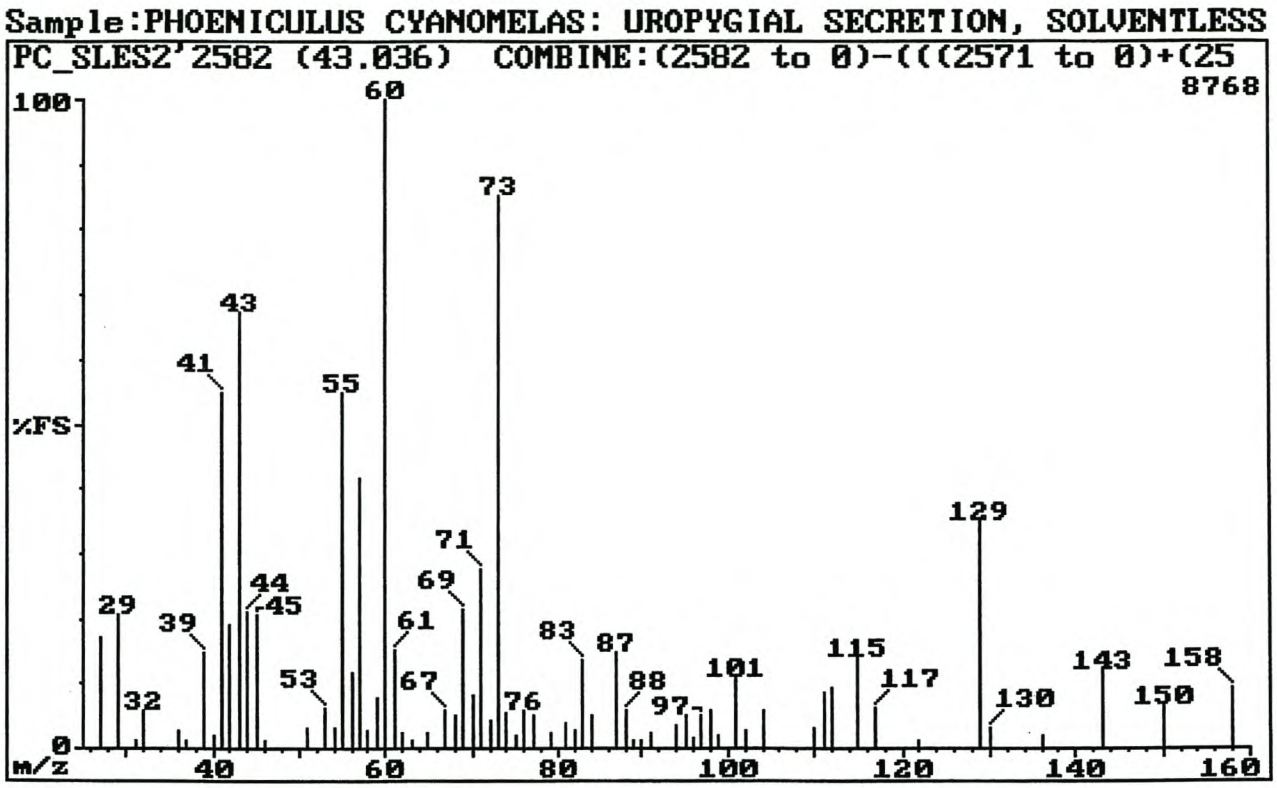

Fig 2.94: EI mass spectrum of component 2582 (nonanoic acid)

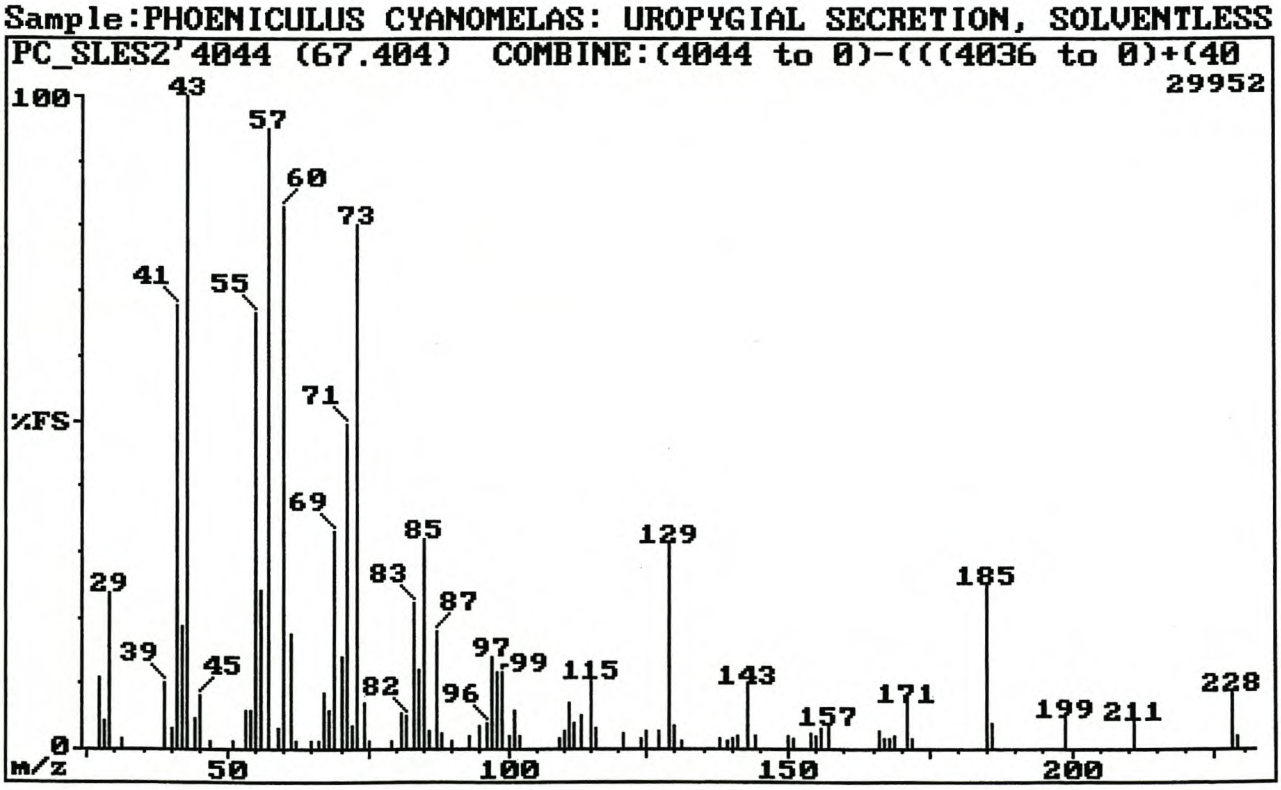

Fig 2.95: EI mass spectrum of component 4044 (tetradecanoic acid)

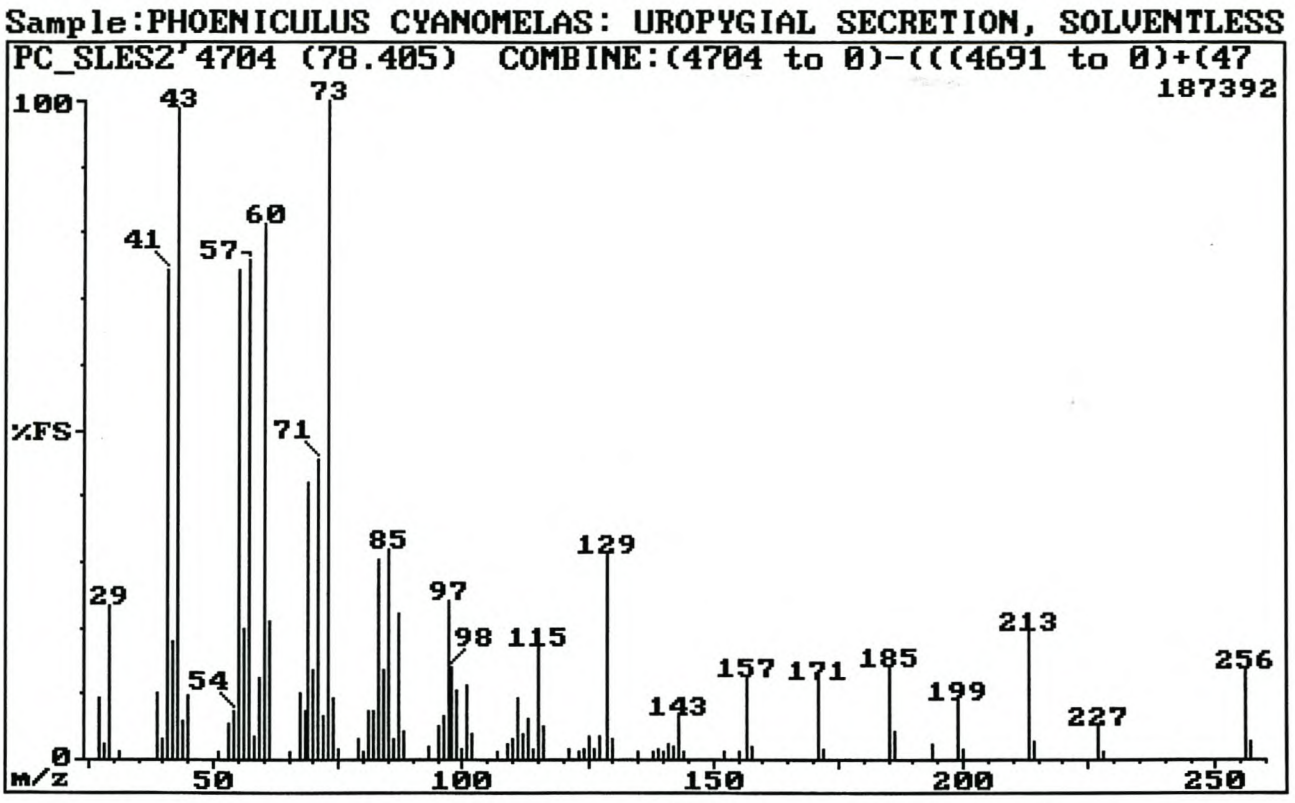

Fig 2.96: EI mass spectrum of component 4704 (hexadecanoic acid)

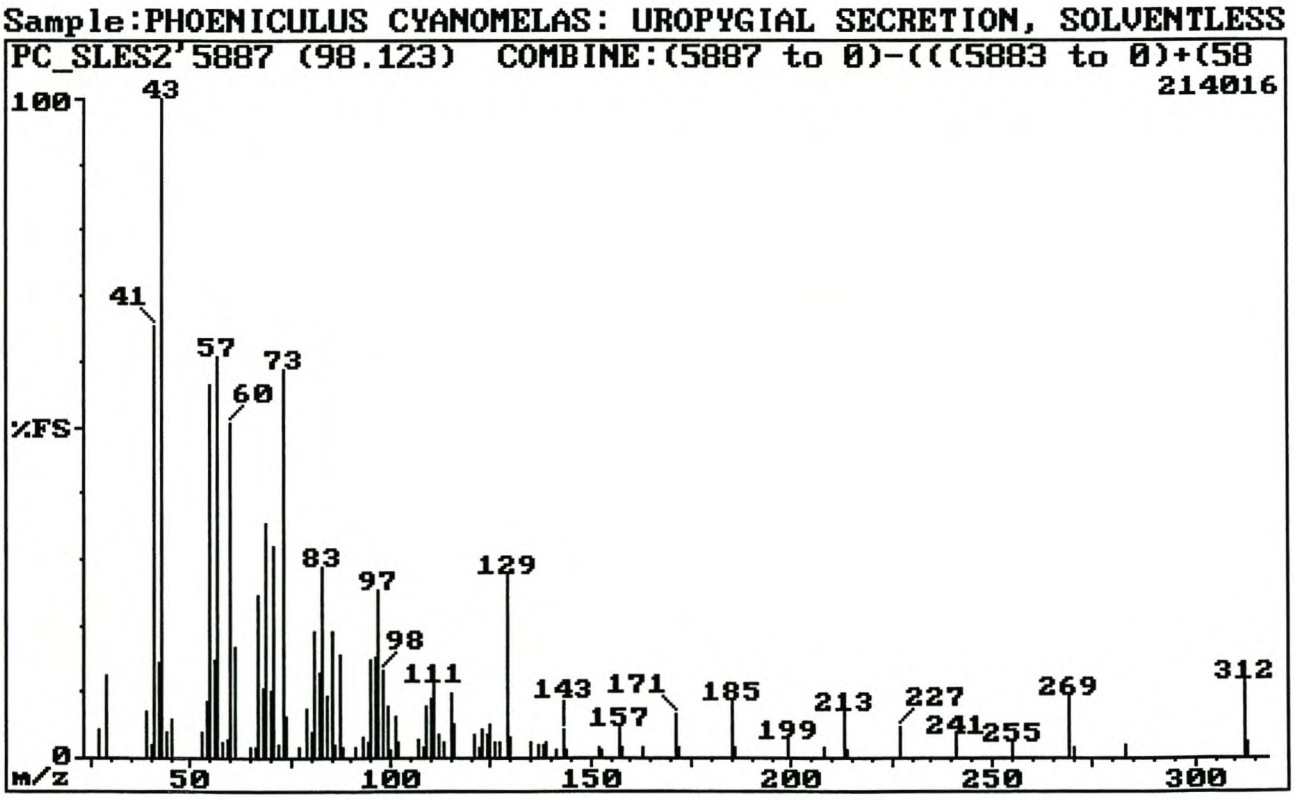

Fig 2.97: EI mass spectrum of component 5887 (eicosanoic acid)

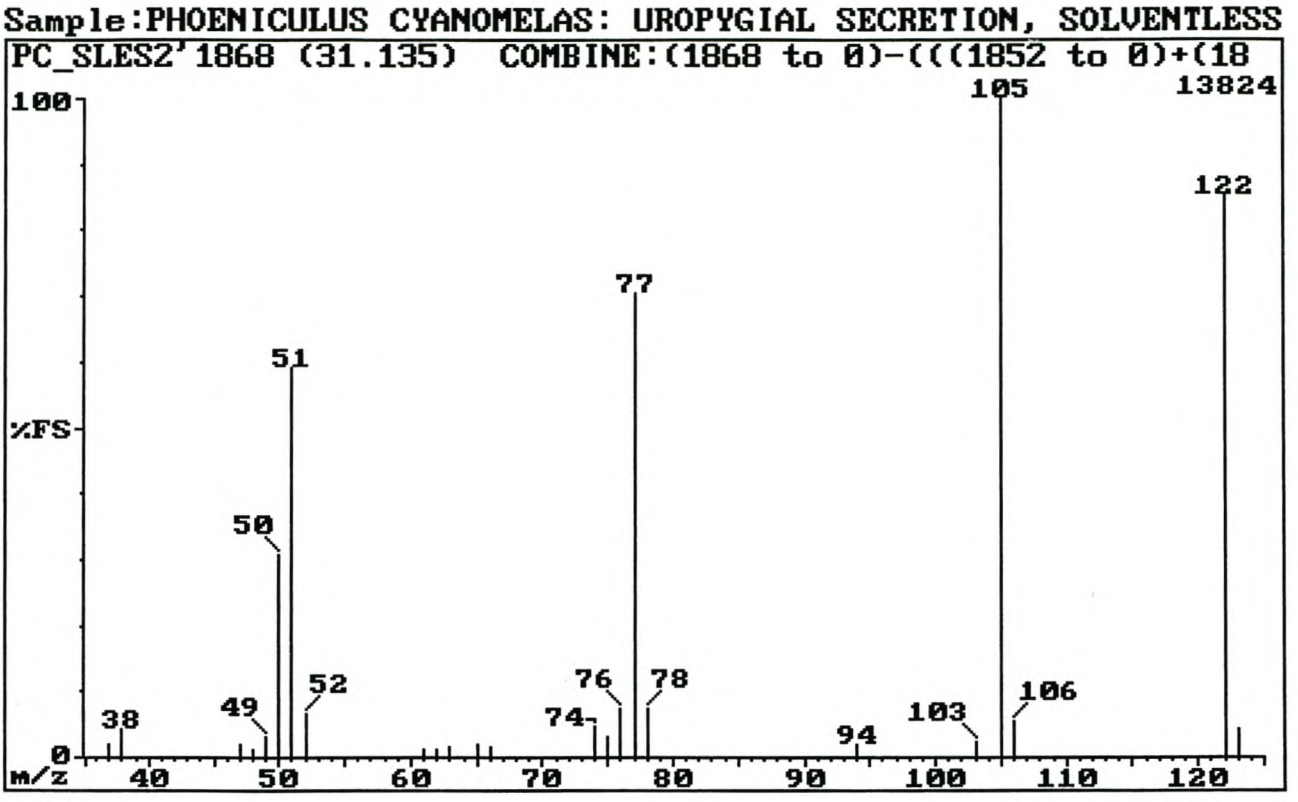

Fig 2.98: EI mass spectrum of component 1868 (benzoic acid)

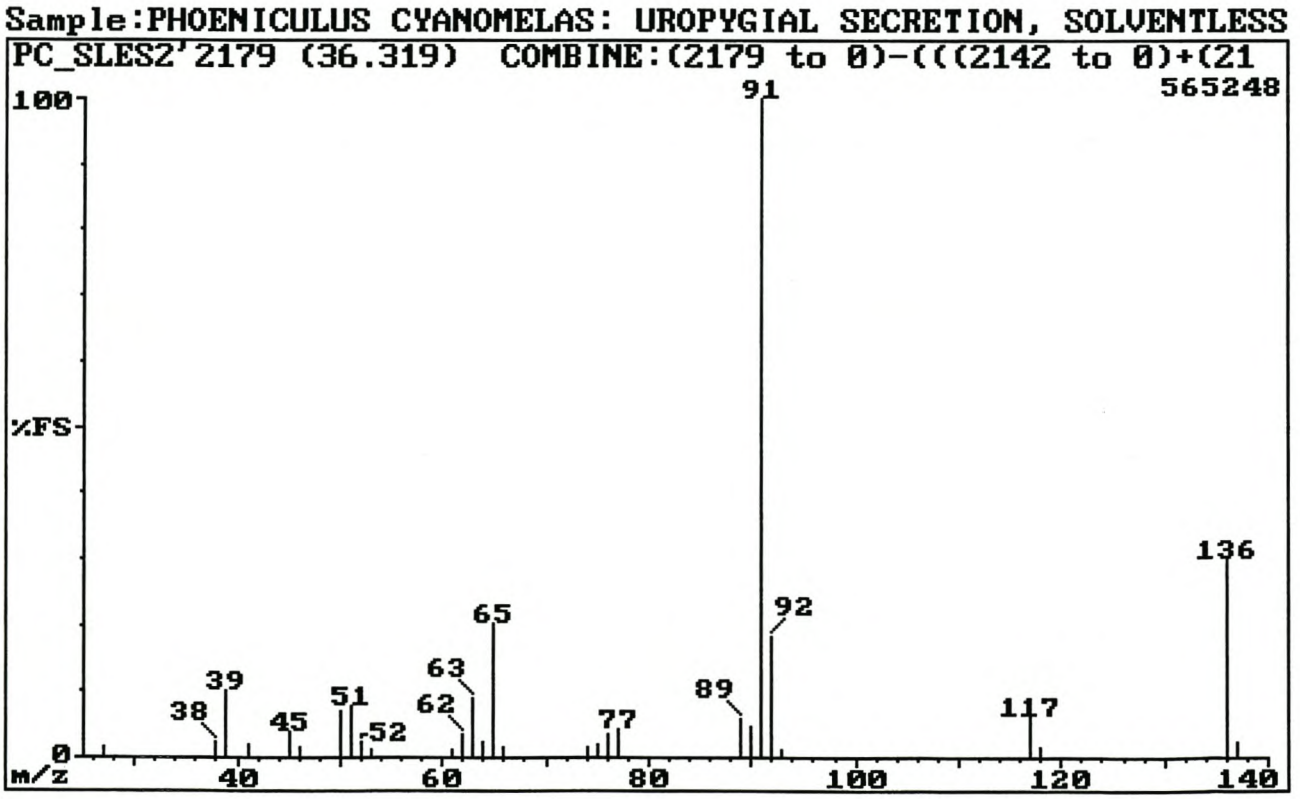

Fig 2.99: EI mass spectrum of component 2179 (phenylacetic acid)

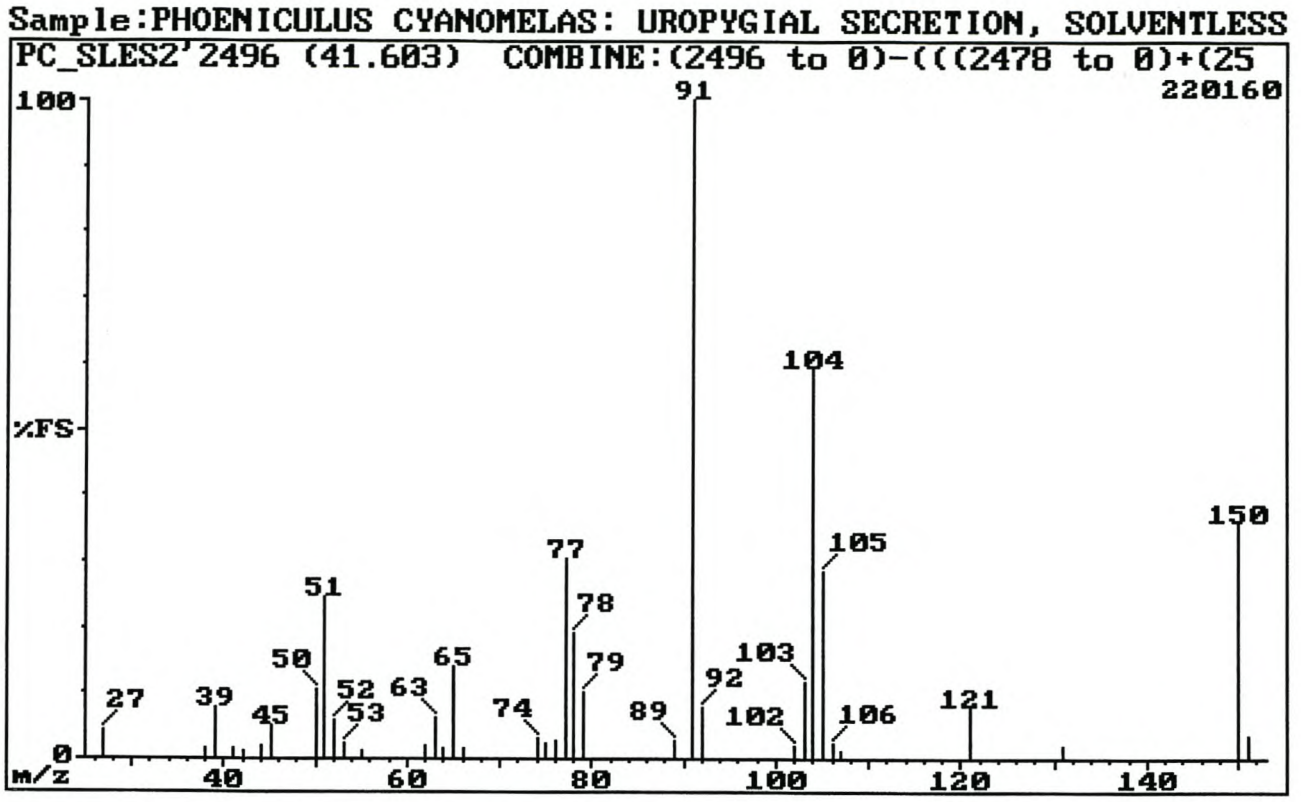

Fig 2.100: EI mass spectrum of component 2496 (3-phenylpropanoic acid)

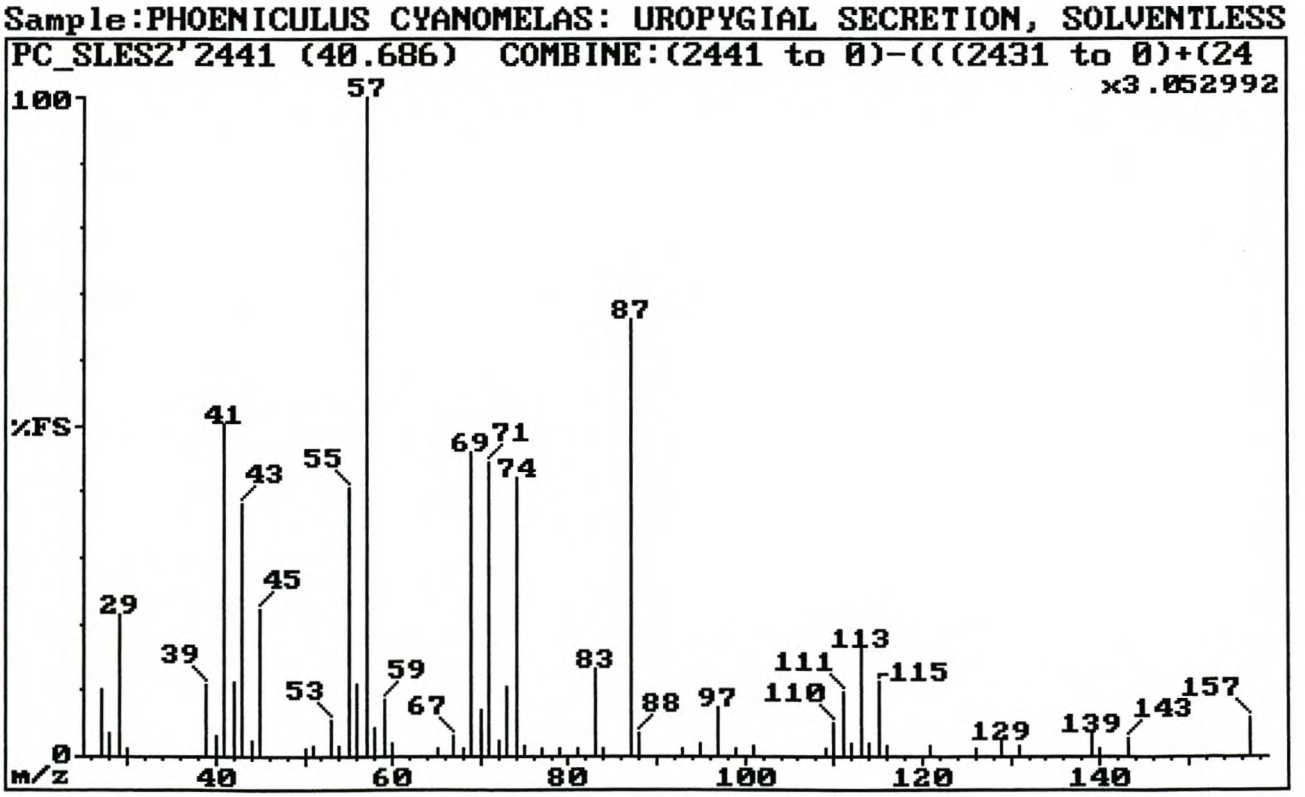

Fig 2.101: EI mass spectrum of component 2441 (methyl 4-methyloctanoate)

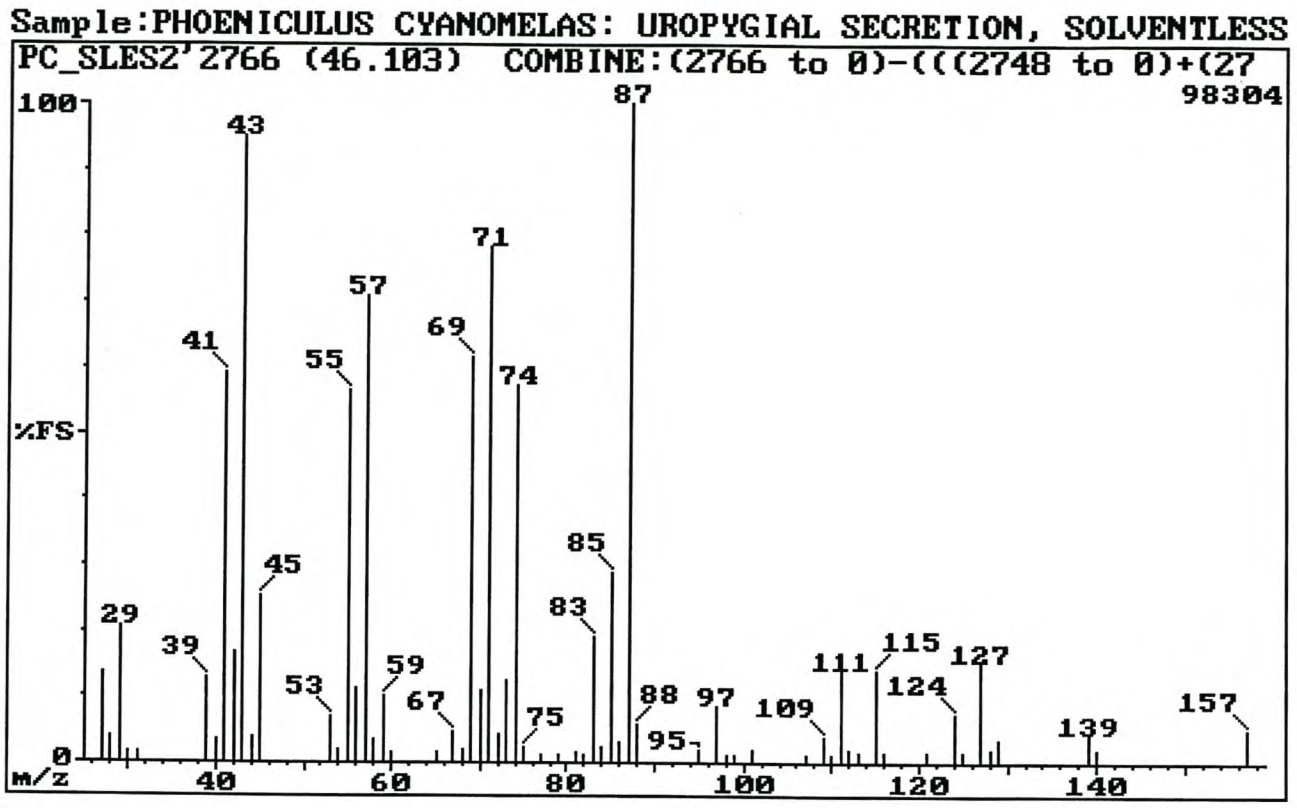

Fig 2.102: EI mass spectrum of component 2766 (methyl 4-methylnonanoate)

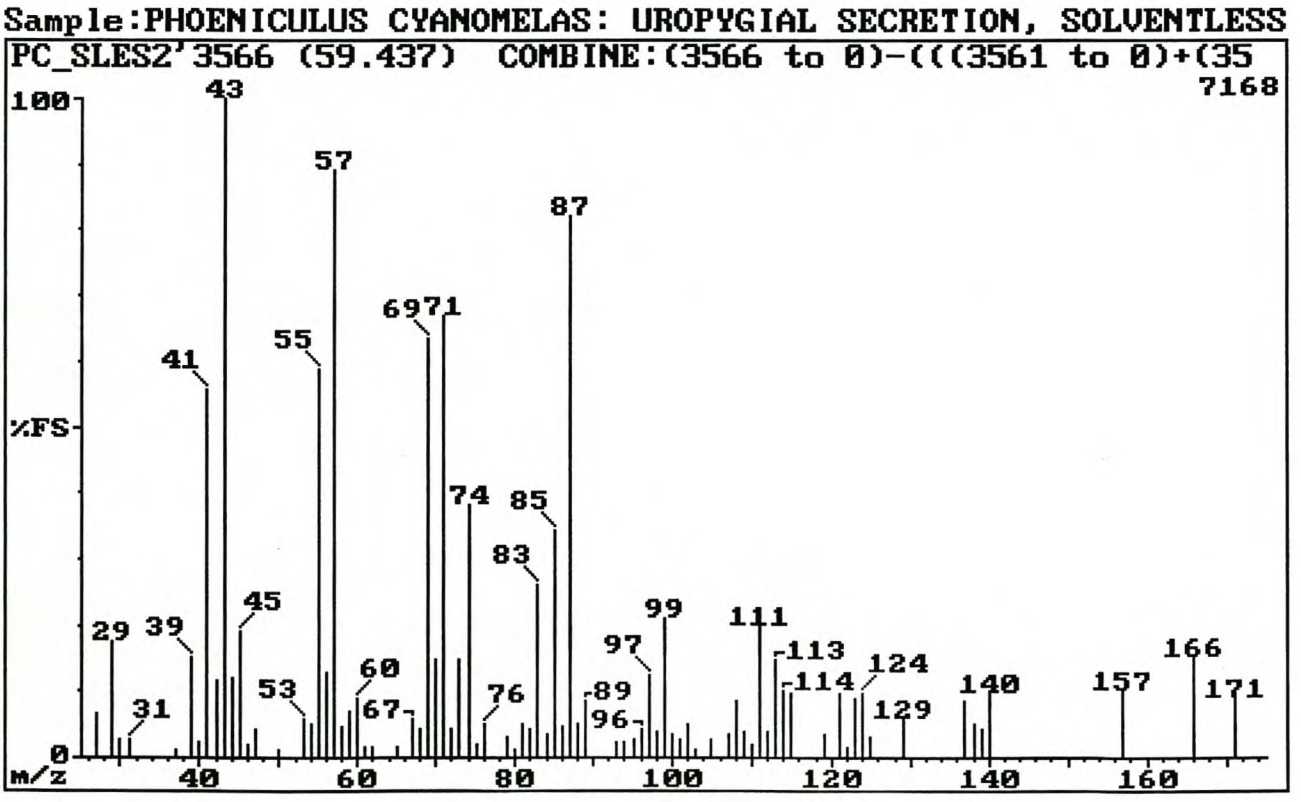

Fig 2.103: EI mass spectrum of component 3566 (methyl 2,6-dimethyloctanoate)

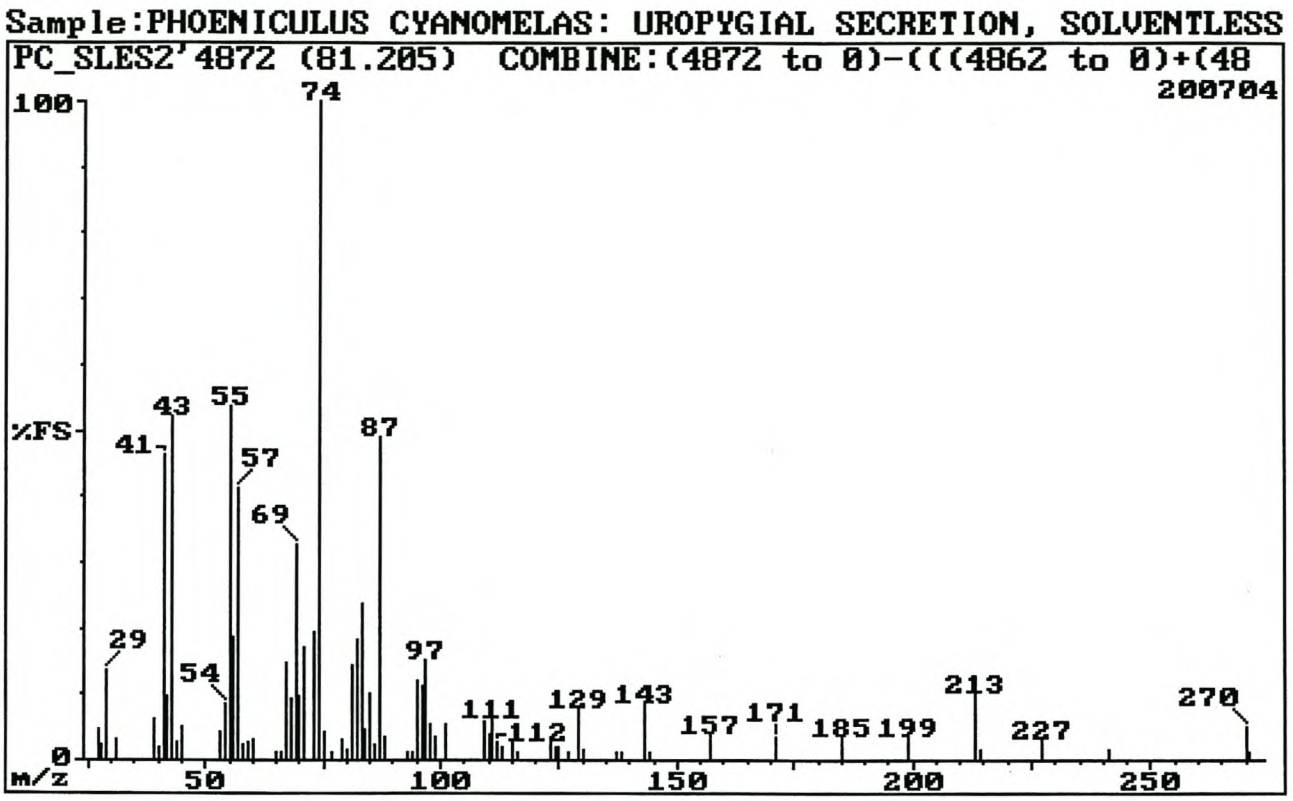

Fig 2.104: EI mass spectrum of component 4872 (methyl 4-methylhexadecanoate)

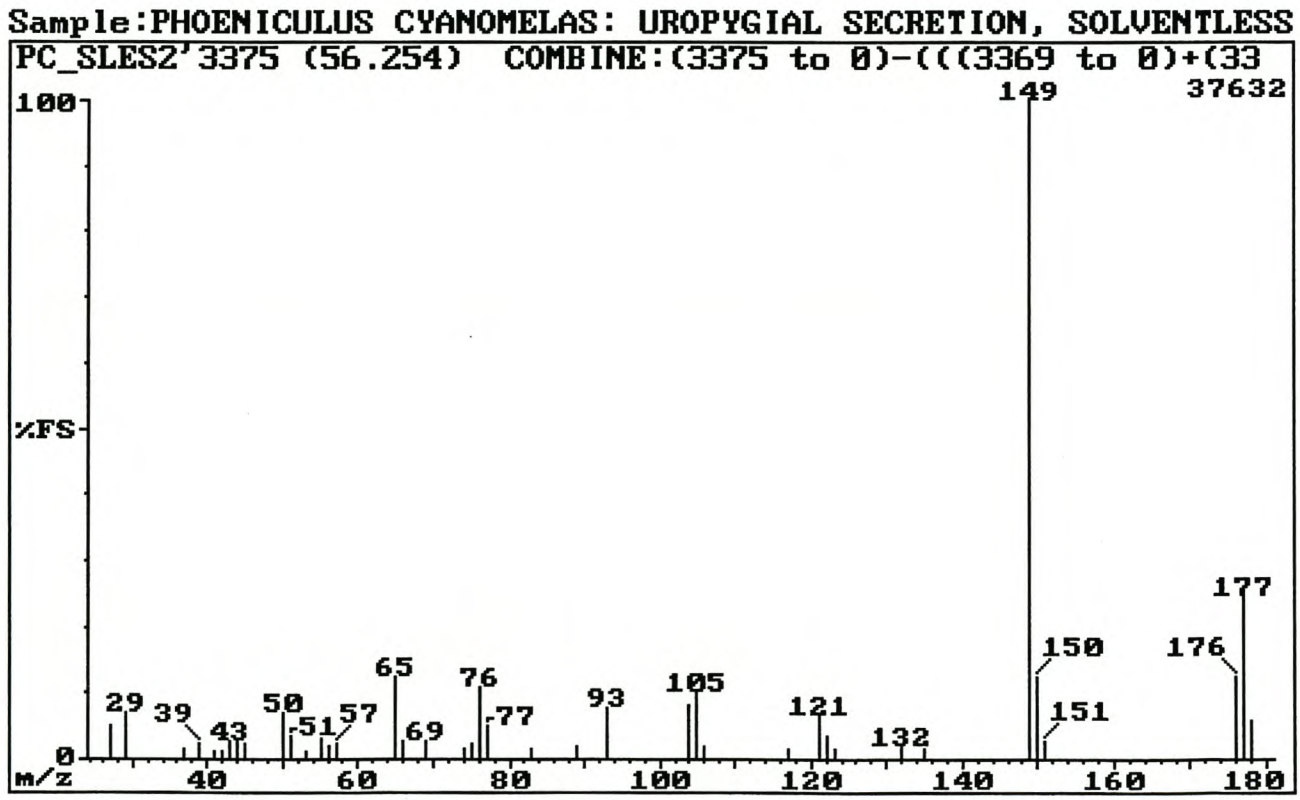

Fig 2.105: EI mass spectrum of component 3375 (diethylphthalate)

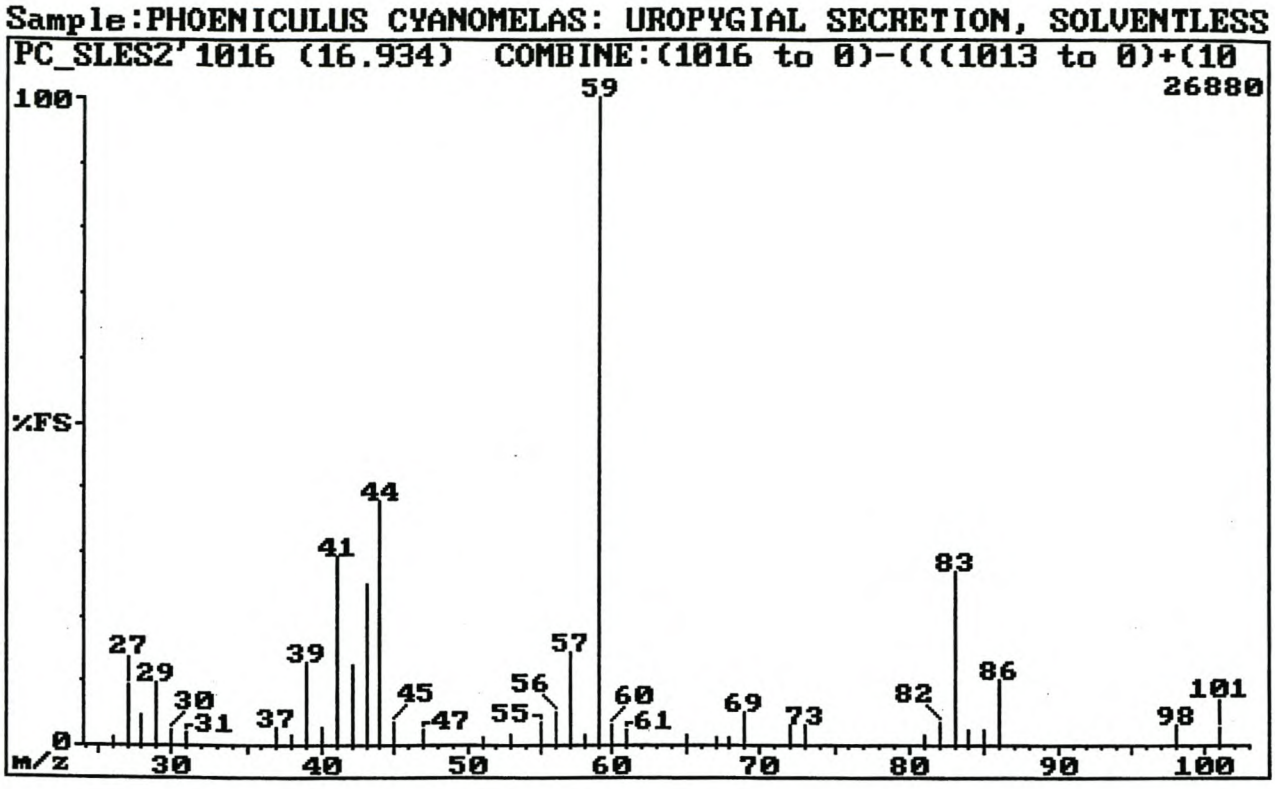

Fig.2.106: EI mass spectrum of component 1016 (pentaneamide)

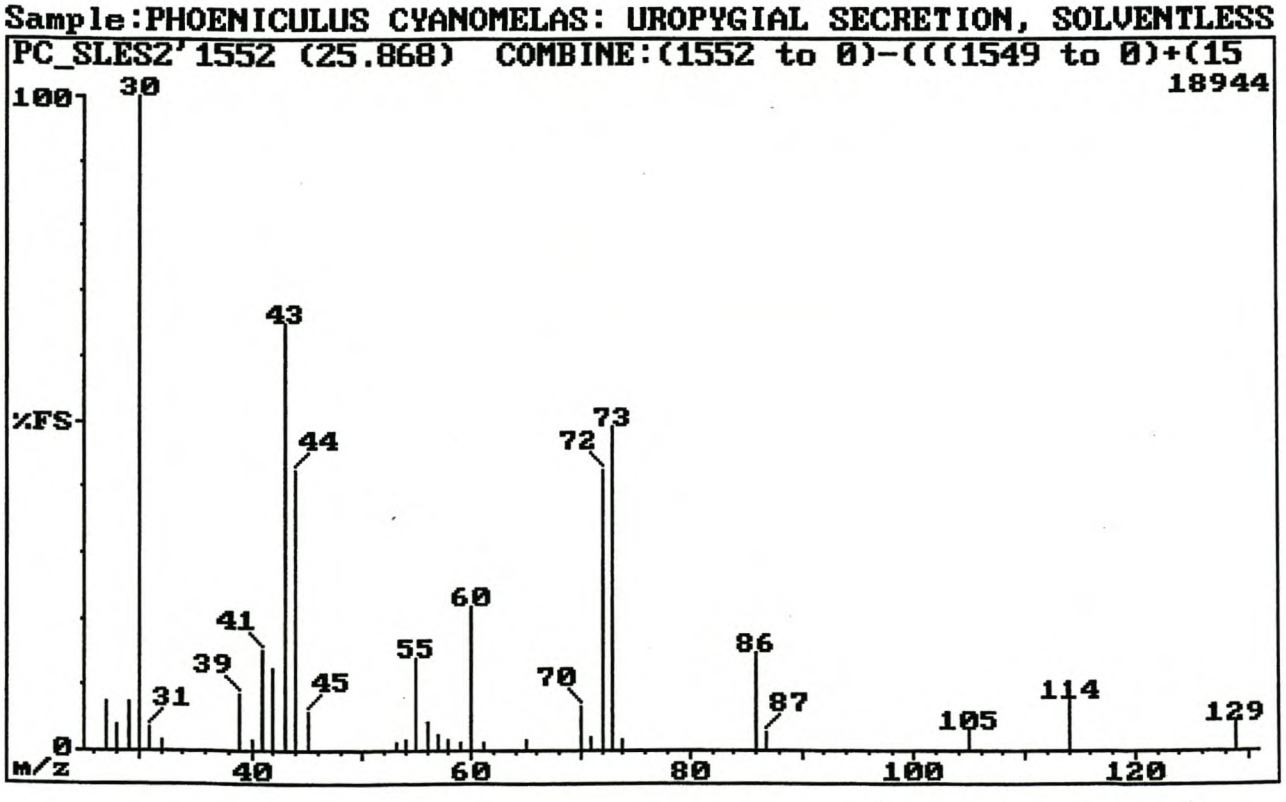

Fig 2.107: EI mass spectrum of component 1552 (pentaneacetamide)

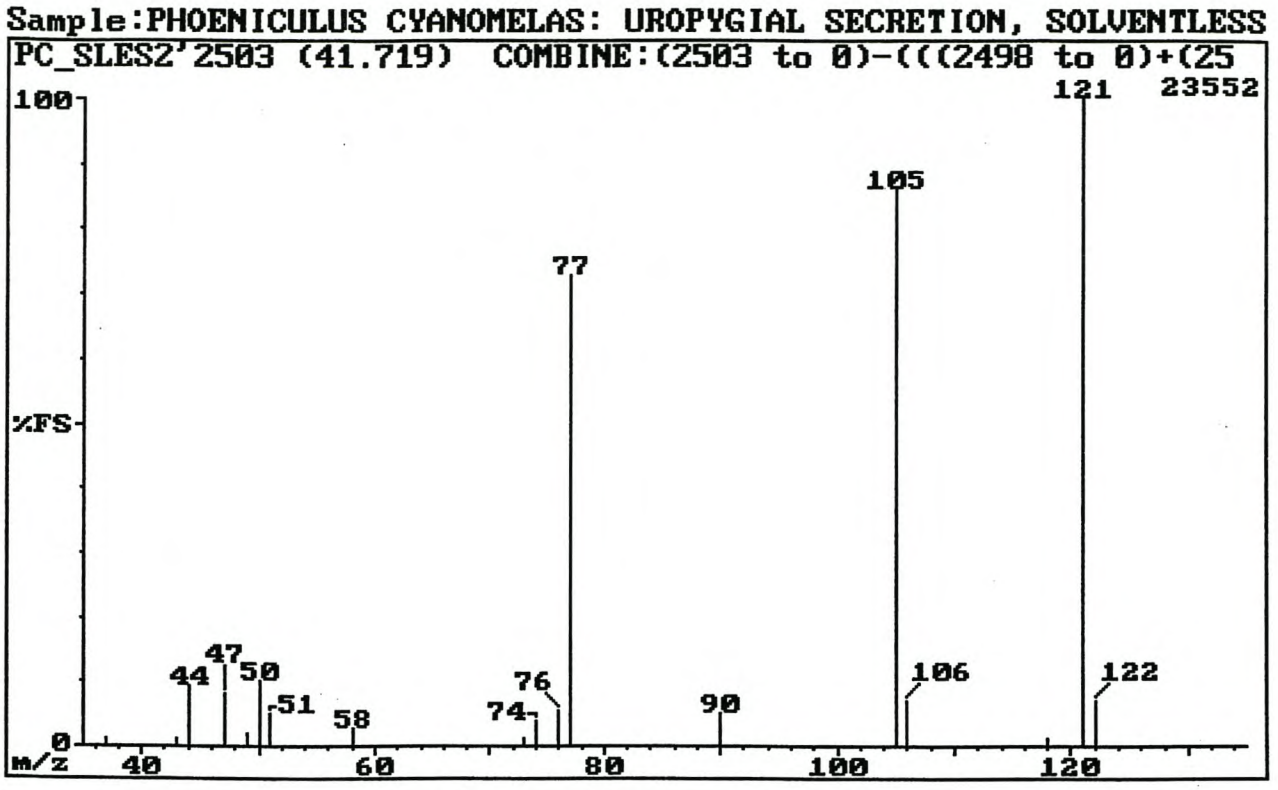

Fig 2.108: EI mass spectrum of component 2503 (benzamide)

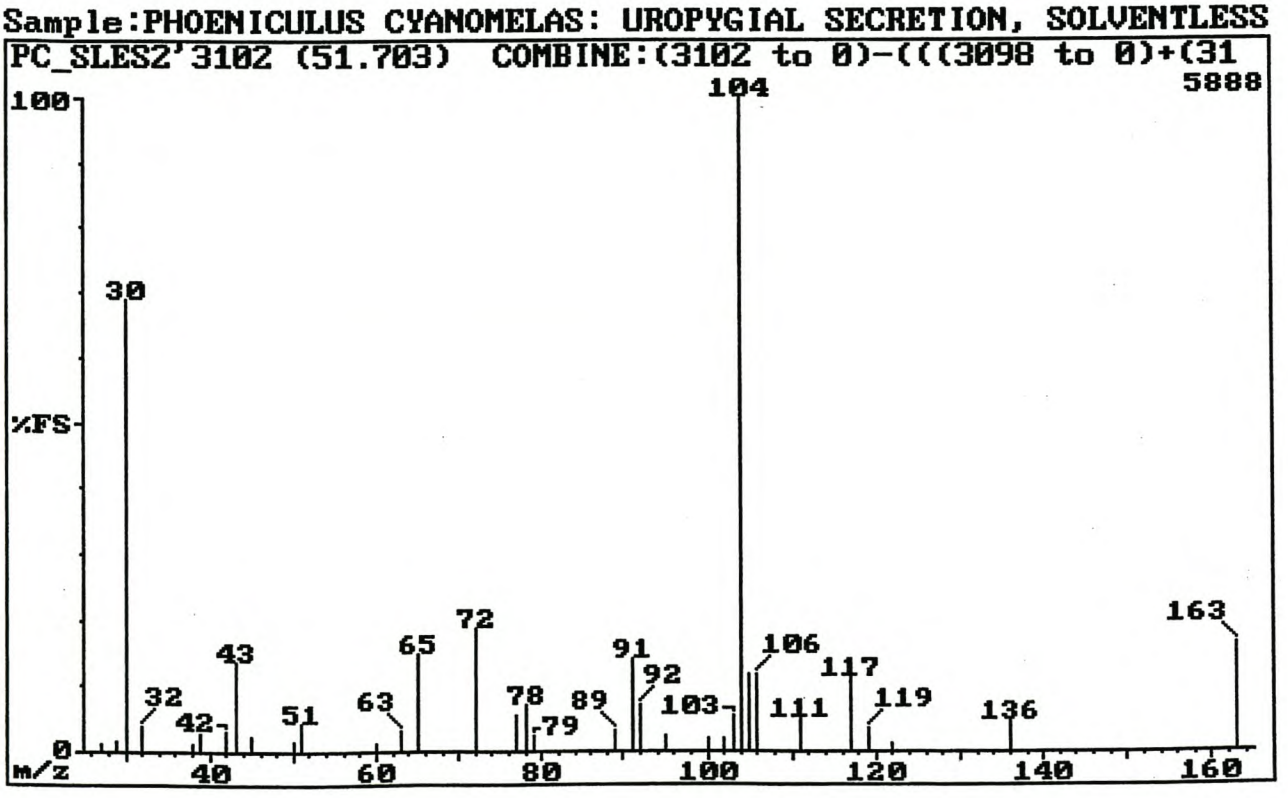

Fig 2.109: EI mass spectrum of component 3102 (N-(2-phenylethyl)-acetamide)

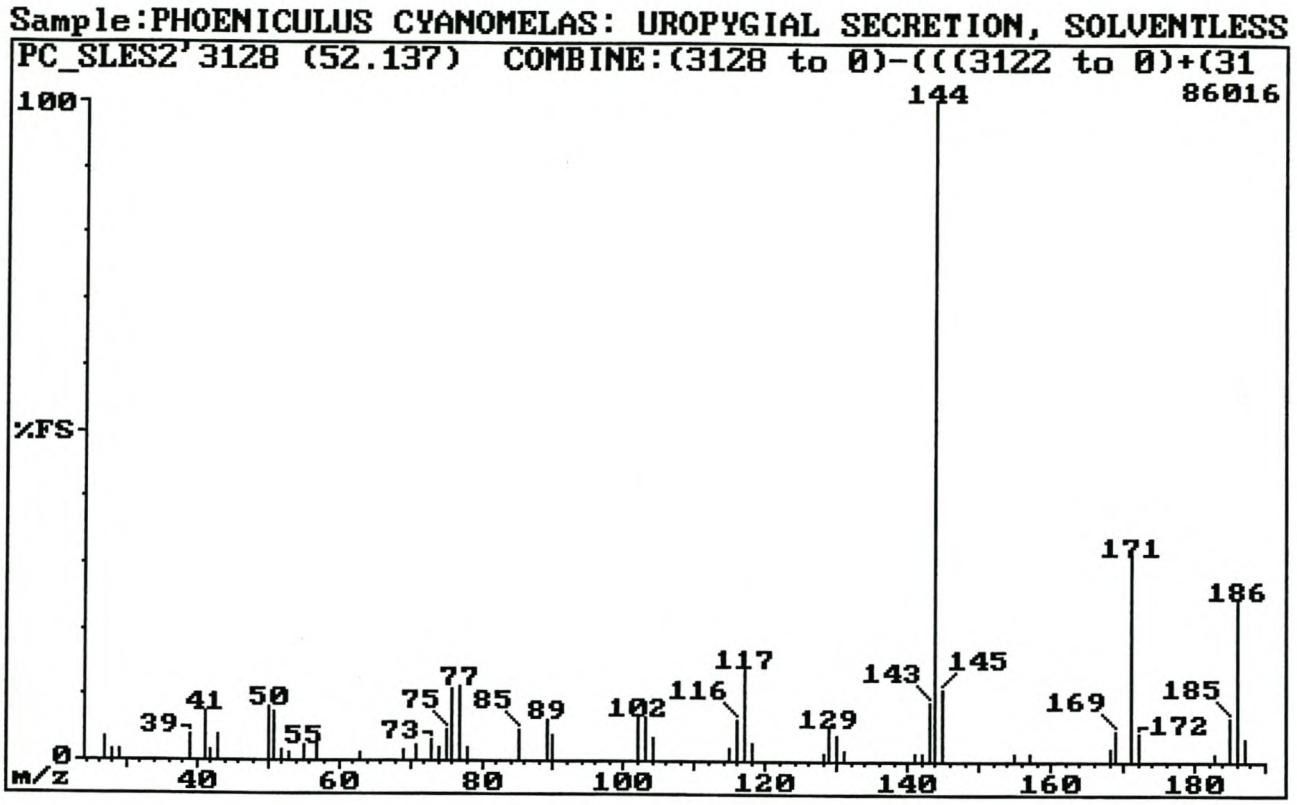

Fig 2.110: EI mass spectrum of component 3128 (N-1-isoquinolinyl acetamide)

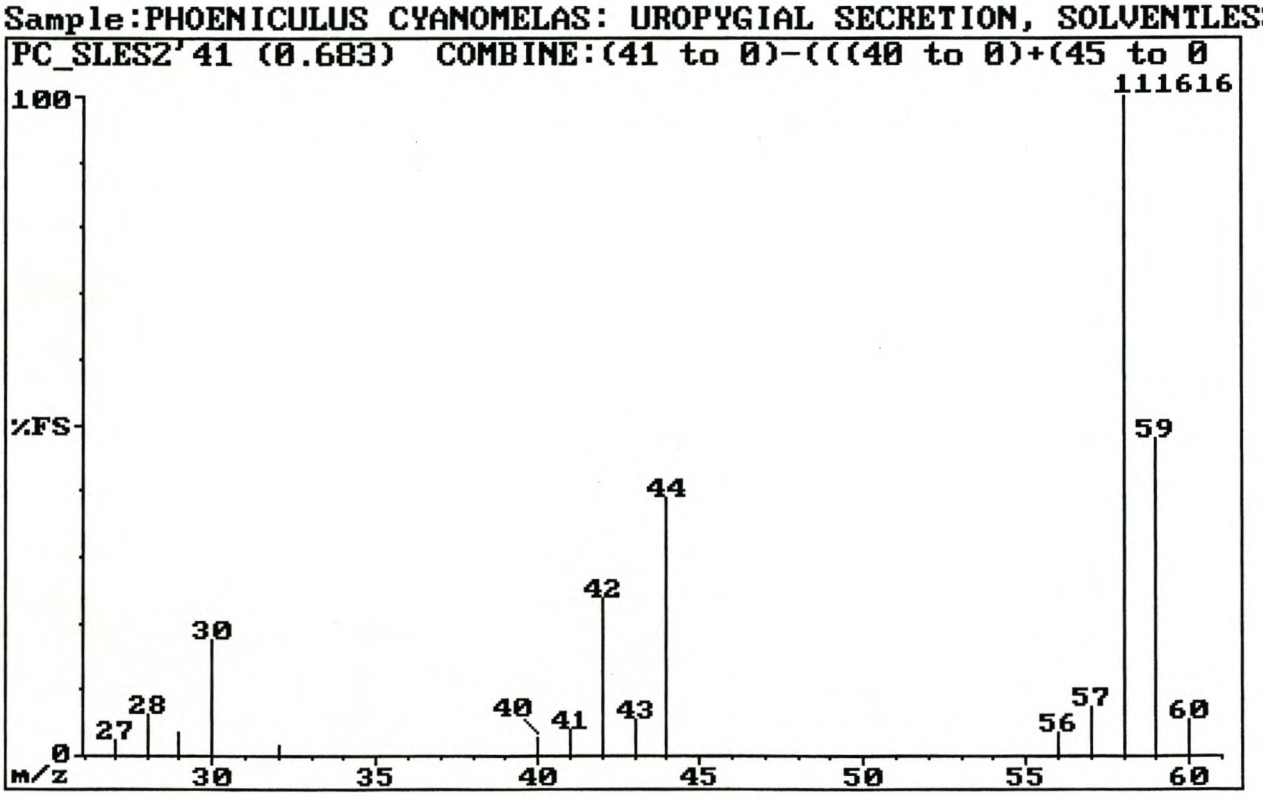

Fig 2.111: EI mass spectrum of component 41 (N,N,N-trimethylamine)

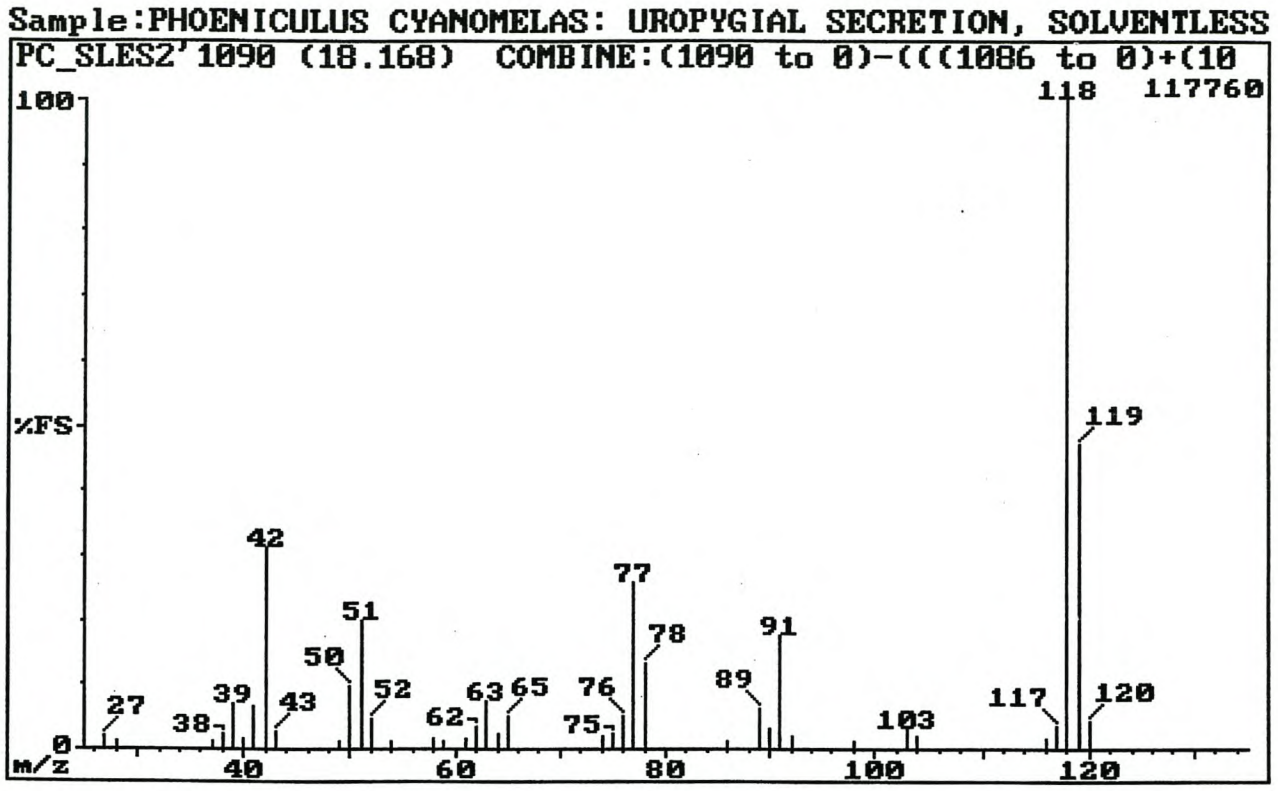

Fig 2.112: EI mass spectrum of component 1090 (*N*-(benzylidene)methyl imine)

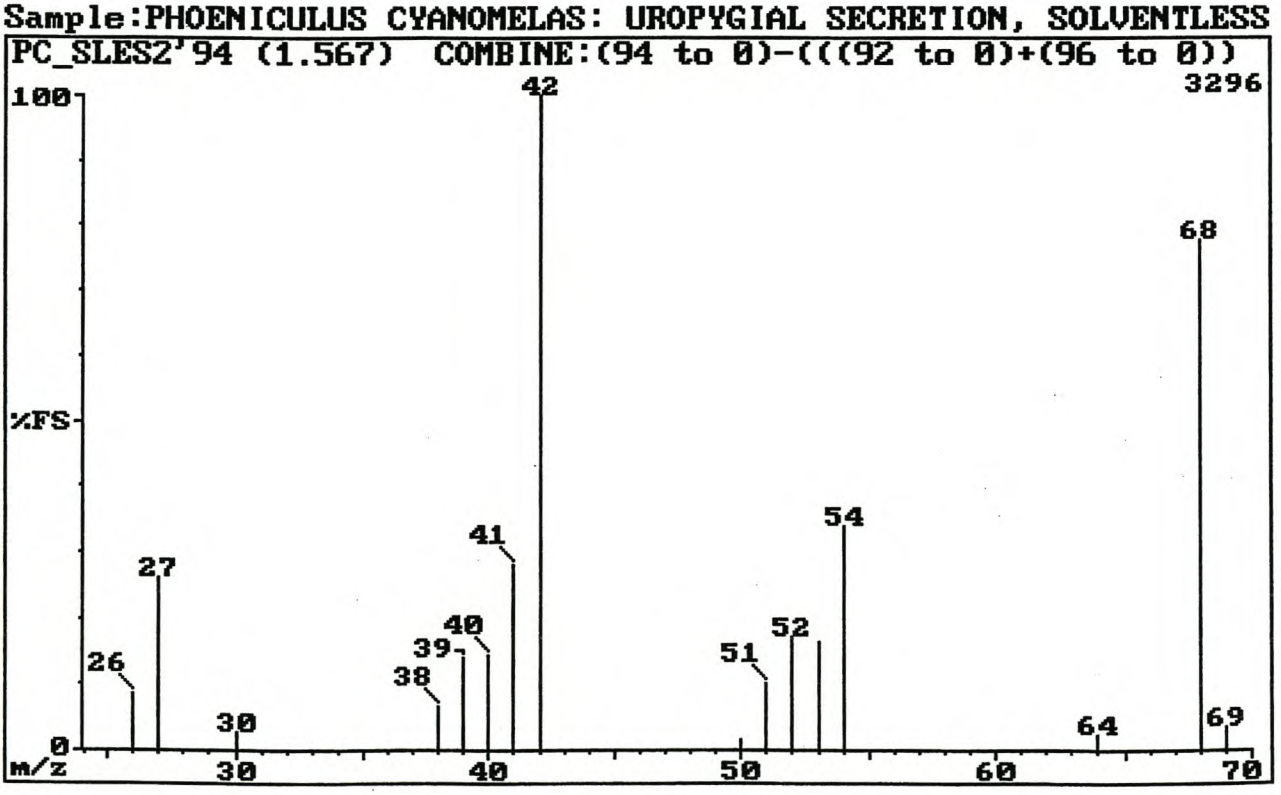

Fig 2.113: EI mass spectrum of component 94 (2-methylpropanenitrile)

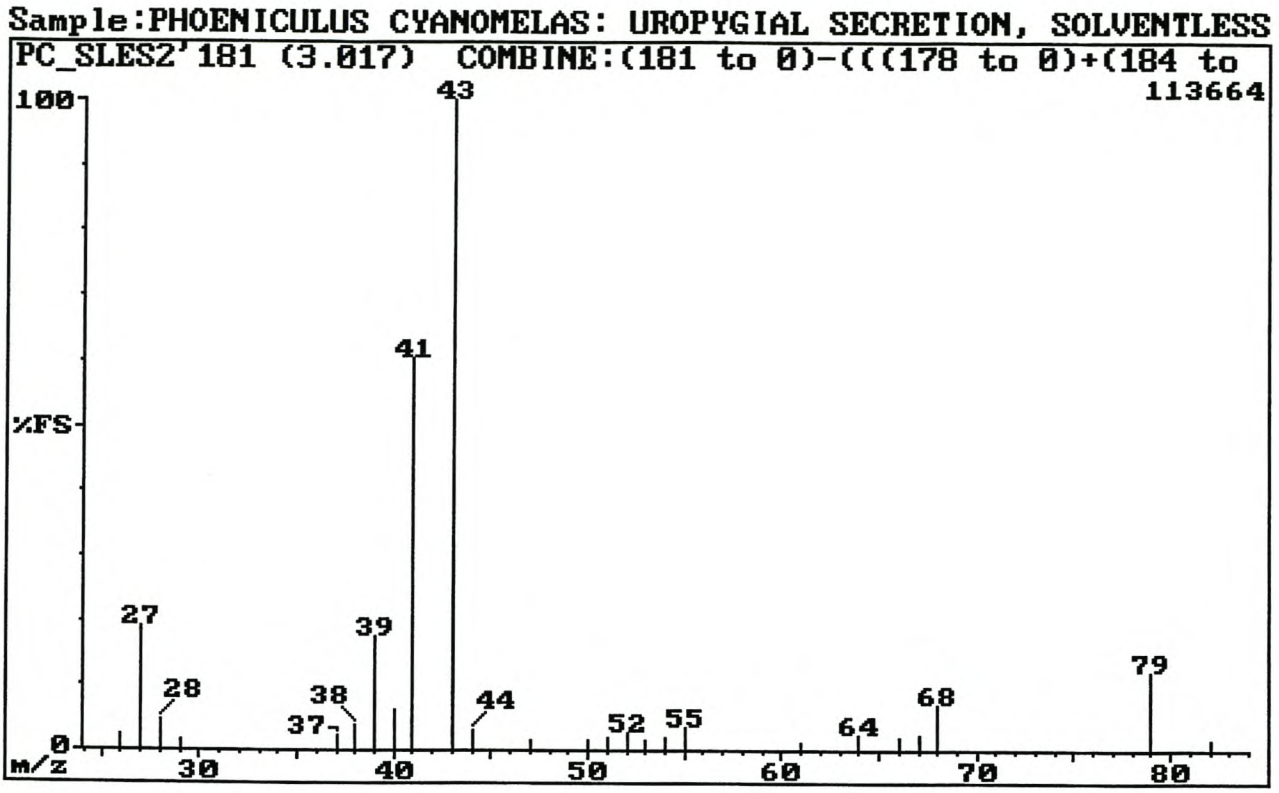

Fig 2.114: EI mass spectrum of component 181 (pentanenitrile)

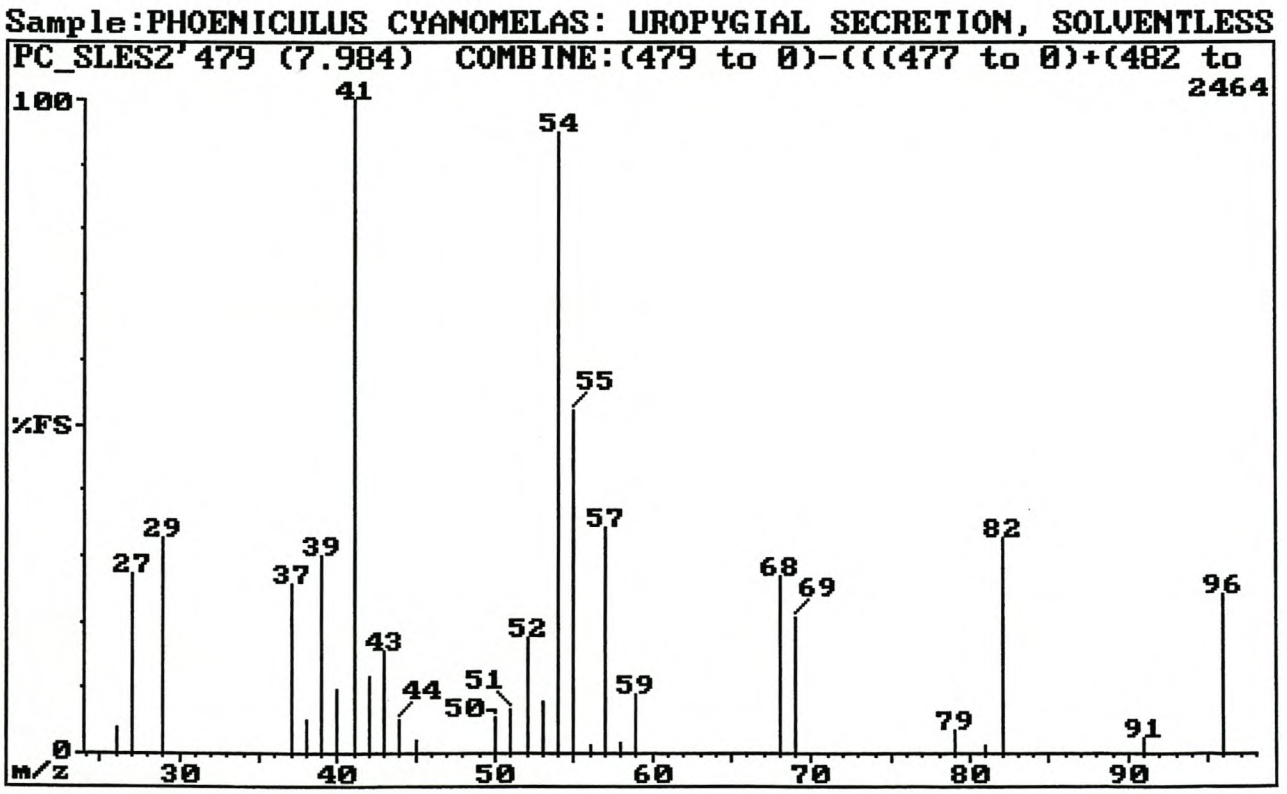

Fig 2.115: EI mass spectrum of component 479 (hexanenitrile)

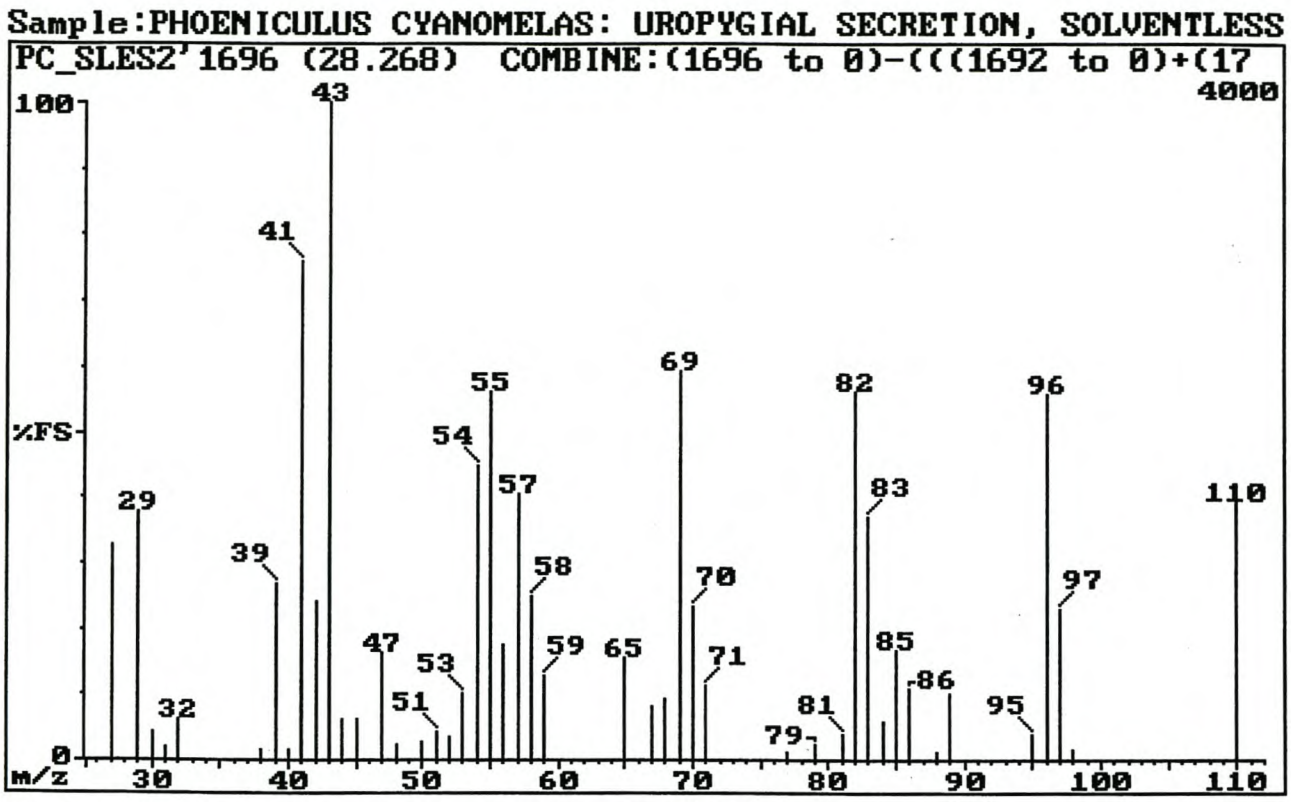

Fig 2.116: EI mass spectrum of component 1696 (nonanenitrile)

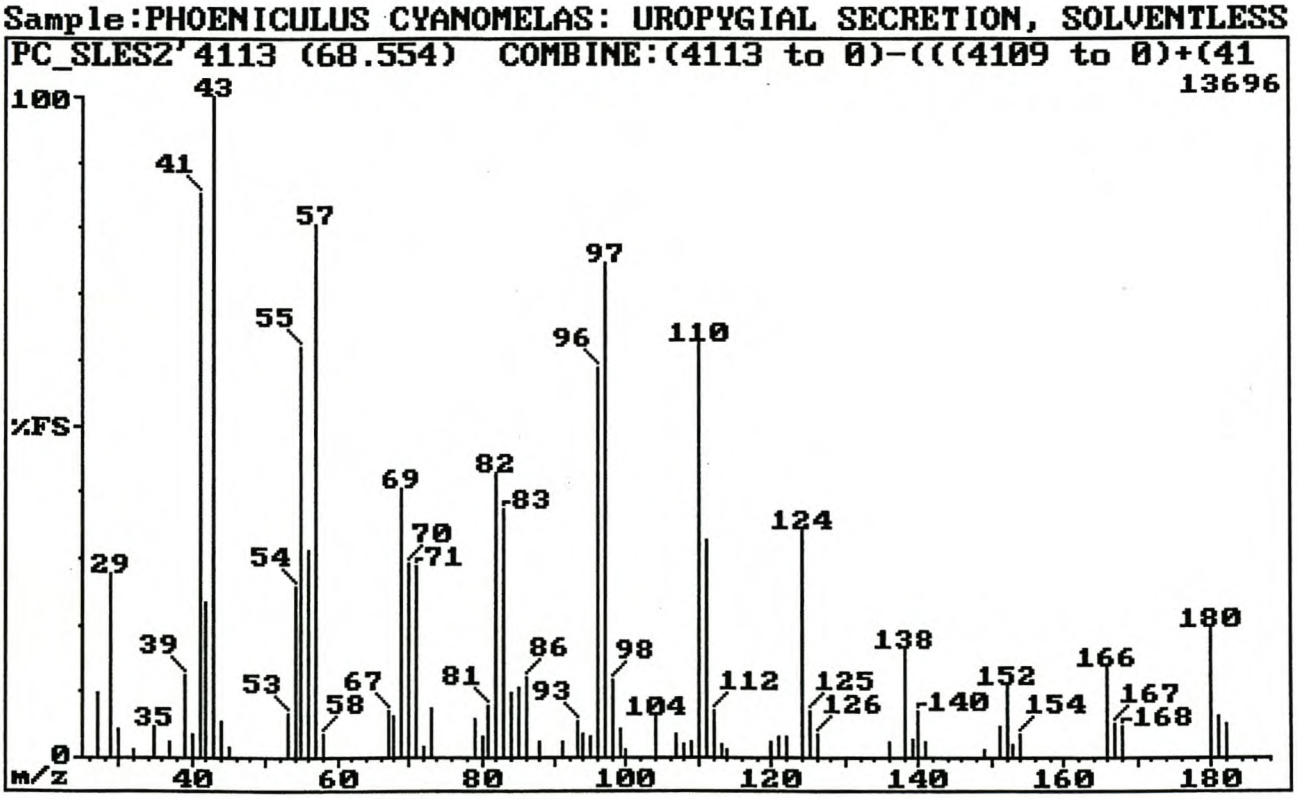

Fig 2.117 EI mass spectrum of component 4113 (undecanenitrile)

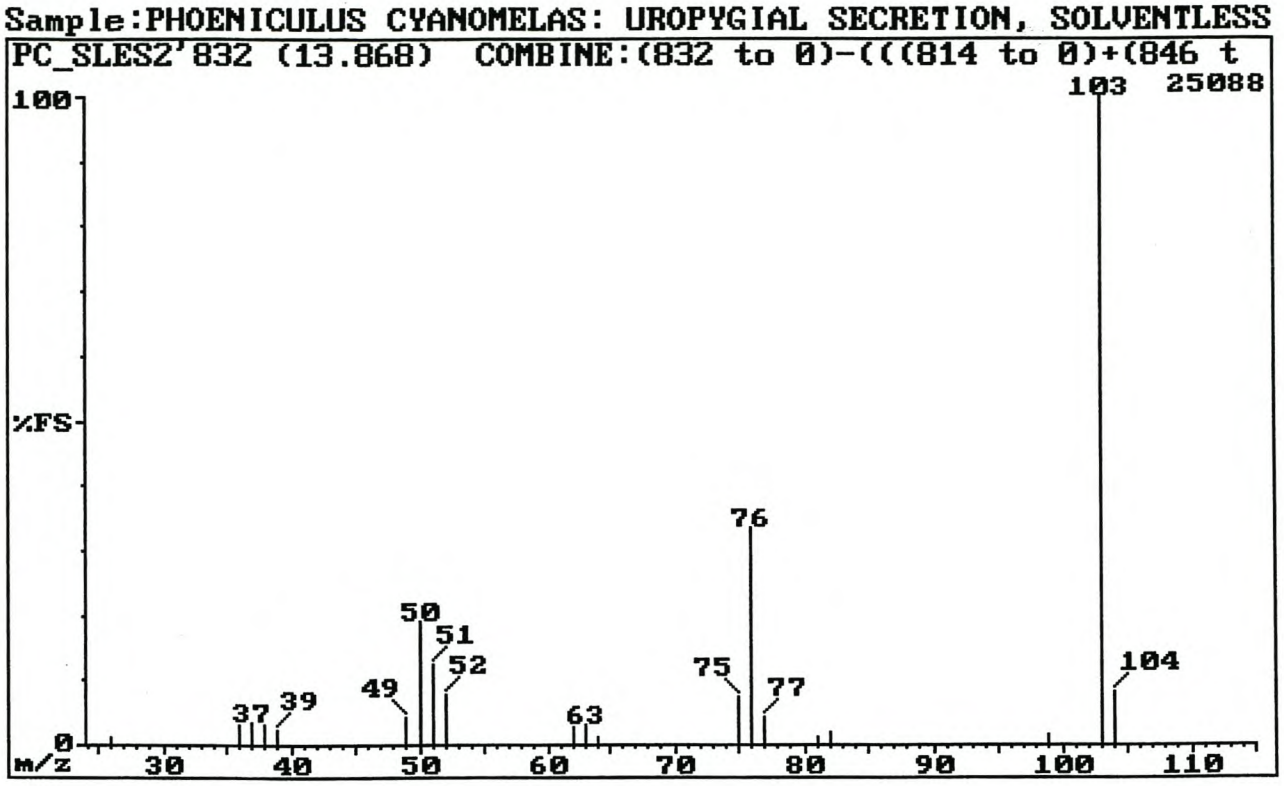

Fig 2.118: EI mass spectrum of component 832 (benzonitrile)

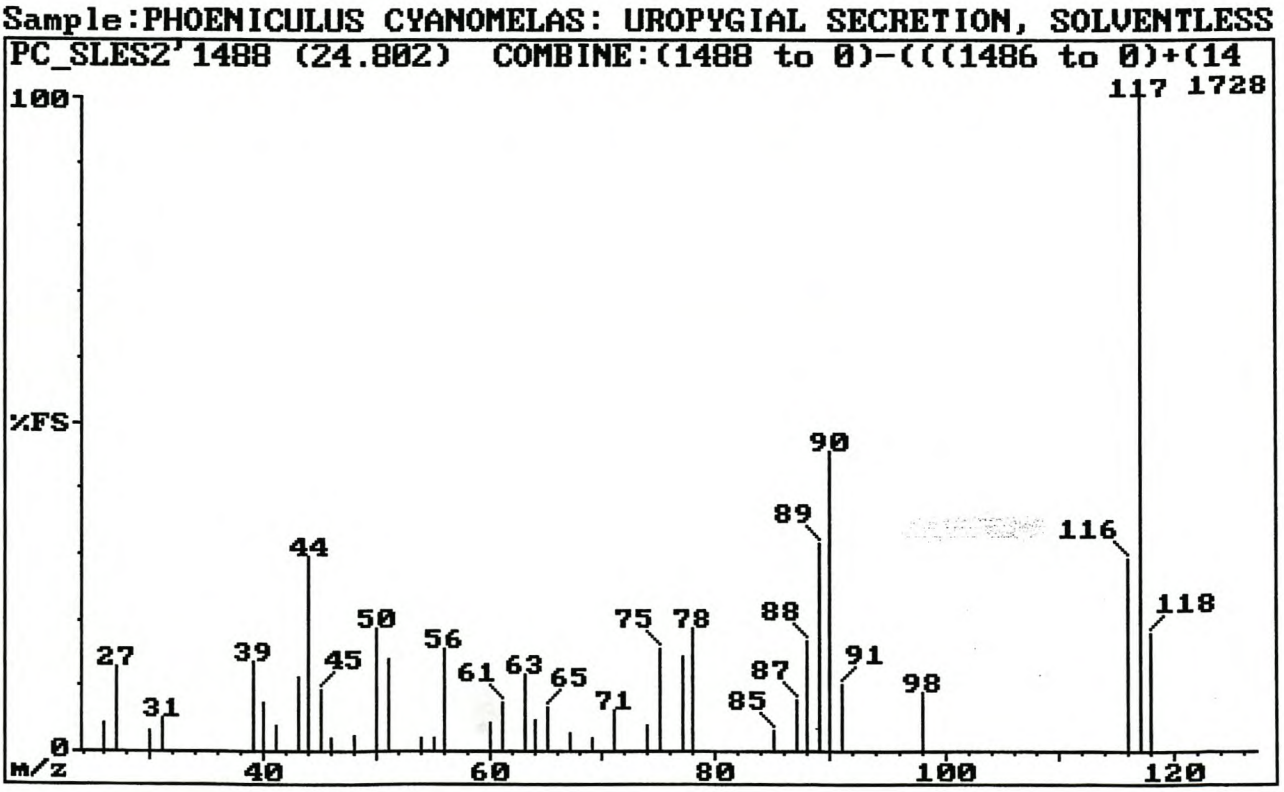

Fig 2.119: EI mass spectrum of component 1488 (phenylacetonitrile)

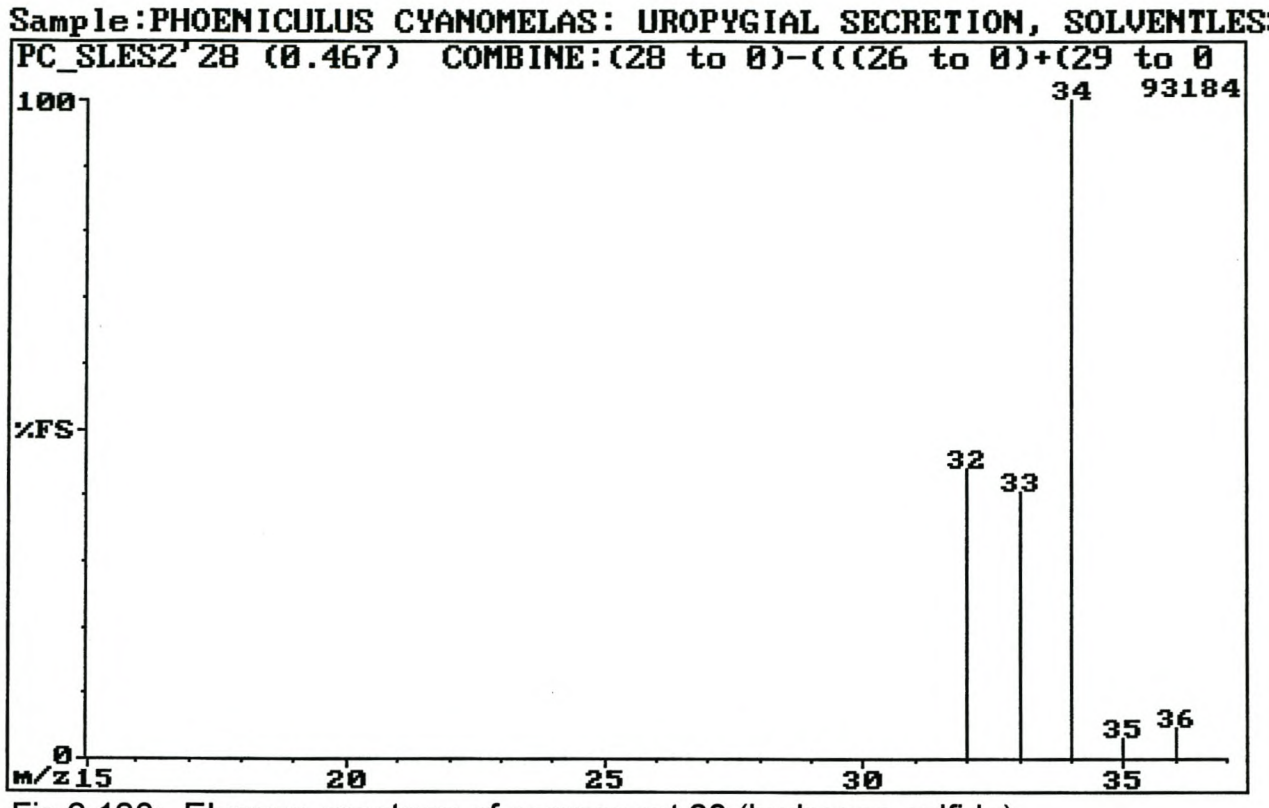

Fig 2.120: EI mass spectrum of component 28 (hydrogen sulfide)

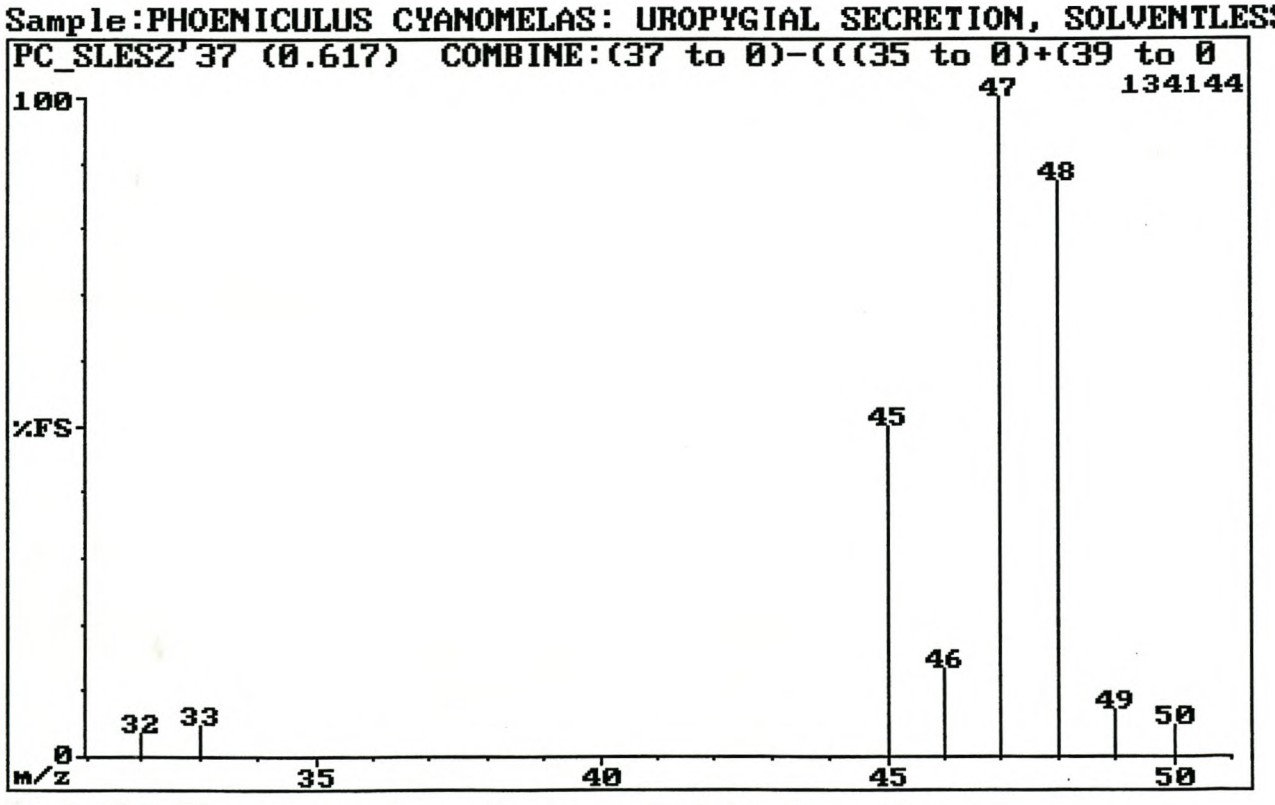

Fig 2.121: EI mass spectrum of component 37 (methanethiol)

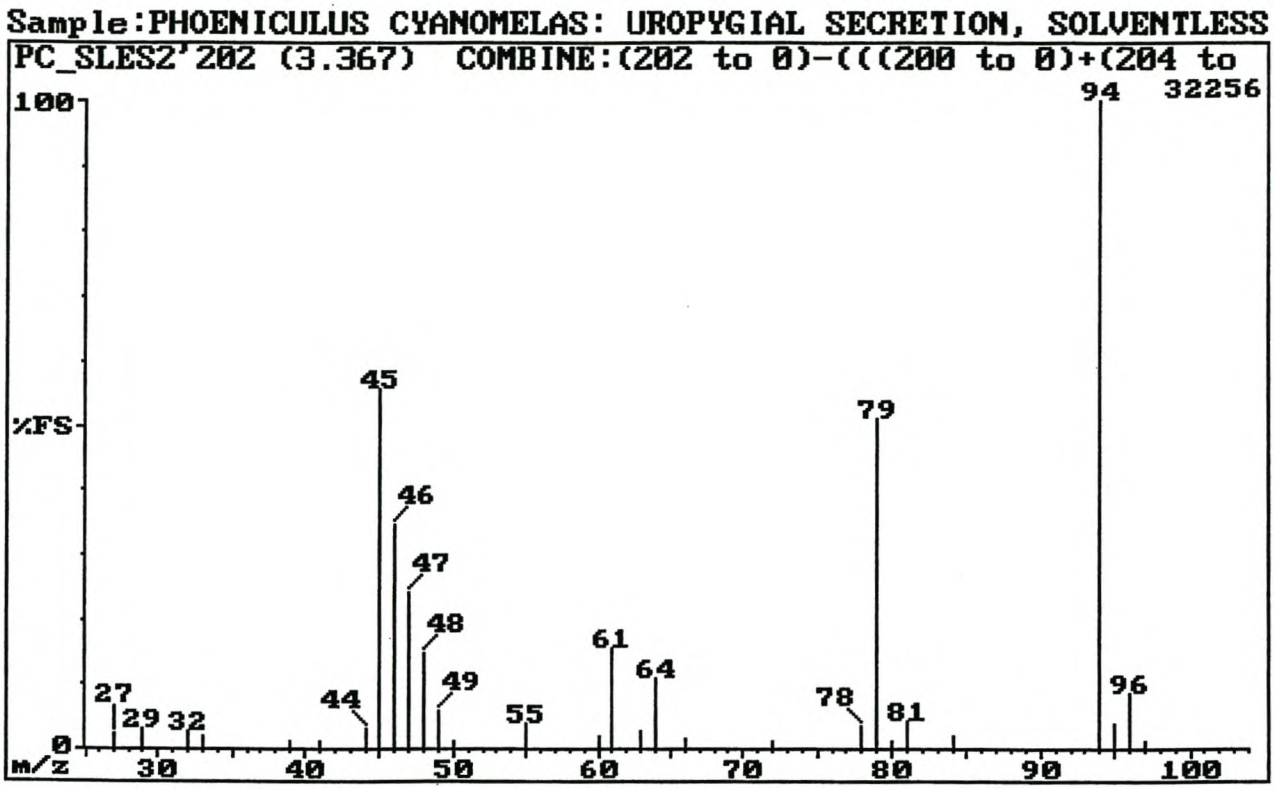

Fig 2.122: EI mass spectrum of component 202 (dimethyl disulfide)

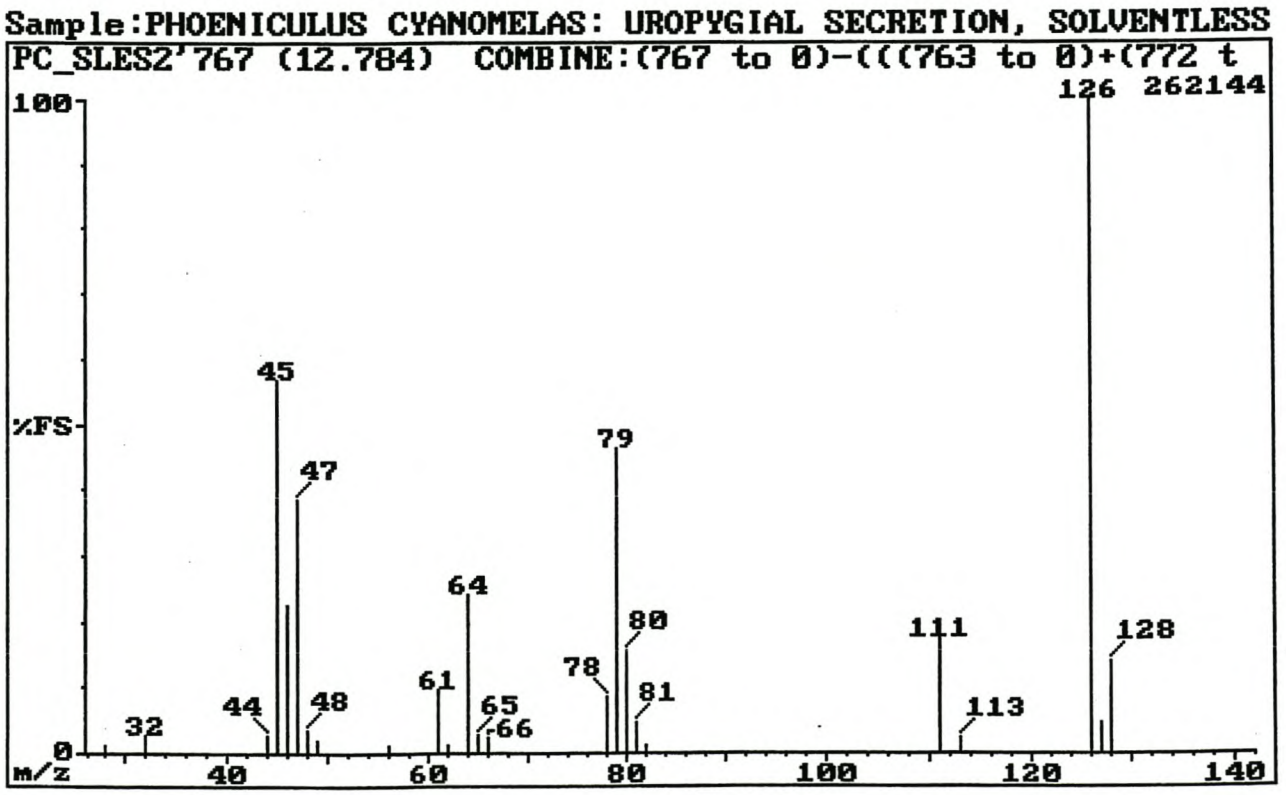

Fig 2.123: EI mass spectrum of component 767 (trimethyl disulfide)

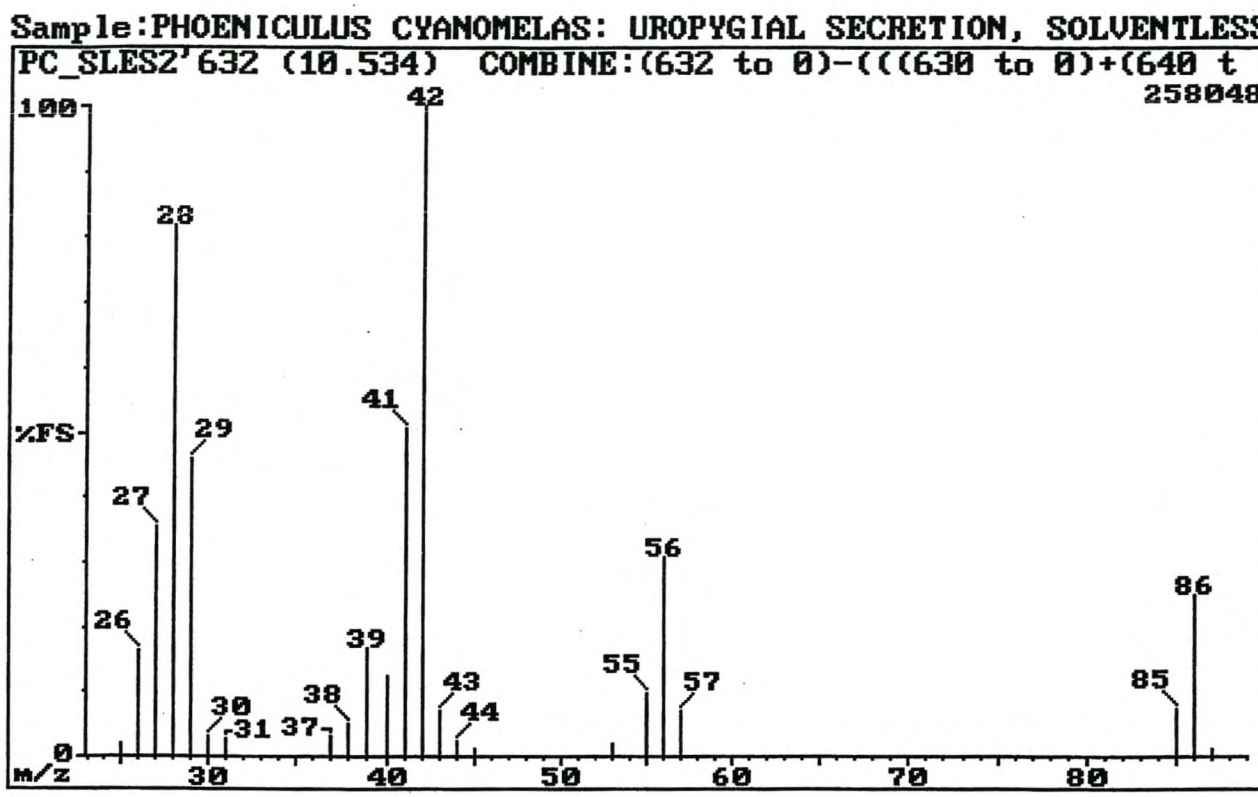

Fig 2.124: EI mass spectrum of component 632 (2-dihydrofuranone)

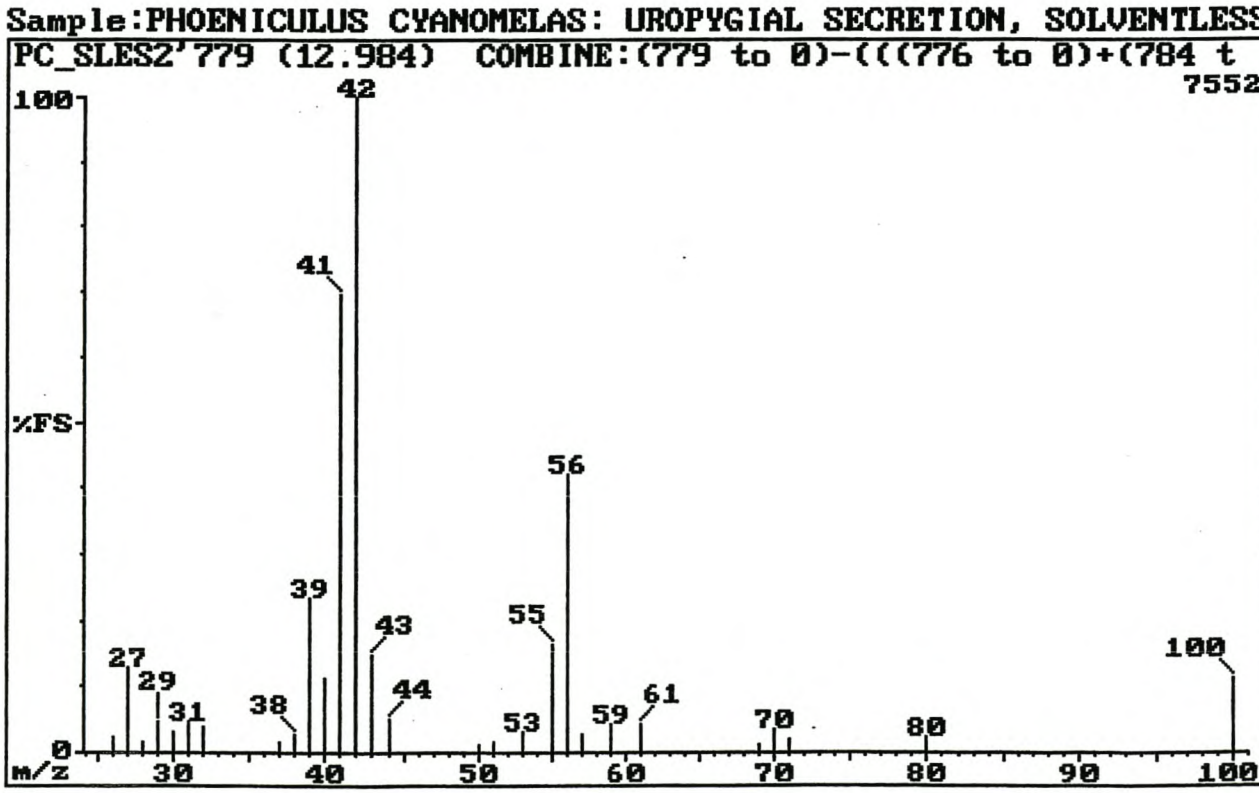

Fig 2.125: EI mass spectrum of component 779 (5-pentanolide)

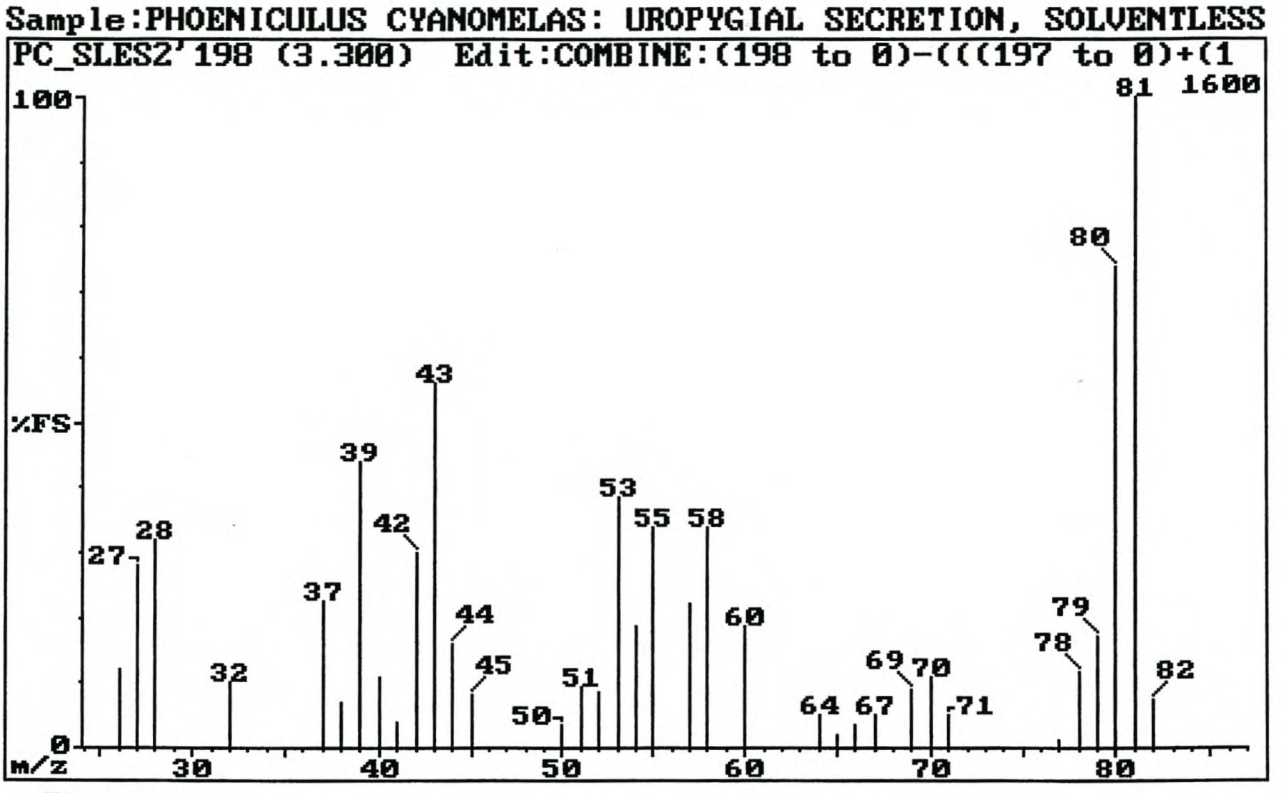

Fig 2.126: EI mass spectrum of component 198 (1-methyl-1H-pyrrole)

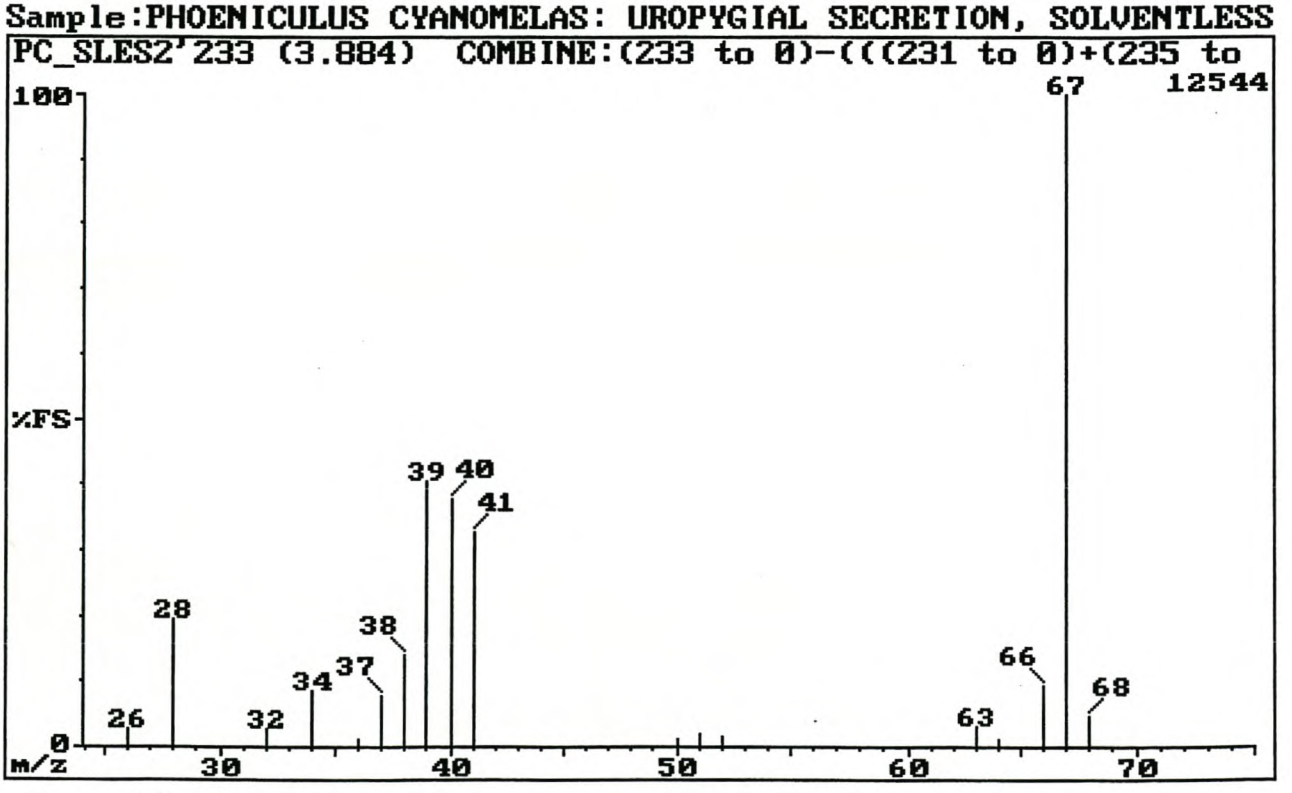

Fig 2.127: EI mass spectrum of component 233 (1H-pyrrole)

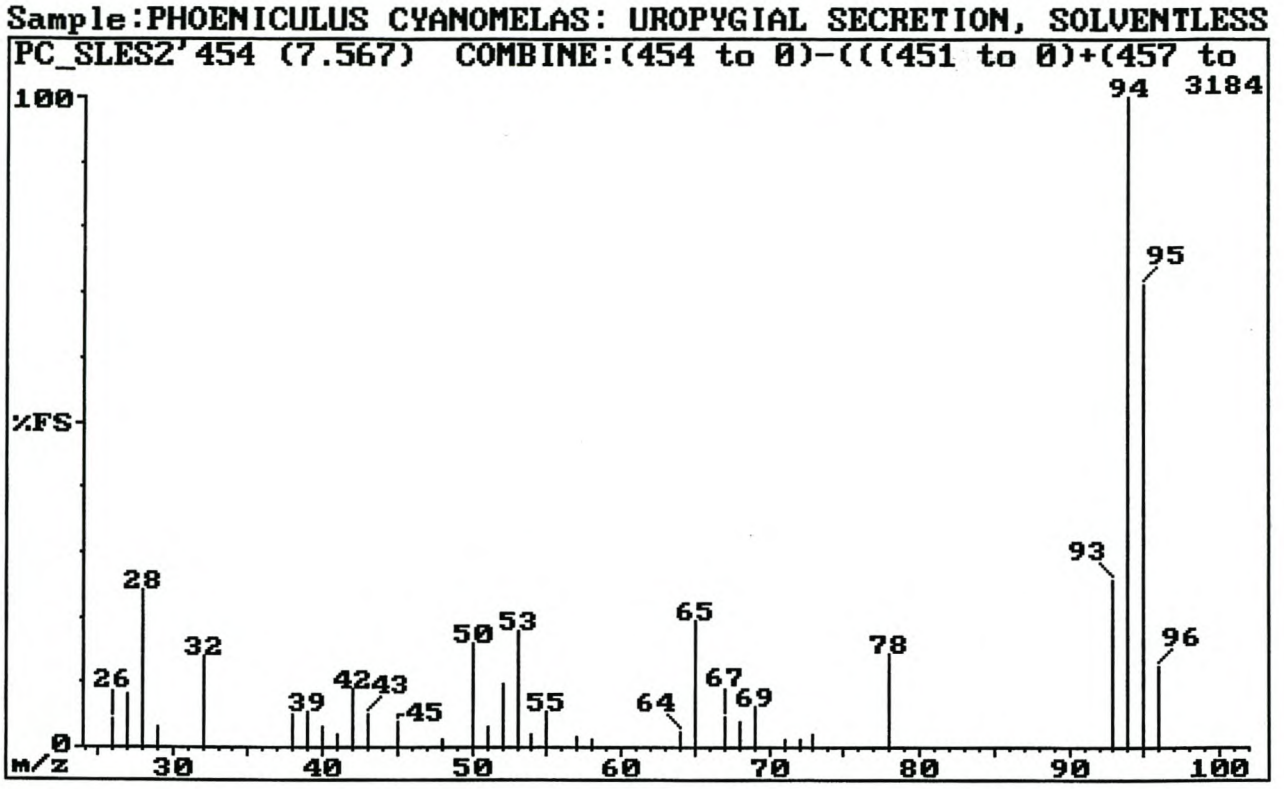

Fig 2.128: EI mass spectrum of component 454 (2,4-dimethyl-1H-pyrrole)

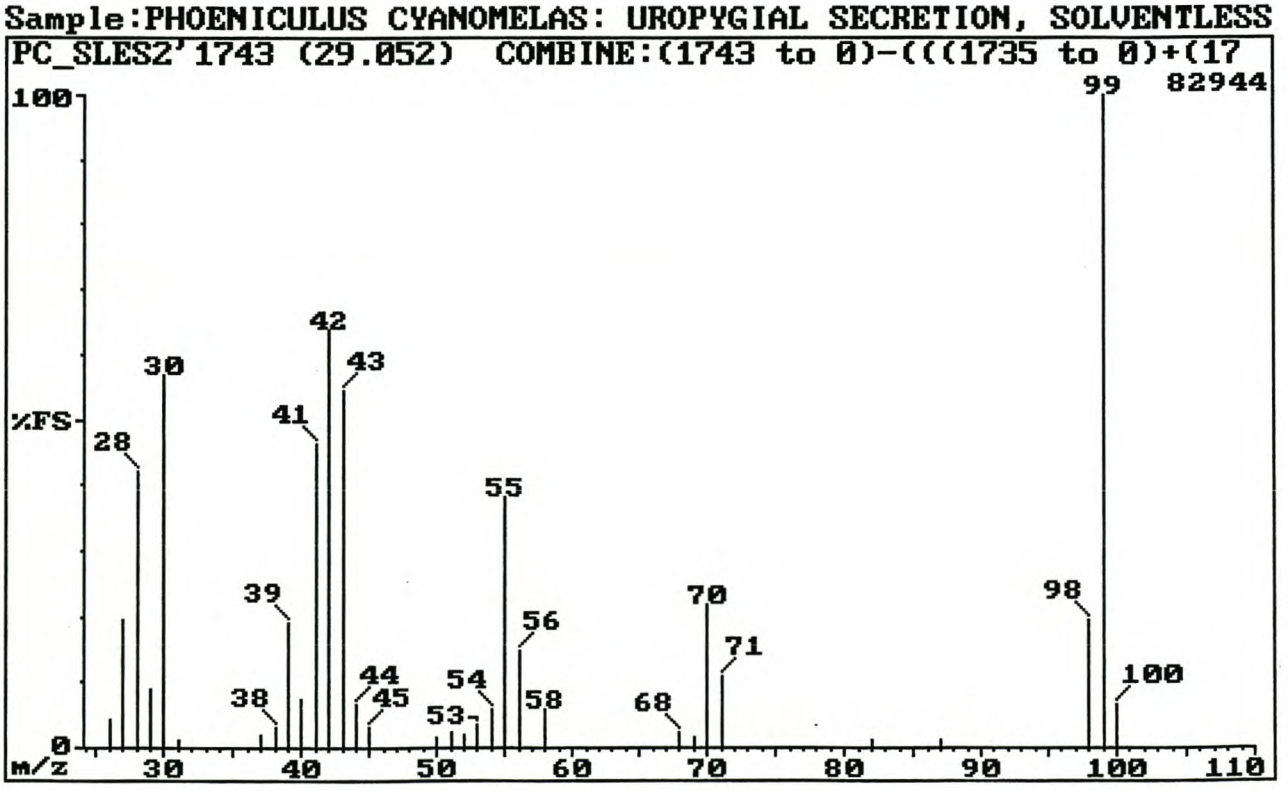

Fig 2.129: EI mass spectrum of component 1743 (2-piperidone)

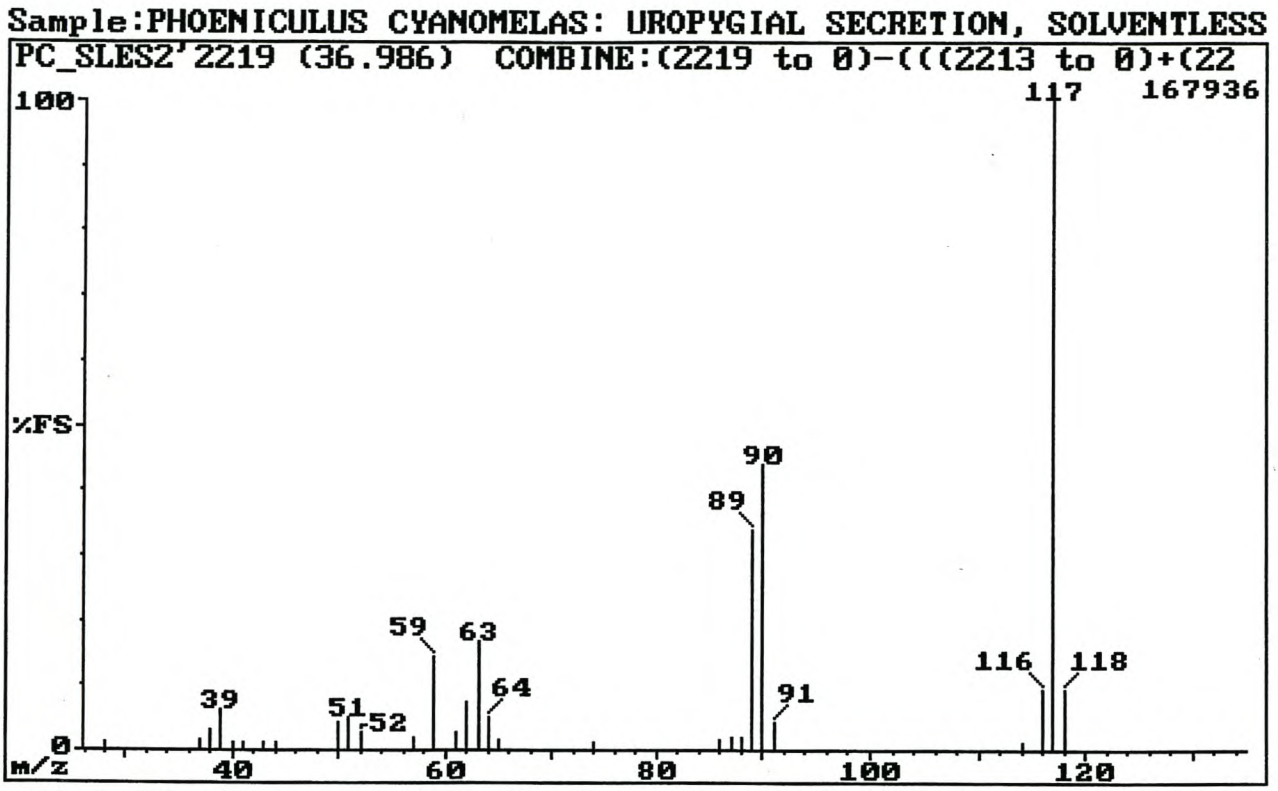

Fig 2.130: EI mass spectrum of component 2219 (1H-indole)

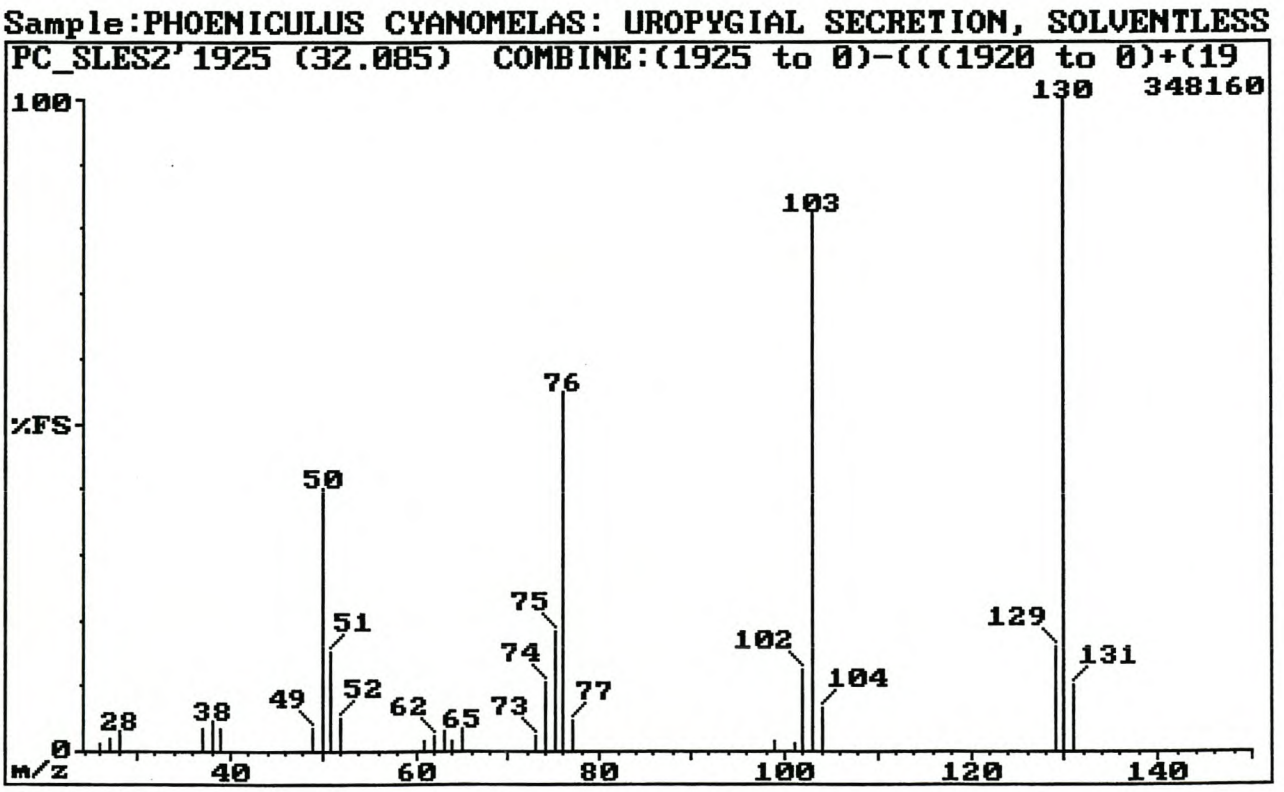

Fig 2.131: EI mass spectrum of component 1925 (quinoxaline)

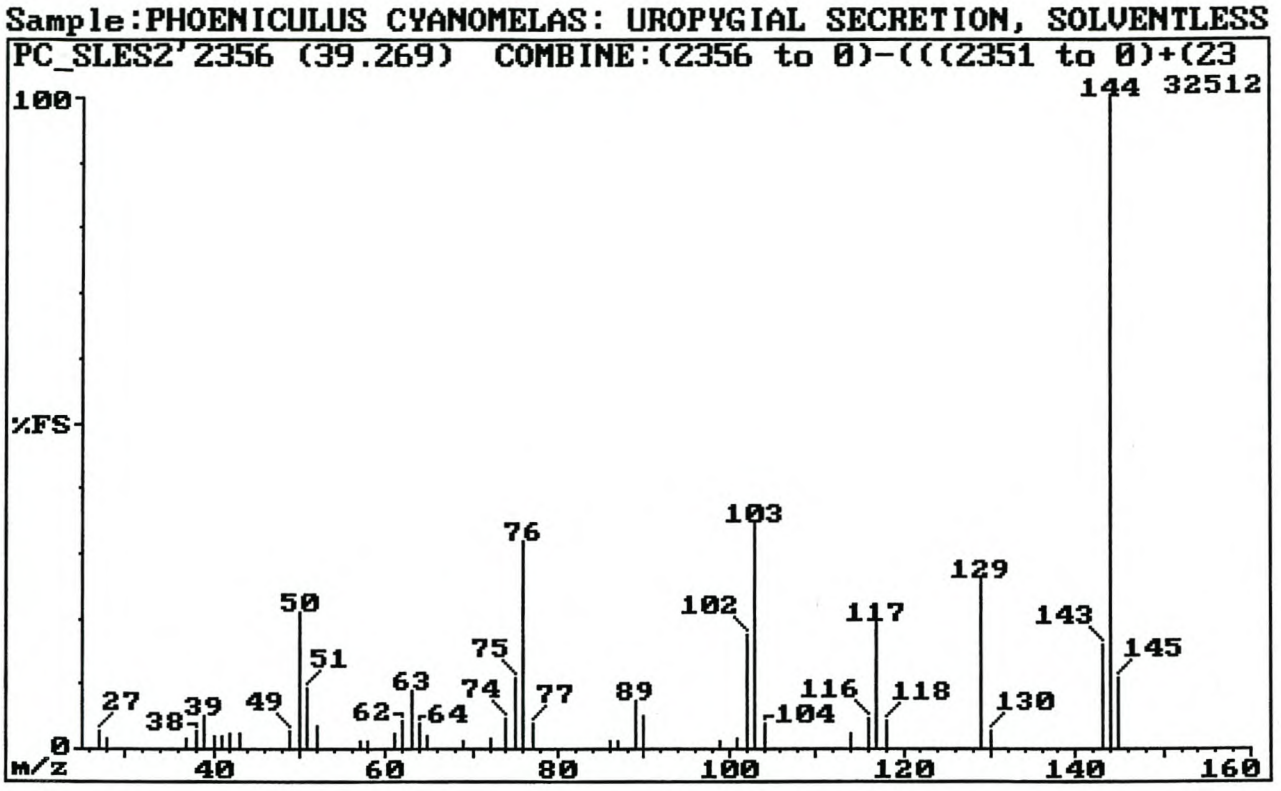

Fig 2.132: EI mass spectrum of component 2356 (4-methylquinazoline)

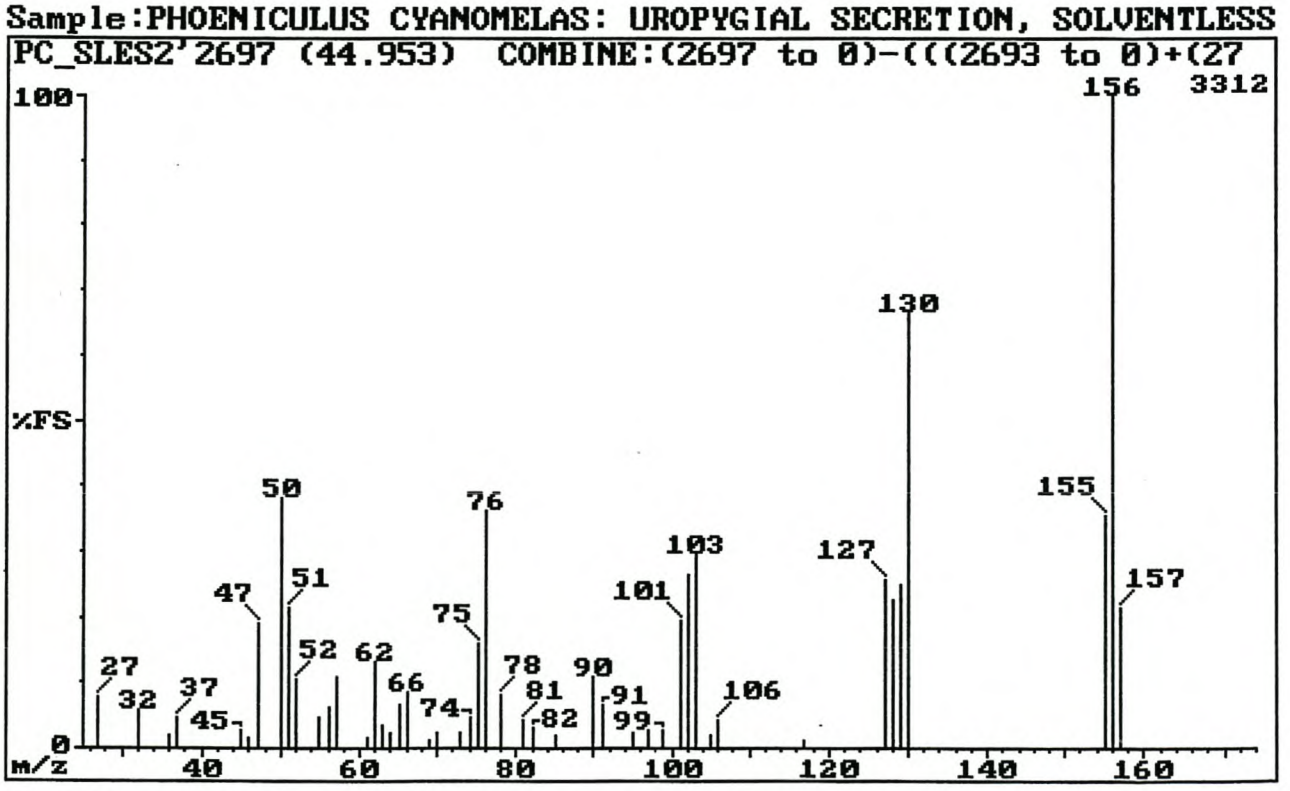

Fig 2.133: EI mass spectrum of component 2697 (4,4-bipyridine)

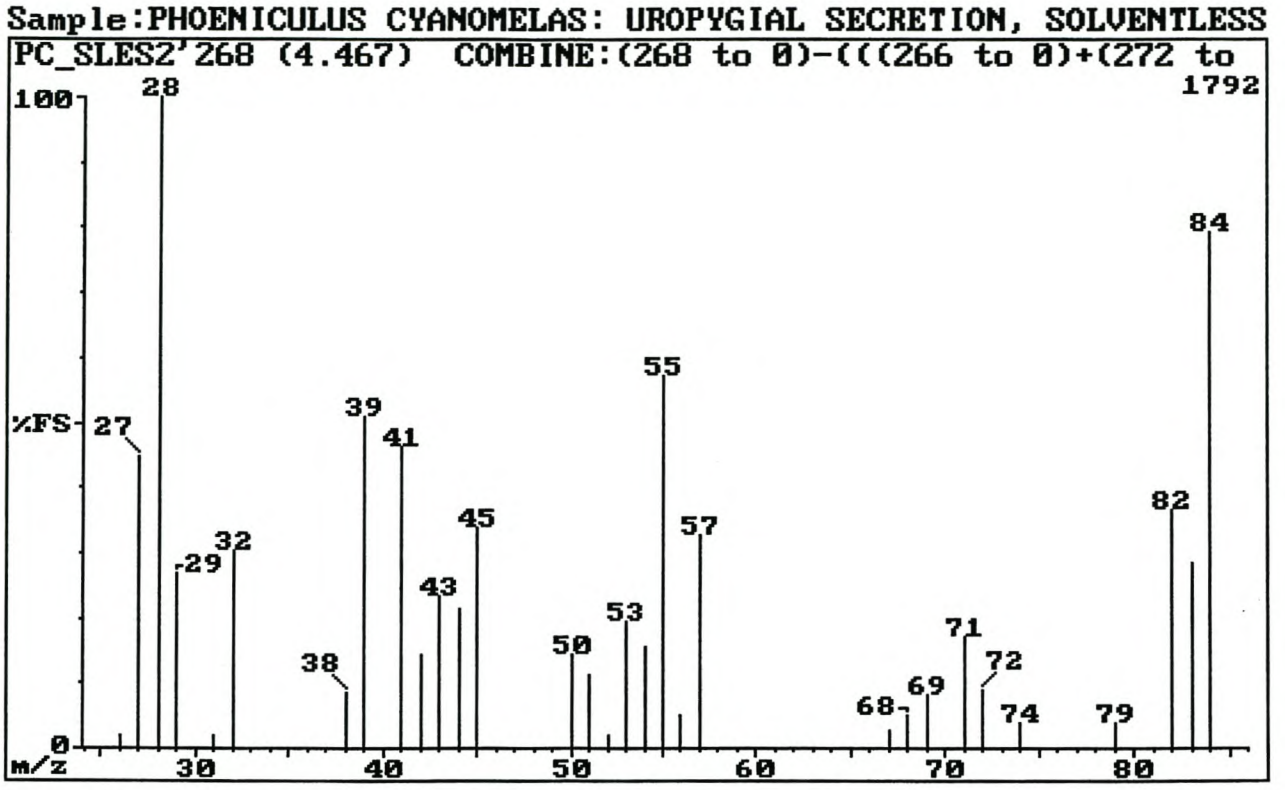

Fig 2.134: EI mass spectrum of component 268 (3,4-dihydro-2H-pyran)

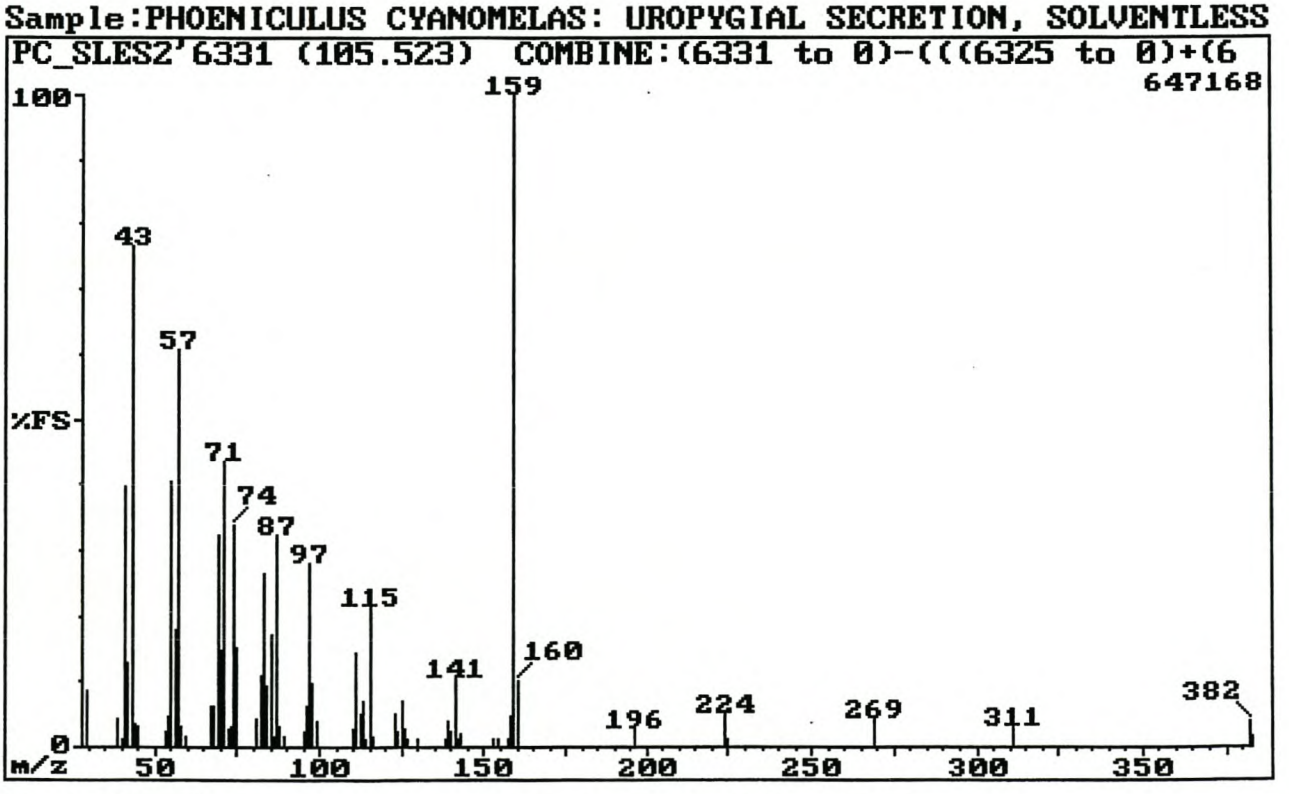

Fig 2.135: EI mass spectrum of component 6331 [25(9;16)]

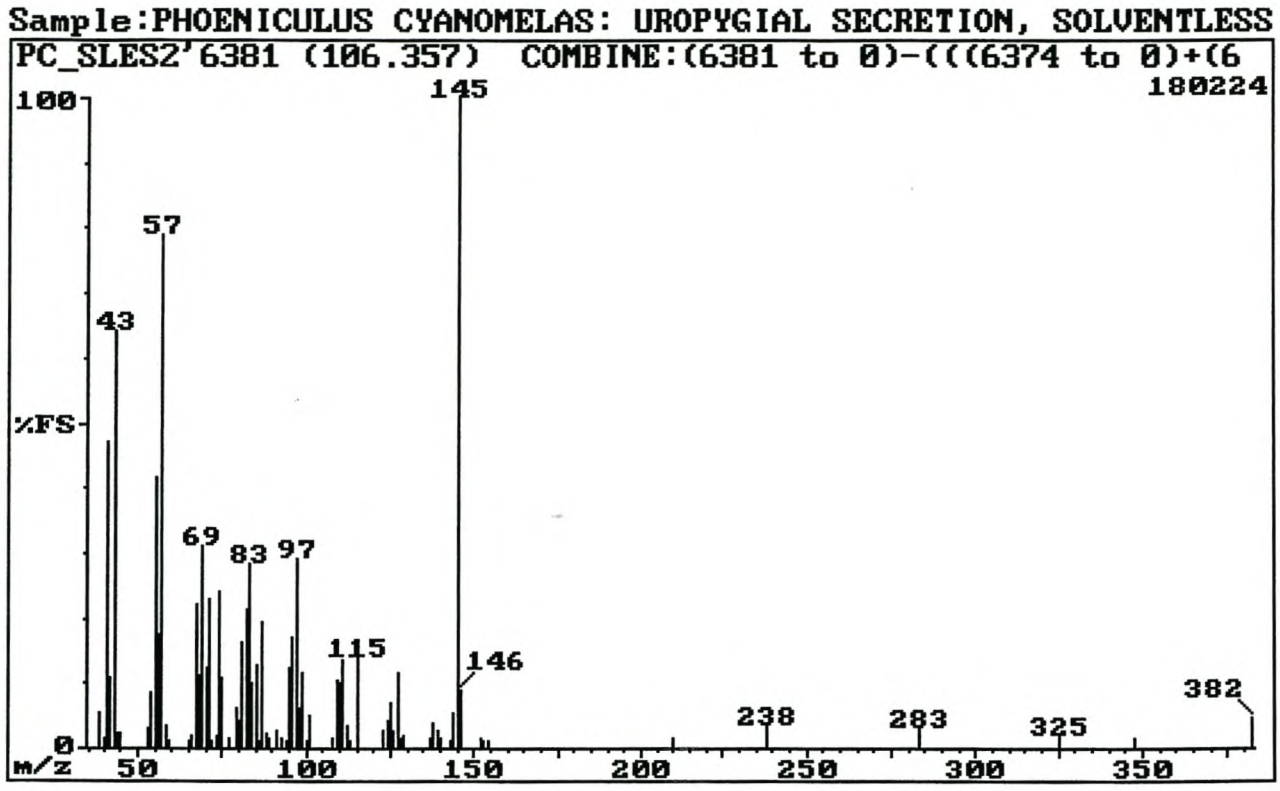

Fig 2.136: EI mass spectrum of component 6381 [25(8;17)]

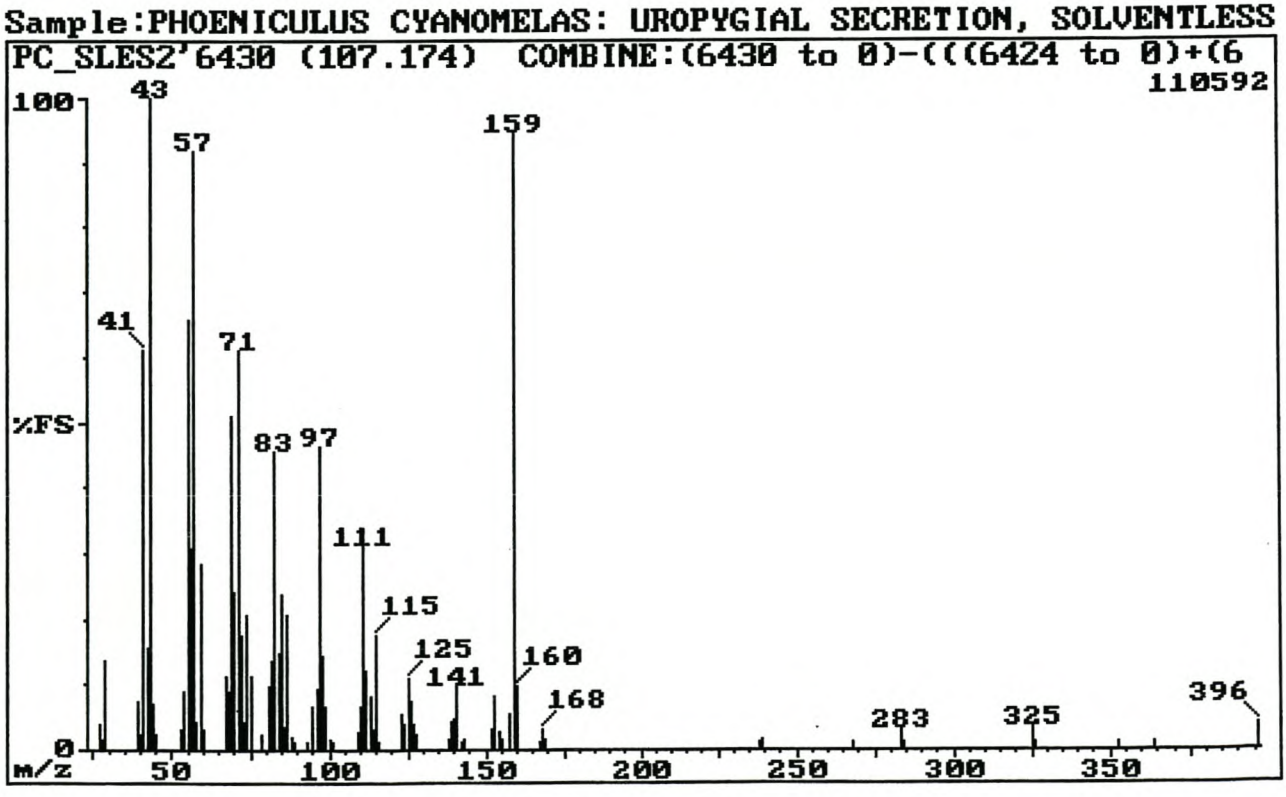

Fig 2.137: EI mass spectrum of component 6430 [26(9;17)]

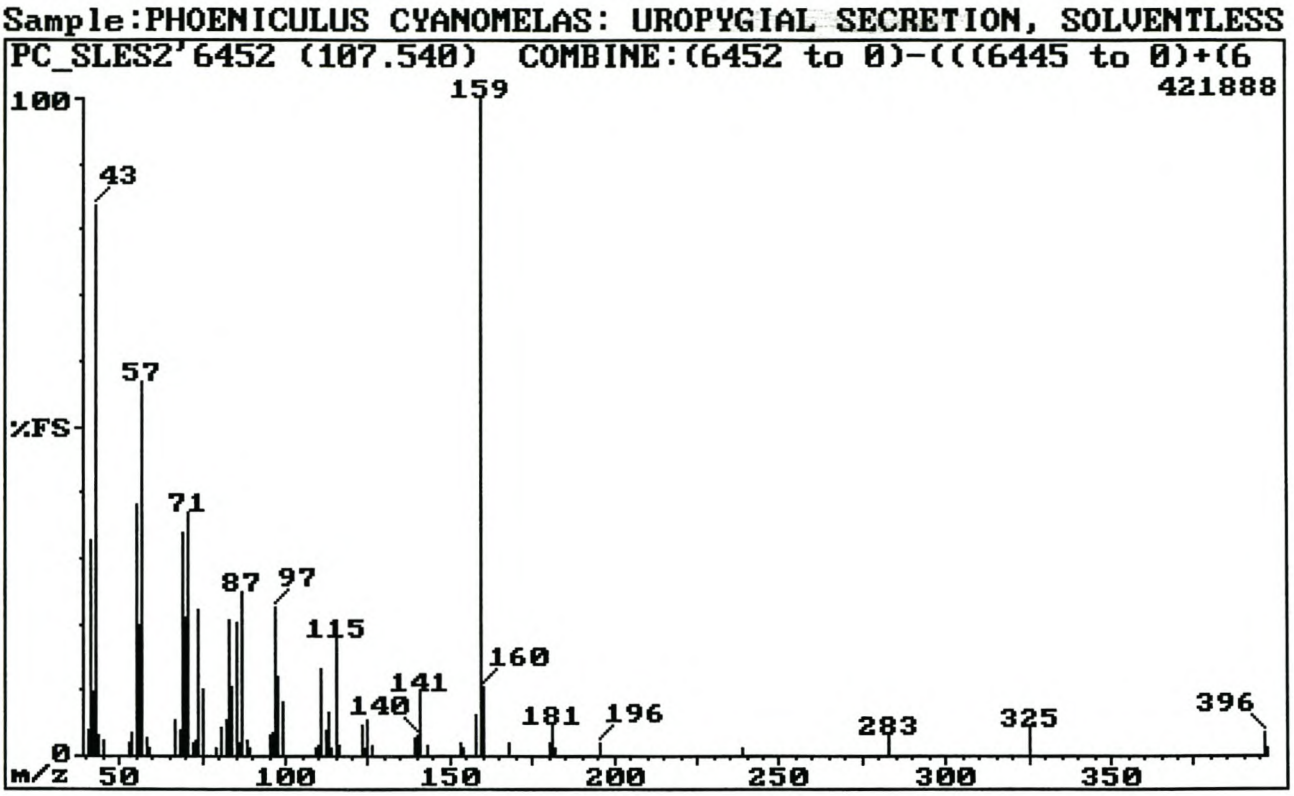

Fig 2.138: EI mass spectrum of component 6452 [26(9;17)]

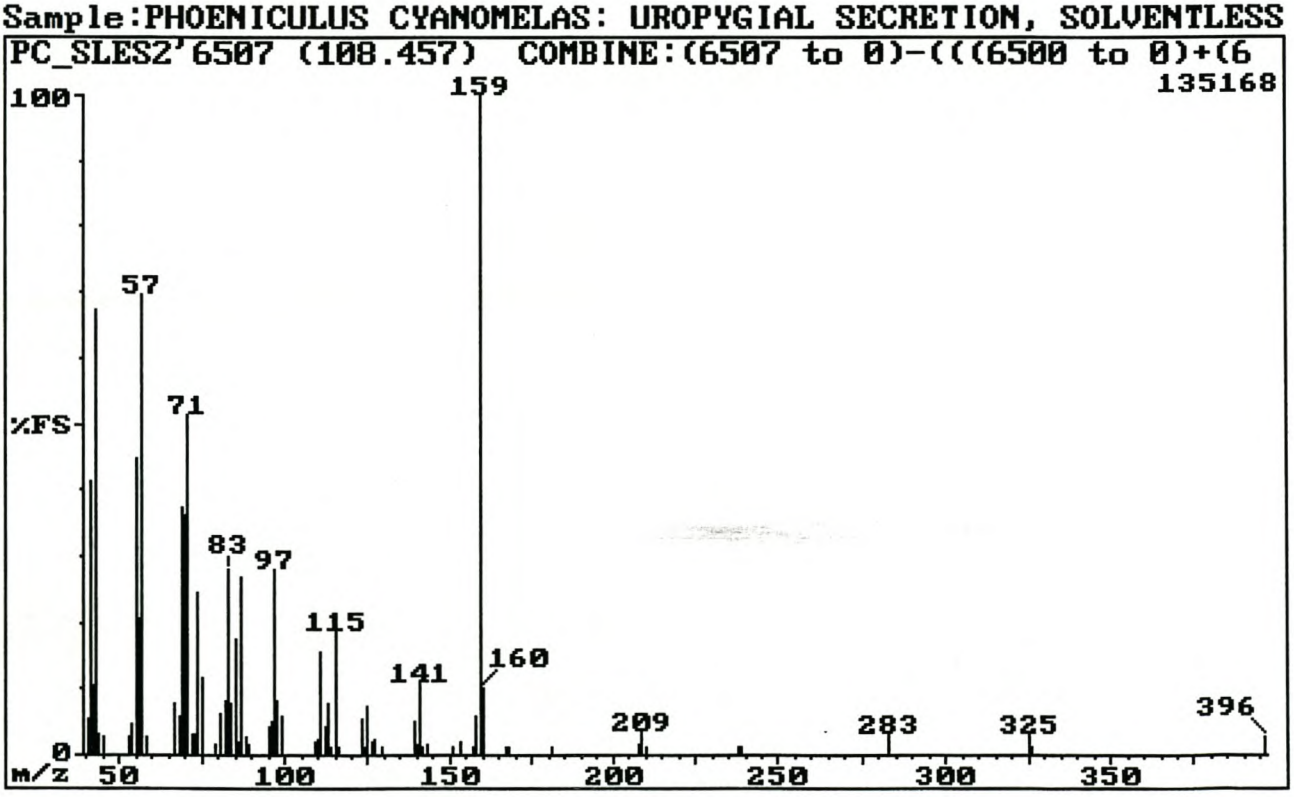

Fig 2.139: EI mass spectrum of component 6507 [26(9;17)]

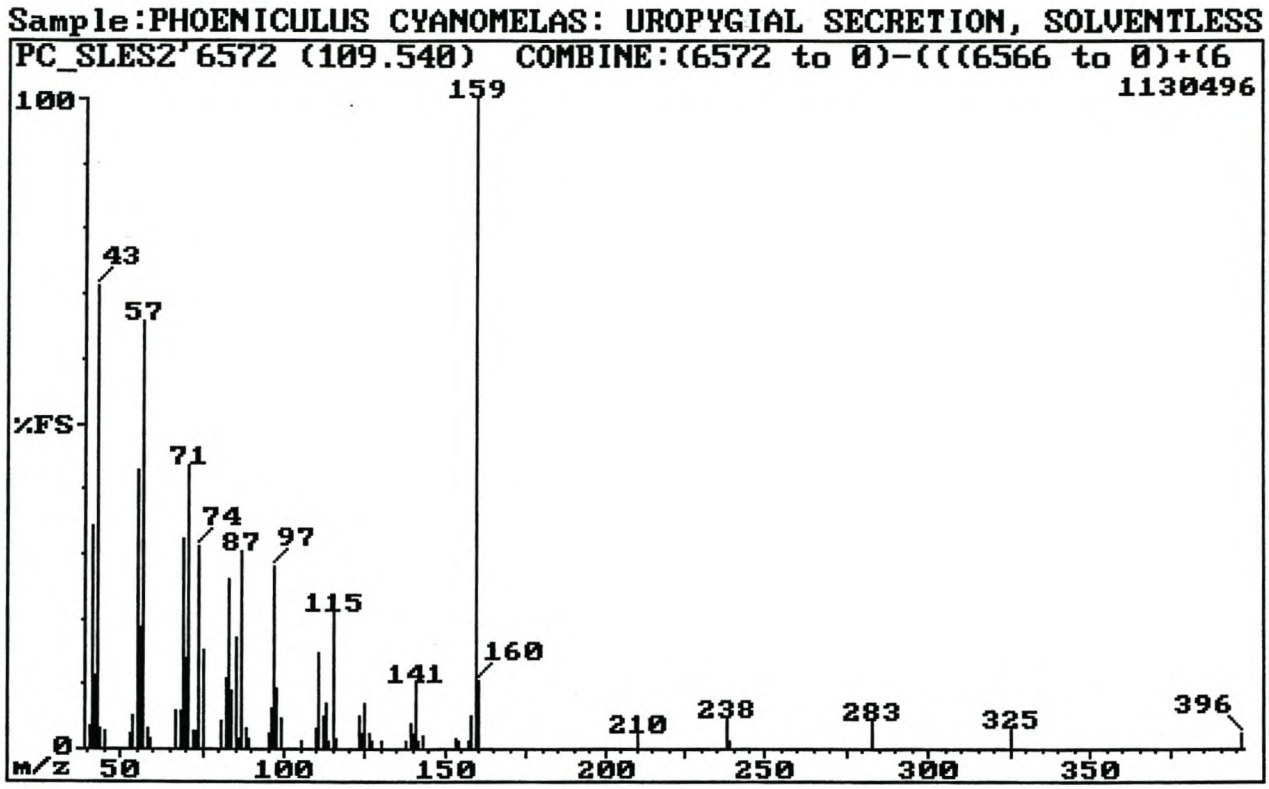

Fig 2.140: EI mass spectrum of component 6572 [26(9;17)]

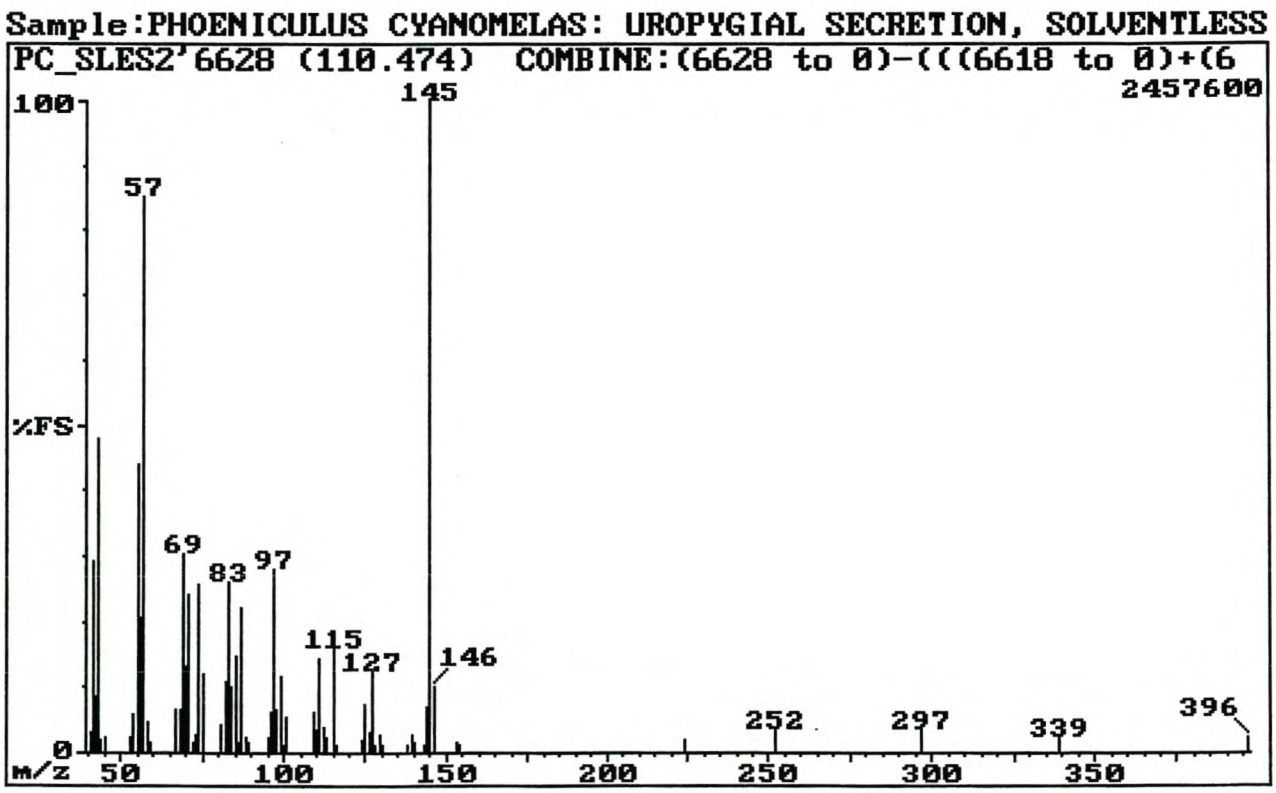

Fig 2.141: EI mass spectrum of component 6628 [26(8;18)]

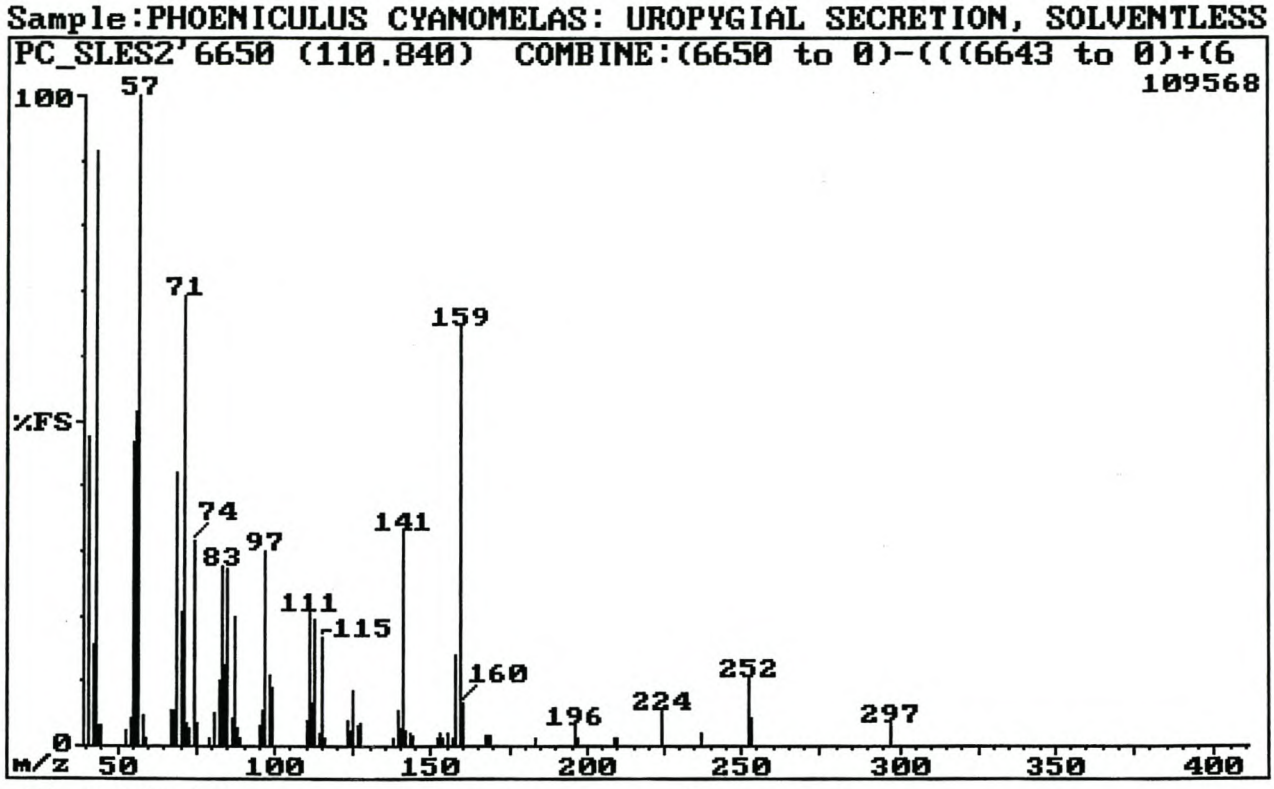

Fig 2.142: EI mass spectrum of component 6650 [27(9;18)]

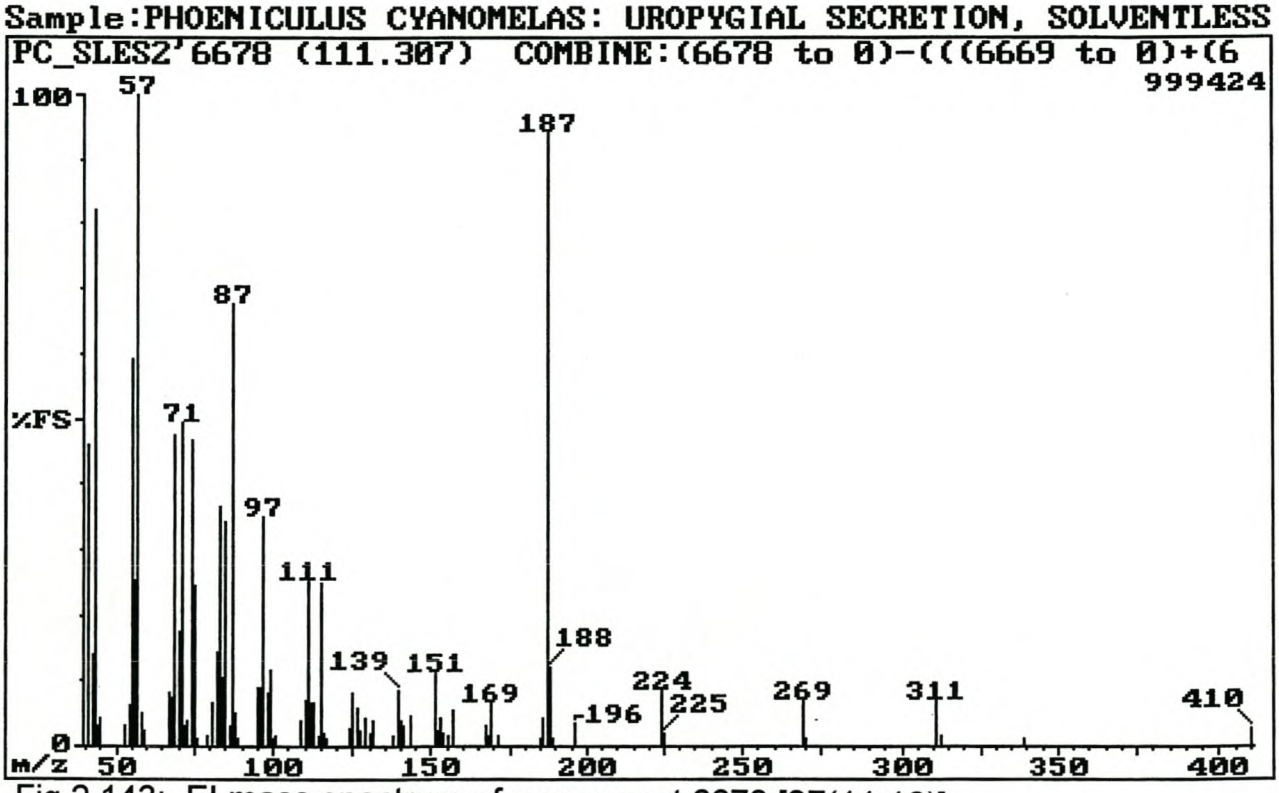

Fig 2.143: EI mass spectrum of component 6678 [27(11;16)]

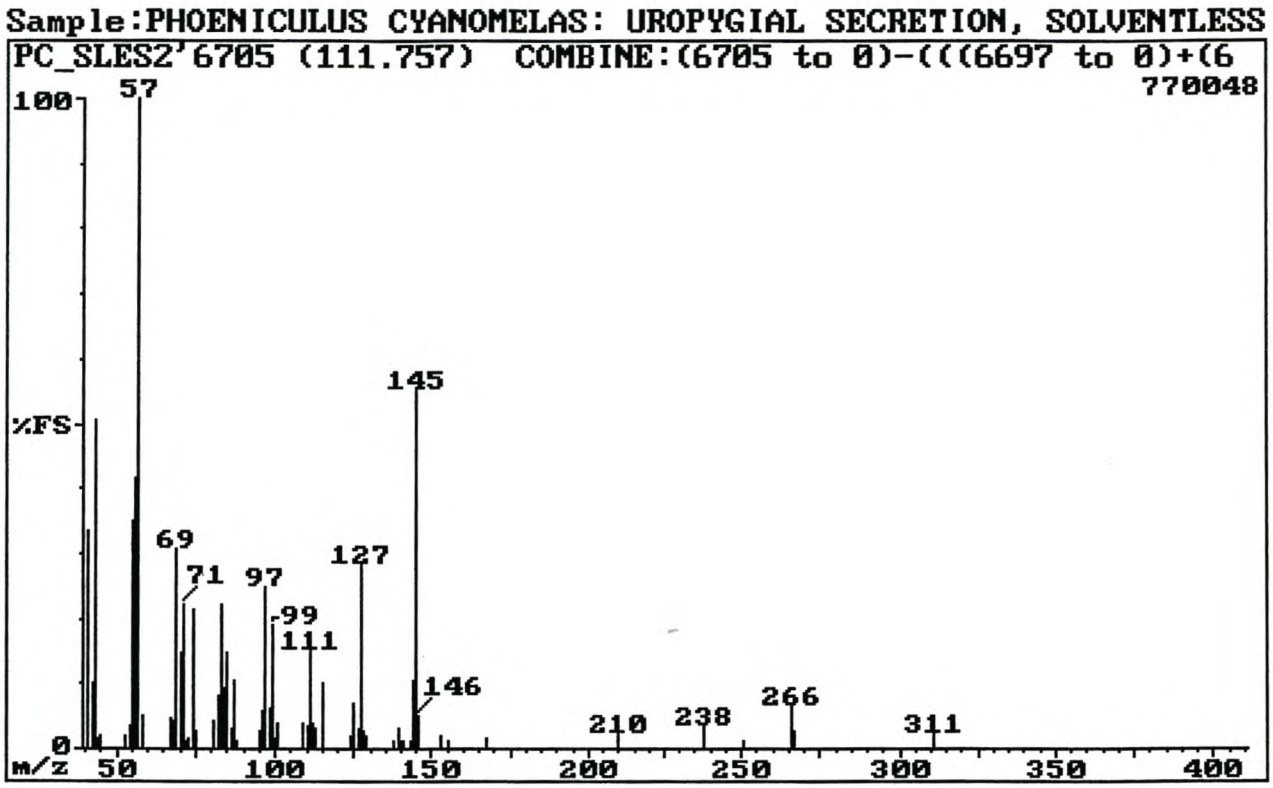

Fig 2.144: EI mass spectrum of component 6705 [27(8;19)]

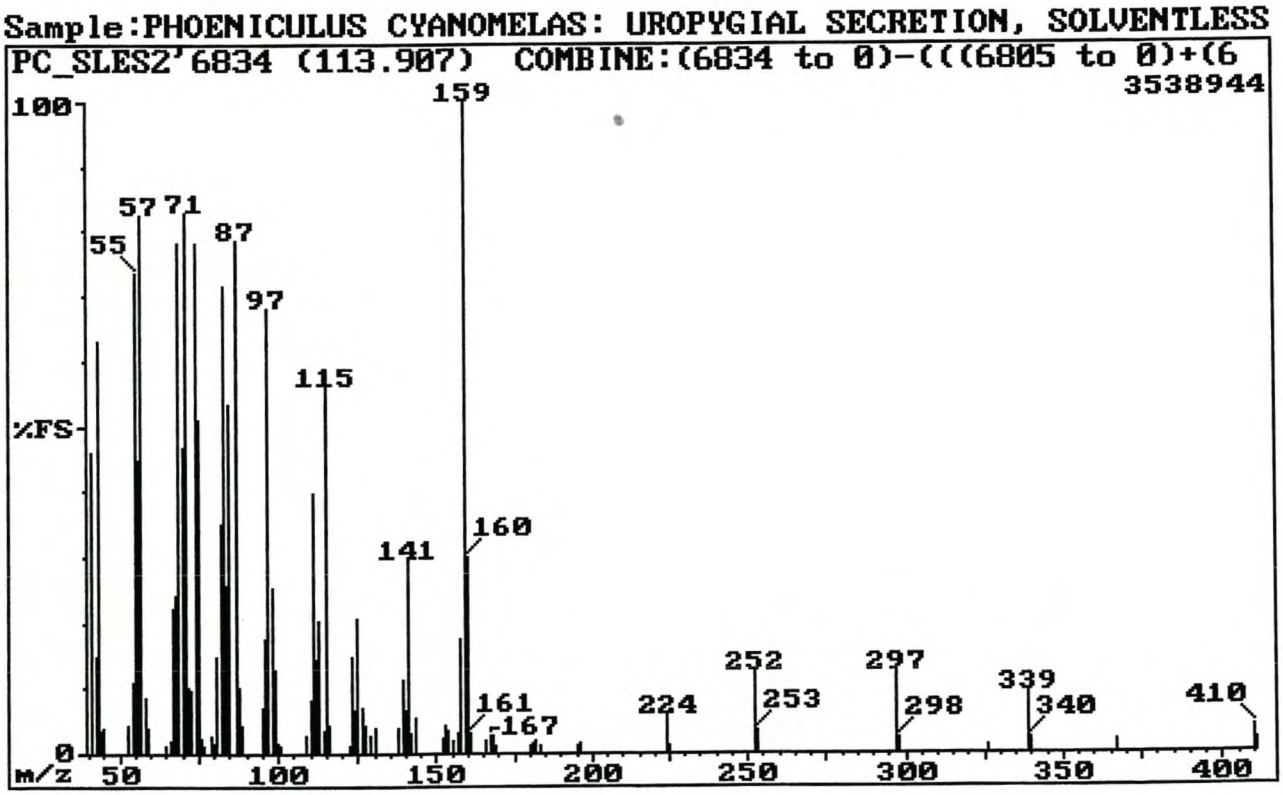

Fig 2.145: EI mass spectrum of component 6834 [27(9;18)]

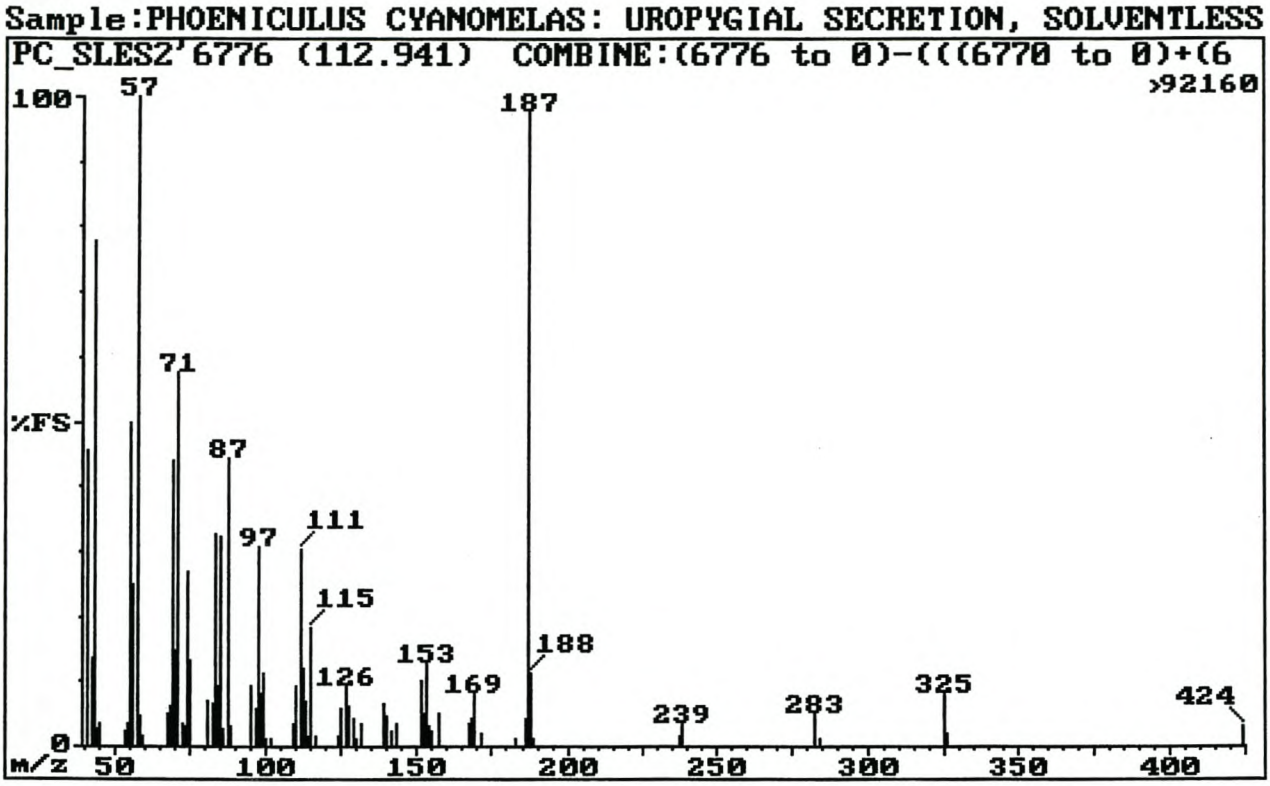

Fig 2.146: EI mass spectrum of component 6776 [28(11;17)]

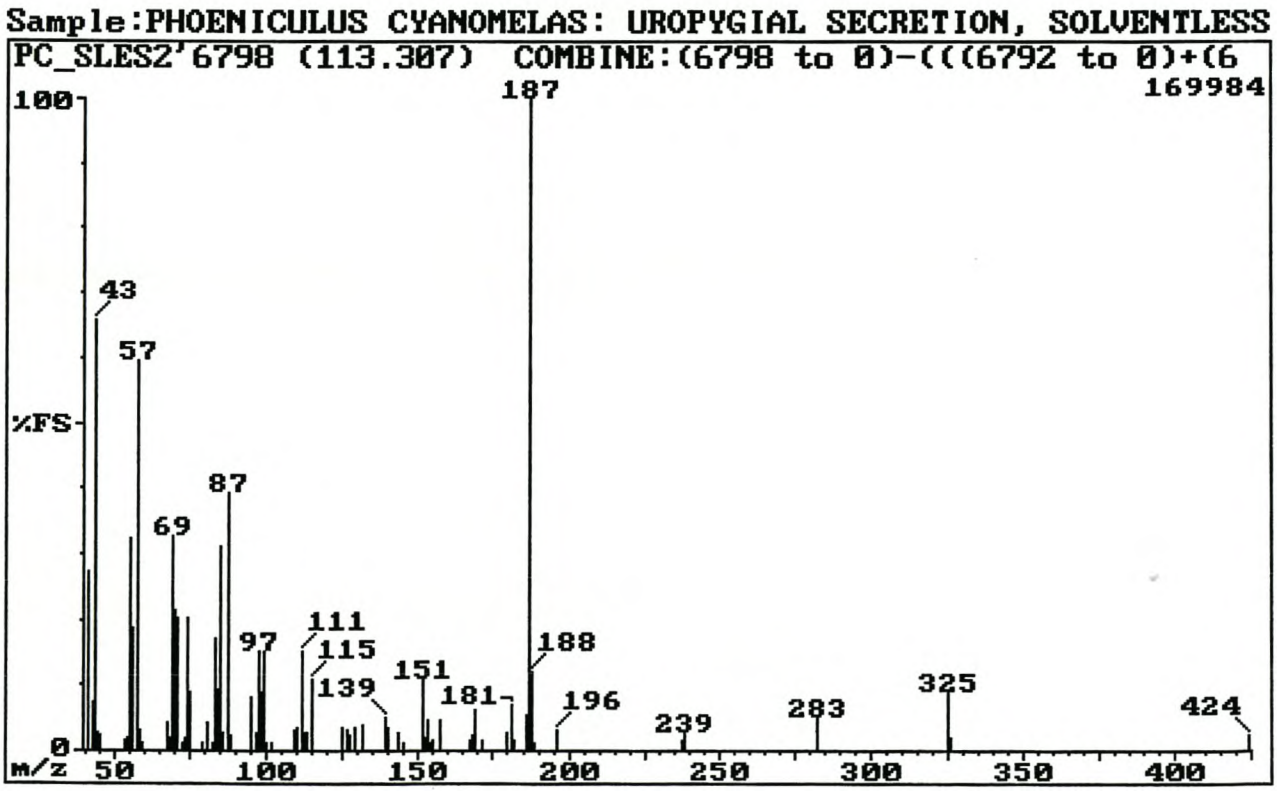

Fig 2.147: EI mass spectrum of component 6798 [28(11;17)]

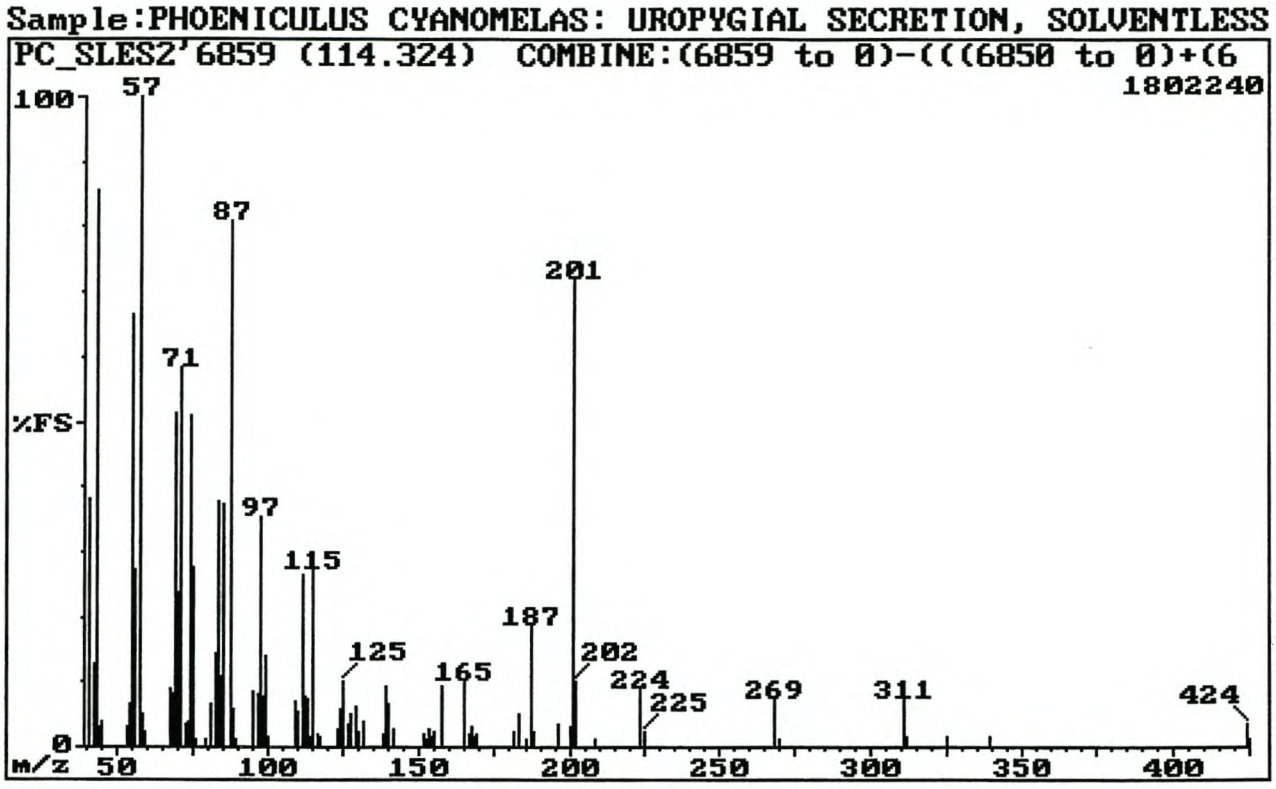

Fig 2.148: EI mass spectrum of component 6859 [28(11;17), 28(12;16)]

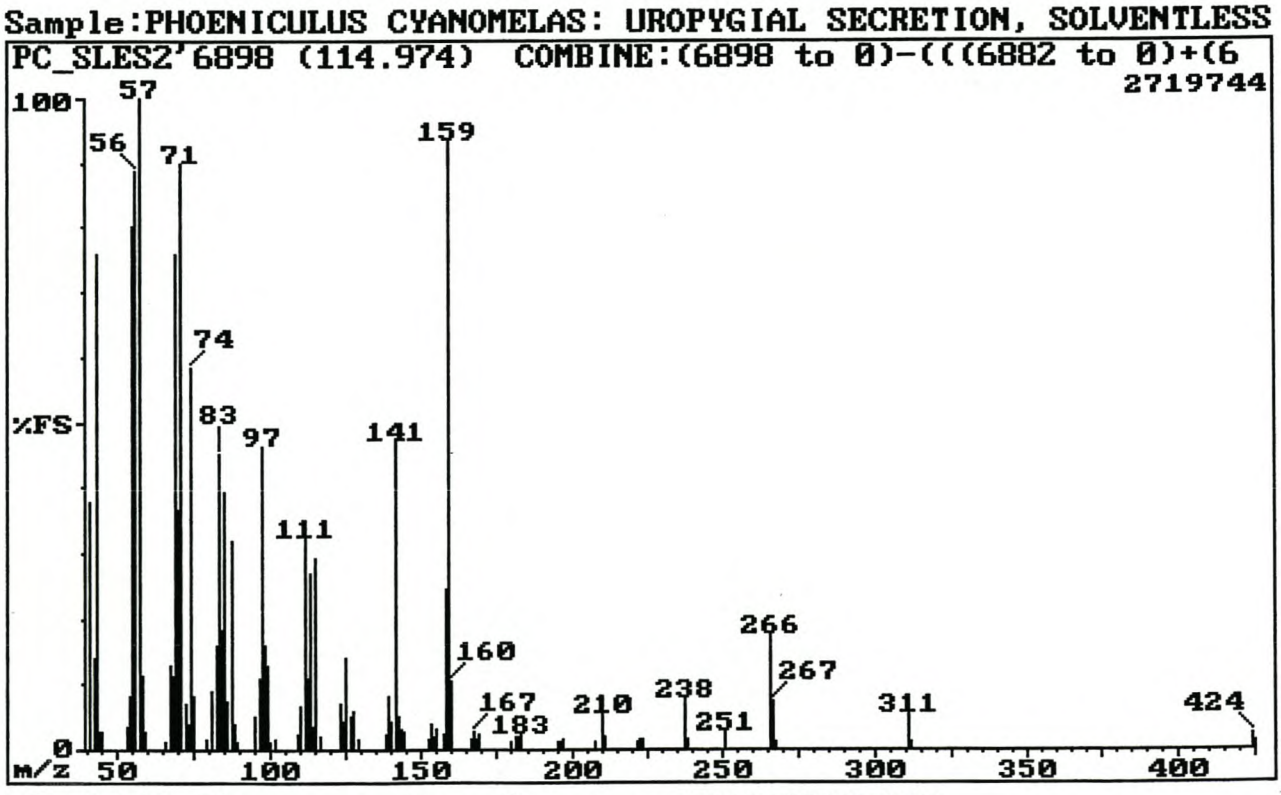

Fig 2.149: EI mass spectrum of component 6898 [28(9;19)]

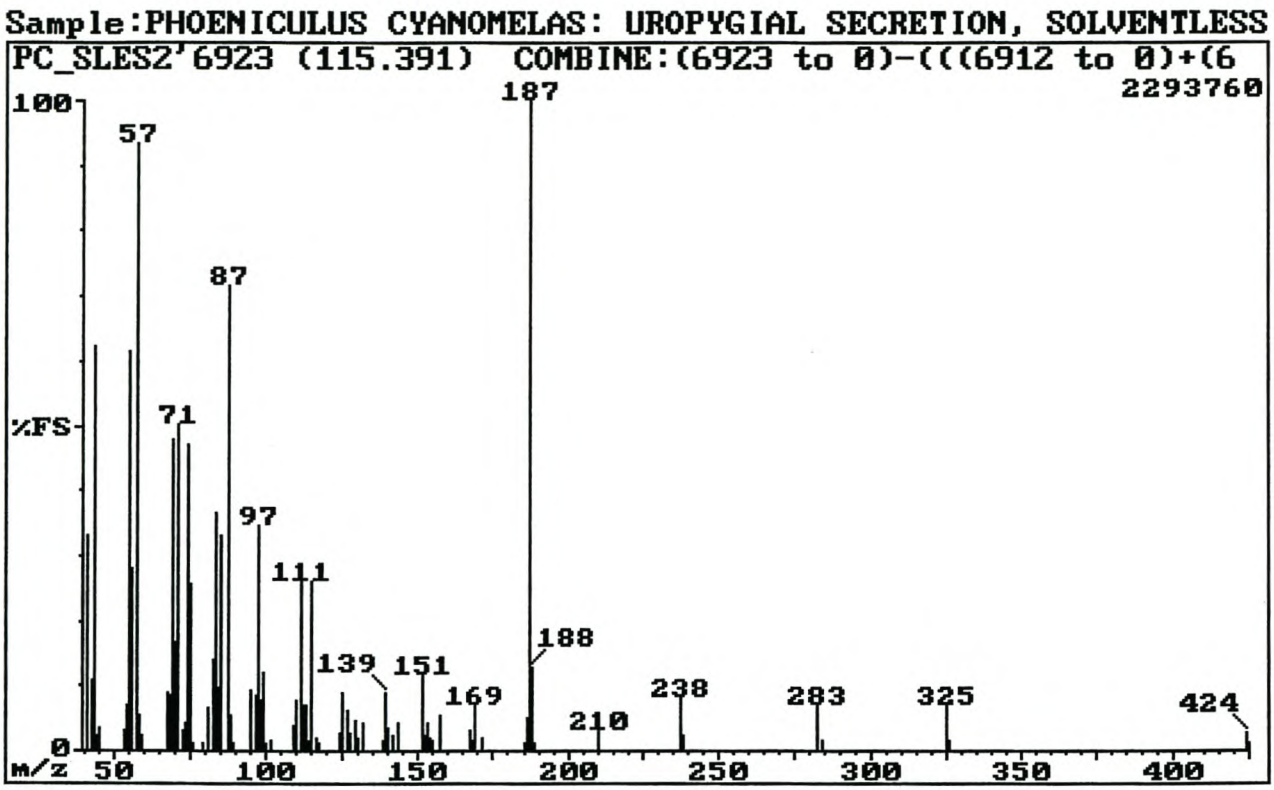

Fig 2.150: EI mass spectrum of component 6923 [28(11;17)]

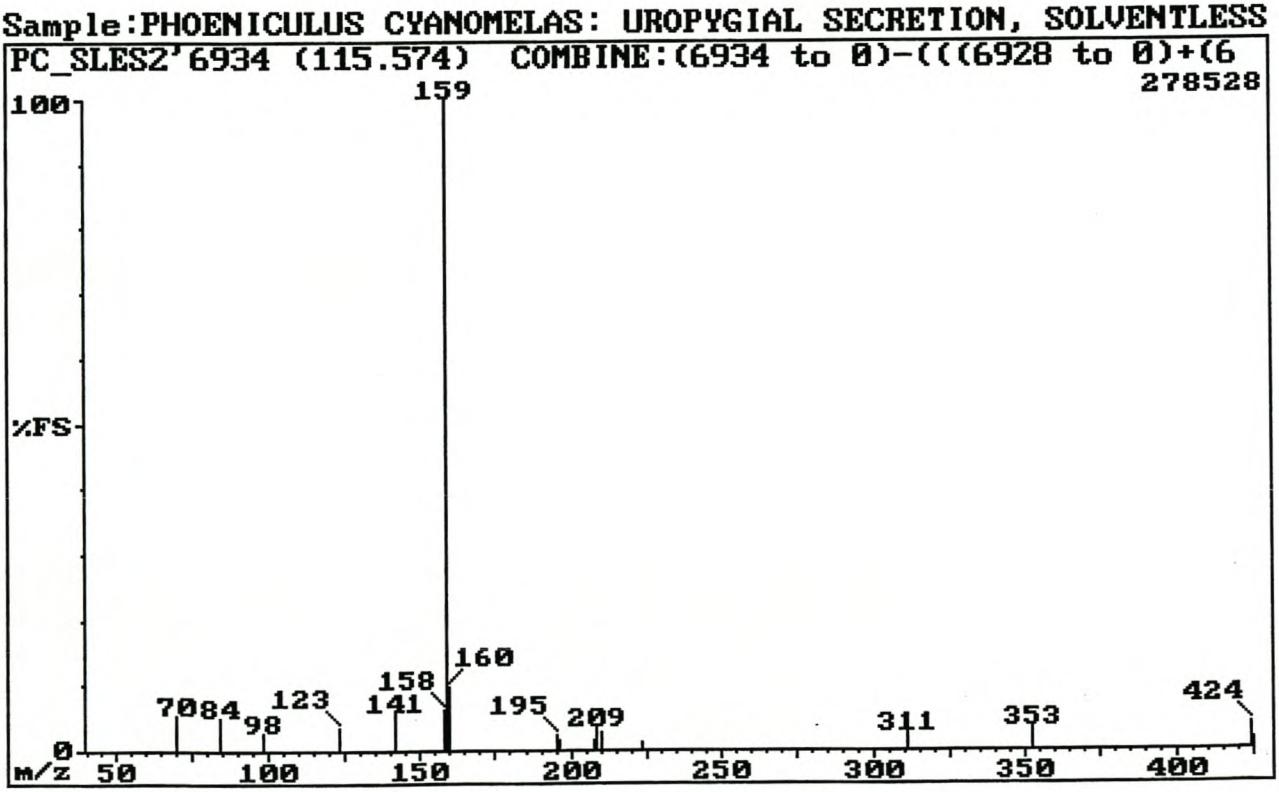

Fig 2.151: EI mass spectrum of component 6934 [28(9;19)]

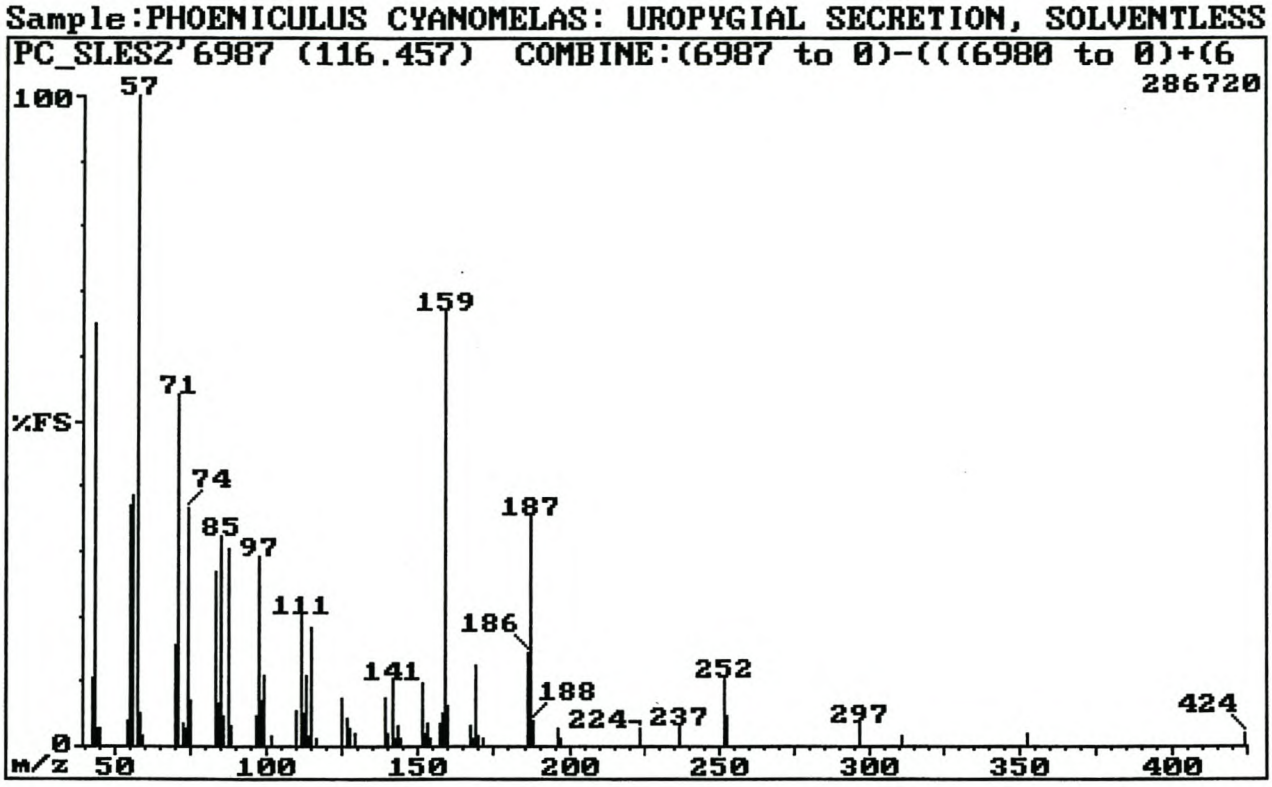

Fig 2.152: EI mass spectrum of component 6987 [28(9;19), 28(11;17)]

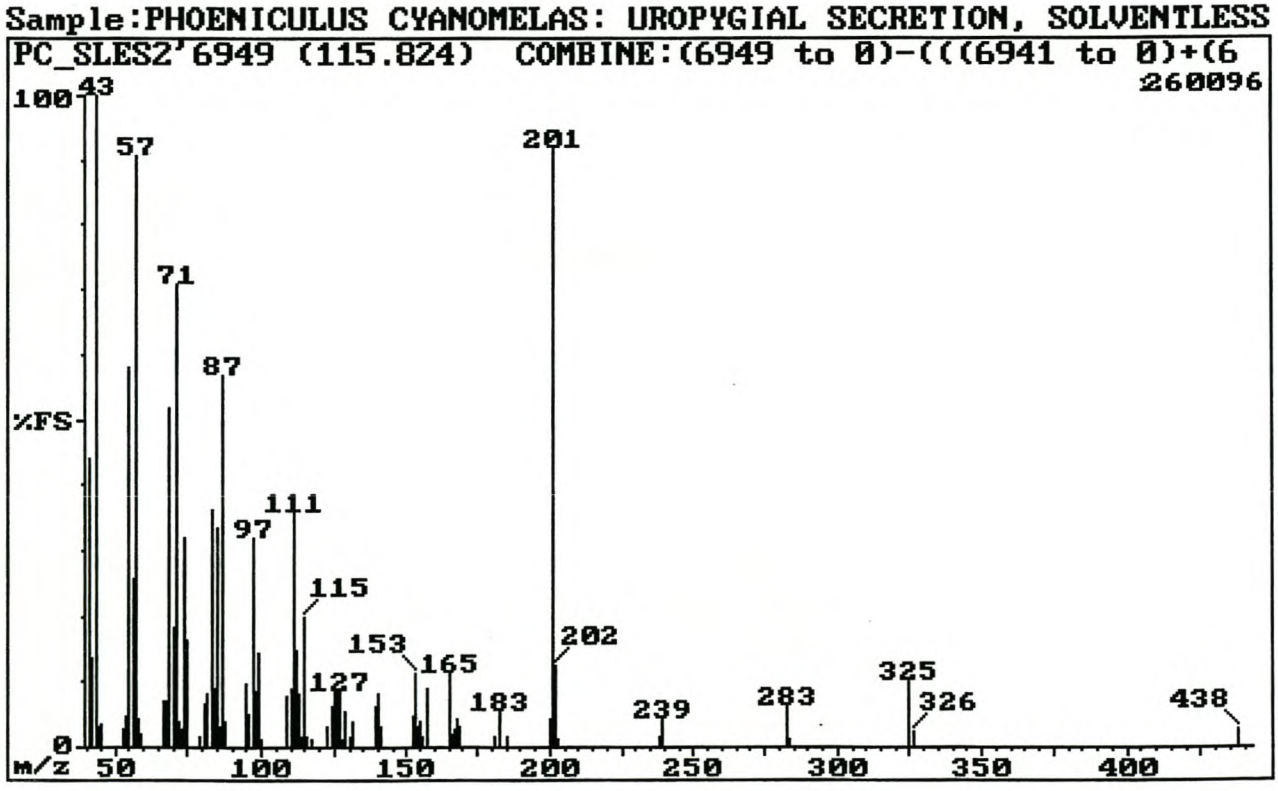

Fig 2.153: EI mass spectrum of component 6949 [29(12;17)]

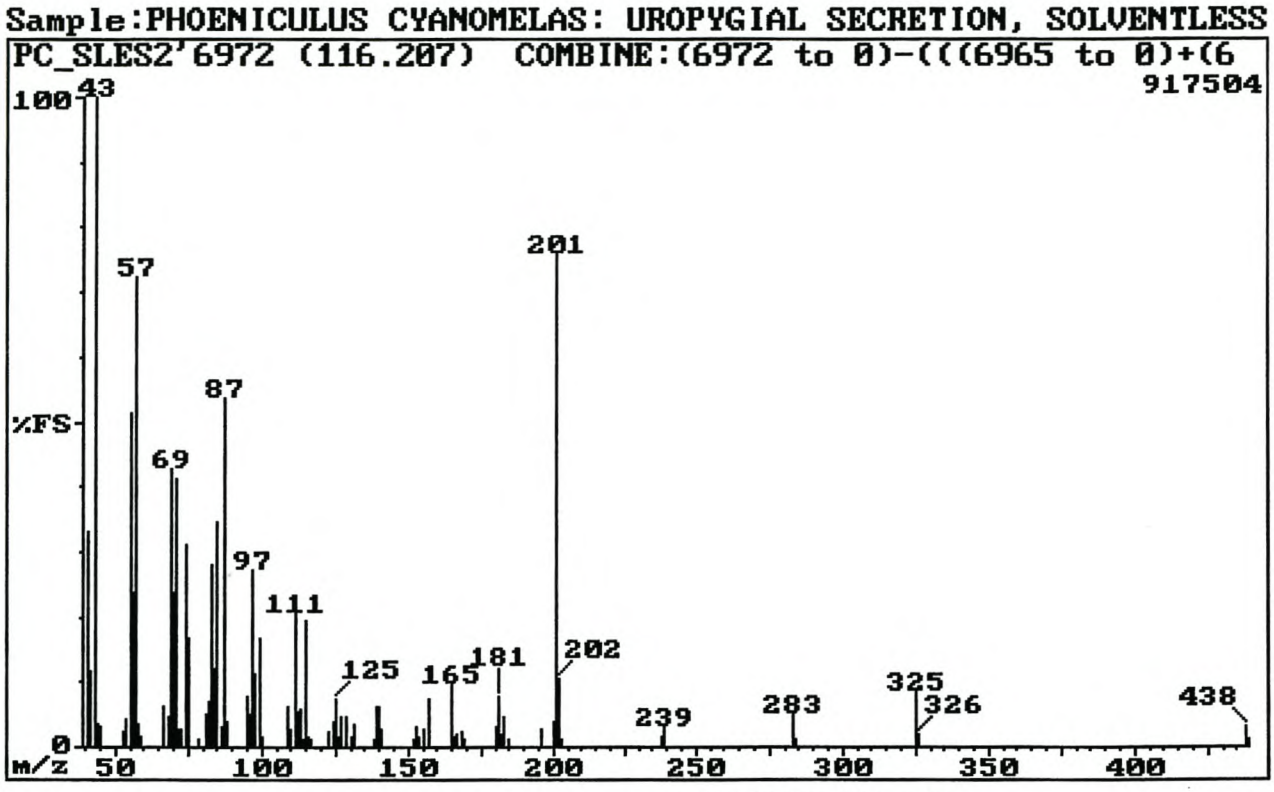

Fig 2.154: EI mass spectrum of component 6972 [29(12;17)]

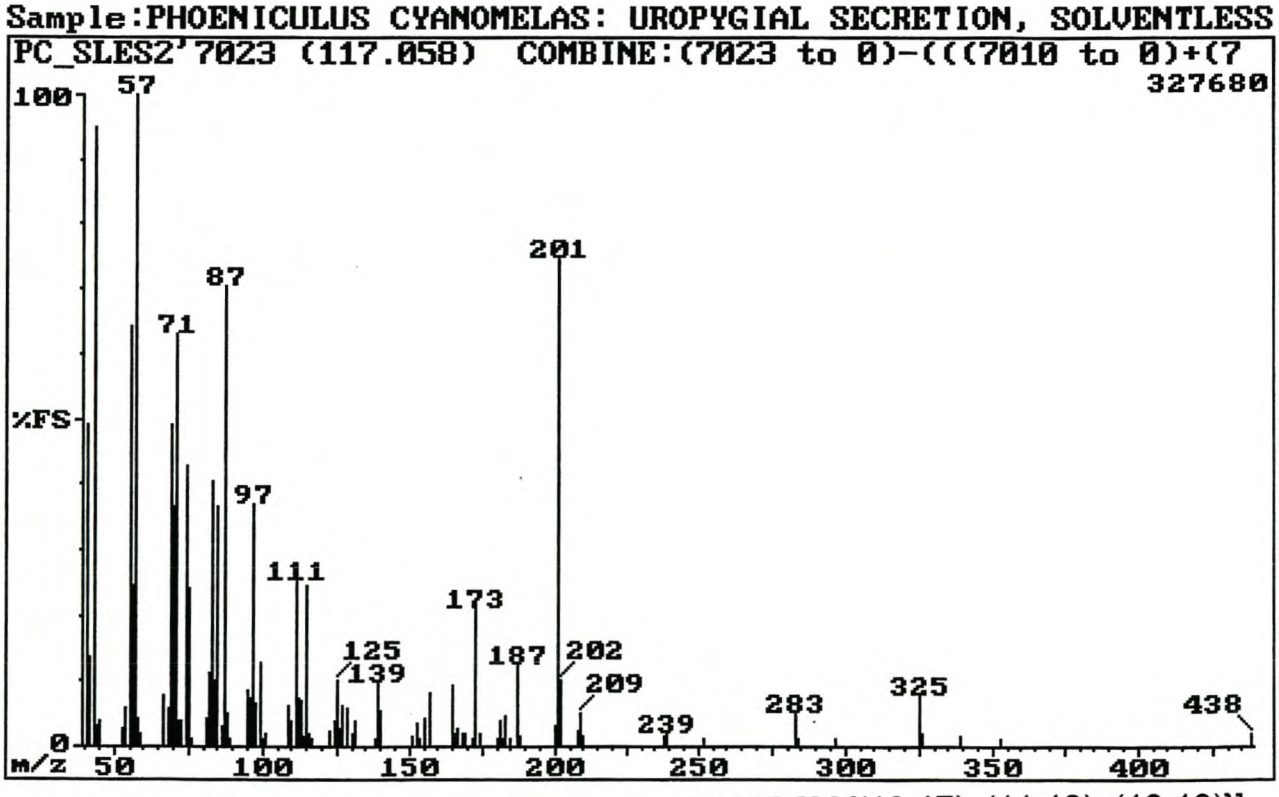

Fig 2.155: EI mass spectrum of component 7023 [29{(12;17), (11;18), (10;19)}]

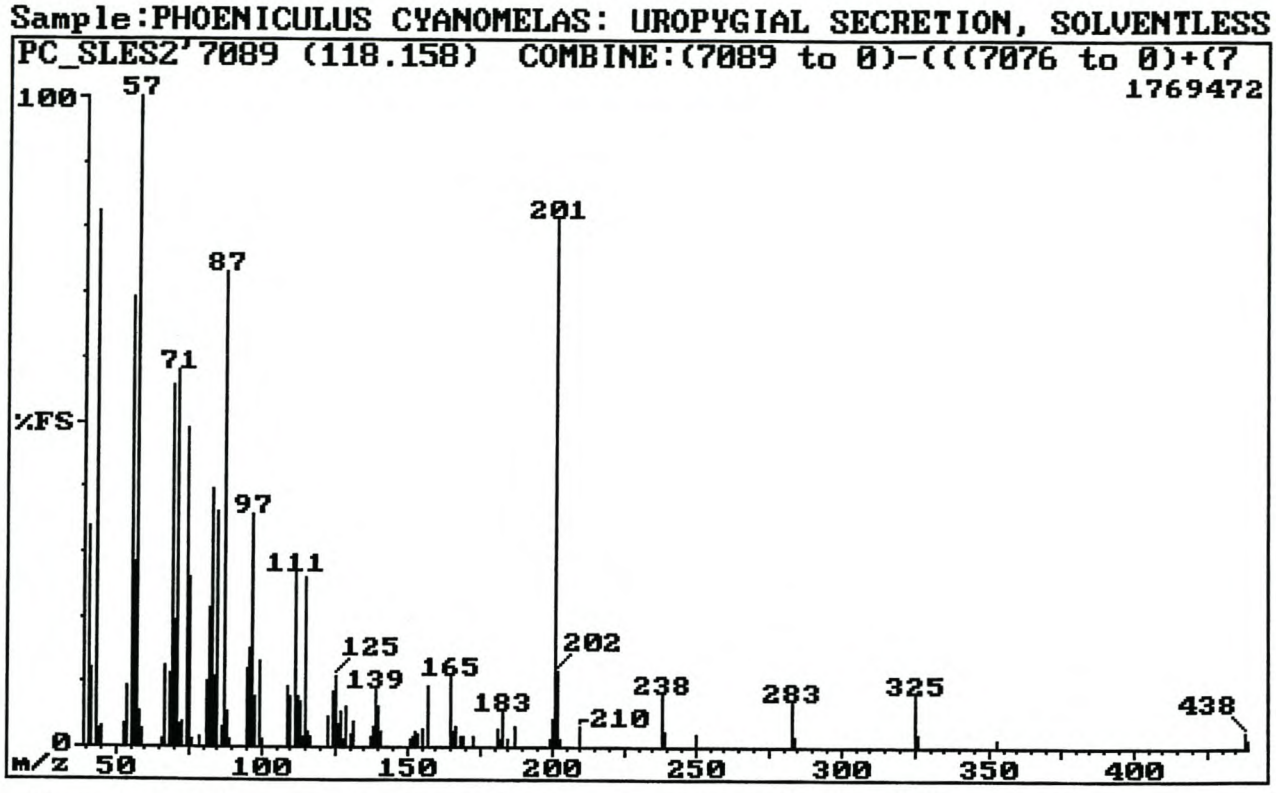

Fig 2.156: EI mass spectrum of component 7089 [29(12;17)]

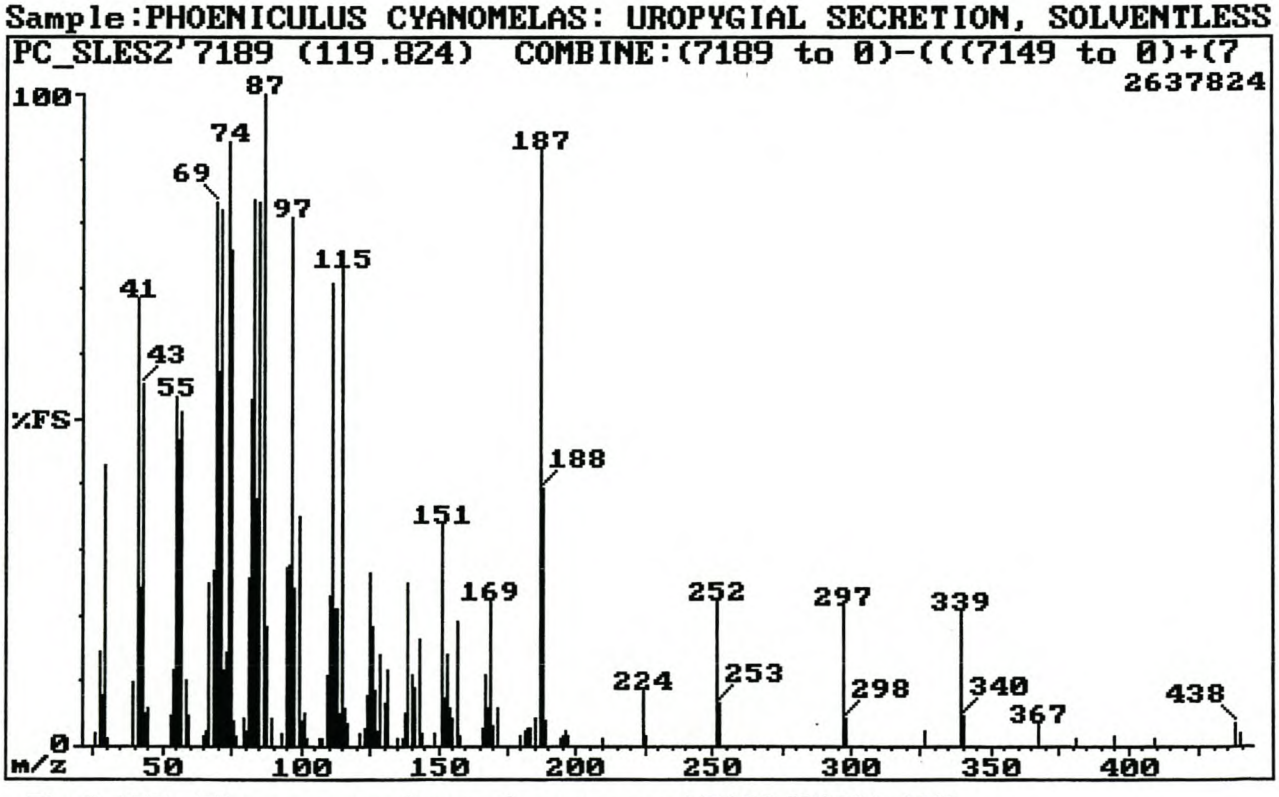

Fig 2.157: EI mass spectrum of component 7189 [29(11;18)]

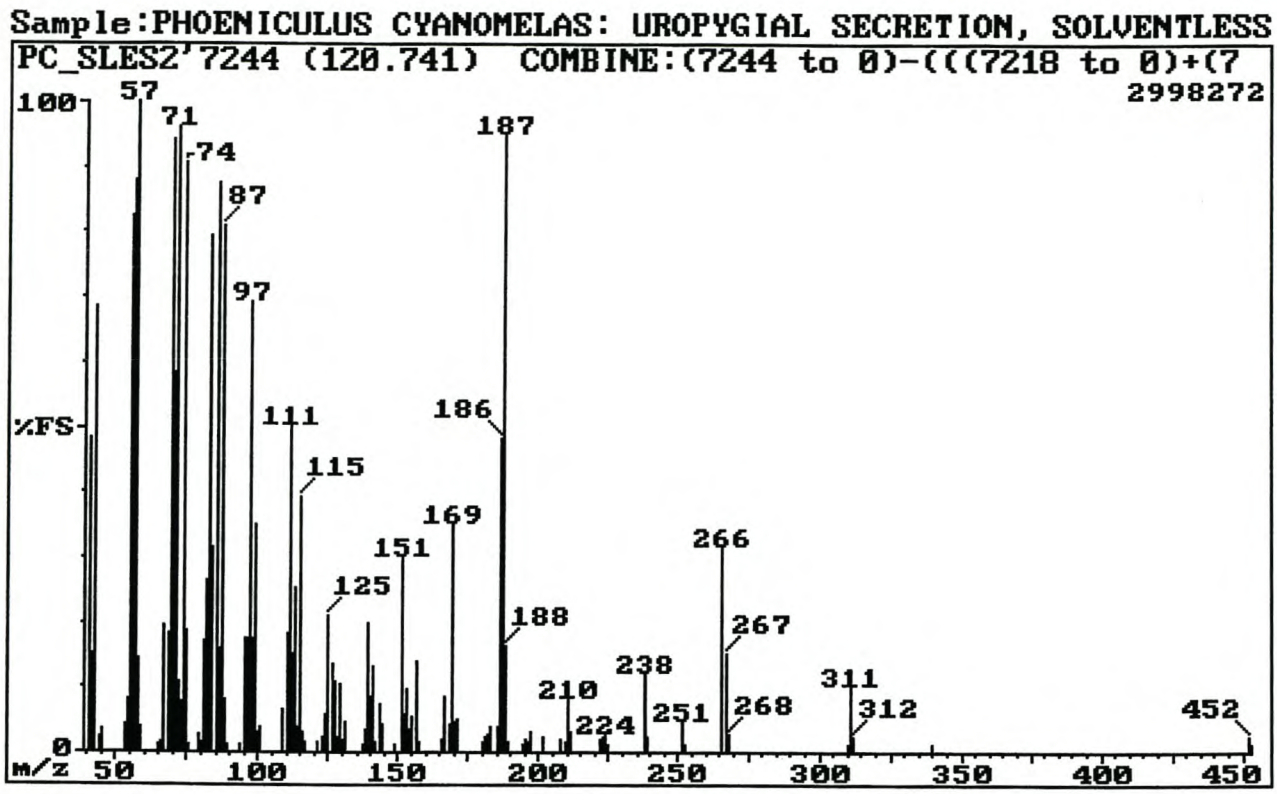

Fig 2.158: EI mass spectrum of component 7244 [30(11;19)]

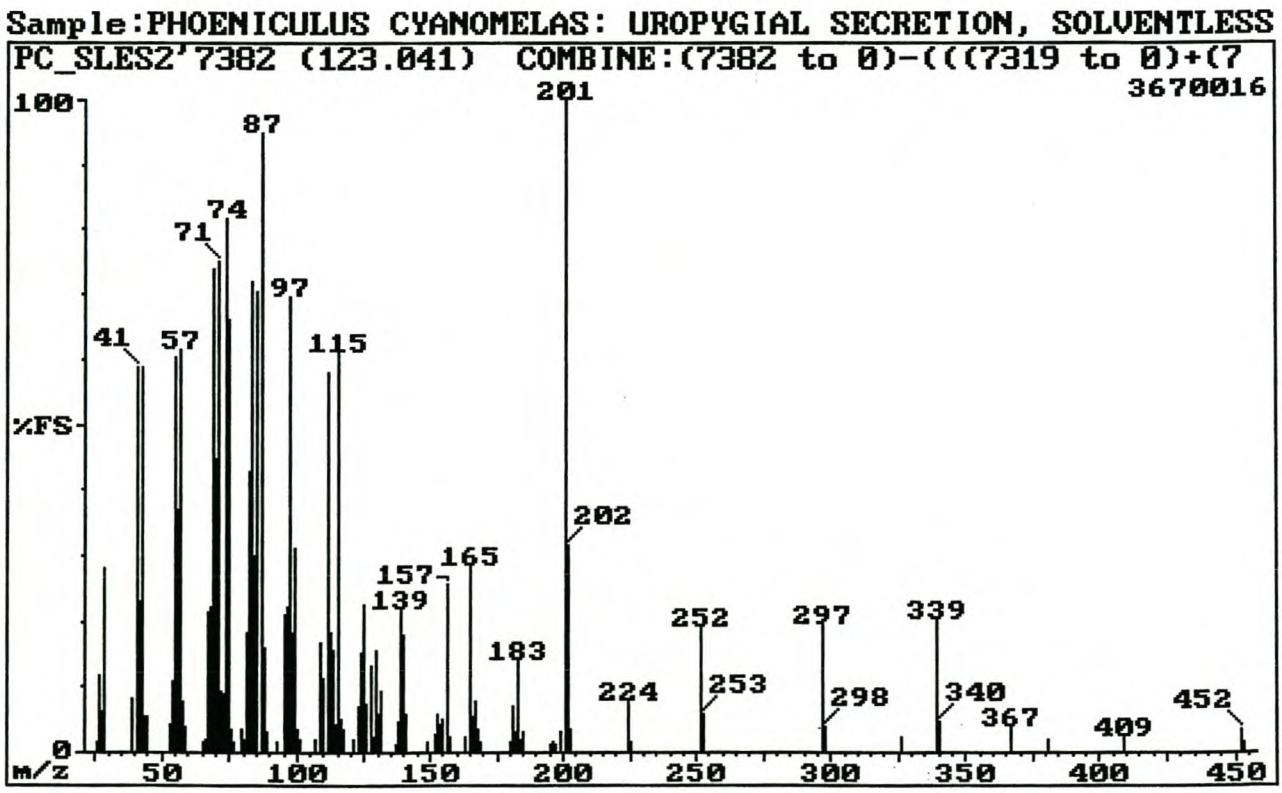

Fig 2.159: EI mass spectrum of component 7382 [30(12;18)]

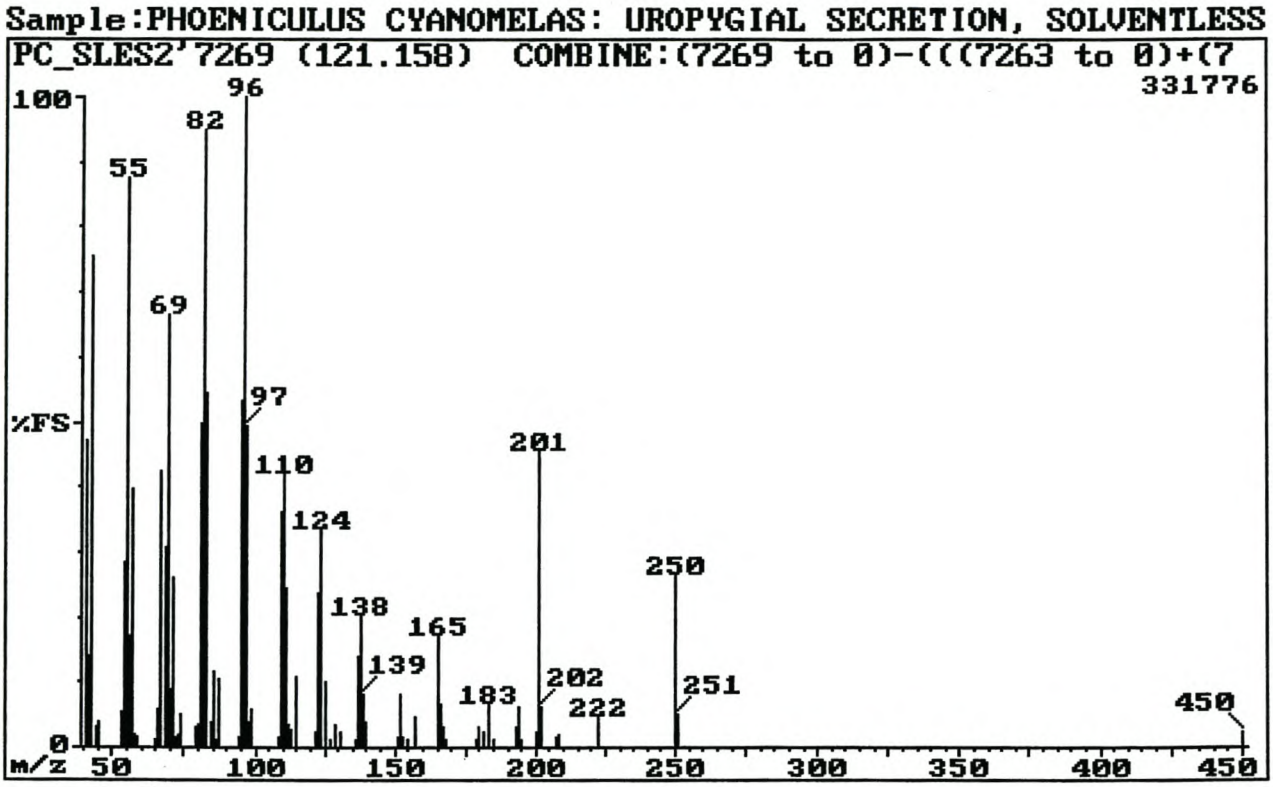

Fig 2.160: EI mass spectrum of component 7269 [30(12;18)]

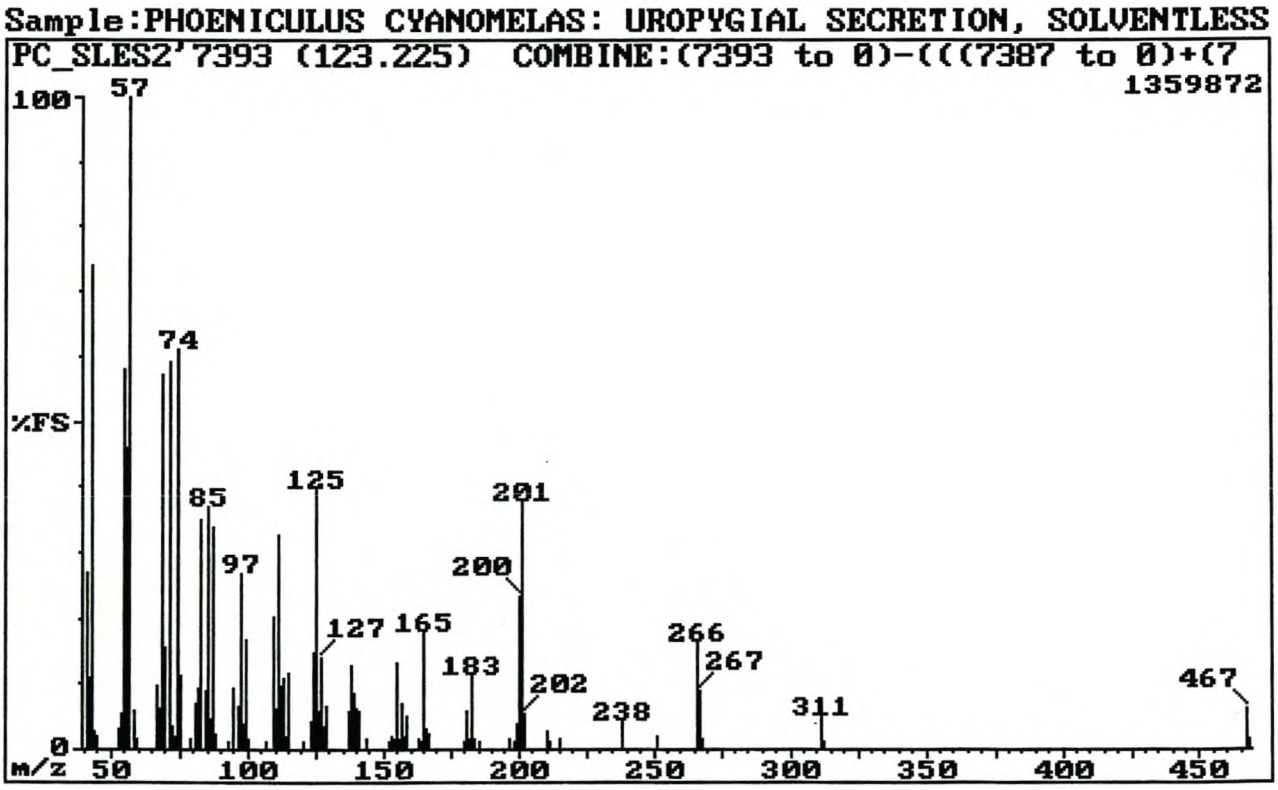

Fig 2.161: EI mass spectrum of component 7393 [31(12;19)]

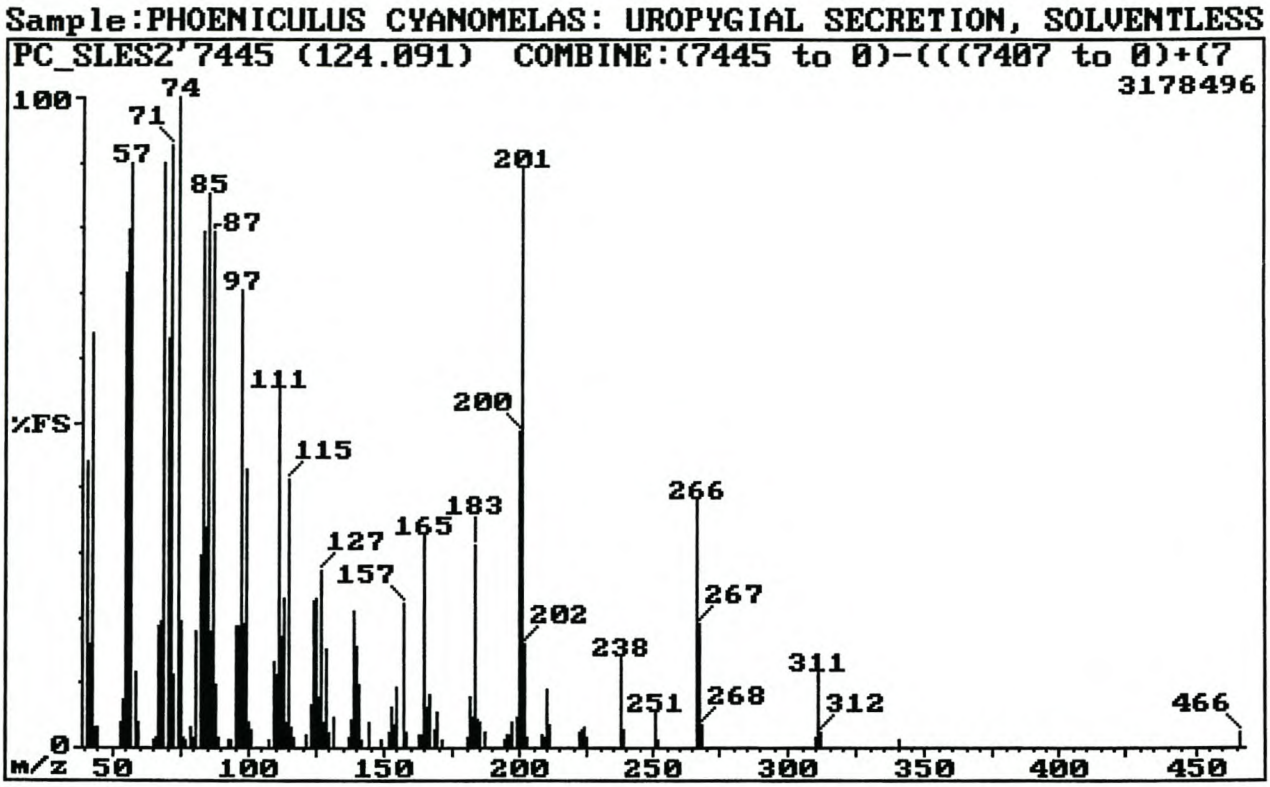

Fig 2.162: EI mass spectrum of component 7445 [31(12;19)]

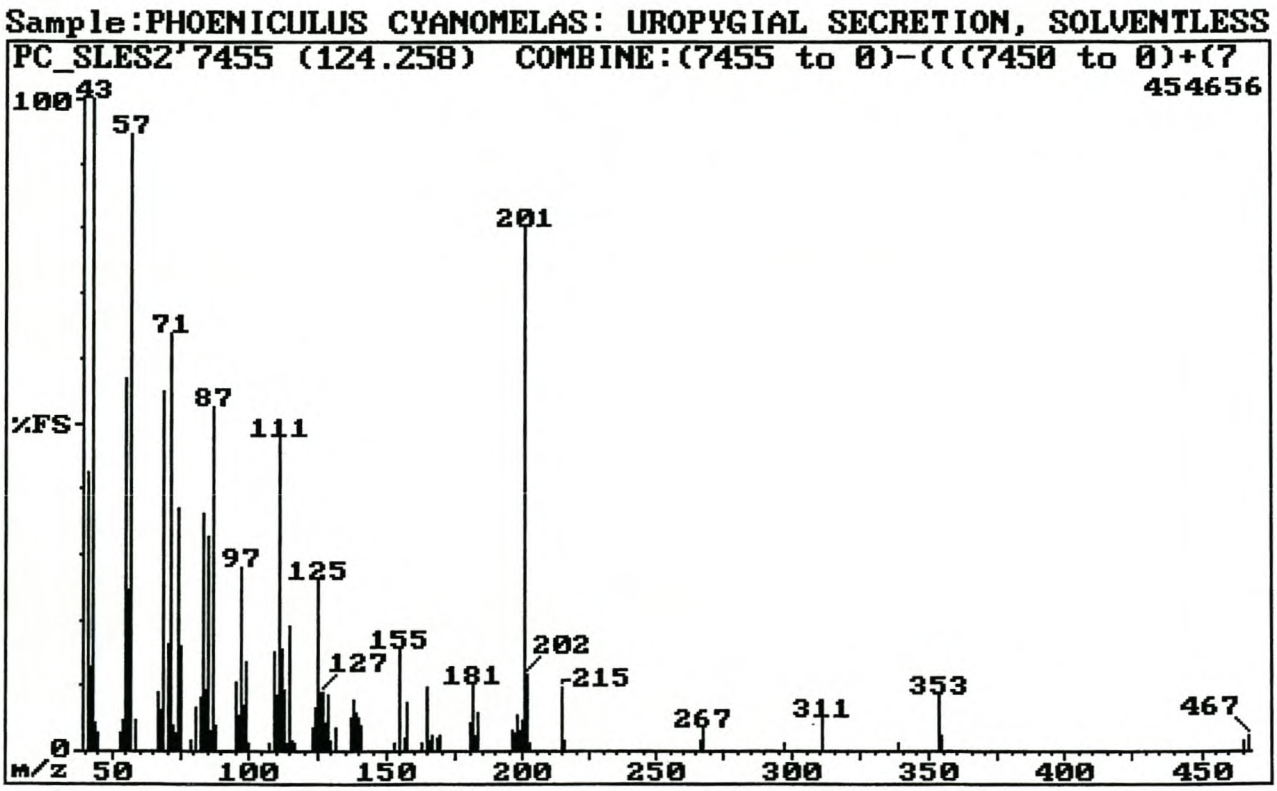

Fig 2.163: EI mass spectrum of component 7455 [31(12;19), 31(13;18)]

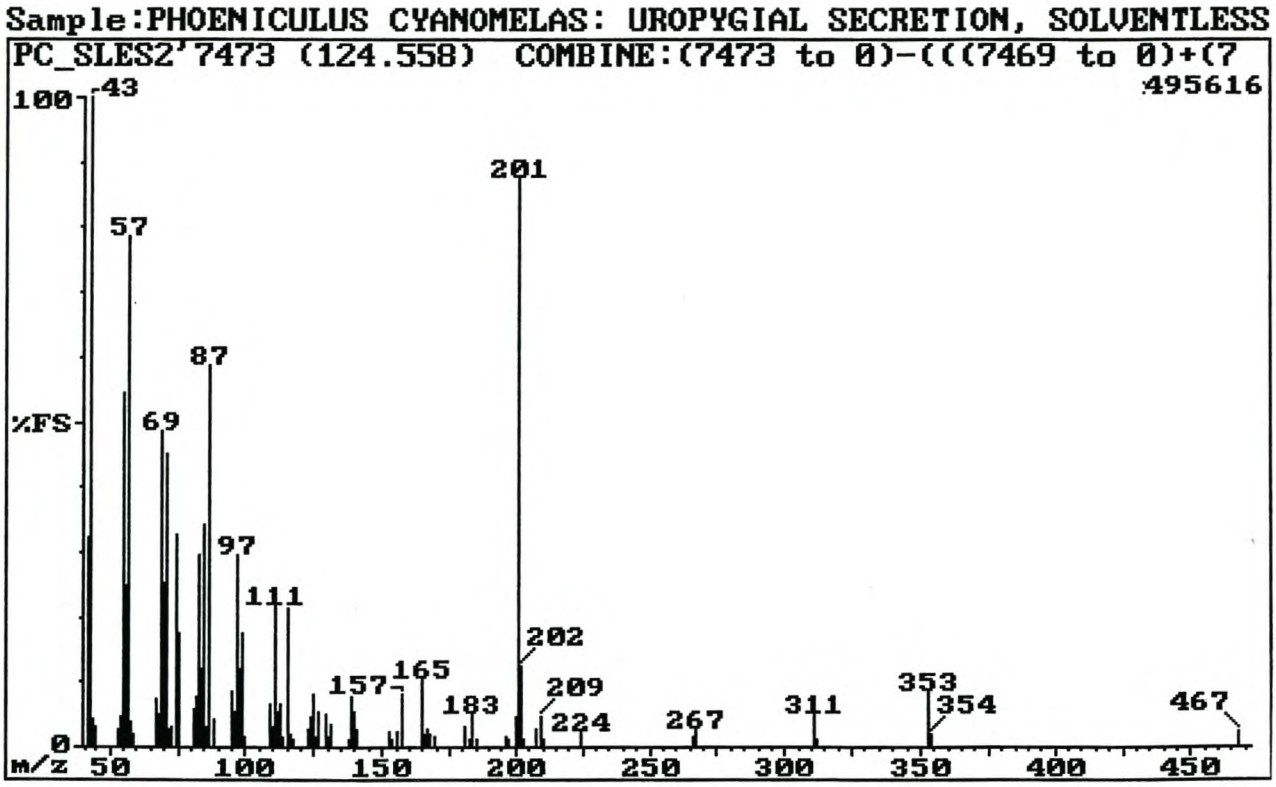

Fig 2.164: EI mass spectrum of component 7473 [31(12;19)]

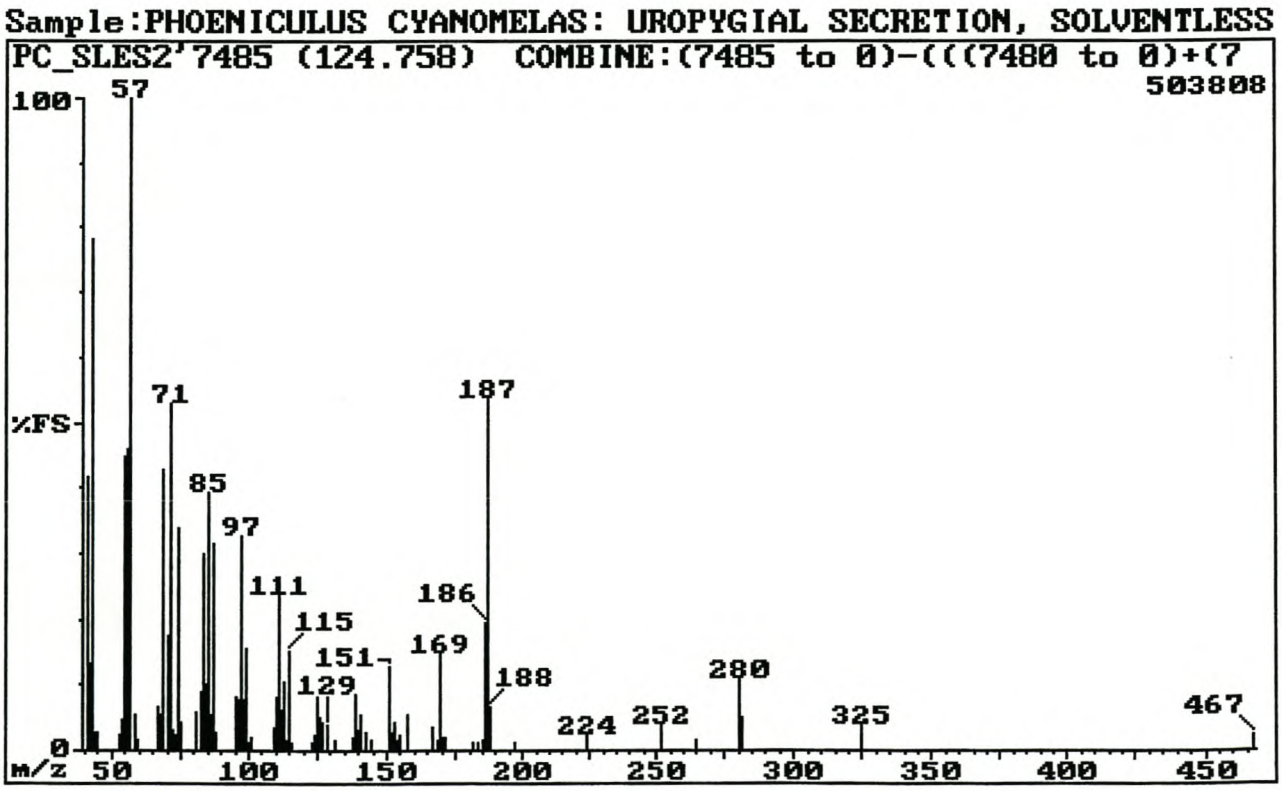

Fig 2.165: EI mass spectrum of component 7485 [31(11;20)]

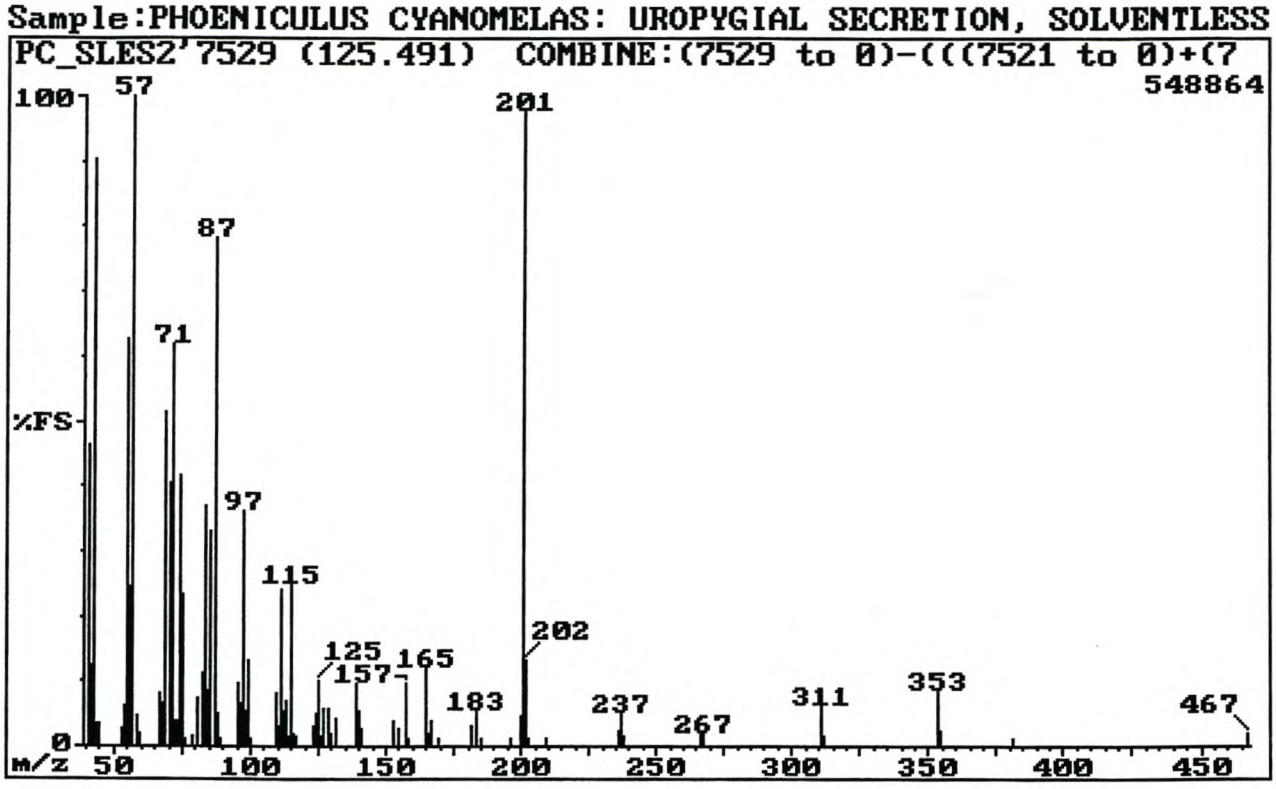

Fig 2.166: EI mass spectrum of component 7529 [31(12;19)]

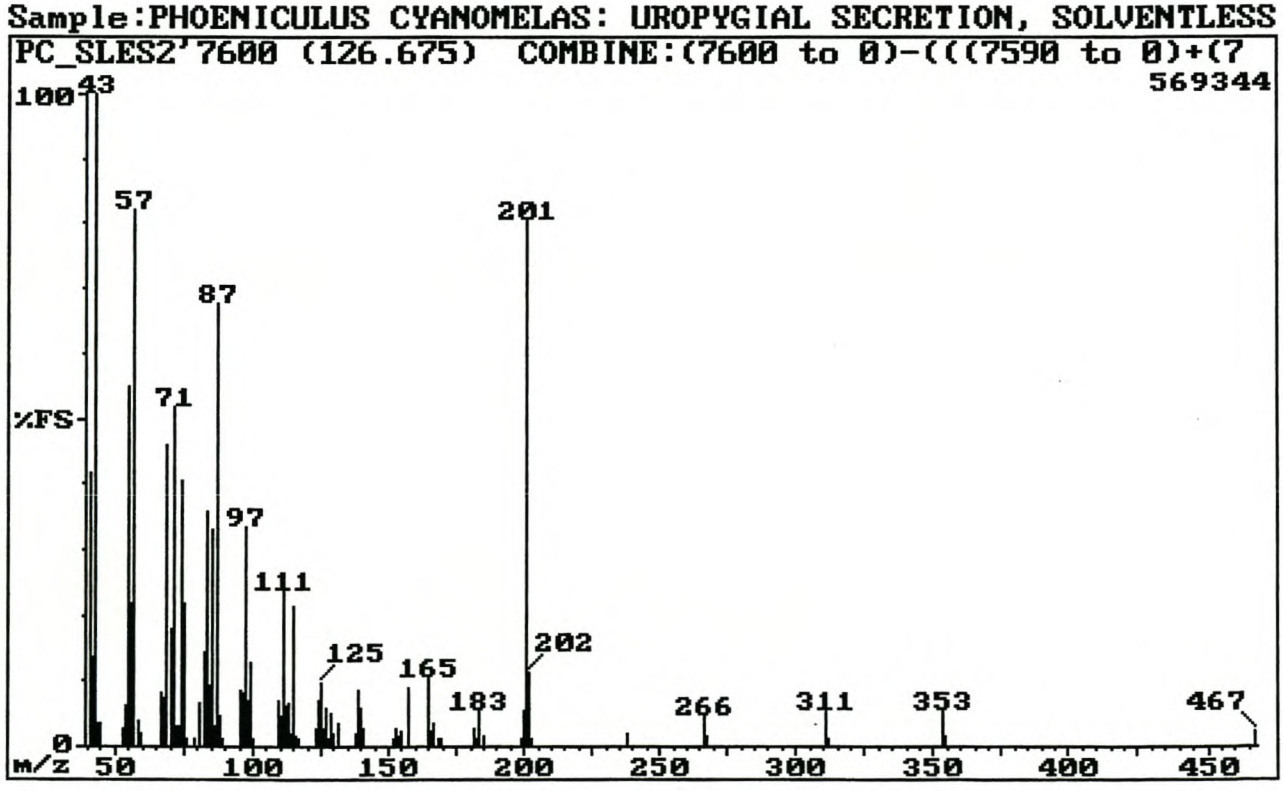

Fig 2.167: EI mass spectrum of component 7600 [31(12;19)]

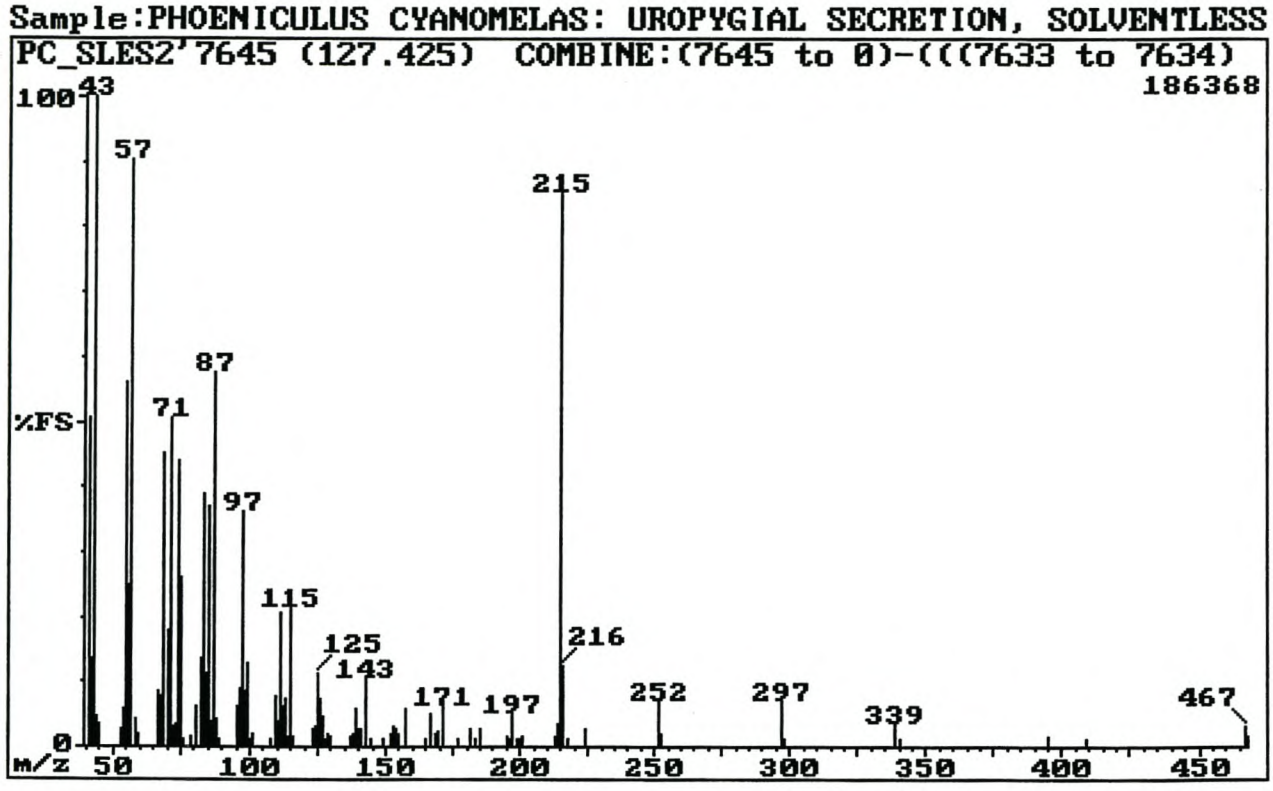

Fig 2.168: EI mass spectrum of component 7645 [31(13;18)]

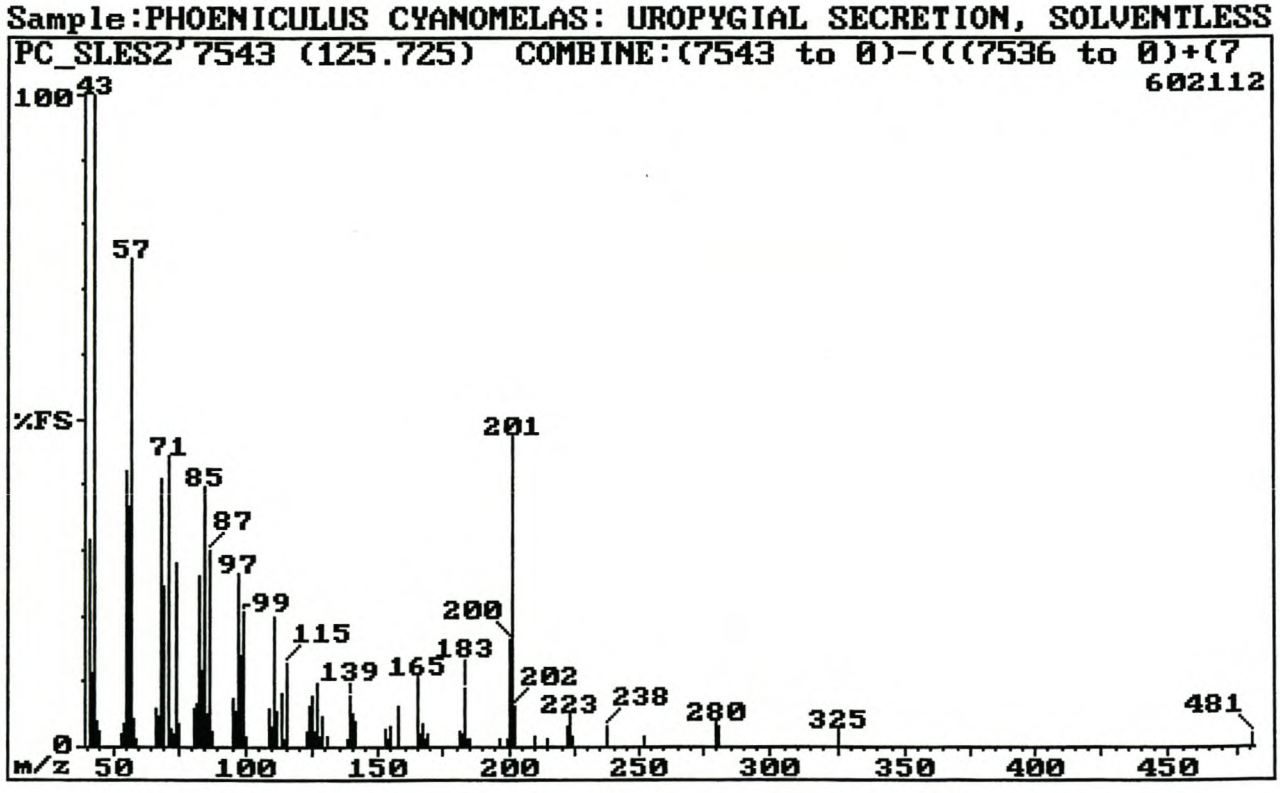

Fig 2.169: EI mass spectrum of component 7543 [32(12;20)]

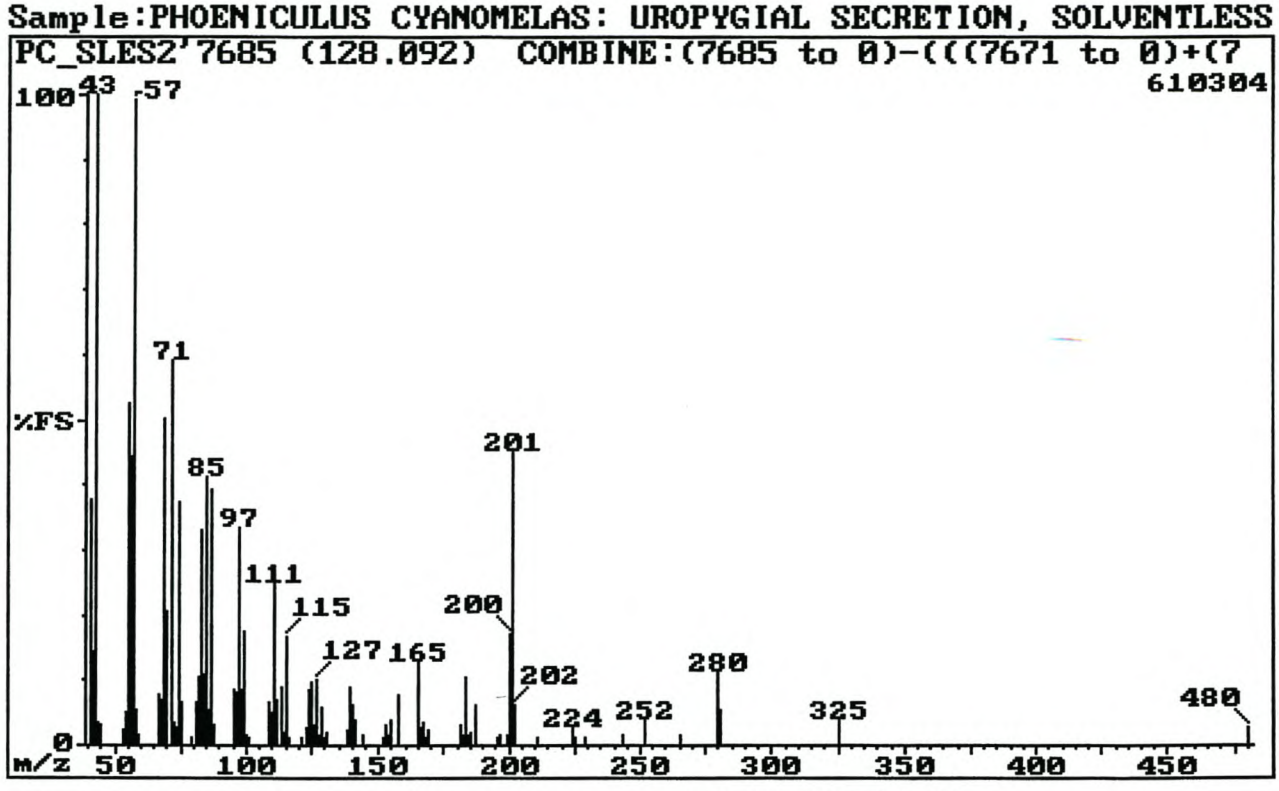

Fig 2.170: EI mass spectrum of component 7685 [32(12;20)]

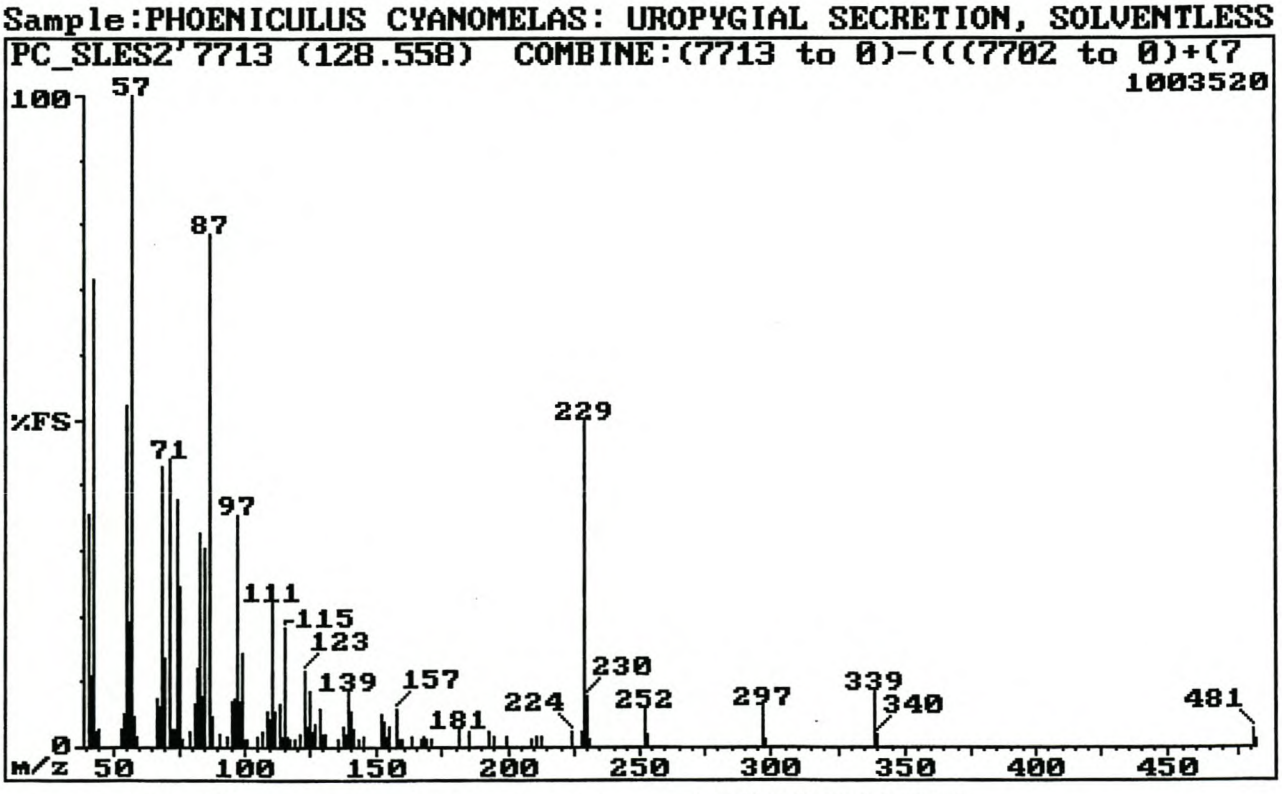

Fig 2.171: EI mass spectrum of component 7713 [32(14;18)]

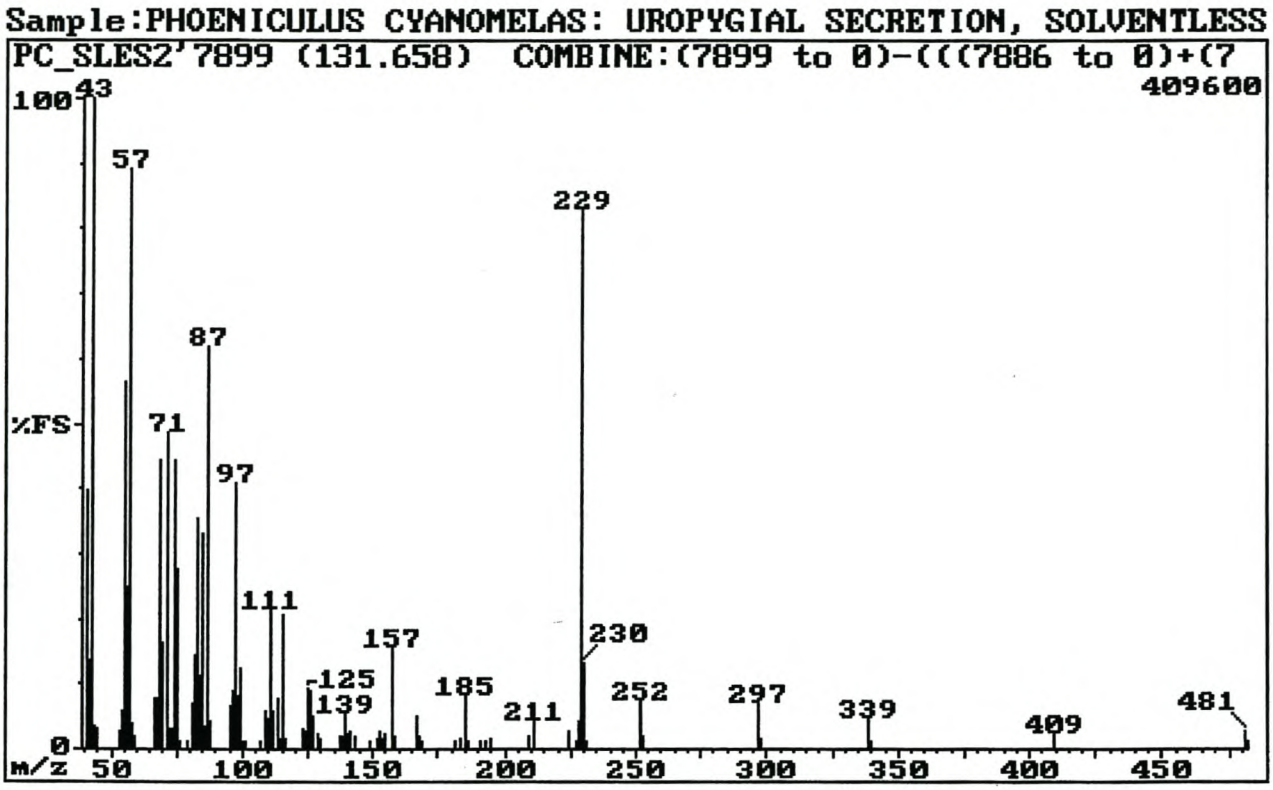

Fig 2.172: EI mass spectrum of component 7899 [32(14;18)]

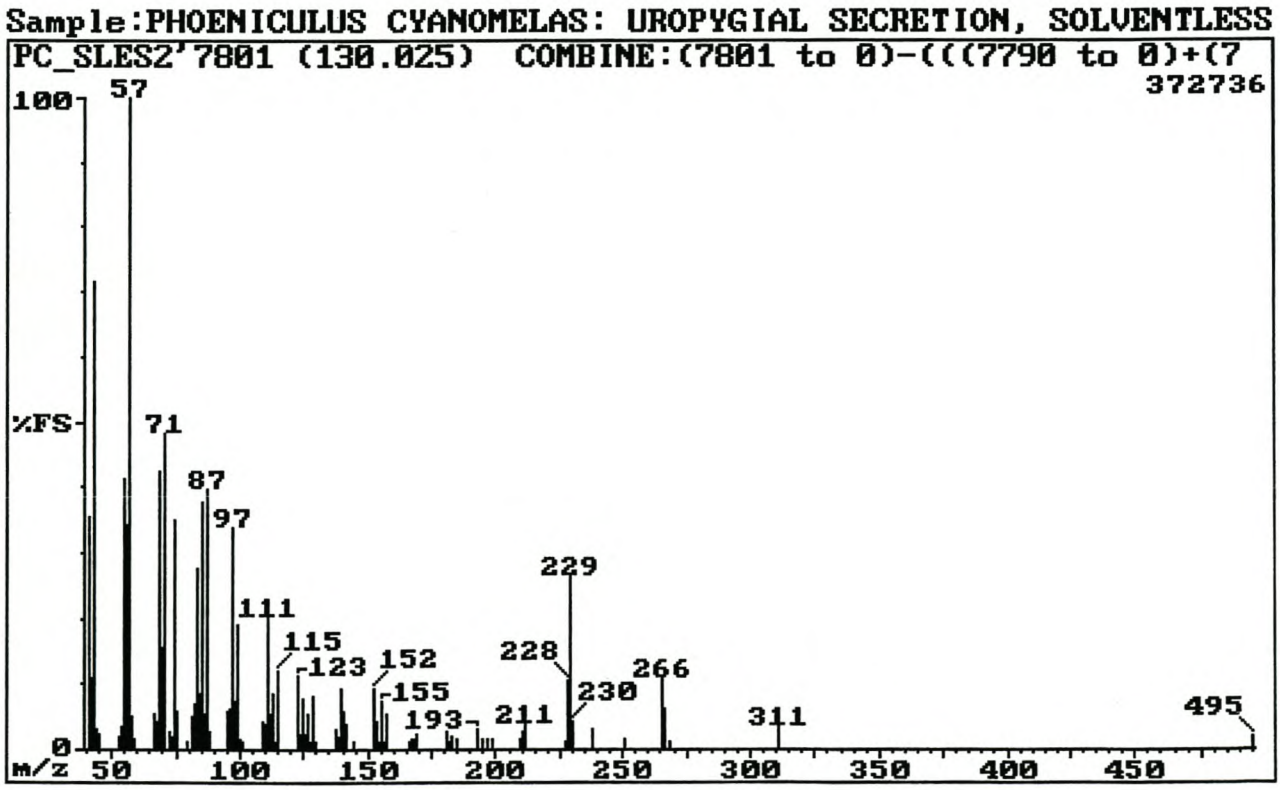

Fig 2.173: EI mass spectrum of component 7801 [33(14;19)]

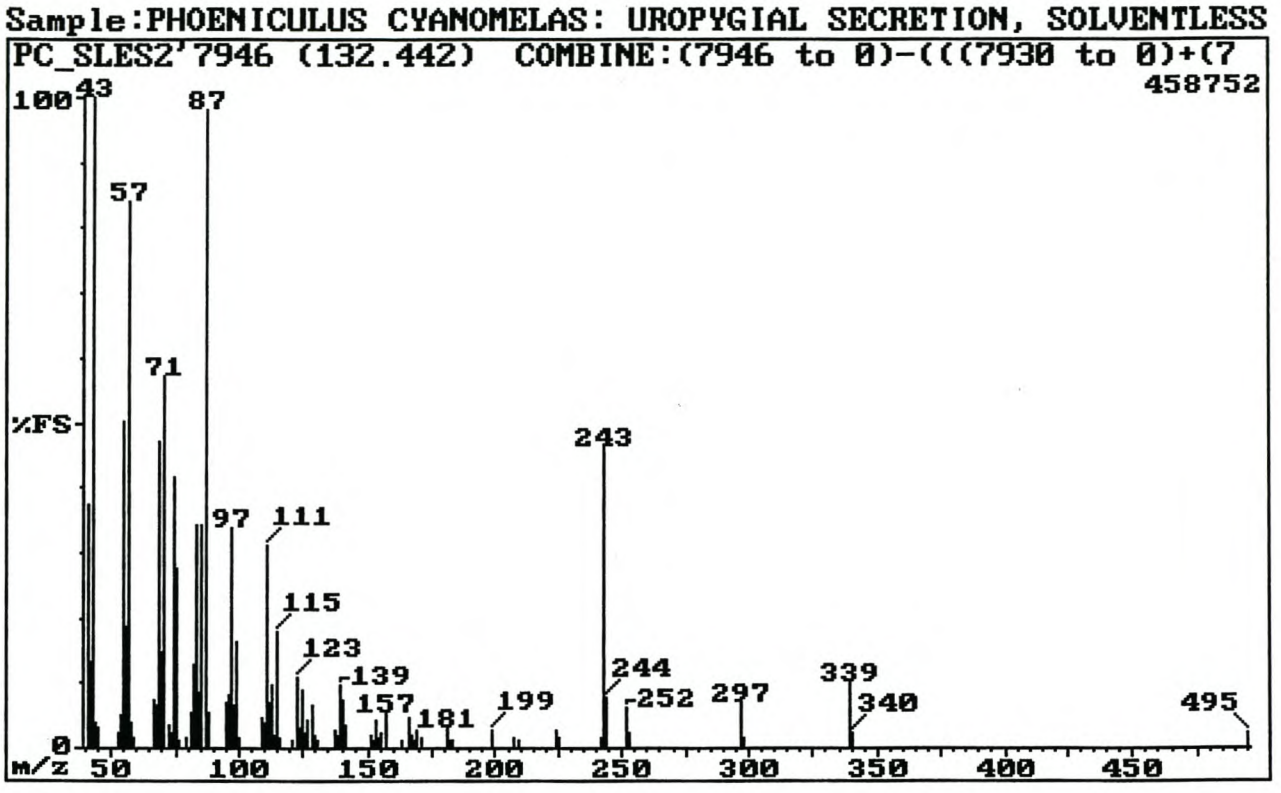

Fig 2.174: EI mass spectrum of component 7946 [33(15;18)]

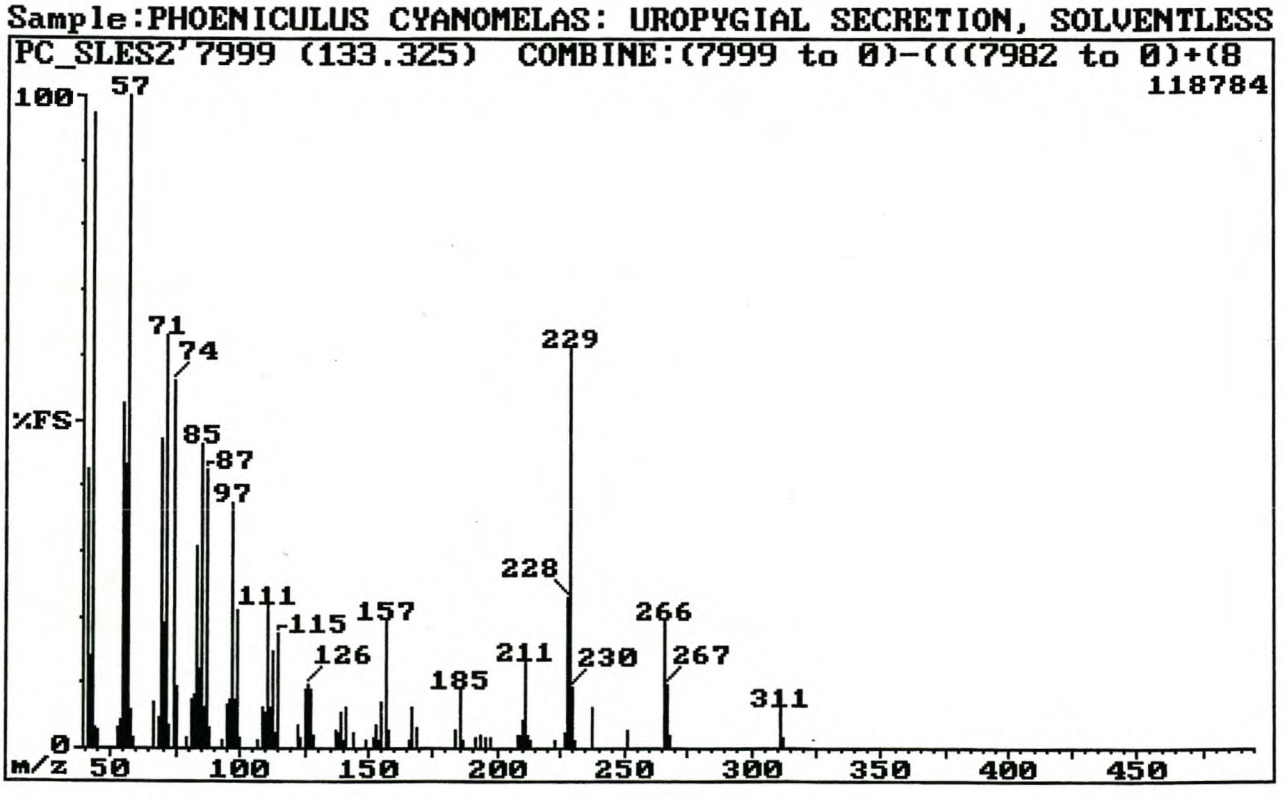

Fig 2.175: EI mass spectrum of component 7999 [33(14;19)]

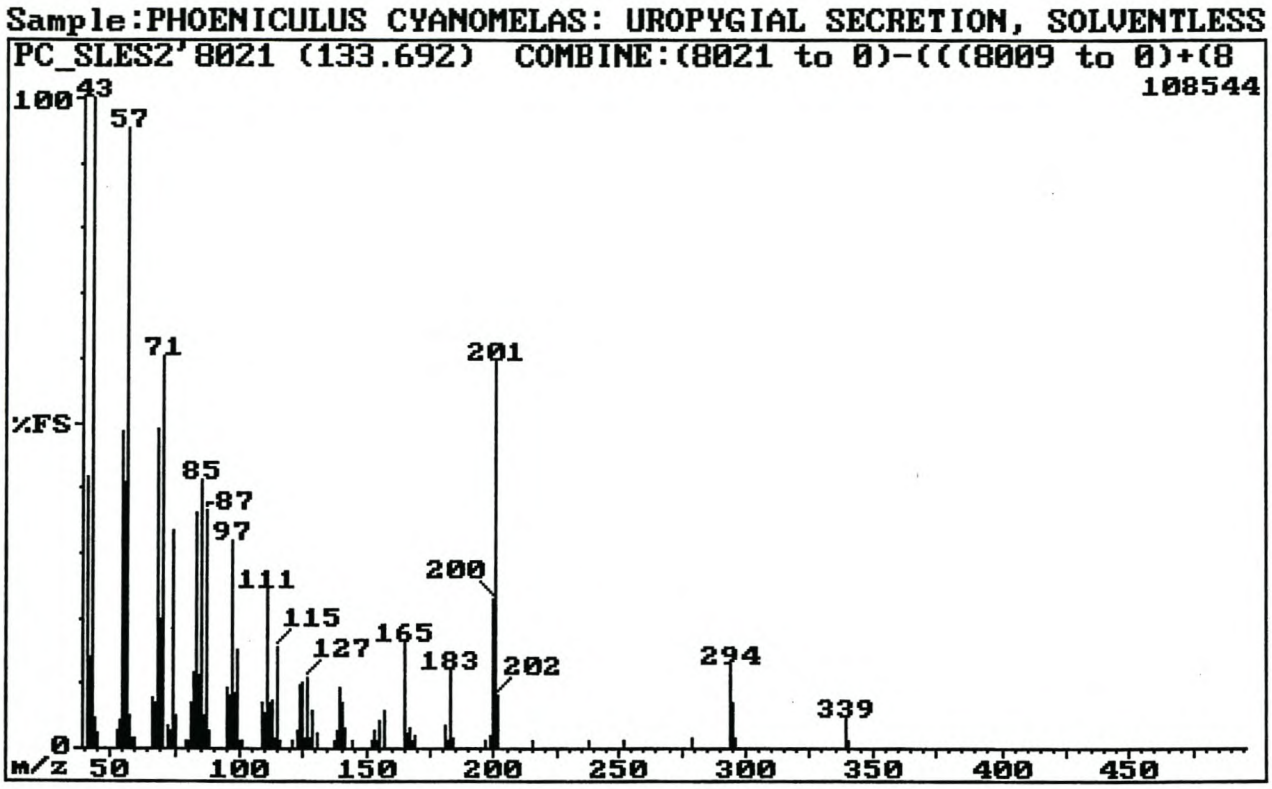

Fig 2.176: EI mass spectrum of component 8021 [33(12;21)]

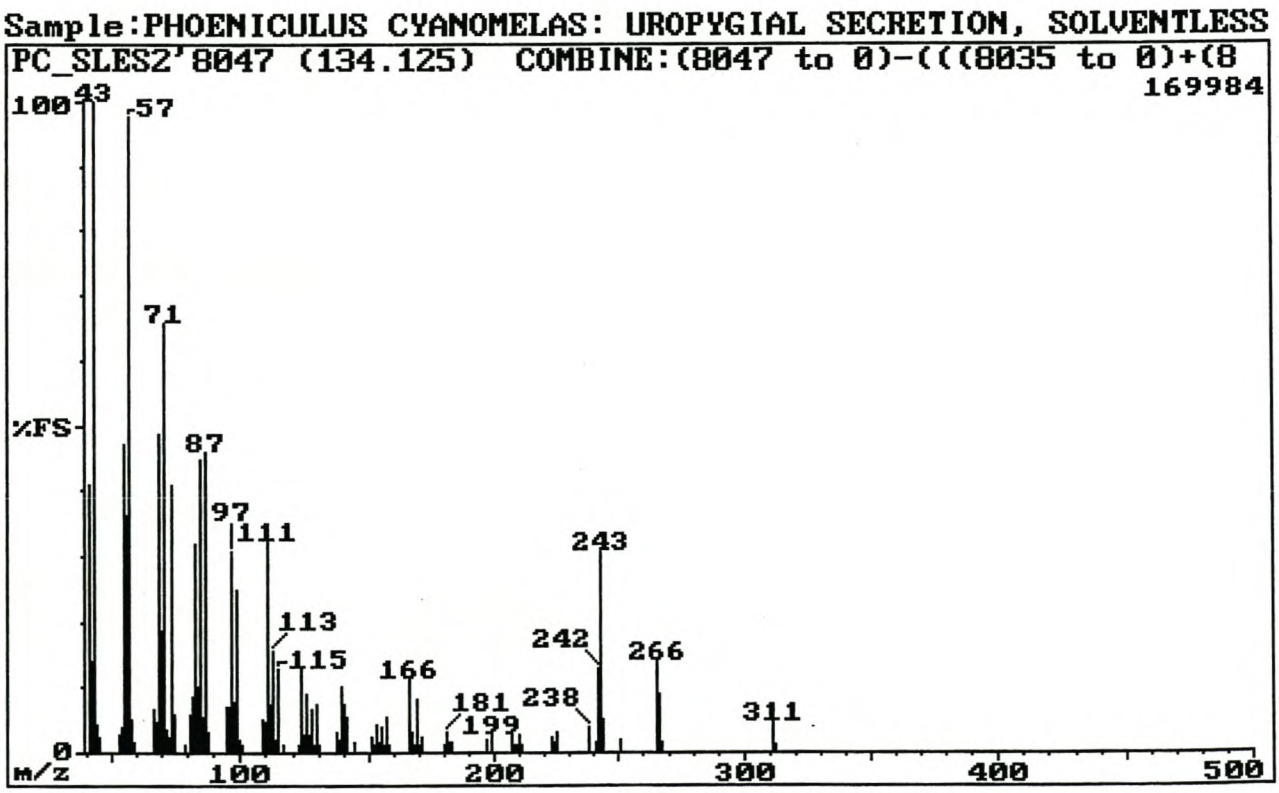

Fig 2.177: EI mass spectrum of component 8047 [34(15;19)]

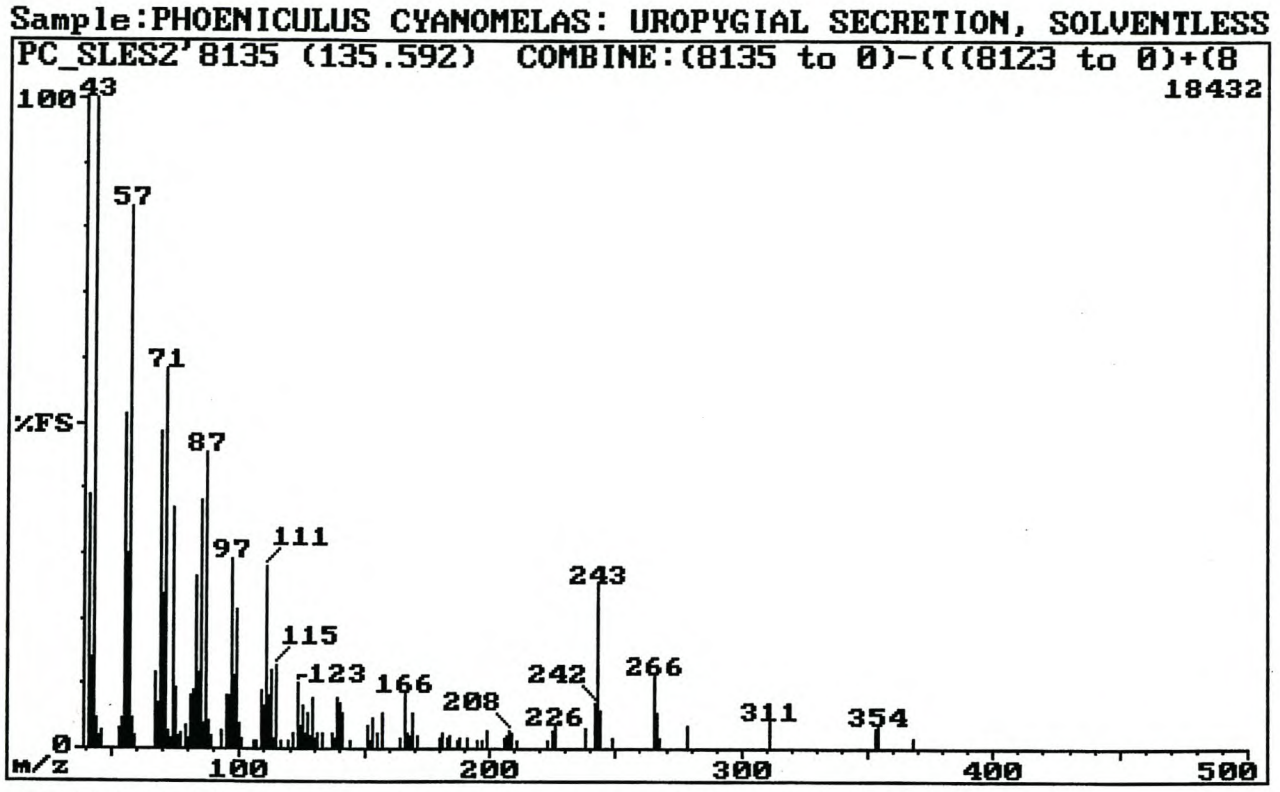

Fig 2.178: EI mass spectrum of component 8135 [34(15;19)]

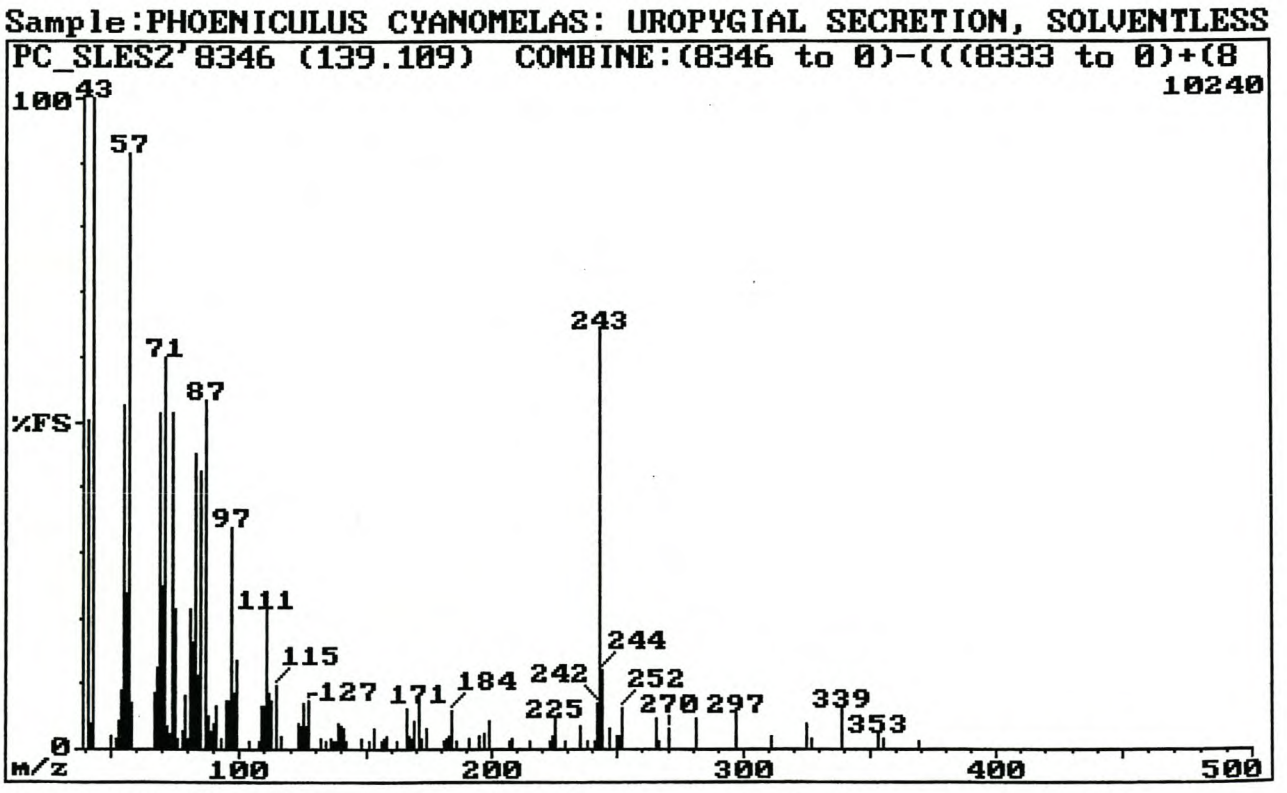

Fig 2.179: EI mass spectrum of component 8346 [35(15;20)]

References: Chapter 2

1. S.F. Dyke, A.J. Floyd, M. Sainsbury and R.S. Theobald, "Organic Chemistry", Longman, London, p. 194 (1978)
2. F.W. McLafferty and F. Turecek, "Interpretation of Mass Spectra", University Science Books, California, p. 226 (1993)
3. R.M. Silverstein, G.C. Bassler and T.C. Morril, "Spectrometric Identification of Organic Compounds", John Willey and Sons., New York, p. 17 (1991)
4. M.J. O'Neal and T.P. Weird, Anal. Chem., **23**, 830 (1951)
5. H. Budzikiewicz, C. Djerassi and D.H. Williams, "Mass Spectrometry of Organic Compounds", Holden-Day, San Francisco, p. 51 (1967)
6. Reference 5, p. 55
7. Reference 2, p. 230
8. W. Kemp, "Organic Spectroscopy", MacMillan Press, p. 207 (1975)
9. F.W. MacLafferty, Anal. Chem., **31**, 2072 (1959)
10. J.H. Beynon, R.A. Saunders and A.E. Williams, "The Mass Spectra of Organic Molecules", Elsevier, Amsterdam, p. 106 (1968)
11. Reference 10, p.107
12. W.H. McFadden, M. Lounsbury, and A.L. Wahrhaflig, Can. J. Chem., **36**, 990 (1958)
13. Reference 5, p. 98
14. R.A. Friedel, J.L. Shultz, and A.G. Sharkey, Anal. Chem., **28**, 926 (1956)
15. S. Meyerson and L.C. Leitch, J. Am. Chem. Soc., **86**, 2555 (1964)

16. W. Benz and K. Biemann, J. Am. Chem. Soc., **86**, 2375 (1964)

17. L. Dolejs, P. Beran, and J. Hradec, Org. Mass. Spec., **1**, 565 (1968)

18. T. Aczel and H.E. Lumpkin, Anal. Chem., **32**, 1819 (1960)

19. Reference 5, p. 617

20. J.H. Beynon, G.R. Lester, and A.E. Williams, J. Phys. Chem., **63**, 1861 (1959)

21. Reference 10, p. 211

22. J.A. Gilpin and F.W. McLafferty, Anal. Chem., **29**, 990 (1957)

23. F.W. McLafferty, Anal. Chem., **31**, 82 (1959)

24. M. Kraft and G. Spiteller, Org. Mass Spec., **2**, 541 (1959)

25. Reference 5, p. 132

26. A. Maccoll and M.N. Mruzek, Org. Mass Spec., **21**, 251 (1986)

27. K. Christiansen, V. Mahadeven, C.V. Viswanathan, and R.T. Holman, Lipids, **4**, 421 (1969)

28. Reference 27

29. D. Goldsmith, D. Becher, S. Sample, and C. Djerassi, Tetrahedron, suppl., **7**, 145 (1966)

30. T. Aczel and H.E. Lumpkin, Anal. Chem., **33**, 386 (1961)

31. Reference 10, p. 213

32. J.D. McCollumand and S. Meyerson, J. Am. Chem. Soc., **85**, 1739 (1963)

33. Reference 1, p. 196

34. Reference 10, p. 191

35. A.G. Sharkey, J.L. Shualtz, and R.A. Friedel, Anal. Chem., **28**, 934 (1956)

36. W. Carpenter, A.M Duffield, and C. Djerassi, J. Am. Chem. Soc., **90**, 160 (1968)

37. Reference 5, p. 135

38. J.H. Beynon, R.A. Saunders, and A.E. Williams, Appl. Spec., **14**, 95 (1960)

39. Reference 5, p. 138

40. G.P. Happ, D.W. Stewart, J. Am. Chem. Soc., **74**, 4404 (1952).

41. Reference 5, pp. 179-180

42. Reference 3, p 27

43. F.W. McLafferty and R.S. Gohlke, Anal. Chem., **31**, 2076 (1959),

44. S. Meyerson and J.L. Corbin, J. Am. Chem. Soc., **87**, 3045 (1965)

45. Reference 10, p. 239

46. J.H. Beynon, R.A. Saunders, and A.E. Williams, Anal. Chem., **33**, 221 (1961)

47. A.J. Sharkey, J.L. Shultz, and R.A. Friedel, Anal. Chem., **31**, 87 (1959)

48. J. Asselineau, R. Ryhage, and E. Stenhagen, Acta Chem. Scand., **11**, 196 (1957)

49. S. Meyerson and C. Leitch, J. Am. Chem. Soc., **88**, 56 (1966)

50. C. Djerassi and C. Fenselau, J. Am. Chem. Soc., **87**, 5756 (1965)

51. E.M. Emery, Anal. Chem., **32**, 1495 (1960)

52. Reference 5, p. 336

53. J.L. Gilpin, Anal. Chem., **31**, 935 (1959)

54. Reference 3, p. 31

55. Z. Pelah, M.A. Kielczewski, J.M. Wilson, M. Ohashi, H. Budzikiewicz, and C. Djerassi, J. Am. Chem. Soc., **85**, 2470 (1963)

56. A.M. Duffield and C. Djerassi, J. Am. Chem. Soc., **87**, 4554 (1965)

57. Reference 5, p. 339

58. J.L. Cotter, J. Chem. Soc., 5742 (1965)

59. J.L. Cotter, J. Chem. Soc., 5477 (1964)

60. Reference 5, p. 297

61. Reference 60

62. Reference 2, p. 271

63. R.S. Gohlke and F.W. McLafferty, Anal. Chem., **34**, 1281 (1962)

64. C. Djerassi and C. Fenselau, J. Am. Chem. Soc., **87**, 5752 (1965)

65. P.N. Rylander, S. Peterson, and H.N. Grubb, J. Am. Chem. Soc., **79**, 842 (1957)

66. Reference 5, p. 408

67. R.F. Pottie and F.P. Lossing, J. Am. Chem. Soc., **83**, 4737 (1961)

68. F.W. McLafferty, Anal. Chem., **34**, 26 (1962)

69. Reference 10, p. 309

70. R. Beugelmans, D.H. Williams, H. Budzikiewicz, and C. Djerassi, J. Am. Chem. Soc., **86**, 1386 (1964)

71. Reference 68

72. Reference 10, p.352

73. E.J. Levy and W.A. Stahl, Anal. Chem., **33**, 707 (1961)

74. Reference 10, p. 358

75. A.M. Duffield, W. Carpenter, and C. Djerassi, Chem. Comm., 109 (1967)

76. J.H. Bowie, S.O. Lawesson, J.O. Madsen, C. Nolde, G. Schroll, and D.H. Williams, J. Chem. Soc., (B), 946 (1966)

77. Reference 76

78. L. Friedman and F.A. Long, J. Am. Chem. Soc., **75**, 2832 (1953)

79. W.H. McFadden, E.A. Day, and M.J. Diamond, Anal. Chem., **37**, 89 (1965)

80. E. Honkanen, T. Moisio, and P. Karnoven, Acta Chem. Scand., **19**, 370 (1965)

81. A.M. Duffied, H. Budzikiewicz, and C. Djerassi, J. Am. Chem. Soc., **86**, 5536 (1964)

82. H. Budzikiewicz, C. Djerassi, A.H. Jackson, G.W. Kenner, D.J. Newman, and J.M. Wilson, J. Chem. Soc., 1949 (1964)

83. Reference 5, p. 602

84. J.H. Beynon, R.A. Saunders, and A.E. Williams, Appl. Spec, **13**, 103 (1959)

85. Reference 5, pp. 610-612

86. Reference 10, pp. 75-76

87. J. Ridd, "Physical Methods in Heterocyclic Chemistry", A.R. Katritzky, ed., Academic Press, London, p. 130 (1963) (as sited in Reference 5, p. 567)

88. H. Budzikiewicz, J.I. Brauman, and C. Djerassi, Tetrahedron, **21**, 1855 (1965)

89. Reference 5, p. 254

90. G. Audlsio, A. Rossini, G. Bianchi and P. Avato, J. High Resol. Chromatogr., **10**, 594 (1987)

91. W. Francke, G. Lubke, W. Schroder, A. Reckziegel, V.I. Fonsecab, A. Kleinert, E. Engels, K. Hartfelder, R. Radtke and W. Engels, J. Braz. Chem. Soc., **11**, 562 (2000)

92. R. Ryhage and E. Stenhagen, Arkiv Kemi **15**, 292 (1959)

93. Reference 41 (Chapter 2)

94. Z. Moldovan, E. Jover, and M. Bayona, J. Chromatogr., A, **952**, 193 (2002)

95. B. Reiter, M. Lechner, E. Lorbeer and R. Aichholz, J. High Resol. Chromatogr., **22**, 514 (1999).

CHAPTER 3

COMPARATIVE ANALYSIS OF THE UROPYGIAL SECRETIONS OF THE SCIMITAR-BILLED WOODHOOPOE, GREEN WOODHOOPOE AND AFRICAN HOOPOE.

The African hoopoe (Fig. 3.1) and two woodhoopoes, the Scimitar-billed (Fig. 1.4) and Green woodhoopoe (Fig. 3.2) are closely related and have many similarities in their behaviour and breeding biology[1]. The uropygial secretions of the African hoopoe, *Upupa africana*, and Green woodhoopoe, *Phoeniculus purpureus*, were previously studied in the Laboratory for Ecological Chemistry of the University of Stellenbosch (LECUS) in South Africa and this chapter deals with the comparison of these results with those obtained in the analysis of the uropygial gland secretion of the Scimitar-billed woodhoopoe, *Rhinopomastus cyanomelas*.

Fig. 3.1: The African hoopoe

Fig. 3.2: The Green woodhoopoe

The total ion chromatograms (TICs) of the uropygial secretions of the Scimitar-billed woodhoopoe, African hoopoe[2], and the Green woodhoopoe[3] are shown in Fig. 2.1, Fig. 3.1 and Fig. 3.2 respectively.

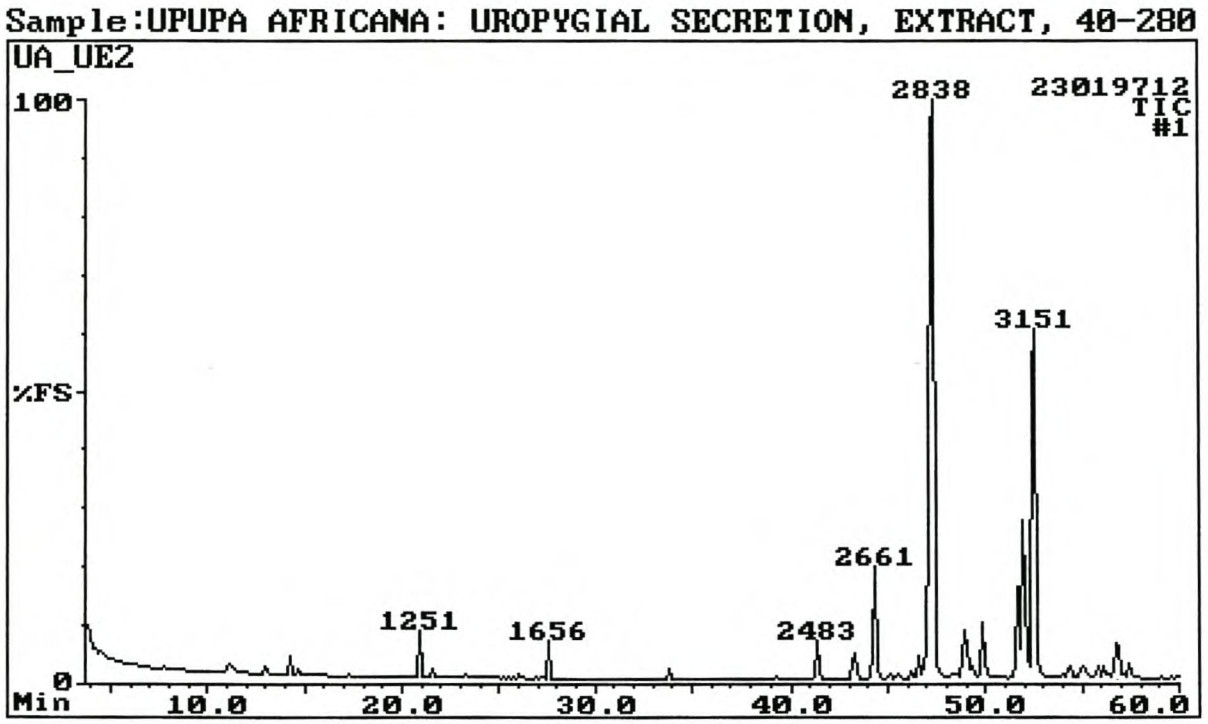

Fig. 3.1: Total ion chromatogram of an extract of the uropygial gland secretion of the African hoopoe.

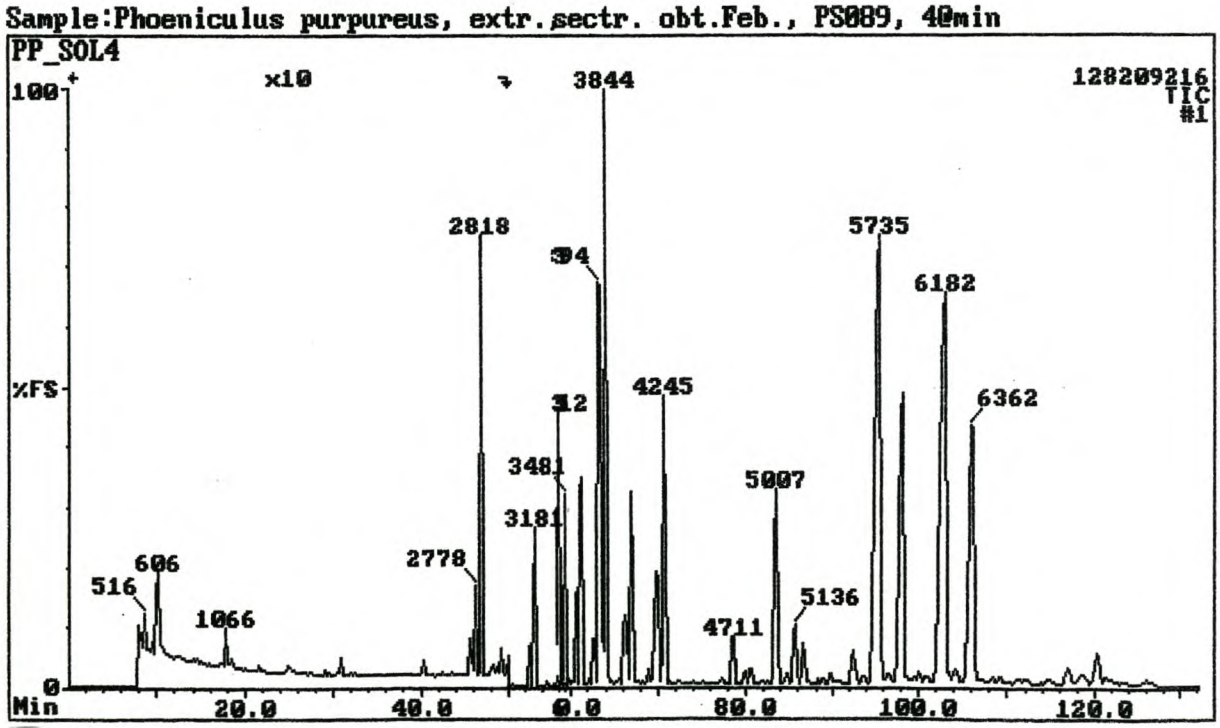

Fig. 3.2: Total ion chromatogram of an extract of the uropygial gland secretion of the Green woodhoopoe.

Quite a large proportion of the constituents of the uropygial gland secretion of the African hoopoe was found to consist of relatively long-chain saturated and unsaturated carboxylic acids. Apart from eicosanoic acid, which is present as three isomers, all the other acids with an even carbon number have unbranched carbon chains. The branched alkanoic acids possess *iso* or *anteiso* structures.

While the carboxylic acids with an odd number of carbon atoms are all saturated compounds, some of the even-numbered ones have saturated and unsaturated carbon skeletons. The C16, C18 and C20 alkenoic acids have two isomers with almost identical mass spectra and similar retention times revealing the presence of *Z*- and *E*-configurations. In all of these unsaturated carboxylic acids, the position of the double bond is at C9.

Table 3.1: Alkanoic acids and their isomers present in the secretion of the African hoopoe

Acid	Straight chain	*Iso*-	*Anteiso*-
C_{14}	√	x	x
C_{15}	√	√	x
C_{16}	√	x	x
C_{17}	√	√	√
C_{18}	√	√	x
C_{19}	√	x	x
C_{20}	√	√	√
C_{22}	√	x	x

In the secretion of the African hoopoe the only compounds of relatively

low mass that are present in the secretion are 2,2-dimethylpropanoic acid, 7-octen-3-ol, 6,9-dimethyloctane, 2,2-dichloroacetamide, methyl salicylate and 6,9-dimethyloctane. Squalene and two ester derivatives of cholesterol are the only high molecular weight compounds found in the secretion. The low molecular weight and more volatile pungent smelling compounds are absent in the secretion of the hoopoe and it also does not contain large quantities of hydrocarbons and wax esters[4].

The composition of the uropygial gland secretion of the Green woodhoopoe varies greatly from that of the African hoopoe. A study on the composition of the secretion of the uropygial gland of Green woodhoopoe showed that a vast number of volatile organic compounds, various hydrocarbons, in particular monounsaturated olefins, and high molecular weight waxes are present in the secretion[5]. In Green woodhoopoes the short-chain fatty acids, trimethylamine, aldehydes, dimethyldisulfide, dimethyl trisulfide and indoles are responsible for the obnoxious smell of the secretion. These constituents are used as a defence when the bird is threatened by predators.

The heavy wax esters are assumed to have two functions. Firstly, because of their hydrophobic nature they form a key water-proofing component when applied to the feathers during preening and keep the feathers in a good condition. Secondly, they are thought to serve as a controlled-release medium for the more volatile constituents of the secretion.

There is a striking similarity between the composition of the uropygial gland secretions of the Scimitar-billed woodhoopoe and the Green woodhoopoe. Most of the more volatile compounds with obnoxious odours are found in both birds. However, the composition of the secretion of the Scimitar-billed is more complex than that of the Green woodhoopoe. The variation and number of the lower molecular weight and more volatile constituents are higher in the case of the Scimitar-bill. Some obnoxious smelling compounds, such as hydrogen sulphide and methanethiol, are restricted only to this bird. The nature and number of the hydrocarbons and wax ester constituents are

much higher in this bird. Only wax esters ranging between C_{27} - C_{33}, with few isomer variations, were found in the secretion of the Green woodhoopoe, whereas in the Scimitar-billed woodhoopoe the numbers and variations of the constituents are vast. Only five additional compounds which are absent in the secretion of the Scimitar-bill were identified in that of the Green woodhoopoe, namely 3-methyl-1-butanol, 2-phenylethanol, 2-phenylethyl acetate, and 14-methyl-1-pentadecanol. A complete list of the compounds identified in the Scimitar-billed woodhoopoe appears in Table 2.1.

From the results so far obtained, it can be seen that, unlike the uropygial secretions of the closely related Scimitar-billed and Green woodhoopoe species, the secretion of the African hoopoe contains only the high molecular weight carboxylic acids with low volatility. The absence of pungent smelling compounds restricts the uropygial gland of the African hoopoe to function only against feather attacking bacteria and as a water-proof coating. In the case of the other two birds however, because of the presence of a wide variety of compounds, the uropygial gland of these birds apparently have a multifunctional role. While the higher esters are used as waterproofing to keep the plumage in good condition and as controlled-release media, the lower molecular weight compounds serve as deterents because of their obnoxious odour, and against attack from bacteria or other feather attacking organisms.

From a chemotaxonomic viewpoint, when compared with the African hoopoe and Green woodhoopoe, the Scimitar-billed woodhoopoe is more closely related to the Green woodhoopoe. As mentioned, both possess predominantly waxes of fatty acids of about the same chain-length. the characteristics of fatty acid have been used as markers in the chemotaxomonic studies[6].

The African hoopoe, in fact, belongs to the family of *Upupidea* (hoopoes) whereas the Scimitar-billed and Green woodhoopoes belong to the same family, the *Phoeniculidae* (woodhoopoes), though they are of different species[7]. This is in agreement with the results and conclusions of this study of the chemical nature of the respective uropygial secretions.

References: Chapter 3

1. P. Steyn, "Nesting birds, The Breeding Habits of Southern African Birds", Farnwood Press, Vlaeberg, 128 (1996)
2. N.G. Kahsai, M.le Roux, B.V. Burger, and M.A. Du Plessis (unpublished results)
3. B.V. Burger, B. Reiter, O. Borzyk, and M.A. Du Plessis, (unpublished)
4. Reference 2
5. Reference 3
6. Reference[75], Chapter 1
7. *http://www.hbw.com/ibc/phtml/familia.phtml?idFamilia*

CHAPTER 4

EXPERIMENTAL

4.1 Secretion Collection and Sample Preparation.

Production of the secretion was induced by exerting gentle pressure on the uropygial gland, which normally results in a drop of liquid being released at the terminal end of the papilla. The suspended drop of secretion was touched with the tip of a capillary tube (0.5 mm i.d.) that had been scored at a point about 10 mm from its tip. Capillary forces caused the secretion to move into the capillary. The end of the capillary containing the secretion was inserted into the mouth of a small conical vial (Reacti-Vial) and broken off at the scored position. The back end of the capillary, which served as a handle during the collection process, was discarded. The collected secretion normally flowed out of the capillary into the lower part of the conical vial.

4.2 Analytical Methods

Gas chromatographic (GC) analyses were carried out with a Carlo Erba 5300 gas chromatograph equipped with a flame ionization detector and a Grob split/splitless injector. The glass capillary column was manufactured by the Laboratory for Ecological Chemistry and was coated with 0.25 μm of the apolar stationary phase PS-089 (DB-5 equivalent). Hydrogen was used as carrier gas at a linear velocity of 50.0 cm/sec at 40°C. The flame ionization detector was operated at 280°C and the injector was normally used at 220°C.

Solventless sample introduction for GC-MS analysis was done using a sample introduction probe[1]. Headspace analyses were done by SPME[2] using a 100-m polymethylsiloxane fiber and some of the secretion was extracted with dichloromethane (Merck, residue analysis grade) for conventional liquid sample introduction.

Low-resolution electron impact mass spectra (EI-MS) were obtained at 70 eV on a Carlo Erba QMD 1000 GC-MS instrument using the above column

and conditions. Mass spectra were recorded at 70 eV. The injector temperature was set at 220°C, the interface temperature at 250°C, and the ion source temperature at 180°C. The pressure in the source housing was *ca*. 2 x 10^{-5} Torr at a column temperature of 40°C, decreasing to *ca*. 1 x 10^{-5} Torr towards the end of the temperature program. A scan rate of 0.9 sec/scan with an interval of 0.1 seconds between the scans was employed. Helium was used as carrier gas at a linear velocity of 28.6 cm/sec at 40°C.

References: Chapter 4

1. B.V. Burger, Z. Munro, D. Smit, U. Shmidt, C.L. Wu, and F.C. Tien, J. Chromotogr., **518**, 207 (1990)

2. Z. Zhang and J. Pawliszyn, J. High Resol. Chromatogr., **16**, 689 (1993)